# SYMPATHETIC NERVES: NOVEL THERAPEUTIC TARGETS IN THE TREATMENT OF INFLAMMATORY DISEASE?

An anatomical study on sympathetic innervation of the human:

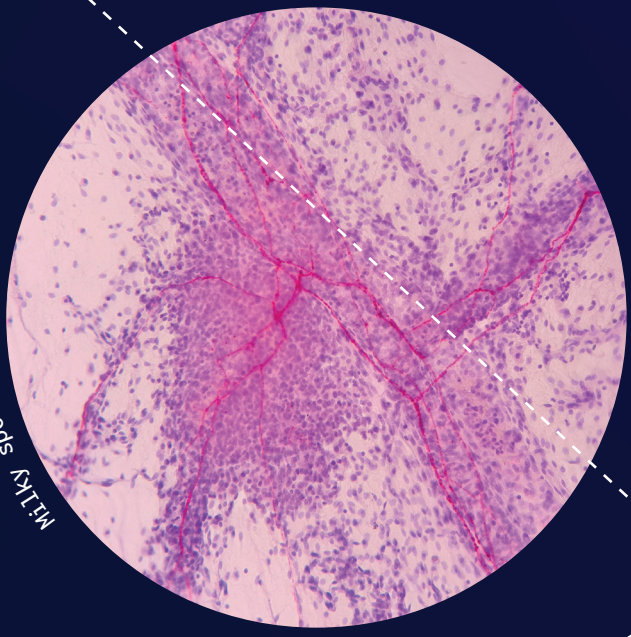

Milky spots

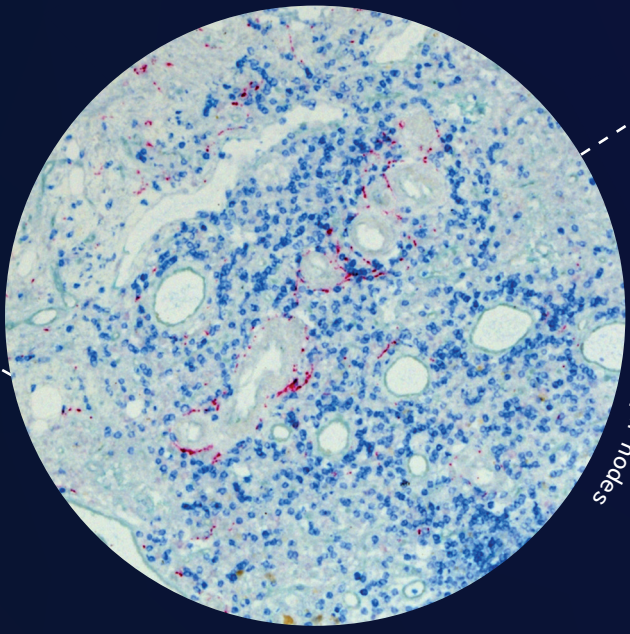

Lymph nodes

Cindy Cleypool

# SYMPATHETIC NERVES: NOVEL THERAPEUTIC TARGETS IN THE TREATMENT OF INFLAMMATORY DISEASE?

## An anatomical study on sympathetic innervation of the human spleen, milky spots, lymph nodes and dorsal root ganglia

Cindy Gerritje Johanna Cleypool

ISBN: 978-94-93197-77-0

Cover design: Ralph Bruens en Brigit van Eijk (Upmost, Amsterdam)

Layout and printing: Off Page, Amsterdam

# SYMPATHETIC NERVES: NOVEL THERAPEUTIC TARGETS IN THE TREATMENT OF INFLAMMATORY DISEASE?

## An anatomical study on sympathetic innervation of the human spleen, milky spots, lymph nodes and dorsal root ganglia

# SYMPATHISCHE ZENUWEN: NIEUWE THERAPEUTISCHE AANGRIJPINGSPUNTEN VOOR DE BEHANDELING VAN ONTSTEKINGSZIEKTEN?

## Een anatomische studie naar de sympathische innervatie van de humane milt, milky spots, lymfeklieren en spinale ganglia

(met een samenvatting in het Nederlands)

**PROEFSCHRIFT**

ter verkrijging van de graad van doctor aan de Universiteit Utrecht
op gezag van de rector magnificus, prof.dr. H.R.B.M. Kummeling,
ingevolge het besluit van het college voor promoties
in het openbaar te verdedigen op

dinsdag 5 oktober 2021 des middags te 2.15 uur

door

**Cindy Gerritje Johanna Cleypool**
geboren op 24 augustus 1976
te Zevenbergen

**Promotor:** Prof. Dr. R.L.A.W. Bleys

De studies beschreven in hoofdstuk 2 en 3 van dit proefschrift zijn mede mogelijk gemaakt met financiële steun van Galvani Bioelectronics.

# TABLE OF CONTENTS

# ABBREVIATIONS

| | |
|---|---|
| α | Alpha |
| Ach | Acetylcholine |
| ANS | Autonomic nervous system |
| AR | Adrenergic receptor |
| ASN | Apical splenic nerve |
| β | Beta |
| BSA | Bovine serum albumin |
| BV | Blood vessel |
| C | Capsule |
| CAIP | Cholinergic anti-inflammatory pathway |
| CGRP | Calcitonin gene related product |
| ChAT | Choline acetyl transferase |
| CNS | Central nervous system |
| CID | Chronic inflammatory disease |
| CT | Coeliac trunk |
| DBH | Dopamine beta hydroxylase |
| DRG | Dorsal root ganglia |
| FDC | Follicular dendritic cell |
| FRC | Follicular reticular cell |
| GSL | Gastrosplenic ligament |
| HE | Hematoxylin / eosin |
| HIER | Heat induced epitope retrieval |
| IR | Immune reactive |
| LGA | Left gastric artery |
| LGEA | Left gastric epiploic artery |
| LN | Lymph node |
| LPR | Liquid permanent red |
| MS | Milky spots |
| NE | Norepinephrine |
| OMS | Omental milky spot |
| PA | Pancreatic artery |
| PBS | Phosphate buffered saline |
| PALS | Periarteriolar lymphatic sheath |
| PGP9.5 | Protein gene product 9.5 |
| Podo | Podoplanin |
| PSL | Pherincosplenic ligament |
| PSNS | Primary sensory nerve soma |
| PSR | Picrosirius red |

| | |
|---|---|
| RGEA | Right gastro epiploic artery |
| RP | Red pulp |
| RT | Room temperature |
| SCS | Subcapsular sinus |
| SGA | Short gastric artery |
| SGC | Satellite glial cell |
| SA | Splenic artery |
| SMA | Smooth muscle actin |
| SMC | Smooth muscle cell |
| SMP | Sympathetic maintained pain |
| T | Trabecula |
| TB | Terminal branch |
| TBS | Tris buffered saline |
| TH | Tyrosine hydroxylase |
| TNF | Tumour necrosis factor |
| VNS | Vagus nerve stimulation |
| vWF | von Willebrand factor |

# 1

# GENERAL INTRODUCTION

# GENERAL INTRODUCTION



Chronic inflammatory diseases (CID), which include diabetes mellitus, several cardiovascular diseases, joint disease, allergies and chronic obstructive pulmonary disease, represent the leading cause of disability and mortality worldwide with a prevalence of 5-7% in Western society (El-Gabalawy et al., 2010). In the last decade our understanding of CIDs has been transformed by new insights in the central role of the immune system in their pathogenesis (Bennett et al., 2018)(Furman et al., 2019). Under normal conditions, the immune system monitors the body for pathogens and tissue damage and, if such a threat is encountered, initiates a temporary restricted upregulation of its inflammatory activity. Once the threat has passed, repair and regulatory processes are activated in order to restore tissue integrity. If the immune system is dysregulated, the inflammatory response can shift from a temporary to a long-lived response thereby setting the stage for CID development (Bennett et al., 2018)(Furman et al., 2019).

To dampen the inflammatory response and mitigate irreversible tissue damage, many anti-inflammatory drugs have been developed including the commonly used nonsteroidal anti-inflammatory drugs (NSAIDs, e.g. aspirin and ibuprofen) and corticosteroids (e.g. prednisone). Although effective, anti-inflammatory drugs come with a variety of side effects and most of these drugs can only be used temporary. Therefore, the development of less harmful anti-inflammatory therapies is desirable and warrants the exploration of the therapeutic potential of lymphoid tissue specific nerves involved in regulating immunity and inflammation.

Animal studies have demonstrated that lymphoid organs receive autonomic, predominantly sympathetic innervation (Bellinger et al., 1993)(Felten et al., 1985), and that sympathetic nerve terminals have been observed in proximity to immune cells with whom they formed synaptic connections (Felten and Olschowka, 1987). Electrical stimulation of splenic sympathetic nerves results in a significant decrease in the systemic anti-inflammatory response (Pavlov and Tracey, 2017)(Chavan and Tracey, 2017) and therefore these nerves hold potential as therapeutic target for the treatment of CIDs.

Further assessment of whether neuroimmune modulation in humans holds potential as a novel anti-inflammatory therapy requires detailed information on sympathetic innervation of lymphoid organs. Since relevant data on human lymphoid organ innervation is limited, this thesis aimed to investigate sympathetic innervation in a subset of these organs, being the spleen, omental milky spots (OMSs) and lymph nodes (LNs).

Sympathetic maintained pain (SMP) is a specific type of chronic pain which is aggravated by sympathetic activity. This type of pain is the result of inflammation induced sympathetic-sensory nerve connections that can develop in dorsal root ganglia (DRGs), along peripheral sensory nerve axons or at sensory nerve receptor endings (Schlereth and Birklein, 2008)(Chen and Zhang, 2015).

Patients with a CID, might be at risk for the development of such nerve connections and increased sympathetic activity, e.g. by stimulation of sympathetic nerves, might result in exacerbation of pain. To assess the risk of this potential side effect in sympathetic nerve based anti-inflammatory therapies, it is of significance to increase our understanding of this phenomenon. Little is known on sympathetic-sensory nerve coupling in humans and this thesis includes a pilot study that reports on our first attempt to gain further insight into its presence in human DRGs.

## Aims of this thesis

The primary goal of this thesis is to provide anatomical data on sympathetic innervation of the human spleen, OMSs, LNs and DRG. This knowledge may contribute to further development of sympathetic nerve based anti-inflammatory therapies in humans. The thesis outline contains more detailed information on separate formulated study goals.

# BACKGROUND INFORMATION



The following paragraphs provide relevant background information with respect to the concept of reflexive neuro immune regulation of inflammation, the therapeutic efficacy of electrical stimulation of a specific anti-inflammatory neural pathway and, the general morphology and current knowledge of sympathetic innervation of human lymphoid organs (spleen, OMSs and LNs) and DRGs.

## Reflexive neuro immune regulation during inflammation

The immune system has long been considered to function independently, however, the last decades it has become evident that immune homeostasis is under neural control (Pavlov and Tracey, 2017). Conjoined efforts in the fields of neuroscience and immunology have identified various neural pathways that regulate the immune response reflexively; sensory (afferent) nerves transmit local immune information (e.g. on the presence of pathogens or inflammatory mediators) to an integrative center in the central nervous system (CNS), which activates motor (efferent) nerves of the ANS that travel back to the peripheral site where they release their neurotransmitter thereby adjusting the immune response via activation of specific receptors on immune cells (Pavlov and Tracey, 2017) (Chavan and Tracey, 2017) (Figure 1). This reflexive immune regulation prevents production of excessive pro-inflammatory cytokines and thereby dampens inflammation and prevents risk of tissue damage, spreading to other tissues and sepsis. Neural reflexive control of cytokine production therefore is vital.

The anti-inflammatory reflex is the most studied of these immune regulatory reflex pathways (Chavan and Tracey, 2017) and rodent studies show that selective stimulation of its efferent arm holds therapeutic potential. If activated, this efferent arm, also known as the cholinergic anti-inflammatory pathway (CAIP), dampens the systemic inflammatory response via the spleen and involves sequential activation of the efferent vagus nerve and sympathetic splenic nerves ) (Pavlov and Tracey, 2017). Activation of sympathetic splenic nerves in turn results in a cascade of intrasplenic events, starting with the release of norepinephrine (NE) (Kees et al, 2003). NE then activates beta (ß) 2-adrenergic receptors (ARs) on $CD4^+$ $ChAT^+$ T lymphocytes (Vida et al., 2011) (Rosas-Ballina et al., 2011)(Vida et al., 2017), which in turn produce and secrete acetylcholine (ACh) (Rosas-Ballina et al., 2011)(Borovikova et al., 2000). ACh then inhibits the release of the pro-inflammatory cytokine tumor necrosis factor alpha (TNFa) from activated macrophages via nicotinergic receptor signaling (Borovikova et al., 2000)(Lu and Kwan, 2014)(de Jonge et al., 2005)(Kox et al., 2009), thereby dampening inflammation. The mechanism described above will be further referred to as the intrasplenic NE-Ach-TNFa-mechanism.

## Therapeutic potential of selective activation of anti-inflammatory pathways

The anti-inflammatory effect of CAIP activation has been studied using electrical stimulation of the vagus nerve (VNS) in sepsis and inflammatory disease models in rodents, and rheumatoid arthritis in humans (Bassi et al., 2017)(Borovikova et al., 2000)(Ghia et al., 2006)(Koopman et al.,

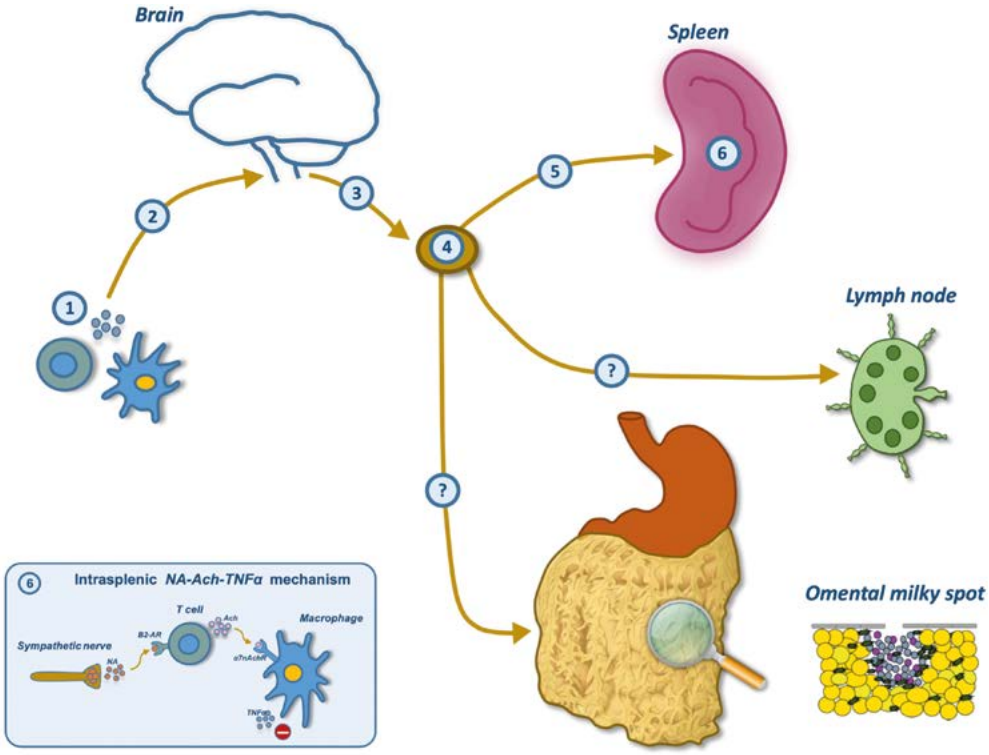


**Figure 1. Reflexive regulation of the immune response.** Local immune information, such as pro-inflammatory cytokines secreted by activated immune cells (**1**), is detected by afferent (sensory) nerves (**2**) and transmitted to an integrative center in the central nervous system (CNS). Subsequently, an efferent (motor) pathway gets activated that will lead to local release of neurotransmitters which can adjust the immune response. One of the most studied efferent pathways is the cholinergic anti-inflammatory pathway (CAIP = 3, 4, 5 and 6) The CAIP is comprised of the vagus nerve (**3**) which transmits information to sympathetic neurons in a sympathetic ganglion (**4**) (in case of the CAIP the coeliac ganglion) from which postganglionic sympathetic nerves run towards the spleen (**5**). In the spleen, these nerves activate the intrasplenic NA-Ach-TNFα mechanism (**6**). Sympathetic nerves release their neurotransmitter noradrenaline (NA) which will then activate beta 2-adrenergic receptors (ß2-ARs) on T cells, which vin turn produce and secrete acetylcholine (Ach). Ach then inhibits the release of the pro-inflammatory cytokine tumor necrosis factor alpha (TNFα) from activated macrophages via nicotinergic receptor (α7nAchR) signaling, thereby dampening inflammation. Details about neural pathways involved in reflexive regulation of the immune response in other secondary lymphoid structures, such as lymph nodes or omental milky spots, is largely unknown.

2016). Although stimulation of the CAIP, using VNS, has been shown to modulate inflammation and hence has therapeutic potential, VNS is associated with a variety of side effects including cough, hoarseness and paresthesia (Ben-Menachem, 2001)(Cristancho et al., 2011). Furthermore, controversy remains as to whether the anti-inflammatory effect of VNS is the result of activation of efferent or afferent vagal nerve fibers, since vagal efferent neurons neither synapse with splenic sympathetic neurons nor drive their ongoing activity (Bratton et al., 2012)(Martelli et al., 2014) (Komega et al., 2018). If the observed anti-inflammatory effect of VNS is the result of afferent

stimulation, activation of the CAIP might be preceded by an unknown central pathway and the distal part of the CAIP, represented by post-ganglionic sympathetic fibers of the splenic plexus (Niijima et al., 1991)(Kees et al., 2003)(Vida et al., 2011), may serve as a more direct stimulation target. Further consideration of splenic plexus stimulation in humans requires knowledge on the course of sympathetic nerves towards the spleen and on splenic intrinsic innervation.

## The spleen

The spleen is the largest lymphoid organ and is positioned in the left upper quadrant of the abdomen. It is covered by visceral peritoneum and is suspended by the gastrosplenic (GSL), splenorenal and phrenicosplenic ligament (PSL) to the stomach, dorsal body wall and diaphragm, respectively. The splenic artery (SA) supplies the spleen with oxygenated blood and originates from celiac trunk, while the splenic vein drains the spleen and empties into the portal vein. The outer part of the spleen is composed of a dense connective tissue capsule from which trabeculae arise to penetrate the deeper parts of the parenchyma. The parenchyma of the spleen is composed of red and white pulp areas. The red pulp is composed of sinuses and cords of Billroth (containing mainly macrophages) and is involved in the removal of old red blood cells, whereas the white pulp with its periarteriolar lymphatic sheath (PALS) (containing mainly T cells) and follicles (containing mainly B cells) is involved in innate and adaptive immune responses, respectively. The spleen filters the blood and if pathogens, cytokines, or antigen presenting cells are encountered, an immune response is initiated. Neuromodulation of this immune response in humans might be mediated via sympathetic nerves of the splenic plexus, which represent the distal part of the efferent arm of the CAIP (Kees et al., 2003)(Niijima et al., 1991)(Vida et al., 2011). The splenic plexus is a neural network that originates from the coeliac ganglia and runs in a paravascular fashion with the SA towards the splenic hilum (Mitchel,1956). Because of this perivascular plexus-like configuration, the optimal neuro electrode interface may require a circumferential device around the SA neurovascular bundle. Since the SA runs in proximity to the pancreas and occasionally is even embedded in it (Sahni et al., 2003), tortuous SA segments (SA loops), that extend away from the pancreas have been evaluated by us as a safer potential stimulation sites in humans. Data collection on the presence, number, location and dimensions of these loops, and, the organization and composition of their surrounding nerve plexus is of importance for further development of a splenic plexus based anti-inflammatory therapy in humans and is described in **Chapter 2.**

Although efferent splenic innervation in general is considered to be predominantly sympathetic, tracer studies in rats suggest that the spleen is supplied by parasympathetic nerves as well (Buijs et al., 2008). These parasympathetic nerves were thought to enter the spleen at its poles as dissection of polar parts of the GSL abolished the presence of retrograde tracer in the dorsal motor nucleus (Buijs et al., 2008). The presence of such a parasympathetic nerve was confirmed in mice where a discrete nerve was macroscopically observed entering the spleen at its cranial pole (Guyot et al., 2019). This nerve, by the authors referred to as the apical splenic nerve (ASN), contains primarily parasympathetic fibres and electrical stimulation of this nerve resulted in increased levels of splenic

Ach, decreased lipopolysaccharide (LPS) induced levels of systemic TNFa and mitigated clinical symptoms in a mouse model of rheumatoid arthritis (Guyot et al., 2019). If such a discrete ASN exists in humans, this structure could hold potential as a relatively easily accessible electrical stimulation target to treat immune mediated inflammatory diseases. **Chapter 3** describes a study in which the presence of the ASN in humans was explored.

Stimulation of the CAIP results in a series of intrasplenic events, which at least require a close association between sympathetic nerves and T cells. Knowledge on this pathway has mostly been derived from rodent studies and only scarce information is available on the intrinsic sympathetic innervation patterns of the human spleen and whether these nerves are in proximity to T cells. Furthermore, sympathetic innervation is known to reduce with age and determining age-related variation in human splenic innervation is of importance to establish whether splenic plexus stimulation is confined to patients of specific age groups only. Age-related variations of sympathetic nerve distribution in the human spleen are studied and results are reported in **Chapter 4**.

Morphological and functional parallels between the spleen and other secondary lymphoid organs exist. This raised the question if other lymphoid structures are innervated as well and whether their supplying nerves could represent potential therapeutic targets to modulate local immune responses. This led to the exploration of sympathetic innervation of OMSs and LNs.

## Omental milky spots

OMSs are small residential lymphoid structures (0.5-3.5 $mm^2$) of the greater omentum. They are mainly composed of macrophages, B cells and T cells and do not show a clear cellular organization or a covering capsule (Shimotsuma et al., 1991)(Liu et al., 2015). OMSs play an important role in the peritoneal immune response: *1)* peritoneal fluid is absorbed via stomata of the omental mesothelium and gets monitored in OMSs for foreign or pathogenic substances (Wilkosz et al., 2005)(Meza-perez and Randall, 2017)(Vugt et al., 1996) and *2)* OMSs form a gateway for circulating immune cells that are recruited towards the peritoneal cavity during a peritoneal immune challenge (Wijffels et al., 1992) (Figure 2).

OMSs are positioned in proximity to side branches of epiploic arteries (originating from the left and right gastroepiploic arteries (LGEA and RGEA, respectively), also known as gastro-omental arteries) and their immune cells are clustered around small arteries (omental glomeruli) originating from these vessels (Michailova and Usunoff, 2004). Venous blood from OMSs runs with epiploic veins towards the portal vein. Absorbed peritoneal fluid gets transferred to the omental lymphatic system via small efferent OMS lymphatic vessels. Sympathetic nerves of the splenic plexus continue around SA branches towards the stomach and omentum via short gastric arteries and the LGEA respectively, and towards the pancreas via pancreatic arteries (Mitchel, 1956). The omentum is known to receive sympathetic nerves, which is thought to be restricted to the vasculature only. If OMSs receive sympathetic nerves originating from the splenic plexus, stimulation of this plexus

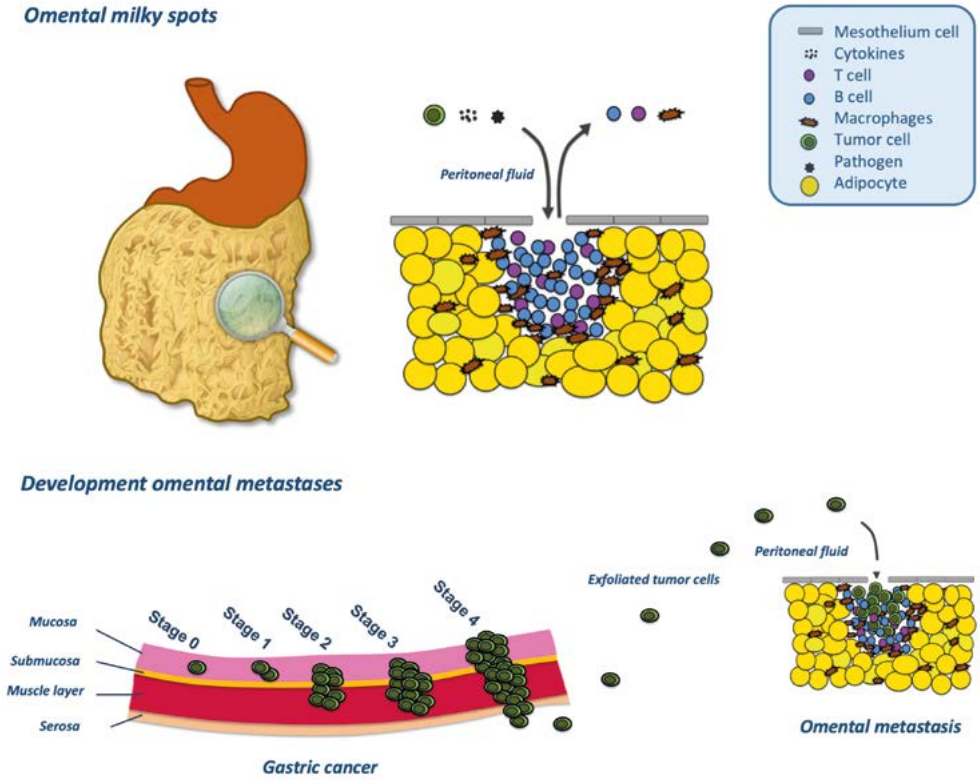


**Figure 2. Omental milky spots and their role in the peritoneal immune response and the development of omental metastases.** Omental milky spots (OMS) are small lymphoid cell clusters residing in the greater omentum. Peritoneal fluid gets absorbed via openings (stomata) in the mesothelial covering of the omentum and gets monitored by OMSs for the presence of immune challenging substances, such as cytokines or pathogens. OMSs then can form a gateway for circulating immune cells that are recruited to the peritoneal cavity. Exfoliated tumor cells, e.g. from stage four gastric cancer, can disseminate to the peritoneal cavity where they end up in the peritoneal fluid. These tumor cells enter OMSs, implant, proliferate and grow into secondary omental tumors (omental metastases).

might, in addition to the systemic immune response, modulate the peritoneal immune response as well. Evaluating the presence of sympathetic nerves in OMSs therefore is of significance.

In addition to their role in immune surveillance of the peritoneal cavity, OMSs are also known for the fact that they form primary implantation sites for disseminated cancer cells in the peritoneal fluid, and hence represent hotbeds for the development of peritoneal metastatic disease (Krist et al., 1998) (Hagiwara et al., 1993)(Hagiwara et al., 1993)(Tsujimoto et al., 1995) (Figure 2). The presence of sympathetic nerves in OMSs might explain why these lymphoid structures represent metastatic hotbeds; the sympathetic neurotransmitter NE is known to be involved in creating a tumor stimulating microenvironment (Cole et al., 2015) and can regulate tumor cells as these cells express adrenergic receptors on their membranes (Coelho et al., 2017).

OMSs cannot be observed with the naked eye and a staining method allowing their macroscopic recognition was developed **(Chapter 5).** This method allowed for targeted isolation of OMSs and subsequent microscopic studies to evaluate the presence of sympathetic nerves **(Chapter 6)**.

Although in the anatomical literature OMSs are considered to represent the only lymphoid structures of the greater omentum, clinical studies have reported the presence of lymph nodes (LNs). This difference might be explained by the fact that activated OMSs may erroneously be mistaken for LNs. In response to inflammation OMSs form specialized B and T cell areas (Dux et al., 1986) (Jackson-Jones et al., 2016)(Bénézech et al., 2015), features also present in, but apparently not restricted to LNs. Establishing which lymphoid structures reside in the greater omentum and how they are interconnected is indispensable for our general understanding of omental immune function, but also contributes to our understanding of cancer dissemination patterns. Since (activated) OMSs and LNs share morphological characteristics, a discriminative method allowing to distinguish omental lymphoid structures was developed **(Chapter 7).** Pathology reports of gastric cancer patients frequently list the presence of LNs in the greater omentum. These lymphoid structures were re-evaluated with the before mentioned discriminative method in order to ascertain the presence of LNs in the greater omentum **(Chapter 8)**.

## Lymph nodes

LNs are lymphoid organs that can be found throughout the body. They are covered by a connective tissue capsule from which trabeculae arise, dividing the LN in functional compartments, also known as lobules. From the outside in, LNs show a layered organization with a capsule, cortex, paracortex and medulla. The cortex contains follicles with B cells, the paracortex contains mostly T cells and the medullary cords are mainly composed of plasma cells, B cells and macrophages. LNs receive lymph from the surrounding tissue via afferent lymph vessels. These vessels enter the capsule and are in continuation with the subcapsular sinus, transverse sinuses and medullary sinuses. Lymph eventually leaves the LN via an efferent lymph vessel at the hilum. The hilum also contains an artery and a vein. Lymph entering the LN gets screened for the presence of pathogens, antigen presenting cells and inflammatory substances such as cytokines, and, if encountered, a proper local immune response is initiated. From animal studies it is known that LNs are under neural control and that this occurs predominantly via sympathetic nerves and moreover its neurotransmitter NE: NE influences LN lymphocyte proliferation, antibody secretion, blood perfusion, inflammatory cytokine production, and lymphocyte migration and egression, as shown in various rodent studies (Madden et al., 1989) (Madden et al., 1994)(Rogausch et al., 2004)(Nakai et al., 2014)(Suzuki et al., 2016)(Guyot et al., 2019). In rodents, sympathetic nerves have been observed in LNs where they were in close relation to lymphocytes (Giron et al., 1980)(Felten et al., 1984). Studies addressing sympathetic nerve distribution in human lymph nodes were limited and very concise (Fink and Weihe, 1988) (Panucio et al., 1998). A microscopic study of sympathetic nerve distribution in human LNs was performed supplying a comprehensive and accurate representation of the presence and location of these nerves as well as on their relation with T cells **(Chapter 9)**. This information could contribute to further consideration of local, LN-based neuro immune modulatory therapies in humans.

## Sympathetic-sensory nerve coupling in dorsal root ganglia

A DRG is a cluster of cell bodies of first order (primary) sensory neurons in the dorsal root of a spinal nerve. DRG neurons are pseudo unipolar in nature; a single axon projects from its cell body which then bifurcates into a peripheral axon (extending to receptor endings in the periphery) and a central axon (extending to the central nervous system). Sensory information, including nociception (pain) from peripheral tissues is transmitted via a peripheral axon towards first order sensory neurons in the DRG from where the signal is then further transferred to the spinal cord via a central axon. Under normal conditions, DRGs are mostly devoid of sympathetic nerves with the exception of perivascular sympathetic nerves. However, aberrant sympathetic neural networks, also referred to as sympathetic baskets, have been observed in DRGs where they surround sensory neurons and their associated supporting satellite glial cells (García-Poblete et al., 2003). These sympathetic baskets result is direct sympathetic-sensory nerve coupling and rodent studies have shown that if such baskets are present, sympathetic activation can initiate or aggravate pain (Chung et al., 1993) (Ramer and Bisby, 1998). When considering sympathetic nerve based anti-inflammatory therapy in humans, it is inevitable to understand the nature of these sympathetic baskets in order to avoid sympathetic nerve stimulation induced / aggravated pain. The development of these sympathetic baskets is inflammation induced and is known to develop in rodents as a result of neuropathy and peripheral tissue inflammation such as colitis (Schlereth and Birklein 2008)(Xia et al. 2011). In humans however, data on sympathetic baskets is very concise and hence a pilot study was performed as a first attempt to increase our understanding of this phenomenon. The presence of sympathetic baskets and their corresponding adrenergic receptors were microscopically investigated in human dorsal root ganglia **(Chapter 10)**. Since an influx of macrophages and T cells is known to precede the development of these baskets in rodents (Hu and McLachlan, 2002), the presence of these immune cells was studied as well.

# THESIS OUTLINE

## Part I: The spleen

Electrical stimulation of sympathetic splenic nerves in rodents results in a dampening of the systemic inflammatory response. The equivalent of these nerves in humans, the splenic plexus, could potentially represent a therapeutic target for the treatment of CIDs. Tortuous SA segments (SA loops), including the surrounding splenic nerve plexus, have been evaluated as potential stimulation sites in humans (**Chapter 2).**

A recent study showed that in addition to the sympathetic splenic nerves, the murine spleen is supplied with a discrete ASN which enters the spleen at its cranial pole. Electrical stimulation of this nerve resulted in an anti-inflammatory response. **Chapter 3** describes a study that evaluated the topographic anatomy of this nerve in mice and explores the presence of an equivalent structure in humans.

Anti-inflammatory effectivity of splenic plexus stimulation requires close association of sympathetic nerves and T cells. **Chapter 4** addresses the distribution of sympathetic nerves in the human spleen and investigates whether these nerves are in proximity to T cells of the PALS. Age-related variations in splenic sympathetic innervation were evaluated as well as these might narrow the window of application of future splenic plexus mediated anti-inflammatory therapies.

## Part II: Omental milky spots

The greater omentum contains small clusters of lymphoid tissue also known as OMS. These structures are involved in immune homeostasis of the peritoneal cavity and play a role in the formation of omental metastatic disease. In order to visualize these tiny structures in large fixed tissue samples of the greater omentum in humans, a visualization technique was developed (**Chapter 5**). The presence of sympathetic nerves in OMSs was studied and findings are described in **Chapter 6**. OMS might erroneously be confused with LNs and a method allowing their proper discrimination was developed **(Chapter 7).** In **Chapter 8** this method was applied to characterize lymphoid structures in the greater omenta of gastric cancer patients.

## Part III: Lymph nodes

The immune response in LNs is regulated by sympathetic nerves as shown in various rodent experiments. These nerves could represent potential therapeutic targets and their presence in human LNs was explored and described in **Chapter 9.**

## Part IV: Dorsal root ganglia

Activated immune cells can migrate to DRGs and stimulate sympathetic nerve outgrowth and the formation of sympathetic nerve baskets around primary sensory nerve somata. Activation of

these sympathetic baskets might result in pain. Detailed knowledge on the nature of sympathetic-sensory nerve coupling might contribute to our general understanding of a specific type of chronic pain, also referred to as sympathetic maintained pain (SMP), and help to estimate if electrical stimulation of sympathetic nerves can aggravate SMP. The presence of DRG related sympathetic nerves was studied in two human cadavers. The preliminary findings of this pilot study are described in **Chapter 10** as well as recommendations for further studies.

## Discussion

In **Chapter 11**, the overall implications of the findings described in this thesis are discussed with respect to our general understanding of neuro immune regulation and sympathetic nerve based anti-inflammatory therapy development. In the discussion new hypotheses are generated, suggestions for future research are presented, issues of concern are raised and a main conclusion is provided.

# SPLEEN

# 2

# SPLENIC ARTERY LOOPS: POTENTIAL SPLENIC PLEXUS STIMULATION SITES FOR NEUROIMMUNOMODULATORY-BASED ANTI-INFLAMMATORY THERAPY?

Cindy G.J. Cleypool[1]; Dyonne Lotgerink Bruinenberg[1], Tom Roeling[1], Eric Irwin[2,3], and Ronald L.A.W. Bleys[1]

[1] Department of Anatomy, Division of Surgical Specialties, University Medical Center Utrecht, Utrecht University, the Netherlands.
[2] Galvani Bioelectronics, Stevenage, United Kingdom.
[3] Department of Surgery, University of Minnesota School of Medicine, Minneapolis, United States of America.

*Clinical Anatomy. 2021*

# ABSTRACT

## Introduction

The splenic plexus might represent a novel neuroimmunomodulatory therapeutic target as electrical stimulation of this tissue has been shown to have beneficial anti-inflammatory effects. Tortuous splenic artery segments (splenic artery loops), including their surrounding nerve plexus, have been evaluated as potential stimulation sites in humans. At present, however, our understanding of these loops and their surrounding nerve plexus is incomplete. This study aims to characterize the dimensions of these loops and their surrounding nerve tissue.

## Materials & methods

Six formaldehyde fixed human cadavers were dissected and qualitative and quantitative macro- and microscopic data on splenic artery loops and their surrounding nerve plexus were collected.

## Results

One or multiple loops were observed in 83% of the studied specimens. These loops, including their surrounding nerve plexus could be easily dissected free circumferentially thereby providing sufficient space for further surgical intervention. The splenic plexus surrounding the loops contained a significant amount of nerves that contained predominantly sympathetic fibers.

## Conclusion

The results of this study support that splenic artery loops could represent suitable electrical splenic plexus stimulation sites in humans. Dimensions with respect to loop height and width, provide sufficient space for introduction of surgical instruments and electrode implantation, and, the dissected neurovascular bundles contain a substantial amount of sympathetic nerve tissue. This knowledge may contribute to further development of surgical techniques and neuroelectrode interface design.

# INTRODUCTION



Neural regulation of the immune system, also known as neuro-immunomodulation, has gained attention for its potential as a new anti-inflammatory therapeutic method. Various neural pathways are suggested to be involved in neuro-immunomodulation with one of these pathways, the cholinergic anti-inflammatory pathway (CAIP), also known as the inflammatory reflex, having been studied most extensively (Chavan and Tracey, 2017). The CAIP comprises an efferent neural pathway that dampens the systemic inflammatory response via the spleen and involves sequential activation of the efferent vagus nerve and sympathetic splenic nerve tissue (Reardon, 2016)(Pavlov and Tracey, 2017).

The anti-inflammatory effect of the CAIP has been studied using electrical stimulation of the vagus nerve (VNS) in both rodent and human inflammatory models (Bassi et al., 2017) (Borovikova et al., 2000)(Ghia et al., 2006)(Koopman et al., 2016). Although stimulation of the CAIP, using VNS, has been shown to modulate inflammation, VNS is associated with a variety of side effects including cough, hoarseness and paresthesia (Ben-Menachem, 2001)(Cristancho et al., 2011). Furthermore, controversy remains as to whether the anti-inflammatory effect of VNS is the result of activation of efferent or afferent vagal nerve fibers, since vagal efferent neurons neither synapse with splenic sympathetic neurons nor drive their ongoing activity (Bratton et al., 2012). If the observed anti-inflammatory effect of VNS is the result of afferent stimulation, activation of the CAIP most likely is preceded by an unknown central reflex and the distal part of the CAIP, represented by post-ganglionic sympathetic fibers of the splenic plexus (Niijima et al., 1991)(Kees et al., 2003)(Vida et al., 2011), may serve as a more direct stimulation target.

Electrical stimulation of the splenic plexus, in rats, has been shown to reduce levels of systemic tumor necrosis factor (TNF) after administration of the endotoxin lipopolysaccharide (Kees et al., 2003) (Vida et al., 2011) and mitigated clinical symptoms in a mouse model of rheumatoid arthritis (Guyot et al., 2019). Therefore, electrical splenic plexus stimulation (SPS) in humans might hold potential as an anti-inflammatory therapy and knowledge on the anatomy of this specific nerve tissue is essential for further therapeutic design.

The human spleen is reported to be innervated by sympathetic nerve fibers (Kuntz, 1953) (Heusermann and Stutte, 1977) (Verlinden et al., 2018). These fibers originate in the celiac ganglia and run in a perivascular nerve plexus around the celiac trunk and subsequently the splenic artery (SA) as they travel towards the splenic hilum (Mitchel, 1956). At the hilum the SA ramifies and the surrounding splenic plexus continues around these smaller branches entering the splenic pulp (Mitchel, 1956). Because of this perivascular plexus-like configuration, the optimal neuro-electrode interface may require a circumferential device around the SA neurovascular bundle. Due to the close proximity of the SA to the pancreas and the fact that it can even be embedded within the pancreatic parenchyma, concern has been raised about the risk of damaging or irritating

pancreatic tissue during circumferential dissection of the SA neurovascular bundle in preparation for electrode application. To address this concern, segments of the SA with increased tortuosity where the artery moves away from the pancreas (Michels, 1942) (Sahni et al., 2003) have been considered as intervention points. These segments, further referred to as SA loops, may represent safe intervention sites for electrical SPS.

In order to assess the feasibility of SA loops as electrical SPS sites in humans, morphological information on these structures is needed to inform surgical and engineering activities. Although the human SA and its tortuosity has been previously studied (Michels, 1942)(Sahni et al., 2003), these studies do not supply all required information for neuroelectrode interface design and surgical implantation technique development. Therefore, this study aims to provide both descriptive and quantitative information on the presence, number, location, and dimensions of SA loops, and, on the presence, amount, type and organization of their perivascular nerve tissue.

# MATERIALS & METHODS

Six human cadavers were used for this study: four females and two males with a median age of 93 years at death (interquartile range (IQR): 79-98). Whole body preservation was accomplished by arterial perfusion with 3% formaldehyde. The spleen, stomach, pancreas, splenorenal ligament, greater omentum, and gastrosplenic ligament were removed *in toto* and stored in 2% formaldehyde until further dissection. All bodies entered the Anatomy department through a body donation program and by prior written informed consent, the donors allowed their bodies to be used for educational and research purposes.

## Macroscopic examination

Dissection was performed macroscopically. Occasionally a surgical microscope (Topcon, OMS75, Tokyo, Japan) was used for more detailed dissections. Descriptive data were collected on the SA, its loops and surrounding structures. Quantitative data were collected on the SA length, the distance of the spleen to the origin of the SA, the SA branching pattern and the number of SA loops. For each SA loop, the height and width of the loop, and the diameter of the ascending and descending limbs of the loop were determined (Figures 1A-B). Distances and diameters were measured using a ruler and calliper, respectively.

## Microscopic examination

Following dissection and investigation of macroscopic parameters, part of SA loops and their surrounding nerve plexus, from now on referred to as the SA loop neurovascular bundle, were removed from halfway up the ascending limbs of the loops and processed for microscopic examination.

## Preparation of tissue sections

All samples were decalcified with EDTA for six days (12,5% EDTA in distilled water, pH 7.5) and sequentially placed in increasing percentages of ethanol, xylene and paraffin. Samples were embedded in paraffin and cut on a microtome (Leica 2050 Super Cut, Nussloch, Germany) and 5 µm thick cross sections of one level of the neurovascular bundles were collected on glass slides, airdried and subsequently heat fixed for two hours on a slide drying table of 60°C (Medax, 14801, Kiel, Germany). Adjacent sections of each sample were stained with antibodies raised against Protein Gene Product 9.5 (PGP9.5), Tyrosine Hydroxylase (TH), Choline acetyltransferase (ChAT) and Calcitonin Gene-Related Peptide (CGRP), staining for general, sympathetic, parasympathetic and afferent nerve tissue, respectively.

## Immunohistochemistry

Sections were deparaffinated and rehydrated followed by 20 minutes of antigen retrieval in 95°C citrate buffer on a hot plate. After washing in Tris-buffered saline (TBS) with 0.05% tween, sections were pre-incubated with 5% Normal Human Serum in TBS for ten minutes, followed by incubation with primary antibodies (rabbit anti-PGP (DAKO Z5116 Glostrup Denmark) 1:2000 for 48 hours at 4°C, rabbit anti-TH (Pel Freez P40101, Rogers USA ) 1:1500 overnight at room temperature (RT), goat anti-ChAT (Milipore AB144P, Burlington USA) 1:50 overnight at 4°C, or mouse anti-CGRP (Sigma C7133, Saint Louis, USA) 1:1500 overnight at 4°C) in TBS with 3% bovine serum albumin. Sections were washed with TBS-0.05% Tween several times and incubated for 30 minutes at RT with Brightvision Poly-AP Goat-anti-Rabbit (ImmunoLogic, Duiven, the Netherlands) (PGP and TH) or Brightvision Poly-AP Goat-anti-Mouse (ImmunoLogic, Duiven, the Netherlands) (CGRP). In case of staining with ChAT, sections were incubated for 60 minutes with biotinylated horse anti goat (Vector, Burlingame, USA) 1:500 at RT followed by washing with TBS-0.05% Tween and incubation with Streptavidin-AP (Vector, Burlingame, USA) 1:500 for 60 minutes. After incubation with secondary antibodies, all sections were washed with TBS and incubated with Liquid Permanent Red (LPR) (DAKO, Glostrup, Denmark) for ten minutes. Tissue sections were then washed with distilled water and counterstained with hematoxylin, airdried at 60°C for 90 minutes and cover slipped using Entellan (Merck, Darmstadt, Germany). Negative controls were obtained by incubation with TBS-3%BSA without primary antibodies. Human vagus nerve sections were included as a positive control for general, afferent and parasympathetic nerve tissue and sympathetic trunk slides for sympathetic nerve tissue.

## Microscopic imaging

Brightfield and fluorescent single images and stitched overview images (also known as tile scans) were captured of the same sample using a DM6 microscope with a motorized scanning stage, a DFC7000 T camera and LASX software (all from Leica, Nussloch, Germany). Single images were obtained with various magnifications whereas the 20x objective was used for tile scans.

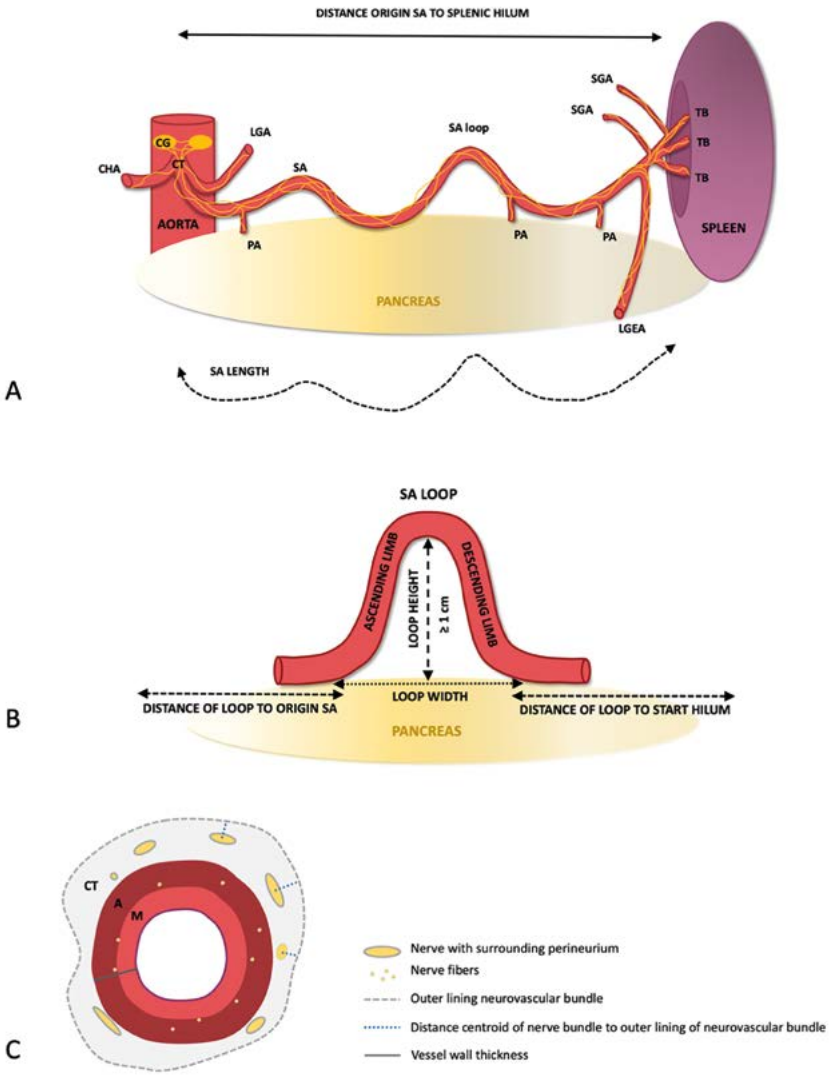


**Figure 1. Schematic representation of investigated macro- and microscopic morphometric parameters. A: Macroscopic parameters SA.** Distance of the spleen to the origin of the SA, measured in a straight line from the start of the splenic hilum to the origin of the SA at the celiac trunk. SA length, was measured by placing a cord alongside the SA, from the origin of the SA at the celiac trunk to the start of the splenic hilum. ***CT****: celiac trunk,* ***LGA:*** *left gastric artery,* ***LGEA****: left gastroepiploic artery,* ***PA****: pancreatic artery,* ***SGA****: short gastric artery,* ***TB****: terminal branch.* **B: Macroscopic parameters SA loop.** Loops are defined as parts of the SA that extend away from the pancreas with a height of minimal 1 cm, measured from the inside of the apex of the loop and the surface of the pancreas. The loops contain a proximal ascending and a distal descending limb. The width of the loop is measured between the start of the ascending - and descending loop. Loop location is determined as the distance of the ascending limb to the origin of the SA and the distance of the descending loop to the start of the hilum. **C: Microscopic parameters SA loop and its surrounding nerve tissue.** Cross section of a SA loop neurovascular bundle, containing the SA with its three layers (I, M and A) and its surrounding connective tissue. Nerves are present in the connective tissue layer (CT) and smaller nerves and fibers can be found in the adventitia until the tunica media. ***CT****: connective tissue,* ***I****: Tunica intima,* ***A****: Tunica adventitia,* ***M****: Tunica media*

### Image analysis

Tile scans of cross sections of SA loops stained with different markers were analyzed in Fiji (ImageJ with additional plugins) (Schindelin et al., 2012). The outer and inner lining of the total neurovascular bundle (SA with its surrounding connective tissue and nerve plexus) and, all perivascular nerves with their surrounding perineurium, were selected manually. The perimeter (circumference) of the total neurovascular bundle and its tissue area, the number of nerves, nerve diameter (short axis), nerve area (including perineurium), vessel wall thickness, diameter of the total neurovascular bundle and distance of the nerve's centroid (geometric center) to the outer lining of the neurovascular bundle were measured (Figure 1C).

A threshold was set allowing to select all TH-immune reactive (IR) tissue inside the nerves of the splenic plexus and to calculate their (pixel) area. The area of sympathetic nerve tissue was then calculated for each loop and the amount of sympathetic nerve tissue was then expressed as area% with respect to the total tissue area of the loops.

### Statistics

Descriptive statistics were used to display quantified data which were calculated in SPSS.

## RESULTS

### Macroscopic morphometric data

#### *Number, orientation and relation of SA loops with surrounding structures*

A total of 8 loops were found in 6 specimens. A median of 1 (IQR: 1-2) loop was found per cadaver. One individual did not have any loops, three individuals contained one loop, one individual contained two loops and one individual contained three loops. Seven out of the eight observed SA loops extended in a dorso-cranial direction with respect to the pancreas whereas only one loop extended in a more ventro-caudal direction. All loops were covered with adipose tissue, a layer of loose connective tissue, and an irregular network of firm white strands (Figure 2A), which, on histological analysis, were shown to represent the splenic plexus. In all cases parts of the loops could be visualized prior to dissection. However, in specimens with less adipose tissue loops were more easily identified. Loops were easily separated from surrounding adipose- and connective tissue, using blunt dissection, whereas the splenic plexus remained attached.

In the majority of the studied specimens, the splenic plexus as a whole remained in close proximity to the adventitial surface of the SA while running along the course of the SA and its loops (Figure 2A). In only one case a discrete nerve was observed to cross from one limb to the other, at the lowest part of the loop, and was found to rejoin and continue with the SA after the loop (Figure 2B). The thickness and patterning of the nerves of the splenic plexus varied within each

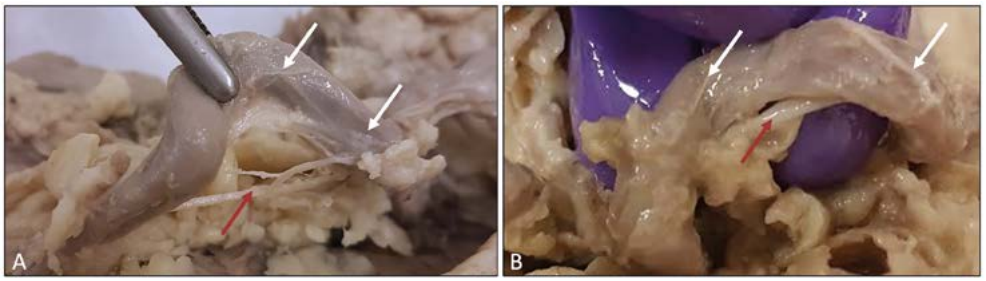


**Figure 2. Splenic plexus in relation with SA loops.** Nerves visible on the SA mostly follow the SA at the loop, but occasionally nerves were observed to run below the inner curvature of the loop and continue with the SA after the loop. **A:** SA loop with nerves following the loop, but also running below the loop. **B**: SA loop showing one relatively thick nerve (arrow) running just below the inner curvature of the loop and smaller nerves running with the loop.

specimen and between specimens. There was no obvious predominant topographical orientation of nerves with respect to the dorsal, ventral, cranial or caudal sides of the vessel wall.

### *SA length, tortuosity and loop location*

The median length of the SA, measured from the origin of the SA to the spleen by placing a cord along the surface of the SA, was 18.9 cm (IQR:12.9-21.1 cm) while the linear distance between the origin of the SA and the spleen was 11.3 cm (IQR: 9.6-13.5 cm), suggesting a median tortuosity of 54% (IQR: 44.3-62.8%). All loops were located at the pancreatic part of the SA. The median distances from the start and ending of the loops to the origin of the SA and splenic hilum, was 6.1 cm (IQR: 3.7 – 8.4 cm) and 3.8 cm (2.1 – 6.4 cm), respectively. Table 1 contains an overview of the macroscopic morphometric data.

### *Height, width and diameter of SA loops*

The average loop height, measured as the distance between the inner curve of the apex of the loop and pancreas, was 1.2 cm (IQR: 1.0 – 1.7cm). Loop width, measured as the distance between the ascending and descending limbs of the SA loop at their origins, was 2.0 cm (IQR: 1.5 – 2.5 cm). The median diameter of loop limbs, irrespectively if these were the ascending or descending limbs, was 0.40 cm (IQR: 0.45 – 0.50 cm).

### *SA course and branching pattern*

In all six specimens the SA originated from the celiac trunk. Its course was mostly suprapancreatic but SA segments were also found to travel in retropancreatic, intrapancreatic or anteropancreatic locations. A number of branches were shown to originate from each SA: One left gastroepiploic artery (LGEA) and a median of five pancreatic arteries (PAs) (IQR: 4-5), three short gastric arteries (SGAs) (IQR: 2-5) and four terminal SA branches (TBs) (IQR: 3-7). Branching arteries were found to originate from each of the eight observed loops. One-to-two PAs were shown to arise from three

of the loops. One-to-two SGAs were found to arise from five loops and the LGEA was found to arise from two loops.

## Microscopic morphometric data

All neurovascular bundle cross sections of SA loops demonstrated a blood vessel with clearly discernible tunica adventitia, media and intima. In some specimens the tunica intima was thickened due to atherosclerotic calcifications. The adventitial layer and surrounding connective tissue were loosely organised and continuous with each other, and no clear borders between the two were observed. Small nerves were present in the tunica adventitia of all specimens, and were observed until the tunica media (Figure 3). In this continuous connective tissue compartment multiple nerves of variable sizes and shapes, were identified around the circumference of the artery. These nerves appeared randomly distributed and oriented around the artery. Thus, in cross-sections of the SA the surrounding nerves, depending on their cutting plane, appear as round, ellipsoid or elongated structures. In ellipsoid and elongated structures, the perimeter and surface area are not representative measures for the amount of excitatory nerve tissue. In order to correct for these misassumptions, the short axis of these structures is allowed to be used to recalculate perimeter and surface area (Weibel 1979).

The median perimeter of the total neurovascular bundle was 26.46 mm (IQR: 19.24-28.78 mm), its tissue area (lumen area excluded) 31.49 $mm^2$ (IQR: 15.83-35.06 $mm^2$) and its vessel wall thickness, measured at locations without calcifications, was 659 µm (IQR:470.8-774.5 µm). The median number of nerves surrounding a SA loop was 28 (IQR: 21-34.5), with a median nerve diameter and tissue area (both including the perineurium) of 33 µm (IQR: 18-87 µm) and 788 $µm^2$ (IQR: 203-5324 $µm^2$), respectively. The average distance of the centroid (geometric center) of a nerve to the outer connective tissue lining of the neurovascular bundle was 446 µm (IQR: 247 –769 µm). Table 2 contains an overview of the microscopic morphometric data.

During a qualitative assessment of all tissue slides it was noticed that the amount and location of PGP9.5 and TH-IR tissue inside nerves appeared equivalent, suggesting the observed nerves contain predominantly sympathetic nerve tissue (Figure 3). This observation was quantitatively confirmed by digitally analysing various microscopic images of both PGP9.5 and TH-stained tissue slides, which resulted in comparable values. As such, further studying of PGP9.5-stained sections would not provide additional information and therefore no further quantitative analysis was performed on these slides. The median area of TH-IR nerve tissue per nerve was 297 $µm^2$ (IQR: 36-2024 $µm^2$) and the median total area of TH-IR tissue surrounding a SA loop was 88190 $µm^2$ (IQR: 10792-197391 $µm^2$), which was 0.34% (IQR: 0.06-0.60%) of the total neurovascular bundle tissue area.

CGRP and ChAT staining were performed on adjacent slides to study whether nerves contained sensory or parasympathetic nerve fibers, respectively. A small amount of CGRP-IR was observed in nerves. CGRP-IR was mostly observed inside small blood vessels whereas merely few CGRP- IR areas

were observed in the nerve tissue itself (Figure 3C). ChAT-IR tissue was observed in nerves as well, but mainly in the wall of small blood vessels and not in structures that could represent nerve fibers (Figure 3D). No further quantitative analysis was performed on CGRP and ChAT-stained slides.

**Table 1.** Quantitative macroscopic morphometric data on the SA and its loops

| Parameter | Median | First quartile | Third quartile |
|---|---|---|---|
| ***SA (n=6)*** | | | |
| SA length (cm) | 18.9 | 12.98 | 21.05 |
| Distance of origin SA to spleen (cm) | 11.25 | 9.63 | 13.5 |
| SA elongation (%) | 54 | 44.25 | 62.75 |
| Number of branching PAs | 5 | 4 | 5 |
| Number of branching SGAs | 3 | 2 | 5 |
| Number of SA TBs | 4 | 3 | 7 |
| Number of loops | 1 | 1 | 2 |
| ***SA loops (n=8)*** | | | |
| Loop width (cm) | 2 | 1.5 | 2.45 |
| Distance of loop to origin SA (cm) | 6.05 | 3.65 | 8.38 |
| Distance of loop to spleen (cm) | 3.75 | 2.13 | 6.43 |
| Loop height (cm) | 1.15 | 1.00 | 1.65 |
| Diameter SA limb (cm) | 0.40 | 0.45 | 0.50 |

**Table 2.** Quantitative microscopic data on SA loops and surrounding nerve tissue

| Parameter | Median | First quartile | Third quartile |
|---|---|---|---|
| ***SA loops*** | | | |
| Perimeter of neurovascular bundle (mm) | 26.46 | 19.24 | 28.78 |
| Tissue area of neurovascular bundle ($mm^2$) | 31.49 | 15.83 | 35.06 |
| Thickness of vessel wall (mm) | 659 | 470.80 | 774.50 |
| ***Nerve tissue*** | | | |
| Number of nerves / loop | 28 | 21 | 34.50 |
| Diameter of nerves (short axis) (mm) | 33 | 18 | 87 |
| Distance of nerves to the outer lining neurovascular bundle (mm) | 446 | 247 | 769 |
| Tissue area of nerves (including perineurium) ($mm^2$) | 788 | 203 | 5324 |
| TH-IR nerve tissue in nerves ($mm^2$) | 297 | 36 | 2024 |
| TH-IR area / loop ($mm^2$) | 88190 | 10792 | 197391 |
| TH-IR tissue / loop (%) | 0.34 | 0.06 | 0.60 |

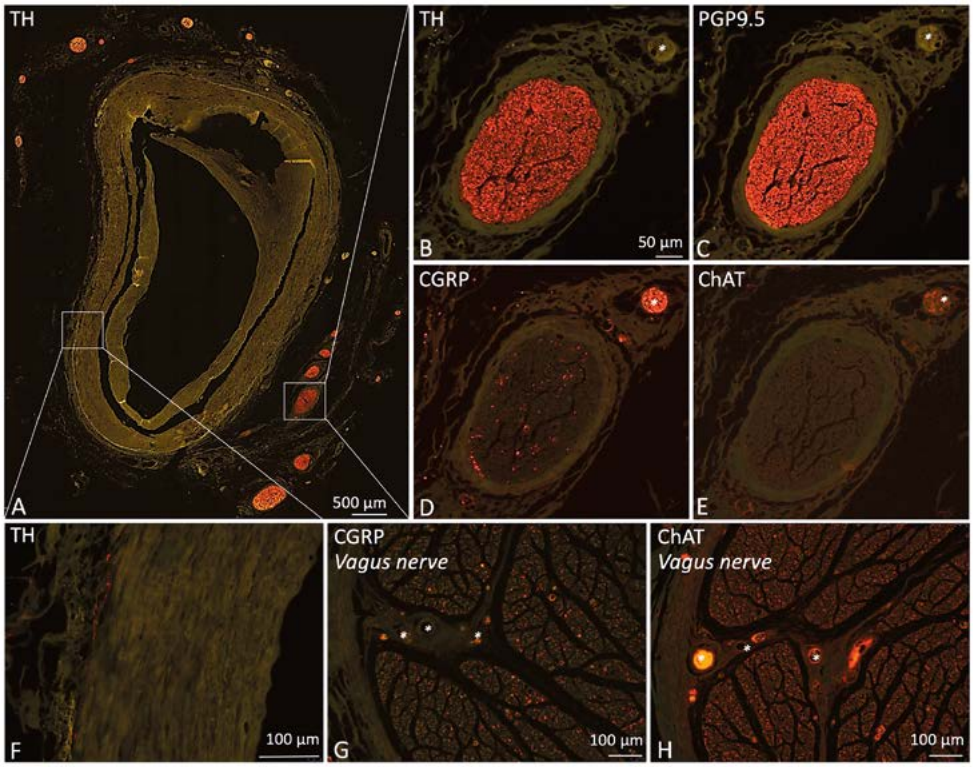


**Figure 3. Microscopic images of SA loop related splenic plexus stained with various nerve markers. A:** Overview image of a SA loop cross section stained with TH, showing the organisation of sympathetic nerves of the splenic plexus. **B-E:** Higher magnifications of an individual nerve stained for TH, PGP, CGRP and ChAT. PGP9.5 and TH-IR patterns are comparable, suggesting the splenic plexus to predominantly be composed of sympathetic nerve fibers. Only a few fibers are stained with CGRP and even less with ChAT, suggesting little sensory and parasympathetic nerve fibers, respectively. CGRP and ChAT-IR was also observed inside blood vessels (asterisk in D, E, G and H) and ChAT-IR was observed in blood vessel walls. **F-H:** Positive controls.

# DISCUSSION

This study shows that one or multiple SA loops are present in the majority of studied subjects and the splenic plexus surrounding these loops contains a substantial amount of predominantly sympathetic nerve tissue.

## Presence, number and location of loops

In the present study, loops were defined as segments of the SA extending away from the pancreas, with a distance of 1 cm or more between the inner curve of the loop and the surface of the pancreas. SA loops were present in 80% (five out of six) of the studied specimens. The occurrence of SA loops was observed in a greater number of cases than reported in two other studies. In the study by Michels (Michels,1942), the SA was found to be straight in 15%, slightly curved in 45% and looped or coiled in

40% of the studied patients. Coiling of the SA was observed in an even lower number of subjects in the study by Sahni et al. ( Sahni et al., 2003) where SA tortuosity was observed in only 10%.

Age related lengthening and widening of the SA is suggested as a cause for the development of loops in older subjects (Michels, 1942)(Sahni et al., 2003). The age of the specimens of the present study was higher than in the other studies (71-100 years versus 18-80 years, respectively) and might have contributed to the finding of splenic artery loops in a greater proportion of patients. Another possible explanation for the variance between the present - and other studies is the lack of a precise definition for tortuosity, coiling or looping, resulting in variable interpretation of these parameters. Given this variability in the ages of subjects studied and the definitions used to define arterial loops, a larger sample of subjects is required to more fully address the contribution of age-related differences in the prevalence of splenic artery loops. Given the wide spread use of cross-sectional radiographical imaging in medical practice this would seem a means to further assess this question *in-vivo*.

A number of potential etiologies for SA tortuosity have been suggested. These reasons were reviewed by Michels (Michels,1942) and included 1) movement and volumetric changes in the spleen require the artery to stretch, 2) tortuosity provides a damping system protecting splenic architecture, 3) tortuosity occurs during growth of the SA while it is tethered to the pancreas by its pancreatic branches, 4) tortuosity represents a developmental peculiarity which is genetically determined and 5) tortuosity is a disease condition associated with atheroma. Little progress on our understanding on tortuosity occurrence has been made since then and so far only the last one has been ruled out as no relationship with the presence of atheroma was observed (Sylvester et al., 1999). The results of our study argue against the hypothesis that tortuosity results from the elongation of the splenic artery between points where the SA is fixed in place by the tethering effects of PAs, with no PAs being expected to arise from with the SA loops. In our study, however, PAs were observed to originate within three out of eight SA loops and prior to SA loop intervention their presence should be carefully evaluated in order to avoid PA damage. This also applies for SGAs and the LGEA, which were observed to originate from five out of eight and two out of eight SA loops, respectively.

The SA can be divided in three segments; the prepancreatic – pancreatic and postpancreatic or perihilar segment, running between the origin of the SA and the neck of the pancreas, along the upper border of the neck and body of the pancreas and in the splenorenal ligament, respectively (Sahni et al., 2003). All SA loops observed in the present study were located at the pancreatic segment of the SA, which is consistent with earlier observations (Michels, 1942) (Pandey et al., 2004).

## Surgical accessibility of the loops

All loops were covered with adipose and loose connective tissue, and a firm irregular network of white fibrous strands, representing nerves as confirmed by histological examination. During dissections one could easily discriminate between the SA loops and the surrounding adipose, connective and nerve tissue based on their appearance and difference in mechanical and tactile properties.

Adipose tissue is yellowish and homogenous. Connective tissue is whitish, and composed of randomly organized loose fibers. Nerve plexus tissue is whitish and composed of moderate nerves, arranged in an irregular perivascular network wherein these nerves took an overall longitudinal course parallel with the SA. In only two loops were nerves observed to take a somewhat different route away from the periadventitial plexus (Figure 2A-B). These were incidental findings and were not associated with a loss of perivascular plexus, thus since they do not interfere with surgical procedures or neuroelectrode implantation on the SA loop limbs, no further attention was payed to these structures.

Nerves of the splenic plexus, which are covered by a firm perineurium, remained structurally intact and maintained their perivascular location, during arterial manipulations as part of dissection activities. In addition, these nerves are part of an irregular perivascular network which is firmly attached to the vessel wall at various locations. It was noted that when the nerves are pulled, tension is transferred to the plexus, and subsequently to the vessel wall. This results in shifting the position of the entire neurovascular bundle. This observation may be of value when the dissection is performed with laparoscopic instruments, where tactile input from the dissection instruments is reduced as compared to dissection using open techniques. While this observation has been replicated in the cadaver lab using laparoscopic dissection on fresh frozen cadavers [personal communication Irwin E.], the more formal characterization of the effects of reduced tactile input during the dissection will require further investigation. In addition, it should be noted that tissue characteristics of embalmed cadavers differ from living individuals and the ease at which the SA and its nerve plexus are dissected from its surrounding structures might differ as well. Fresh frozen cadavers represent more lifelike tissue characteristics and were used to compare these parameters. No noteworthy differences were observed [personal communication Irwin E.].

SA loops provide a space between loop limbs and the pancreas. This allows introduction of surgical instruments for the purpose of exposing the site for intervention, and, for application and stabilization of the neural interface. While these data inform the investigators involved in development of surgical techniques, further validation is required. Additional correlative radiographic and anatomical studies are in progress to meet this need. These studies will use radiographic imaging and anatomic dissections, with histological evaluation, to replicate and validate these gross anatomic findings.

## Amount, type and organization of nerve tissue

During dissection, perivascular white strands remained in close proximity to the wall of the loops and appeared adherent to the SA throughout the curving of the loops. These strands represent nerves of the splenic plexus as was shown by microscopic investigation of PGP9.5 stained tissue slides of SA loops. Furthermore, microscopic assessment showed these nerves to be composed of predominantly TH-IR nerve fibers, suggesting a sympathetic nature, thereby supporting previous anatomical studies (Klein et al., 1982)(Nance and Burns, 1989). Evaluation of CGRP and ChAT stained tissue slides showed minor and doubtful IR for these antibodies, respectively. CGRP-IR was observed

as small dots in nerves in all specimens and its appearance morphologically consistent with nerve fibers, suggesting sensory nerve fiber presence. However, most of the staining was observed inside small blood vessels which, based on their spherical shape and their known CGRP production and secretion most likely presented lymphocytes (Wang et al., 2002).

The contribution of the of CGRP-IR tissue in splenic plexus nerves was determined for SA loops of three different cadavers and varied from 0.64-1.92% of the total amount of nerve tissue. These low numbers were considered negligible, especially since the main source was non-neural tissue. Minor ChAT-IR areas were observed in nerve tissue of the splenic plexus. However, their morphological appearance did not clearly match nerve fibers, but instead more closely resembled cellular structures. Furthermore, ChAT-IR was observed in blood vessel walls and in connective tissue compartments. ChAT appears to be an enzyme that is not only produced in cholinergic nerve tissue, but also in smooth muscle, endothelial and epithelial cells, and T lymphocytes (Ratcliffe et al., 1989). Additionally, this enzyme appears to be present in extracellular fluids such as plasma and CSF (Vijayaraghavan et al., 2013). Altogether, this may explain the seemingly nonspecific ChAT-IR.

Although the spleen itself is considered to lack parasympathetic and sensory innervation (Nance and Burns 1989; Bellinger et al., 1993)(Nance and Burns 1989)(Nance and Burns 1989)(Nance and Burns 1989)(Nance and Burns 1989)(Nance and Burns 1989)(Nance and Burns 1989)(Nance and Burns 1989)(Nance and Burns 1989), the stomach and pancreas receive sensory and parasympathetic fibers (Kuntz, 1953)(Lundberg et al., 2017) which might pass through the splenic plexus, explaining their presence in SA loop samples. To determine whether the observed sensory fibers innervate the spleen, stomach, greater omentum or pancreas, the perivascular plexus surrounding their corresponding supplying arteries is an interesting subject for future studies. Although the splenic plexus continues around SA branches towards the stomach and the greater omentum via SGAs and the LGEA, and towards the pancreas via PAs, animal studies have been performed in rodents and so far, no obvious off-target effects have been observed (Guyot et al., 2019). Future studies in large animals and humans may provide additional information on effects on other nerves.

## Neuroelectrode interface development

The nerves of the splenic plexus, as found in the present study, are predominantly composed of sympathetic nerve fibers. These fibers are reported to originate from the celiac ganglion and are considered to represent postganglionic unmyelinated fibers (Mitchel, 1956). The homogenous composition of nerve fibers in the nerves of the splenic plexus is favorable since less heterogeneity in electrophysiological characteristics of the various nerve fiber types is anticipated. The other parameters, such as the number of nerves, their amount of sympathetic nerve tissue, and their distance to the outer connective tissue lining of the neurovascular bundle, provide information for neuroelectrode interface development and stimulation settings. No studies which address these parameters could be found and no correlation between anatomy and function have been

established. Experimental stimulation studies might provide comparative data which helps to estimate this correlation and to select therapeutic parameters that are appropriate for use in future studies in humans. Macroscopically, the splenic plexus showed the appearance of an irregular network, wrapping the SA, without clear preferential topographical orientation with respect to the dorsal, ventral, cranial or caudal sides of the vessel wall. Topographical orientation of the SA samples was not retained during tissue sampling and therefore these subjective observations could not be confirmed. Therefore, a circumferential neuroelectrode interface would address this until further studies show a preferential distribution. The median diameter of the neurovascular bundle of the SA loop limbs was determined and electrodes should be optimized to fit this dimension.

### Limitations of the study

This study was limited to six specimens of older age and no discrimination was made between sexes. This limited data did not allow for thorough statistical analysis and therefore this study should be considered as exploratory study to characterize the feasibility of SA loops as stimulation sites for electrical SPS in humans.

## CONCLUSION

SA loops and their surrounding splenic plexus could represent suitable electrical stimulation sites in the context of anti-inflammatory therapy in humans. One or multiple SA loops are present in the majority of the studied subjects, their neurovascular bundle can be easily freed from surrounding connective and adipose tissues, and, dimensions with respect to loop height and width, provide sufficient space for introduction of surgical instruments and electrode placement. Furthermore, their surrounding splenic plexus contains a substantial amount of predominantly sympathetic nerve tissue, the target tissue for anti-inflammatory interventions. These data provide support for further development of SPS in humans.

# 3

# A COMPARATIVE ANATOMICAL AND HISTOLOGICAL STUDY ON THE EXISTENCE OF AN APICAL SPLENIC NERVE IN MICE AND HUMANS

Cindy G.J. Cleypool [1], Claire Mackaaij[1],
Suzanne A.M.W. Verlinde-Schellekens[1], Ronald L.A.W. Bleys[1]

[1]Department of Anatomy, Division of Surgical Specialties, University Medical Center Utrecht, Utrecht University, the Netherlands.

*Journal of Anatomy. 2021*

# ABSTRACT

## Introduction

The cranial pole of the mouse spleen is considered to be parasympathetically innervated by a macroscopic observable nerve referred to as apical splenic nerve (ASN). Electrical stimulation of the ASN resulted in increased levels of splenic acetylcholine, decreased lipopolysaccharide induced levels of systemic tumor necrosis factor alpha and mitigated clinical symptoms in a mouse model of rheumatoid arthritis. If such a discrete ASN would be present in humans, this structure is of interest as it might represent a relatively easily accessible electrical stimulation target to treat immune mediated inflammatory diseases. So far it is unknown if a human ASN equivalent exists. This study aimed to explore the existence of an equivalent structure in humans.

## Materials & methods

Six mice and six human cadavers were used to study and compare the ASN, both macro- and microscopically. Macroscopic morphological characteristics of the ASN in both mice and humans were described and photographs were taken. ASN samples were resected, embedded in paraffin, cut in 5 µm thin sections where after adjacent sections were stained with a general, sympathetic and parasympathetic nerve marker, respectively. Neural identity and nerve fiber composition was then evaluated microscopically.

## Results

Macroscopically, the ASN could be clearly identified in all mice and was running in the phrenicosplenic ligament connecting the diaphragm and apical pole of the spleen. If a phrenicosplenic ligament was present in humans, a similar configuration of potential neural structures was observed. Since the gastrosplenic ligament was a continuation of the phrenicosplenic ligament, this ligament was explored as well and contained white, potential discrete nerve like structures as well which could represent an ANS equivalent. Microscopic evaluation of the ASN in mice and human showed that this structure did not represent a nerve, but most likely connective tissue strains.

## Conclusion

White nerve like structures were macroscopically observed in the phrenicosplenic ligament in both mice and human and in the gastrosplenic ligament in humans which could represent the ASN. Microscopic investigation did not confirm a neural identity and therefore this study disclaims the existence of a parasympathetic ASN in both mice and human.

# INTRODUCTION

Splenic sympathetic nerves might represent a novel therapeutic target, as electrical stimulation of these nerves has shown to have beneficial anti-inflammatory effects in rodents (Vida et al., 2011) (Kees et al., 2003)(Komega et al., 2018). Upon stimulation, norepinephrine (NE) is released from these sympathetic nerves followed by b2 adrenergic receptor activation on splenic CD4 positive T cells (Vida et al., 2017)(Rosas-Ballina et al., 2011)(Vida et al., 2011). These activated T cells produce and secrete acetylcholine (Ach) which ultimately inhibits the release of pro-inflammatory cytokines from activated macrophages through a7-nicotinic acetylcholine receptor signalling (Lu and Kwan, 2014)(Borovikova et al., 2000)(de Jonge et al., 2005)(Kox et al., 2009). In addition to these sympathetic nerves, which run with the splenic artery, tracer studies in rats suggest the spleen is supplied by parasympathetic nerves as well (Buijs et al., 2008). These parasympathetic nerves were thought to enter the spleen at its poles as dissection of polar parts of the gastro splenic ligament abolished the presence of retrograde tracer in the dorsal motor nucleus (Buijs et al., 2008). The presence of such a parasympathetic nerve was confirmed in mice where a discrete nerve was macroscopically observed entering the spleen at its cranial pole (Guyot et al., 2019). This nerve, by the authors referred to as the apical splenic nerve (ASN), contains primarily parasympathetic fibers and electrical stimulation of this nerve resulted in increased levels of splenic acetylcholine (Ach), decreased lipopolysaccharide (LPS) induced levels of systemic tumor necrosis factor alpha and mitigated clinical symptoms in a mouse model of rheumatoid arthritis (Guyot et al., 2019). If such a discrete ASN would be present in humans, this structure could hold potential as a relatively easily accessible electrical stimulation target to treat immune mediated inflammatory diseases. So far, the literature does not mention a discrete, macroscopic observable nerve entering the cranial pole of the human spleen. In order to investigate the existence of the ASN in humans, this study first aimed to macroscopically identify this nerve in mice and to describe its location and course. This information was then used for guided exploration of an equivalent structure in humans. Microscopic techniques were additionally used to study ASN nerve identity and composition.

# MATERIALS & METHODS

## Tissue resection

### *Mice*

Fixed surplus cadavers of six 13 weeks old C57BL/6J male mice were used. The use of surplus cadaveric tissues did not require ethics committee approval. These mice were used for another experiment wherein they were anaesthetized with isoflurane and fixation was performed by means of transcardial perfusion with 2.5 ml of 4% paraformaldehyde (PFA). The right atrium was opened to drain excessive fluid. The abdomens were opened and the cadavers were additionally fixed *in toto* by immersion in 4% PFA for 24 hours. After fixation, the cadavers were stored at 4°C in a 0.1 M phosphate buffer, pH 7.4, containing 15% sucrose (PBS/Sucrose) until further investigation. Further dissections were performed

macroscopically and by using a stereomicroscope with both transmission and incident light (Leica EZ4, Nussloch, Germany). The left halve of the liver was removed to get better access to the left upper abdominal quadrant containing the spleen, stomach and left sided part of the diaphragm. While lifting the spleen and pulling it slightly downwards, the ASN became visible (Figure 1A). The stomach and spleen were positioned with needles securing a clear view of all relevant structures. After recording the course of the ASN *in situ,* the stomach, spleen, diaphragm and their connecting ligaments were removed *en block,* placed on a green transparent glass plate and studied with transmission light allowing better visualization of various structures (Figure 1B). Hereafter, the tip of the spleen, its suspending ligaments and the ASN were removed and stained *in toto* with haematoxylin according to a procedure previously described (B Schurink, Cleypool, and Bleys 2019) (Figure 1D). This staining provided better recognition of the ASN and the ligaments, and allowed complete trimming of these ligaments (Figure 1E). The tip of all spleens with its associated ASN were placed on 70% ethanol and further processed for microscopic evaluation. Vagus nerves, which show comparable macroscopic dimensions as the ASN and contain parasympathetic fibers were resected as well and used as controls.

### *Humans*

Seven human cadavers were provided for this study: four female and three male cadavers with a median age of 93 years at death (interquartile range: 79-98). All bodies entered the Anatomy department of the University Medical Centre Utrecht, the Netherlands, through a body donation program. Informed consent was obtained during life, allowing the use of these bodies for educational and research purposes. Whole body preservation was accomplished by arterial perfusion of approximately 10 liters of 3% PFA via the femoral artery. The abdomens were opened, the left halves of the livers were removed and the spleen, stomach, diaphragm and suspending splenic ligaments, being the phrenicosplenic ligament (PSL) and gastrosplenic ligament (GSL), were identified. The presence of ASN-like structures was recorded. In order to further microscopically assess the neural identity of observed ASN-like structures, the PSLs, which is the ligament containing the ASN in mice (as shown in the current study) was isolated as a whole. In humans the PSL was only present in 2/6 cadavers and since the GSL is a caudal continuation of the PSL, it was decided to additionally study the GSL as well. The GSL was sampled at three different locations; at the cranial border of the ligament (or at the border of the GSL with the PSL if a PSL was present) and at locations that showed clear white fibrous strands, which could potentially represent nerves. In addition, one spleen and its associated PSL and GSL was isolated as a whole, allowing microscopic evaluation of these ligaments *in toto* in case discrete neural structures were missed out in the resected parts. All samples were placed on 70% ethanol and further prepared for microscopic evaluation as following.

## Tissue sample preparation for microscopic investigation

All samples were processed for paraffin embedding by placing them in increasing percentages of ethanol, xylene and paraffin. Tissues were then embedded in paraffin in such way that the cutting plane would be perpendicular to the course of presumably neural structures. All resected nerves, spleens (both mice) and ligaments (humans) were cut in 5 µm thick sections on a microtome (Leica

2050 Super Cut, Nussloch, Germany) whereas the human ligament *in toto* was cut in 10 µm thick sections on a microtome (Leica Tetrander, Nussloch, Germany). All sections were placed on glass slides, air dried and subsequently heat fixed for two hours on a slide drying table of 60°C (Medax, 14801, Kiel, Germany). Mouse ASN and spleen slides (the latter containing a substantial amount of hilar and parenchymal tissue) were single stained with antibodies raised against protein gene product 9.5 (PGP9.5) and tubulin III (Tub III) to identify neural structures in general, and antibodies against tyrosine hydroxylase (TH) and choline acetyl transferase (ChAT), to analyse whether neural structures were composed of sympathetic or parasympathetic nerve fibers, respectively. Human splenic ligament slides (both PSL and GSL) were stained with PGP9.5 to verify the neural identity of the macroscopically observed ASN-like structures. Details on all immune histochemical staining procedures can be found in the following paragraph.

### *Immunohistochemical staining (TubIII, ChAT, TH)*

All slides were deparaffinized and rehydrated followed by 20 minutes of antigen retrieval in 95°C citrate buffer on a hot plate. After washing in Tris-buffered saline (TBS) with 0.05% tween (TBS/Tween), mice and human sections were pre-incubated for 10 minutes with 5% normal mouse or human serum, respectively. After preincubation, sections were incubated with primary antibodies in TBS with 3% bovine serum albumin (see table 1 for technical details). Following incubation, sections were washed with TBS/Tween and incubated for 30 minutes at room temperature (RT) with secondary antibodies being undiluted Brightvision Poly-Alkaline phosphatase (see table 1 for specific details) After incubation, all sections were washed with TBS and incubated with Liquid Permanent Red (LPR) (DAKO, Glostrup, Denmark) for 10 minutes. Subsequently, tissue sections were washed with distilled water and counterstained with haematoxylin, airdried at 60°C for 90 minutes, and cover slipped using Entellan (Merck, Darmstadt, Germany). Mouse spleen and vagus nerve sections of the same mice were used as positive controls whereas for human samples, intrinsic paravascular nerves served as positive controls. Negative controls were obtained by incubation of both mice and human slides with TBS-3% BSA without primary antibody. All slides were evaluated using bright field microscopy.

## Image acquisition

Macroscopic images and more detailed images of dissections (through a stereomicroscope) were obtained using a smart phone camera (Samsung S9, Seoul, South Korea). Brightfield microscopic single and stitched overview images were captured at various magnifications using a DM6 microscope with a motorized scanning stage, a DFC7000 T camera and LASX software (all from Leica, Nussloch, Germany).

| | Host + Clone | Vendor | Order # | Dilution, incubation time and temperature |
|---|---|---|---|---|
| TH | Rabbit Polyclonal | PelFreez (Rogers, USA) | P40101 | 1:400, o.n., RT |
| PGP9.5 | Rabbit Polyclonal | Dako (Glostrup, Denmark) | Z5116 | 1:2000, 48 hours, 4ºC |
| ChAT | Goat polyclonal | Millipore (Burlington, USA) | AB144P | 1:50, o.n., 4°C |
| TubIII | Mouse mono IgG2a | R&D systems (Minneapolis, USA) | MAB1195 | 1:10.000, 60 min, RT |

**Table 1.** Technical specifications of used antibodies

# RESULTS

## Macroscopic observations

### *Mice*

All mice showed a whitish neural plexus like structure in the left upper quadrant of the abdomen cranial to the spleen and stomach, interconnecting the spleen, stomach and the diaphragm (Figure 1A). The relevant tissues (stomach, spleen, diaphragm and their interlinking ligaments with its neural plexus like structures) were removed *en block* and placed on a dark green glass plate and studied under the stereomicroscope using only transmission light. This allowed for better determination of all relevant structures (Figure 1B). Three separate white strands could be distinguished in the plexus-like structure. The first strand was connecting the cranial pole of the spleen with the connective tissue of the central tendon of the diaphragm (Figure 1B structure a). From the same location at the diaphragm, a similar structure, which partly runs parallel with structure (a), could be observed running towards the fundus of the stomach (Figure 1B structure b). A third strand was observed running between the stomach and the cranial pole of the spleen (Figure 1B structure c). The spleen is attached to the stomach and diaphragm by various ligaments, which were composed of a double sheet of peritoneum. These ligaments were very thin and difficult to observe both macro - and stereomicroscopically. Only if the incident light of the stereomicroscope hit the ligaments from the right angle, these ligaments became shiny and recognizable. The splenorenal ligament attached the spleen to the dorsal body wall and contained the splenic artery with its terminal branches. The GSL is positioned ventrally with respect to the splenorenal ligament and connected the spleen to the stomach and contained a short gastric artery and structure c (Figure 1B). The PSL connected the spleen to the diaphragm and contained structure a and the final part of structure c (Figure 1B), which together formed the presumably ASN.

### *Humans*

In contrast to the mouse, in humans the suspending splenic ligaments are much thicker and therefore clearly recognisable. Since the ASN, as shown in mice, was positioned within the PSL,

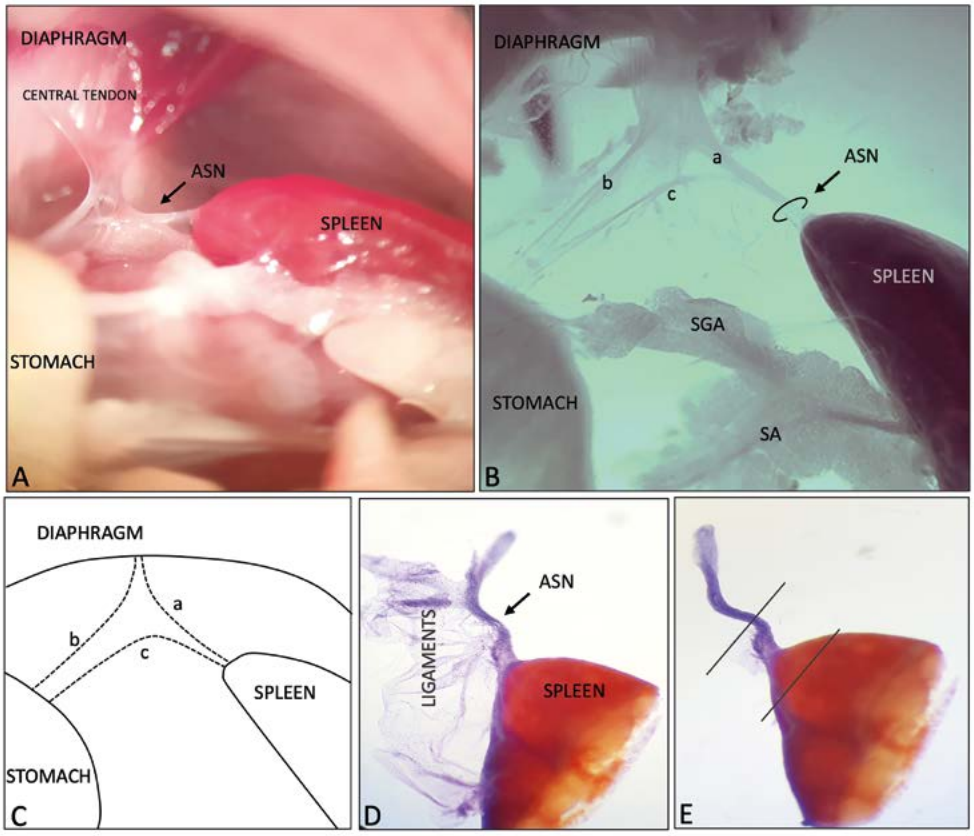


**Figure 1. Apical splenic nerve in mice. A:** Ventral view on the upper left quadrant of the abdominal cavity with the spleen, diaphragm, stomach and connecting splenic ligaments *in situ*. **B:** Ventral view on an isolated spleen, stomach, diaphragm and their connecting ligaments. White fibrous strands can be observed in the phrenicosplenic -, gastrophrenic -, and gastrosplenic ligaments (structures a, b and c respectively). **C:** Schematic representation of the various observed white fibrous strands. **D:** Hematoxylin-stained sample of the cranial tip of the spleen including some of its ligaments and the apical splenic nerve. **E:** The same sample as shown in D. Trimming of the ligaments was performed to ensure microscopic slides to contain the apical splenic nerve only. Black lines illustrate the location of the apical splenic nerve and spleen slides as obtained from each mouse.

the latter was explored for the presence of discrete macroscopically visible nerves in humans. In 2/6 cadavers a PSL was present. This ligament was observed running from the diaphragm to the cranial tip of the spleen (Figure 2AB) and contained white fibrous strands which ran from the central tendon of the diaphragm to the tip of the spleen (Figure 2AE). A clearly observable GSL was present in all cadavers and connected the fundus and part of the greater curvature of the stomach to the spleen. Comparable to the greater omentum in humans, the GSL contains a significant amount of adipose tissue making it difficult to distinguish discrete structures. However, when stretched, white strands could be observed running from the surface of the stomach to the hilum of the spleen (Figure 2D).

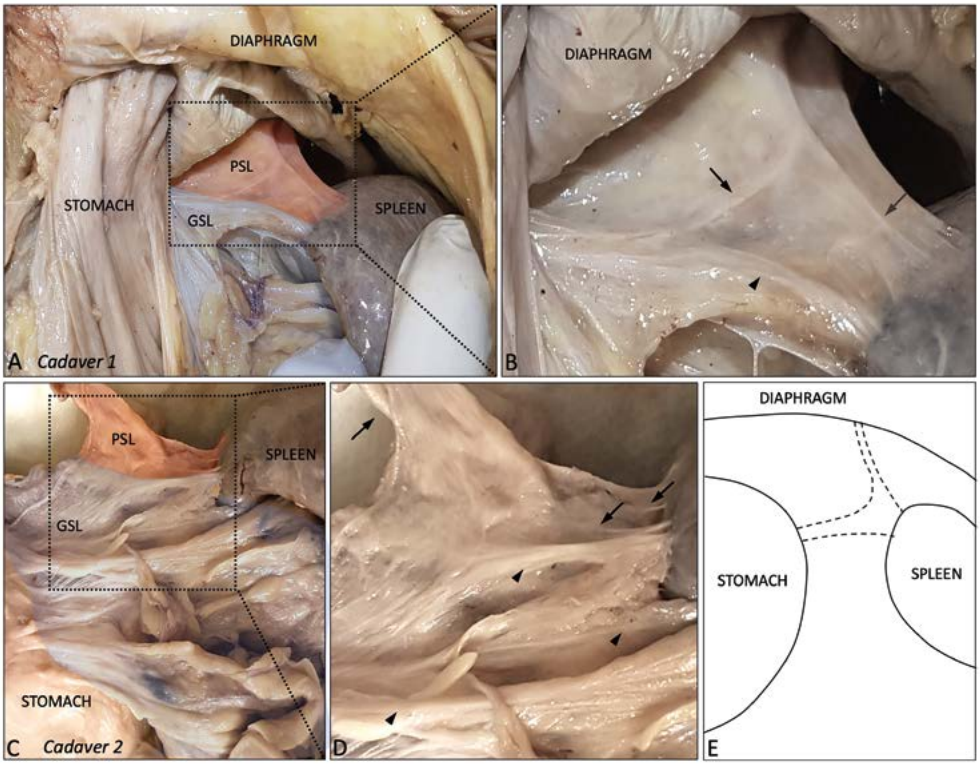


**Figure 2. Apical splenic nerve-like structures in humans. A:** Ventral view on the upper left quadrant of the abdominal cavity of cadaver 1. The spleen, diaphragm, stomach and connecting ligaments can be observed *in situ*. **B:** Close up of the ligaments of Figure A, showing white fibrous strands which might represent equivalent structures to the once observed in mice (Figure 1B). **C:** Ventral view on the upper left quadrant of the abdominal cavity of cadaver 2. **D:** Close up of the ligaments of Figure A, showing white fibrous strands which might represent equivalent structures to the once observed in mice (Figure 1B). **E:** Schematic representation of the various observed white fibrous strands. **Arrows:** white strand like structures running between the diaphragm and the spleen and fundus of the stomach. **Arrow heads:** white nerve-like structures running between the stomach and the spleen.

## Microscopic observations

### *Mice*

All ASNs were composed of a homogenous tissue mass, enclosed by a covering mesothelium (Figure 3AD). None of the ASNs showed immunoreactivity (IR) for the general nerve markers PGP9.5 and TubIII (Fig. 3AB) nor for the sympathetic nerve marker TH (Figure 3C). ChAT staining of the ASN showed a homogenous light pink staining comparable to the aspecific general background staining as observed in e.g. adipose and connective tissue (Figure 3DLP).

All neural controls showed the following expected staining patterns. The splenic hilum contained a SA with peri and paravascular nerves (Figure IJ) which were predominantly sympathetic of nature

(Figure 3K). In the splenic parenchyma, fine sympathetic nerves were observed to run with vascular structures and occasionally branched off and travelled further into the parenchyma (Figure 3M-O). The vagus nerve showed clear staining for both general nerve markers and was composed of a few sympathetic and a significant amount of parasympathetic nerve fibers (Figure 3E-H). Furthermore, strong ChAT-IR was observed in cellular structures that were primarily present in the splenic red pulp and which occasionally interspersed the white pulp (Figure 3P).

### *Humans*

A few small discrete nerves were observed in the connective tissue of both the PSLs and GSLs (Figure 4), but never represented dimensions complying with the macroscopically observed ASN-like structures shown in Figure 2B. Furthermore, moderate sized nerves were observed in association with the short gastric arteries (SGA) (Figure 4D-F). Again, these nerves these could not be observed by the naked eye and could not represent macroscopically observable ASN-like structures as shown in Figure 2D.

## DISCUSSION

Although the presence of noradrenergic nerves in the spleen in various species is well established (Bellinger et al., 1987)(Bellinger et al., 1992) (Murray et al., 2017)(Hoover et al., 2017)(Verlinden et al., 2018), the presence of cholinergic nerves is still under debate. Various studies disclaim the existence of splenic parasympathetic innervation (Bellinger et al., 1993)(Cano et al., 2001)(Hoover et al., 2017) (Verlinden et al., 2018), whereas other reported opposite observations (Buijs et al., 2008)(Gautron et al., 2013). With the recent discovery of the ASN, a macroscopic observable nerve of cholinergic nature as shown by immune histochemical staining and electrical stimulation, this debate might have come to an end. However, the current study shows that the structure that is referred to as the ASN in mice, is mainly composed of connective tissue and does not represent a macroscopic observable nerve. This significant discrepancy could be explained by inaccurate inclusion of non-ASN tissue in the current study. This however seems unlikely as prior to resection of the presumably ASN, the location, appearance and course of what was considered to represent this structure was confirmed via personal communication with the corresponding author of the study of Guyot et al (Guyot et al., 2019). Furthermore, by applying whole mount hematoxylin staining (Figure 1DE), all irrelevant structures were trimmed in order to avoid obscurity of the results. Secondly, it was questioned whether the immunohistochemical staining results of the current study were erroneous. To make sure that the observations were trustworthy, several tissues with known noradrenergic and cholinergic neural staining patterns were included as controls and included the vagus nerve and hilar and parenchymal splenic tissue. All controls showed expected staining patterns, confirming staining accuracy for general, sympathetic and cholinergic nerve markers. It was however noticed, that in addition to nerve fibers as observed in the vagus nerve, ChAT antibodies showed strong IR in various non-neuronal structures such as red pulp associated immune cells, blood vessel content and adipocytes, and, showed light IR in connective tissue rich structures such as the capsule, trabeculae

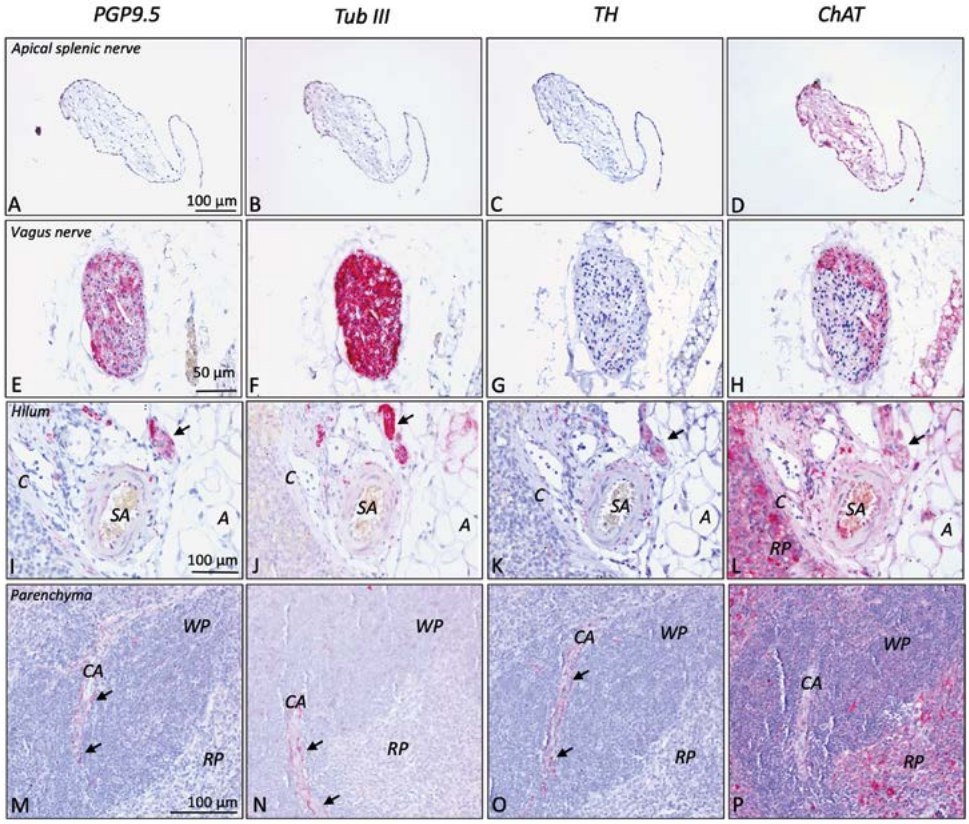


**Figure 3. Microscopic images of the apical splenic nerve in mice stained with various nerve markers.** The apical splenic nerve and various control tissues were stained with general nerve markers (PGP9.5 and TubIII) and a sympathetic (TH) and parasympathetic nerve marker (ChAT), all visualized by a pink chromogen. **A-D:** Apical splenic nerve. Based on the absence of staining with general nerve markers it can be concluded that the ASN does not contain nerve fibers. ChAT staining results are doubtful, but based on staining patterns in the control tissues it can be concluded that this marker shows strong immune reactivity (IR) with non-neuronal tissues (immune cells) and weak IR for a few other tissues such as connective tissue and smooth muscle cells (vessel walls, capsule). **E-H:** Vagus nerve. The vagus nerve is composed of a few sympathetic (TH-IR) nerve fibers, a substantial amount of parasympathetic (ChAT-IR) fibers. The fibers that remain most likely represent afferent fibers. **I-L:** Splenic hilum. At the splenic hilum, splenic artery branches enter the spleen. These arteries are accompanied by sympathetic (TH-IR) nerves. A significant number of ChAT-IR cells are present in the spleen. These cells predominantly reside in the red pulp, but can be observed inside blood vessels and in between the connective tissue of the hilum. **M-P:** Splenic parenchyma. Sympathetic (TH-IR) nerves run with arteries deeper into the splenic parenchyma. A significant number of ChAT-IR cells are present in the spleen. These cells predominantly reside in the red pulp. ***A:*** *Adipocytes.* ***CA:*** *Central artery*. ***RP:*** *Red pulp*. ***SA:*** *Splenic artery.* ***WP:*** *White pulp*. ***Arrow:*** *Nerve.*

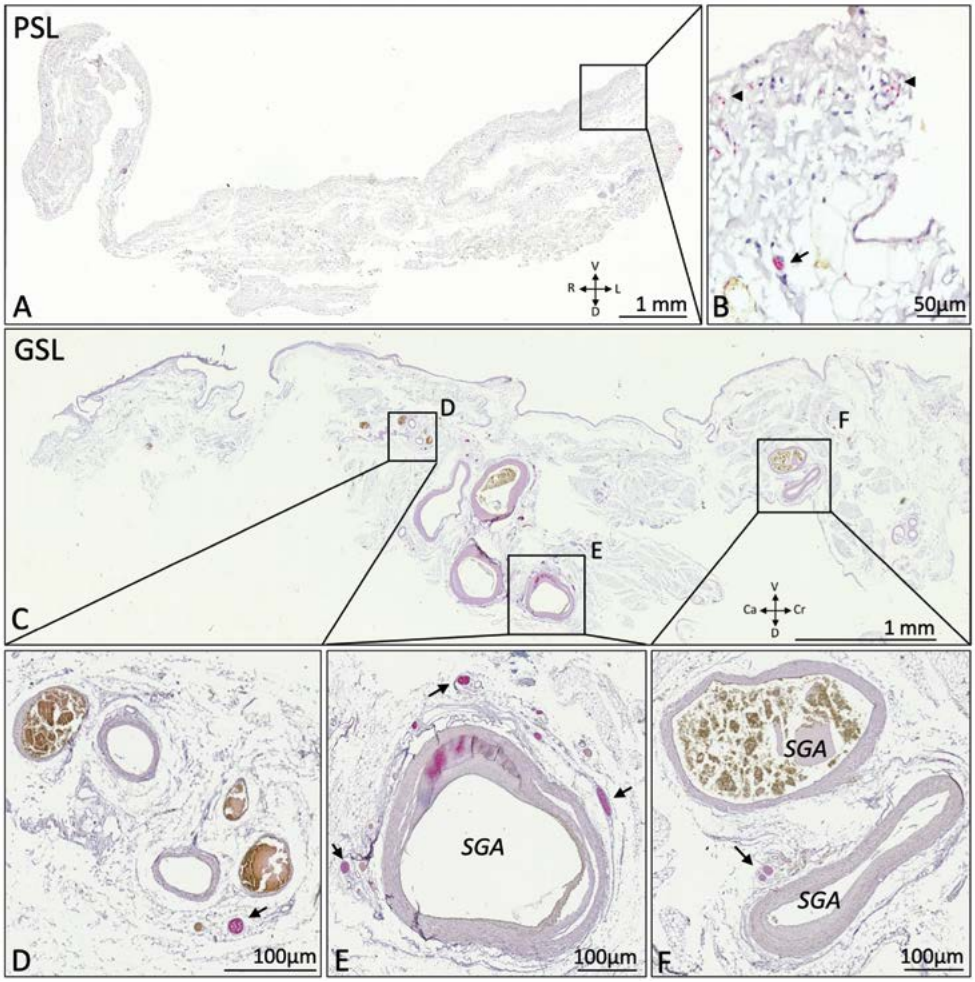


**Figure 4. Microscopic images of splenic ligaments with observed apical splenic nerve-like structures in humans.** Both ligaments are stained with a general nerve marker (PGP9.5) which is visualized by a pink chromogen. **A-B:** Overview image of one of the two phrenicosplenic ligaments (PSL). The ligament is primarily composed of connective tissue with scattered small blood vessels and fine nerves. If nerve bundles were present, these were sparse and small and did not represent the macroscopic observed nerve-like structures as presented in Figure 2B. **C-F:** Overview image of the *in toto* studied gastrosplenic ligament (GSL). Various short gastric arteries and smaller vascular structures can be observed (some blood vessels are filled with blood which has a brownish appearance in these slides). Comparable to the PSL, the GSL was composed of connective tissue. Scattered throughout the ligament fine nerves could be observed (the relatively low magnifications do not allow to observe these). Surrounding the short gastric arteries (SGA), various paravascular nerve bundles can be observed. These, however, do not represent the macroscopic observed nerve-like structures as presented in Figure 2D.

and vessel walls. These non-neuronal and a specific ChAT-IR patterns might explain the observations in ChAT stained ASN slides of Guyot et al. (Guyot et al., 2019). Furthermore, light sheet images of this author did not convincingly show a discrete ChAT-IR nerve at the tip of the spleen and in general ChAT-IR was observed in a fragmented pattern, which is not suggestive for nerves. The fragmented pattern was observed at various locations in the light sheet imaged spleen and might be better explained as ChAT-IR immune cells, since these are largely present as shown in splenic parenchyma slides of the current study.

Thus, from an anatomical point of view the results of the current study cast doubt on the existence of an ASN. However, from a functional point of view, the "ASN" (from now on placed between quotation marks due to its doubtful existence), does represent an interesting structure as electrical stimulation of this structure resulted in increased levels of splenic NE and Ach, whereas stimulation of splenic artery associated nerves resulted in splenic NE increase only. Now that the neural identity of the "ASN" is in doubt and this increase in splenic neurotransmitters could not be attributed to its nerve fibers, could these observations be explained otherwise? Leakage of electrical current could hypothetically result in stimulation of splenic artery associated sympathetic nerves and hence explain the increase of splenic NE levels. The source of non-neuronal Ach could then be explained by subsequent activation of CD4+ T cells. However, Guyot et al (Guyot et al., 2019), showed that this increase of Ach levels was independent to both T cells and adrenergic signaling. These observations lead the authors to conclude that Ach could only be derived from the cholinergic fibers of the ASN, thereby strengthening the assumption of its existence. However ChAT expression has been observed in other immune cells such as B cells (Gautron et al., 2013), dendritic cells and macrophages (Fujii et al., 2017). ChAT-IR cells in the spleen are not a rare entity, but moreover represented a large cell population in normal spleens, as can be observed in the splenic parenchymal control samples of the current study. Moreover, a significant portion of these ChAT-IR cells did not display a typical lymphocyte morphology or overlapping distribution patterns with T cells (unpublished data, Cleypool), supporting the presence of a significant number of alternative cellular Ach sources. Could the "ASN" transmit electrical current towards the spleen, and moreover, directly activate these alternative Ach sources? The current study showed that the "ASN" in mice was composed of homogenous connective tissue positioned between two layers of mesothelium, together constituting the PSL. It is known, that if physiological forces are applied to connective tissue, collagen fibrils will align into orientated bundles (Kalson et al., 2013), a process which might have occurred in the PSL and explain the presence of discrete white fibrous strands, including the "ASN" (Figure 1). Collagen fibrils show electrical conductivity (Bardelmeyer 1973) and "ASN" stimulation might result in transmission of electrical signals to e.g. the splenic capsule. If and how electrical signals could then be further transmitted to e.g. cholinergic B cells, macrophages or dendritic cells remains unknown. However, the splenic capsule, which contains a significant amount of smooth muscle cells, forms a continuous structure with the reticular framework. This framework represents the splenic connective tissue scaffold and is composed of collagen fibers enveloped by myofibroblasts; fibroblasts with smooth muscle cell like characteristics. Smooth muscle cells are known to be electrically coupled via gap junctions and can conduct action potentials from one cell

to another. If such coupling electrically conjoins the splenic capsule and the reticular fiber network, electrical stimulation of the "ASN" and hence the splenic capsule might activate the reticular framework. Since myofibroblasts of this framework can release various chemokines and cytokines, express chemokine receptor ligands, and, is involved in guided migration of immune cells, regulation of immune function (Zhao et al., 2015) (Perez-Shibayama et al., 2019), their activation can have significant effects on the immune response .

Although the ASN does not represent a neural structure, its intermediate role in the activation of an Ach mediated, T cell and adrenergic receptor independent anti-inflammatory mechanism is intriguing and triggers further research. This research might include mechanisms that activate the release of intrasplenic Ach from e.g. macrophages and dendritic cells, and, connective and splenic tissue transmission routes of electrical current and excitability of the reticular network.

## CONCLUSION

Microscopic evaluation of the ASN in mice and humans dismissed its neural identity, thereby casting doubt on its existence. The anti-inflammatory effect upon electrical stimulation of this non-neural structure in mice points out that our understanding of regulation of the splenic immune response is incomplete.

# 4

# AGE-RELATED VARIATION IN SYMPATHETIC NERVE DISTRIBUTION IN THE HUMAN SPLEEN

Cindy G.J. Cleypool[1], David J, Brinkman[2,4], Claire Mackaaij[1], Peter G.J. Nikkels[3], Martijn A. Nolte[5], Misha D. Luyer[4], Wouter J. de Jonge[2,6] and Ronald L.A.W. Bleys[1]

[1] Department of Anatomy, Division of Surgical Specialties, University Medical Center Utrecht, Utrecht University, Utrecht, the Netherlands.
[2] Amsterdam University Medical Centre, University of Amsterdam, Tytgat Institute for Liver and Intestinal Research, Amsterdam, The Netherlands.
[3] Department of Pathology, Division of Laboratory, Pharmacy, Biomedical Genetics and Pathology, University Medical Center Utrecht, Utrecht, The Netherlands.
[4] Department of Surgery, Catharina Hospital, Eindhoven, The Netherlands.
[5] Department of Molecular and Cellular Hemostasis, Sanquin Research and Landsteiner Laboratory, Amsterdam, The Netherlands.
[6] Department of Surgery, University Clinic of Bonn, Bonn, Germany.

*Under review at Frontiers in Neuroscience*

# ABSTRACT

## Introduction

The cholinergic anti-inflammatory pathway (CAIP) has been proposed as an efferent neural pathway dampening the systemic inflammatory response via the spleen. The CAIP activates the splenic neural plexus and a subsequent series of intrasplenic events, which at least require a close association between sympathetic nerves and T cells. Knowledge on this pathway has mostly been derived from rodent studies and only scarce information is available on the intrinsic innervation of the human spleen. This study aimed to investigate the sympathetic innervation of different structures of the human spleen, the topographical association of nerves with T cells and age-related variations in nerve distribution.

## Materials & methods

Spleen samples were retrieved from a diagnostic archive and were allocated to three age groups; neonates, 10-25 and 25-70 years of age. Sympathetic nerves and T cells were identified by immunohistochemistry for tyrosine hydroxylase (TH) and the membrane marker CD3, respectively. The overall amount of sympathetic nerves and T cells were semi-automatically quantified and expressed as total area percentage. A predefined scoring system was used to analyse the distribution of nerves within different splenic structures.

## Results

Sympathetic nerves were observed in all spleens and their number appeared to slightly increase from birth to adulthood and to decrease afterwards. Irrespective to age, more than halve of the periarteriolar lymphatic sheaths (PALSs) contained sympathetic nerves in close association with T cells. Furthermore, discrete sympathetic nerves were observed in the capsule, trabeculae and red pulp and comparable to the total amount of sympathetic nerves, showed a tendency to decrease with age. No correlation was found between the number of T cells and sympathetic nerves.

## Conclusion

The presence of extra-vascular sympathetic nerves in the splenic parenchyma, capsule and trabecular of human spleens could suggest a role in functions other than vasoregulation. In the PALS, sympathetic nerves were observed to be in proximity with T cells and is suggestive for the existence of the CAIP in humans. Since sympathetic nerve distribution shows interspecies and age-related variation, and our general understanding of the relative and spatial contribution of splenic innervation in immuneregulation is incomplete, it remains difficult to estimate the anti-inflammatory potential of targeting splenic nerves in patients.

# INTRODUCTION



The cholinergic anti-inflammatory pathway (CAIP) comprises an efferent neural pathway that dampens the systemic inflammatory response via the spleen and is suggested to involve sequential activation of the efferent vagus nerve and the splenic plexus (Reardon, 2016)(Pavlov and Tracey, 2017). Others have put forward that instead of the efferent vagus nerve, this pathway involves the greater splanchnic nerve (Komega et al., 2018). Irrespective, activation of the splenic plexus results in a cascade of intrasplenic events, starting with the release of norepinephrine (NE) (Kees et al., 2003). Studies have demonstrated that NE then activates adrenergic receptors on $CD4^+$ $ChAT^+$ T lymphocytes (Vida et al. 2011) (Rosas-Ballina et al., 2011)(Vida et al., 2017), which in turn produce and secrete acetylcholine (ACh) (Rosas-Ballina et al., 2011)(Borovikova et al., 2000). ACh then inhibits the release of the pro-inflammatory cytokine tumour necrosis factor alpha (TNFa) from activated macrophages via nicotinergic receptor signaling (Borovikova et al., 2000) (Lu and Kwan, 2014) (de Jonge et al., 2005)(Kox et al., 2009).

Morphological evidence for the presence of sympathetic nerves in proximity with splenic T lymphocytes was provided earlier by Bellinger et al. (Bellinger et al., 1987)(Bellinger et al., 1992). In a study on rat spleen, they observed sympathetic nerves diverging into T lymphocyte specific white pulp areas, also known as periarteriolar lymphatic sheaths (PALSs). In the PALSs these nerves were in close proximity to T lymphocytes and formed synaptic connections (Felten and Olschowka, 1987). The presence of sympathetic nerves which could release NE in the proximity of T lymphocytes in the human spleen might hold potential as a therapeutic target for immune related disease and knowledge on the anatomical configuration of intrinsic splenic innervation in humans is therefore essential.

The presence of sympathetic nerves at the medioadventitial junction in human spleens has been described in various studies (Heusermann and Stutte, 1977)(Kudoh et al., 1979)(Anagnostou et al., 2007)(Verlinden et al., 2018), however, innervation of T cell specific lymphoid tissue has only been reported once (Hoover et al., 2017). In the latter study, sympathetic innervation patterns in spleens of end-stage sepsis patients were investigated and sympathetic nerves were observed to be in close association with lymphocytes in the PALS of the control group (trauma patients who died after haemorrhagic stroke). The results of this study were descriptive and it remains unclear whether this was a common feature and observed in all PALSs, or only occasionally. Since, PALS related sympathetic nerves were seldom observed in end-stage sepsis patients, the authors suggested this difference to be disease-related (Hoover et al., 2017). However, other factors, such as aging, are known to contribute to decline of sympathetic innervation as well, as shown in the rat spleen (Bellinger et al., 1987)(Bellinger et al., 1992) and human cerebral arteries (Bleys and Cowen, 2001). If human splenic innervation is subject to age-related decline as well, this information is of relevance because it might determine the window of application of anti-inflammatory neuromodulation along age. Since the age profile of a substantial amount of patients of the control group in the study of

Hoover *et al* (Hoover et al., 2017) was lacking, as well as comprehensive data on the prevalence of PALS related sympathetic nerves, our understanding of human splenic innervation remains incomplete.

Therefore, in this study, quantitative and semi-quantitative analytical methods were used to investigate the presence of sympathetic nerves in human spleens of various age groups. Although the PALS is considered to represent the primary structure of T cell neuromodulation, T cells migrate through the spleen and exposure to NE might occur at any location they pass while entering or exiting the spleen. Therefore, blood vessels, red pulp, trabeculae and the capsule were evaluated for the presence of sympathetic nerve tissue as well.

# MATERIALS & METHODS

## Tissue samples

A total of 26 paraffin embedded splenic samples were provided the Pathology Department of the University Medical Center Utrecht. Samples were divided into three age groups, being 40 weeks of gestation (from now on referred to as neonatal), 10-25 years and 25-70 years. These archived autopsy samples were allowed to use for research purposes based on informed consent provided by next of kin. None of the individuals was known with immunological - or splenic clinical conditions. Table 1 contains data on age, sex and cause of death.

## Sample processing

Samples were obtained from the splenic hilar region and were cut in the transversal plane. Paraffin embedded splenic samples were cut on a microtome (Leica 2050 Super Cut, Nussloch, Germany) and 5 µm thick sections of splenic tissue were collected on glass slides, air dried and subsequently heat fixed for two hours on a slide drying table of 60°C (Medax, 14801, Kiel, Germany). All slides were deparaffinized, rehydrated and further processed for histochemical – or immunohistochemical staining. Hematoxylin/Eosin (HE) was used to evaluate technical tissue quality, to generate a tissue overview, and to screen for general pathological changes. A double T and B cell staining, using antibodies against specific membrane proteins, being CD3 and CD20 respectively, was used to screen the white pulp for distinct pathological abnormalities. To quantify and compare the total amount of sympathetic nerves and T cells, and the distribution of sympathetic nerves in the PALS and other splenic structures (capsule, trabeculae, rep pulp and arteries), a double staining for sympathetic nerves and T cells was performed. In this procedure antibodies against CD3 and tyrosine hydroxylase (TH), were used, the latter being an enzyme involved in the synthesis of NE. The general nerve marker, protein gene product 9.5 (PGP9.5) was used on adjacent slides to confirm neural identity of TH-immune reactive (IR) structures.

## Staining procedures

Tissue sections were dewaxed in xylene and rehydrated through graded alcohols prior to histochemical or immunohistochemical staining. Prior to immunohistochemistry, sections were pretreated with Heat Induced Epitope Retrieval (HIER) in citrate buffer (pH6.0) for 20 min at 95°C.

**Table 1.** Patient profiles. Age is represented in years for the 25-70 years and 10-25 years age groups and in weeks of gestation and postnatal days for the 40 weeks group (e.g. 41 6/7 w 7 = 41 weeks and 6 days of gestation whereafter the newly born lived for 7 days).

| **25-70 years (N=7)** | | | |
|---|---|---|---|
| **#** | **sex** | **age** | **Cause of death** |
| 1 | F | 46 | Pancreatic tail cyst |
| 2 | F | 66 | Myocardial infarct |
| 3 | F | 52 | Subarachnoid hemorrhage |
| 4 | F | 48 | Traumatic motor bike accident |
| 5 | M | 66 | Unknown |
| 6 | M | 26 | Arrythmia |
| 7 | M | 29 | Long QT syndrome |
| **10-25 years (N=7)** | | | |
| **#** | **sex** | **age** | **Cause of death** |
| 8 | F | 14 | Acute unexpected death, probably due to cardiac arrest |
| 9 | M | 16 | Arrythmia |
| 10 | M | 11 | Sudden unexpected death due to coronary artery anomaly |
| 11 | M | 11 | New diabetes mellitus with keto-acidosis |
| 12 | F | 12 | Unknown |
| 13 | M | 11 | Herniation of the sigmoid due to congenital mesenterial defect |
| 14 | F | 24 | Lung emboly |
| **40 weeks (N=12)** | | | |
| **#** | **sex** | **age** | **Cause of death** |
| 15 | M | 40w 2d | Perinatal asphyxia |
| 16 | F | 39 2/7w 2d | Perinatal asphyxia |
| 17 | M | 40w 1d | Perinatal asphyxia |
| 18 | M | 42 1/7w 3d | Perinatal asphyxia |
| 19 | F | 41w 10d | Perinatal asphyxia |
| 20 | M | 40 6/7w 4d | Perinatal asphyxia |
| 21 | M | 40 2/7w 1d | Perinatal asphyxia |
| 22 | M | 40 2/7w 1d | Perinatal asphyxia, congenital heart defect |
| 23 | M | 40 2/7w 4d | Perinatal asphyxia |
| 24 | M | 41 5/7w 3d | Perinatal asphyxia |
| 25 | F | 35w 1d | Perinatal asphyxia, first born of dichorionic twin |
| 26 | M | 41 6/7w 7d | Perinatal asphyxia |

### *HE staining*

Tissue sections were stained with hematoxylin for 10 min at room temperature (RT). After rinsing in running tap water, sections were dipped in ethanol 50%, stained with eosin for 1 min and dehydrated in graded alcohols and xylene. Slides were coverslipped with Entellan (Merck, Darmstadt, Germany).

### *Single immunohistochemical staining procedures (PGP9.5 and TH)*

After the HIER procedure, sections were incubated with 5% Normal Human Serum (NHS) in TBS prior to incubation with rabbit anti human PGP9.5 antibody (1:2000 in TBS-T + 3% BSA, 48 hr, 4°C, Dako, Glostrup, Denmark) or rabbit anti-human TH (1:1500 in TBT-T + 1% BSA, overnight RT, Pel-Freez, Rogers AR). Visualization of bound antibodies was performed with undiluted Brightvision Poly-Alkaline Phosphatase (AP) Goat-anti-Rabbit (ImmunoLogic, Amsterdam, the Netherlands) and Liquid Permanent Red (LPR, Dako). All sections were counterstained with hematoxylin (Klinipath), dried on a hotplate for 15 min at 60°C and coverslipped with Entellan (Merck). Tris-buffered saline with 0.05% Tween20 (TBS-T) was used for all regular washing steps. Negative controls were obtained by incubation with TBS-3%BSA without primary antibodies. Human vagus nerve – and sympathetic trunk sections were included as a positive control for general – and sympathetic nerve tissue respectively.

### *Sequential double immunohistochemical staining procedure (CD20/CD3 and CD3/TH)*

After HIER, sections were incubated with 3% Normal Goat Serum (NGS) (CD20/CD3) or 5% NHS (CD3/TH). In the first staining sequence, sections were incubated with CD20 or CD3 antibodies (details of the used antibodies, including dilution, incubation time are presented in table 2) and visualized with Brightvision Poly-AP Goat-anti-Mouse or Goat-anti-rabbit Mouse (ImmunoLogic) respectively followed by PermaBlue plus/AP (Diagnostics Biosystems, Pleasanton, USA). Details of the used antibodies, including dilution and incubation time are presented in table 2. Prior to the second staining sequence a HIER in citrate buffer (pH6.0, 15 min RT) was performed, removing unbound antibodies but leaving chromogens unhanged (Van der Loos 2010). Sections were then incubated with 3% NGS (CD20/CD3) or 5% NHS (CD3/TH) followed by incubation with CD3 and TH antibodies, whereafter they were visualized with Brightvision Poly-AP Goat-anti-Rabbit (ImmunoLogic) and LPR (Dako, Glostrup, Denmark). Sections were dried on a hotplate for 15 min at 60°C and coverslipped with Entellan (Merck, Darmstadt, Germany). Tris-buffered saline with 0.05% Tween20 (TBS-T) was used for all regular washing steps. Negative controls were obtained by incubation with TBS-3% BSA without primary antibodies. Human spleen sections that were previously confirmed to show proper staining for B cells, T cells and sympathetic nerves were included as positive controls.

## Microscopic evaluation

HE and CD3 and CD20 stain was evaluated by bright field microscopy. The chromogen LPR was used to visualize sympathetic nerves. This marker has stable fluorescent characteristics and allows the user to alternately use bright field - and fluorescent microscopy on the same slide. This can be beneficial as both modalities have their own advantages, e.g. fluorescent microscopy is more

**Table 2.** Detailed information on antibodies used in sequential double staining procedures

| Double stain | Staining sequence | Primary antibody | Host | Vendor | Dilution, incubation time and temperature | Secondary antibody | Chromogen |
|---|---|---|---|---|---|---|---|
| CD3/TH | 1 | CD3 | Rabbit | Dako A0452 | 1:50, 90 min, RT | Brighvision-anti-Rabbit/AP | PermaBlue |
| | 2 | TH | Rabbit | Pel-Freez P40101 | 1:1500, overnight, RT | Brighvision-anti-Rabbit/AP | LPR |
| CD20/CD3 | 1 | CD20 | Mouse | Dako M0755 | 1:400, 90 min, RT | Brighvision-anti-Mouse/AP | PermaBlue |
| | 2 | CD3 | Rabbit | Dako A0452 | 1:100, 90 min, RT | Brighvision-anti-Rabbit/AP | LPR |

sensitive allowing small nerves to be more easily recognized, whereas bright field allowed better discrimination between lymphocytes and other cells. Instead of using a band pass filter suited for LPR, a long pass filter was used which allowed emission of a broader range of wave lengths. This resulted in a green/yellow autofluoresce of connective tissue, which was used to determine if the observed nerve tissue extended beyond e.g. perivascular connective tissue. All samples were studied using a DM6 microscope (Leica, Nussloch, Germany) with an I3 fluorescent filter.

## Image acquisition

Single images were captured at various magnifications. These images were either brightfield or fluorescent images, depending on which modality appeared most suited to visualize the structures of interest. Both brightfield and fluorescent tile scans (stitched overlapping images) were captured for digital image analysis. Tile scans were either used to quantify the total amount of sympathetic nerves and T cells or to automatically select PALS regions which were then further studied in detail regarding their innervation (all tile scans were obtained using a 10x objective). Image acquisition was performed using a DM6 microscope with a motorized scanning stage, a I3 fluorescent filter, a DFC7000 T camera and LASX software (all from Leica, Nussloch, Germany).

## Quantitative analysis of the total amount of sympathetic nerves and T-cells

Bright field and fluorescent tile scans of CD3 and TH stained slides, respectively, were optimized and analysed in Fiji (ImageJ with additional plugins) (Schindelin et al., 2012). Optimization of the images included removal of irrelevant tissue (e.g. hilar connective tissue and vasculature), artefacts and large trabecular arteries with a lot of surrounding nerves. Both the total splenic tissue area and the area of TH - and CD3-IR tissue were selected using standardized thresholds. The selected areas were expressed in pixels and the amount of sympathetic nerves and T cells was then calculated and expressed as area% with respect to the total tissue area. Table 3 contains an overview of the different parameters investigated in this study, including a short description of the quantification method and how the data are expressed.

**Table 3.** Studied parameters, their method of quantification and data expression.

| Quantitative analysis of: | Method of quantification | Expressed as |
|---|---|---|
| Total amount of sympathetic nerve tissue | Automated counting of TH-IR pixels | Area % |
| Total amount of T cells | Automated counting of CD3-IR pixels | Area % |
| **Semi-quantitative analysis of:** | **Method of quantification** | **Expressed as** |
| # PALSs with sympathetic nerves | Automated selection of PALSs & manually counting of + PALSs | % |
| Amount of sympathetic nerves in: | | |
| PALS | Microscopic evaluation of automated selected PALS | Score 1-3 |
| Capsule | General microscopic evaluation | Score 1-3 |
| Trabeculae | General microscopic evaluation | Score 1-3 |
| Red pulp | General microscopic evaluation | Score 1-3 |
| Arteries | General microscopic evaluation | Score 1-3 |

## Semi quantitative analysis of sympathetic nerves in various splenic structures

### *PALS*

For each sample a series of PALS regions was automatically selected and further studied in detail. Automated selection was performed in Fiji, using tile scans of CD3/TH-stained slides. A threshold was set to select all CD3-IR areas, which were turned into solid regions using a blur function. Solid regions of 40.000 pixels or more were then selected. This approach resulted in a selection of 23-60 PALSs of substantial size. A maximum of 40 selected PALSs were then evaluated for the presence of sympathetic nerves. The number of positive PALSs was counted and expressed as percentage of the total number of studied PALSs. The association of sympathetic nerves with T cells was then graded as follows; 1: only one or two sympathetic nerves were observed to extend beyond the connective tissue of the vessel wall and to be in close proximity with T cells immediately lining the vessel wall 2: multiple sympathetic nerves extended beyond the connective tissue of the vessel wall and were in close proximity with T cells immediately lining the vessel wall and 3: comparable to 2, but nerves extended beyond T cells immediately lining the vessel wall.

### *Capsule, trabeculae, red pulp and arteries*

With respect to the capsule, trabeculae, red pulp, sympathetic innervation was considered to be present if discrete nerves were observed or when nerves extended beyond the adventitial connective tissue of blood vessels running within these compartments. With respect to the arteries a division was made into large and small arteries. Large arteries represented penetrating arteries, also referred to as trabecular arteries (these were surrounded by a substantial amount of connective tissue). Small arteries represented arteries that could be observed in the red and white pulp, also referred to as central – and sheathed arteries. All samples were studied microscopically using a 20x objective and alternately switching between brightfield and fluorescent microscopy for reasons described in paragraph 2.4. The amount of nerves were quantified by means of scoring

according to the following grading scale: 0: complete absence, 1: low amount, 2: moderate amount and 3: high amount. These scores were assigned when the observation was representative for the whole sample.

Prior to scoring the amount of sympathetic nerve tissue in PALSs and other splenic compartments, various samples of the different age groups were evaluated by the observers in order to obtain a general idea of low and high amounts. Each sample was examined independently by two observers (CC and DB) who were blinded for the age group. When there was disagreement between the observers the samples were re-examined and scored by consensus.

### Statistical analysis

Statistical analysis and graph conception were performed using Graphpad Prism 8. A Kruskall-Wallis test was used to compare the three age groups for their total amount of sympathetic nerves and T cells, and, for the amount of sympathetic nerves in various splenic structures. An uncorrected Dunn's test was used to provide a p value for each separate group comparison. All parameters were expressed as median followed by their inter quartile range. Association between the total amount of sympathetic nerves and T cells was tested by means of Pearson's correlation coefficient.

## RESULTS

All spleens showed well defined white pulp with distinct T and B cell regions (PALS and follicles, respectively) and red pulp with well-defined splenic cords red pulp sinusoids were more indistinctly present. All samples contained blood vessels of various sizes, trabeculae and most samples contained a significant bit of capsule. No pathological abnormalities were observed. TH-IR structures showed comparable patterns to PGP9.5-IR structures in adjacent slides confirming they represented nerves and not TH-IR cells. Figure 1 shows examples of normal splenic morphology.

### Total amount of sympathetic nerves and T cells and their age-related variation

Sympathetic nerves were detected in 26/26 samples (100%). Nerves were mostly observed surrounding vascular structures and to a lesser extent as discrete structures in the PALS, capsule, trabeculae and red pulp. T cells were observed in all samples and were primarily present in the PALS and to a lesser extent in follicles and in the red pulp. Relatively more sympathetic nerves were observed in the 10-25 group (0.1 [0.09-0.18]) compared to the neonatal group (0.02 [0.01-0.07], p=0.0034) as well as compared to the 25-70 group (0.04 [0.02-0.05], p = 0.0192) (Figure 2A). No significant difference in the number of T cells was observed between the different age groups (Figure 2B). No correlation was found between the amount of sympathetic nerves and the amount of T cells (r=0.076, p=0.71). Table 4 contains an overview of quantified median data per age group and lists age-related significant differences. Data of all separate individuals can be found in the supplementary data.

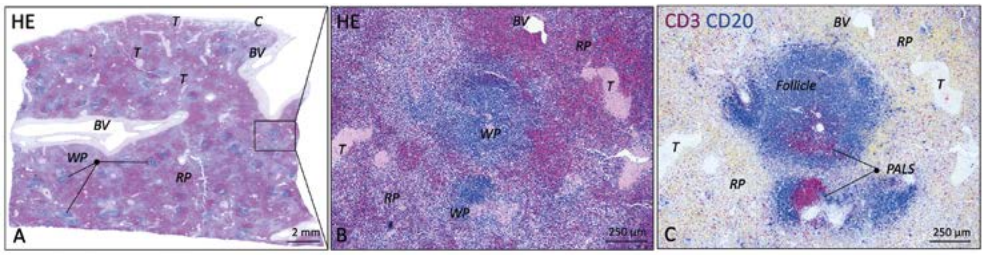


**Figure 1. Microscopic images of a normal spleen. A:** Overview image of a splenic sample of a patient from the 10-20 years group (HE staining). White and red pulp can be clearly distinguished as well as vascular structures and connective tissue structures such as trabeculae. **B:** Close up image of the boxed splenic region in figure A, showing normal splenic pulp morphology with clear white and red pulp areas (HE staining). **C:** Similar region as in figure B, showing the presence of T and B cells (CD3 and CD20, respectively) in periarteriolar lymphatic sheaths (PALSs) and follicles, respectively. ***BV:*** *blood vessel.* ***C:*** *capsule.* ***WP:*** *white pulp.* ***RP:*** *red pulp.* ***T:*** *trabecula.*

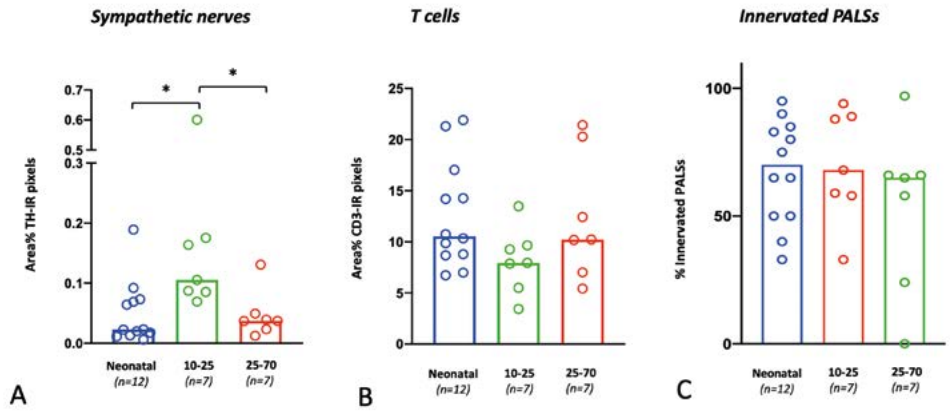


**Figure 2. Age related variations in the total amount of T cells and sympathetic nerves, and, the percentage of innervated PALS. A:** The total number of T cells per sample is calculated as the number of CD3 positive pixels and expressed as area % with respect to the total area of each sample. **B:** The total amount of sympathetic nerves per sample is calculated as the number of TH positive pixels and expressed as area % with respect to the total area of each sample. **C:** The total amount of sympathetic innervated PALSs per sample expressed as percentage of the total amount of PALS in each sample. * $P<0.05$.

## Sympathetic nerve distribution in PALS and its age-related variation

In 25/26 subjects (96%), sympathetic nerves were occasionally observed to extend beyond the adventitial lining of the central artery into the lymphatic tissue where they were in close proximity with T cells. To gain an objectified understanding of the number of innervated PALSs, a series of PALSs was automatically selected for each sample and further studied in detail (Figure 3A). PALSs with sympathetic nerves in close proximity with T cells were observed in 614 of the in total studied 1027 PALSs (60%). No significant difference in the percentage of innervated

**Table 4.** Age related variations of T cell and sympathetic nerve presence. Data is expressed as median values (interquartile range is placed between brackets). Observed significant differences between groups are listed including their p value. NS: no significant difference observed.

| | Neonatal | 10-25 years | 25-70 years | Significant difference |
|---|---|---|---|---|
| Total amount of sympathetic nerve tissue (Area %) | *0.02 (0.01-0.07)* | *0.10 (0.09-0.18)* | 0.04 *(0.02-0.05)* | 10-25 >neonatal p=0.0034<br>10-25 >25-70 p=0.0192 |
| Total amount of T cells (Area %) | 10.55 *(8.70-16.34)* | 7.95 *(5.50-9.66)* | 10.23 *(7.02-20.29)* | NS |
| # PALSs with sympathetic nerves (%) | 70 *(50-95)* | 68 *(58-89)* | 65 *(24-66)* | NS |
| Score 1 (%) | 38 *(28.5-60)* | 34 *(21-41)* | 21 *(8-41)* | Neonatal >25-70 p= 0.0059 |
| Score 2 (%) | 10 *(5-14.75)* | 9 *(4-19)* | 8 *(1-11)* | NS |
| Score 3 (%) | 4 *(0-9.5)* | 6 *(0-12)* | 9 *(0-11)* | NS |
| Amount of sympathetic nerves in: | | | | |
| Capsule | 2 (1-2) | 0 (0-0) | 0 (0-1.25) | Neonatal >10-25 p=0.0003<br>Neonatal >25-70 p=0.008 |
| Trabeculae | 1 *(1-2)* | 1 *(1-3)* | 1 *(1-2)* | NS |
| Large arteries | 3 *(2-3)* | 2 *(2-3)* | 2 *(1-2)* | Neonatal >25-70 p=0.0098 |
| Small arteries | 3 *(2-3)* | 2 *(2-3)* | 2 *(1-2)* | NS |
| Red pulp | 2 (1-2) | 1 (0-2) | 0 (0-1) | Neonatal >25-70 p=0.0016 |



PALSs was observed between the different age groups (Figure 2C). All PALSs that contained sympathetic nerves were additionally evaluated with respect to the amount of nerves that were in association with T cells and whether these nerves would travel further into the lymphatic tissue. Of the in total 1027 studied PALSs, 302 (29%) PALSs contained one paravascular nerve in proximity with T cells (score 1), 249 (24%) PALSs contained multiple nerves (score 2) and 63 (6%) PALSs contained nerves which travelled further into the lymphatic tissue (score 3) (Figure 3B-H contains examples of all scores). The neonatal group showed a higher percentage of PALSs with a score 1 (38 [28.5-60]) compared to the 25-70 group (21 [8-41], p=0.0059). For the other scores no age-related differences were observed.

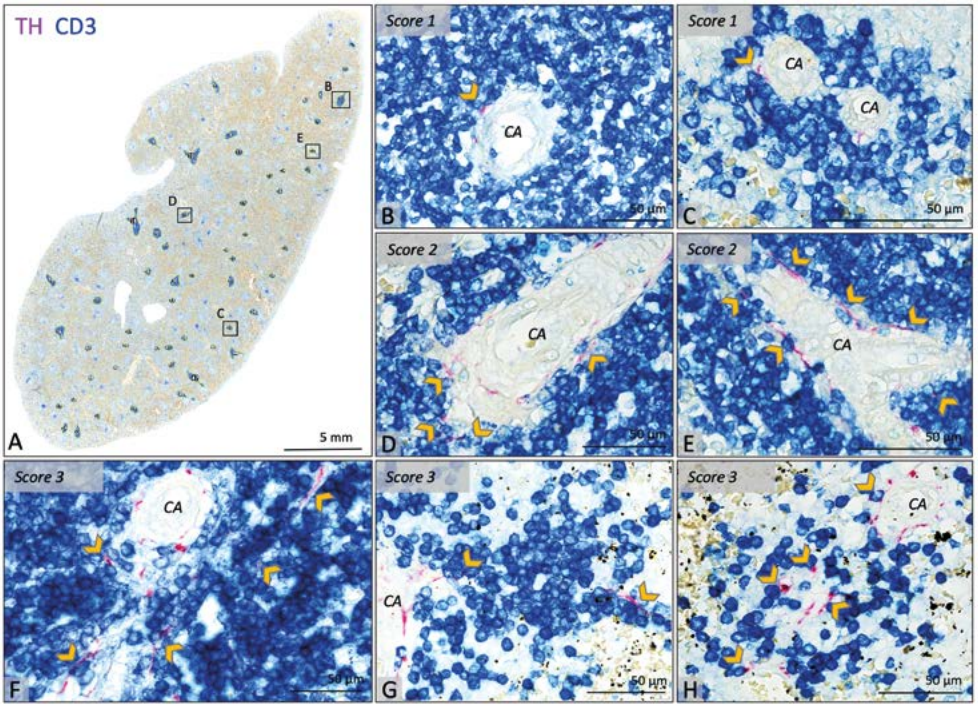


**Figure 3. Bright field microscopic images of PALS related sympathetic nerves in CD3/TH double stained splenic tissue slides of various individuals. A:** Overview image of a splenic sample showing automatically selected T cell regions which were further investigated for the presence of sympathetic nerves and their relation with T cells. **B-E:** Close up images of the marked regions in figure A representing PALSs with a score 1 or 2. **F-H:** Close up images of PALSs (from different spleens) with a score 3. ***Score 1:*** *Only one or two sympathetic nerves were observed to extend beyond the connective tissue of the vessel wall of the central artery (CA) and to be in close proximity with T cells immediately lining the vessel wall.* ***Score2:*** *multiple sympathetic nerves extended beyond the connective tissue of the CA and were in close proximity with T cells immediately lining the vessel wall.* ***Score 3:*** *comparable to 2, but nerves extended beyond T cells immediately lining the vessel wall.* ***CA:*** *central artery.* ***Arrow heads****: pointing out sympathetic nerves that are in close proximity with T cells, but might be obscured by the blue stain.*

## Sympathetic nerve distribution in other splenic structures and their age-related variation

### *Capsule*

In 25/26 subjects (96%) a substantial amount of capsule was present of which 15 (60%) contained sympathetic nerves. These nerves were scattered and were mainly observed in the part of the capsule which was in close proximity to the hilum, where vascular structures with surrounding nerves entered the spleen. In the hilar region, the capsule was less distinct and showed continuity with hilar specific structures such as the adventitia of incoming vascular structures or the connective tissue of suspending splenic ligaments (Figure 4AB). Most observed capsular nerve tissue was present in

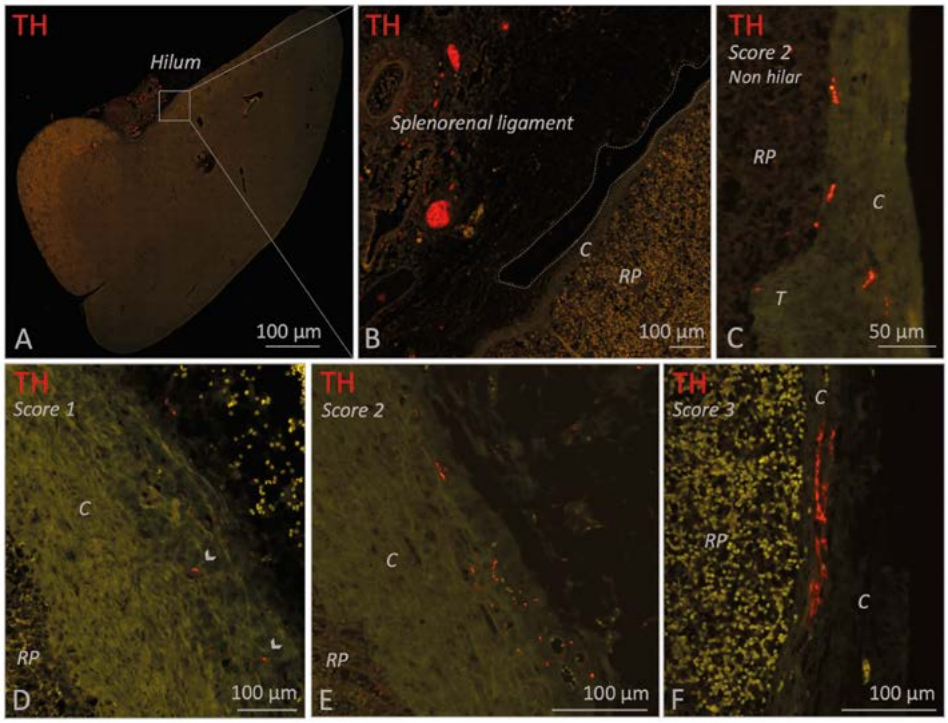


**Figure 4. Fluorescence microscopic images of various quantities of capsule related sympathetic nerves (TH staining). A:** Overview image of a neonatal spleen. Large blood vessels with a perivascular nerve plexus reside in the splenorenal ligament an enter the spleen at the hilum. **B:** Close up images of the boxed region in figure A. The splenorenal ligament contains connective tissue, vascular structures and sympathetic nerves. The lining of the splenorenal ligament reflects over the hilar capsule and on its distal continuation thins out (dotted line shows the lining of the ligament). **C:** Close up image of a part of a capsule obtained from a non hilar part of the spleen. A moderate amount (score 2) of sympathetic nerves can be observed. **D-F:** Close up images of hilar capsule samples containing a low (score 1), moderate (score 2) or high (score 3) amount of sympathetic nerves. Nerves were mostly observed in the more superficial and middle part of the capsule and only sporadically in the deeper part where they were in direct contact with the red pulp (as shown in C). ***C:*** *capsule*. ***RP:*** *red pulp*. ***T:*** *trabecula*. ***Arrow heads:*** *small capsular nerves*

the more superficial and middle part of the capsule (Figure 4DE) and only sporadically in the deeper part, where it was in direct contact with the red pulp (Figure 4C).

### *Trabeculae*

All subjects showed trabeculae which, as a result of the cutting plane of the samples, were observed either as immediate extensions of the capsule, or as discrete structures deeper in the parenchyma (Figure 5A). The deeper parts of the trabeculae frequently contained large vascular structures (Figure 5CE). In 25/26 (96%) subjects, trabecular sympathetic nerves were present to some extent and were often observed in the deeper parts of trabeculae, whereas the trabeculae that extended immediately from the capsule were mostly devoid of nerves. Trabecular sympathetic nerves were observed as discrete structures (Figure 5BF), or as a nerve plexus surrounding vascular structures (Figure 5CE). In both cases nerves could extend up to the external border of the trabecular tissue where nerves were in proximity with the surrounding red pulp.

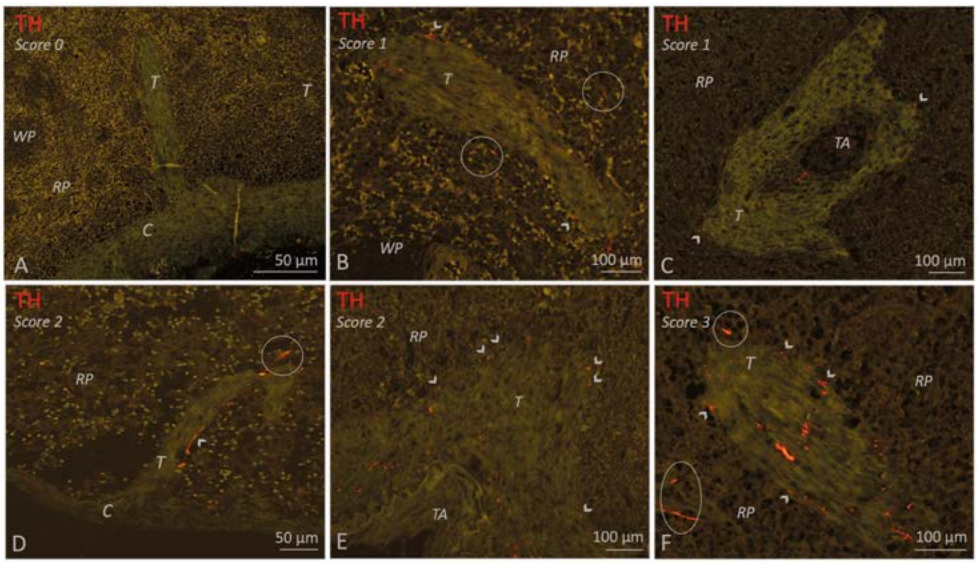


**Figure 5. Fluorescence microscopic images of various quantities of trabecula related sympathetic nerves (TH staining). A:** Spleen without trabecular sympathetic nerves (score 0). **B:** Trabecula with a low amount (score 1) of sympathetic nerves. A few small nerves are present within the connective tissue of the trabecular and a few nerves can be observed on its outer margin where they are in proximity with the RP. **C:** Trabecula with a low amount (score 1) of sympathetic nerves. Perivascular nerves can be observed in the adventitia of a small blood vessel (trabecular artery) and in the connective tissue of the trabecula from where it diverges to its outer margins were a few nerves are bordering the RP. **D:** Trabecula extending from the capsule with a moderate amount (score 2) of sympathetic nerves. Most nerves are in proximity to the RP and on its cranial site a nerve extents into the RP. Note: sympathetic nerves in parts of trabeculae directly extending from the capsule were very sparse. **E:** Comparable to figure C but this figure contains a larger trabecular artery and shows a moderate amount (score 2) of sympathetic nerves. **F:** Trabecula with a high amount (score 3) of sympathetic nerves which diverge to the trabecula's outer border to be in proximity with the RP.

### Arteries

All 26 subjects had clear recognizable vascular structures of various sizes which were to some extent surrounded with perivascular sympathetic nerves (Figure 6). In case of splenic artery branches in the hilum or large incoming trabecular arteries, nerve tissue was presented as large nerve bundles running in the adventitia or trabecular connective tissue, respectively, or as finer neural structures. In case of smaller arteries, nerve tissue was organised in a more delicate network of small nerves that were in close proximity to the vessel wall. Occasionally, perivascular nerves extended beyond the adventitial connective tissue. This was observed in central arteries, trabecular arteries and to a lesser extent in small arteries in the red pulp.

### Red pulp

The red pulp of all subjects contained clearly recognisable lymphoid tissue, also known as the splenic cords (Figure 7A). Sinusoids were easily recognized if they contained a substantial amount of blood, but otherwise were less distinct. Sympathetic nerves were observed in the red pulp of 20/26 (77%) subjects. These nerves comprised either small solitary nerves in between the red pulp (Figure 7BD), or nerves bordering parenchymal trabeculae (Figure 5BEF and 7C) or small vascular structures (Figure 5F and 7ADE).

### Age-related variations

Age-related differences were observed with respect to the capsule, large arteries and the red pulp. The neonatal group showed significant more sympathetic nerves in its capsule compared to both the 10-25 and 25-70 group, and, surrounding its large arteries and in its red pulp when compared to the 25-70 group. No age-related differences were observed in trabeculae and small arteries. Table 4 contains detailed information on median group data and p values.

## DISCUSSION

This study shows that the human spleen contains sympathetic nerves, not only associated with the splenic vasculature, but also as discrete structures in the PALS, capsule, trabeculae and red pulp. Furthermore, the number of sympathetic nerves shows a mild tendency to decrease with age. These findings are of relevance for understanding the role of splenic sympathetic nerves in regulation of the systemic immune response in humans and for the development of neuromodulatory anti-inflammatory therapies.

Sympathetic nerves were observed in all spleens but their presence was most prominent in the 10-25 age group, suggesting that from birth their number increases whereafter it decreases from adulthood on. This observation fits in with the fact that organ systems, including the peripheral nervous system, mature after birth until the onset of adulthood whereafter they subsequently show signs of aging (Verdú et al., 2000). More specifically, animal studies have shown that an age-related

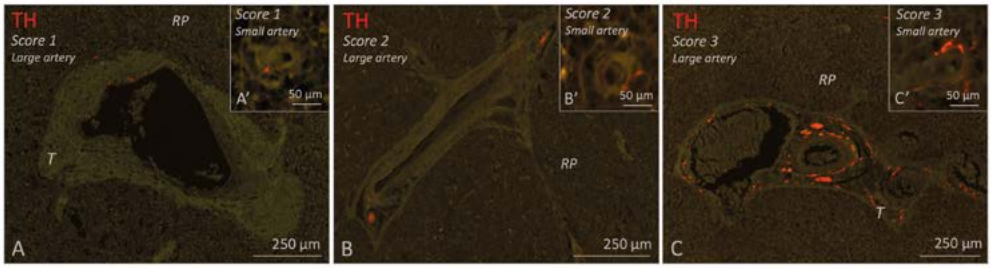


**Figure 6. Fluorescence microscopic images of various quantities of blood vessel related sympathetic nerves (TH staining).** Each figure contains a representative example of a large vessel and a small vessel with a specific amount of sympathetic nerves (score 1-3). A-C: Splenic samples with a low, moderate or high amount of sympathetic nerves surrounding large arteries (score 1-3). A'-C': Splenic samples with a low, moderate or high amount of sympathetic nerves surrounding small arteries (score 1-3). ***RP:*** *red pulp.* ***T:*** *trabecula.*

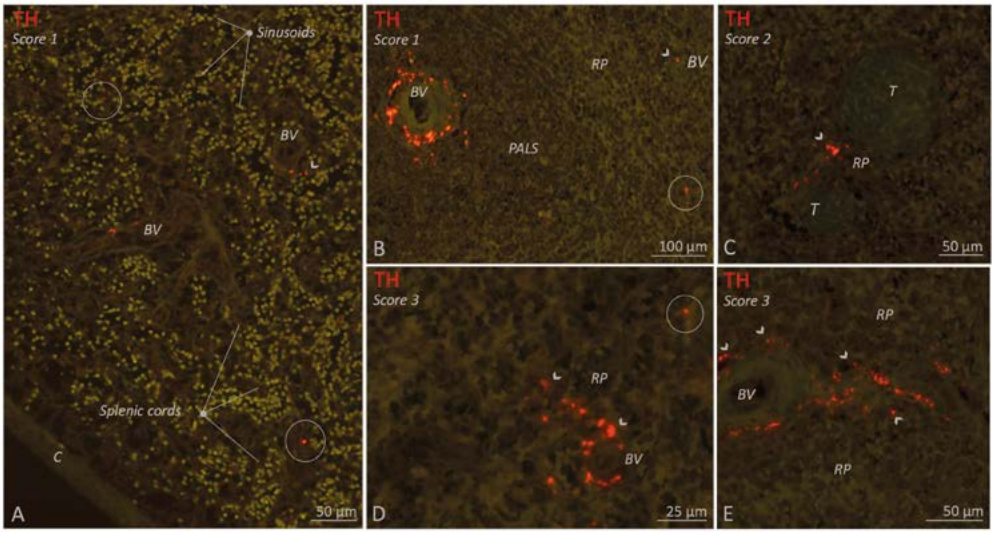


**Figure 7. Fluorescence microscopic images of various quantities of red pulp related sympathetic nerves (TH staining).** Sympathetic nerves are present as discrete structures running in the splenic cords (encircled structures) or as nerves that originate from a perivascular or trabecular plexus and from there diverge further into the red pulp (RP) (arrow heads). **A:** Splenic sample with clear splenic cords and sinusoids and a low amount (score 1) of sympathetic nerves. **B-E:** Various examples of spleens with RP related nerves either as a low amount (score 1), a moderate amount (score 2) or a high amount (score 3). ***C:*** *capsule.* ***BV:*** *blood vessel.* ***PALS****: periarteriolar lymphatic sheath.* ***RP:*** *red pulp.* ***T:*** *trabecula.*

decline applies for splenic sympathetic innervation as well (Bellinger et al., 1987)(Bellinger et al., 1992) (Madden et al., 1997).

A decrease in the number of T cells has been put forward as another explanation for a decrease in sympathetic nerves (Hoover et al., 2017). The authors observed the number of T cells to

correlate to the number of sympathetic nerves and suggested the lack of specific nerve growth factors produced by these T cells to be of relevance. In the current study, however, no correlation between sympathetic nerve and T cell quantities was found, thereby further emphasizing aging to be the most plausible explanation for the observed decline of sympathetic innervation in spleens of healthy persons.

In 96% of the studied individuals, PALSs were observed to contain sympathetic nerves that extended beyond the adventitia of central arteries and to be in apposition with T cells. So far PALS innervation in humans have only been reported once (Hoover et al., 2017). The authors, however, did not supply information on the number of innervated PALSs per individual, deeming it impossible to estimate whether PALS innervation represented a structural entity of normal healthy spleens or a more coincidental heterogenous finding. The current study shows that human PALSs innervation was observed in 60% of the studied PALSs and therefore represents a structural phenomenon. Furthermore, no significant age-related differences could be determined with respect to the innervation of the number of PALSs, or the extent to which nerves travelled further into the parenchyma.

The sympathetic innervation patterns observed so far in human PALSs, however, seem to differ significantly from other species. In rats, mice and rabbits nerves were more abundant and also travelled further into the parenchyma (Felten et al., 1987) (Bellinger et al., 1992) (Felten et al., 1997). This questions whether splenic plexus stimulation in humans, with only a few T cells in direct contact with sympathetic nerves, would target enough of these cells to establish a similar systemic anti-inflammatory effect as observed in rodents. Most T cells are migratory cells and reside in the PALS for only a certain amount of time whereafter they disseminate to the red pulp and return to the systemic circulation. If, during this migration, enough $CD4^+$T cells pass sympathetic nerves and short term synaptic connections are formed, a phenomenon referred to as short term plasticity (Song et al., 2018), a significant amount of adrenergic receptors on $CD4^+$T cells might indeed get activated. Another potential mechanism to overcome this issue might be volume transmission; a process wherein a neurotransmitter is not released in a synaptic cleft but is expelled into the extracellular matrix and reaches its effector cells by diffusion (Fuxe et al., 2013).

Other studies have casted doubt on the prevailing mechanisms of the cholinergic anti-inflammatory pathway involving the sequence of NE release, ACh production, and subsequent TNFα reduction through cholinergic receptor activation on macrophages, both with respect to the mechanism itself and with respect to its location (Murray et al., 2017)(Rosas-Ballina et al., 2008). In a recent study wherein the relationship between sympathetic neurons and $ChAT^+$ lymphocytes were mapped in complete mouse spleens, it was shown that overall few $ChAT^+$ T cells were juxtaposed to sympathetic fibers and that their distance to these fibers exceeded that of traditional synapses (Murray et al. 2017). Moreover, the authors showed that sympathetic innervation was involved in homing of $ChAT^+$T cells to appropriate physical regions in the spleen by increasing the expression of the chemokine CXCL13 in stromal cells (Murray et al., 2017). Such homing processes are vital as it conjoins the right cells for

a properly aligned immune response (reviewed by Zhao et al., 2015). In case of conjoining the key mediators of the intrasplenic NE-ACh-TNFα mechanism, this requires homing of $ChAT^{+}$T cells towards macrophage rich areas such as the marginal zone and the the red pulp, where adrenergic receptors on these T cells need to be activated prior to release of ACh in proximity of these macrophages. Interestingly, vagus nerve stimulation in mice specifically attenuated TNFα production by splenic macrophages in these two areas 30 minutes after endotoxin administration. The authors observed nerve terminals adjacent to these TNFα producing macrophages, but did not provide information on the local presence of $ChAT^{+}$ T cells. With the above discussed topics in mind, it would be more plausible that the intrasplenic NE-Ach-TNFα mechanism occurs in the marginal zone and red pulp, instead of the PALS. Further support for favouring the red pulp and marginal zone over the PALS as designated immune regulation areas, is the difference in T cell transit time. T cell passage through the red pulp and marginal zone takes 5 and 50 minutes respectively whereas passage through the PALS takes 2.5-6 hours (Hammond, 1975) (Ford, 1979) (Ganusov and Auerbach, 2014) and the latter may take too long to provoke the fast systemic response which peaks at 90 minutes after electrical stimulation (Rosas-Ballina et al., 2008)(Komega et al., 2018)(Guyot et al., 2019).

According to recent literature, human spleens do not have a marginal zone but their red pulp is considered to be morphologically and functionally comparable to mice and rats (reviewed by Steiniger, 2015). In the current study, it was confirmed that human spleens of all age groups contain low amounts of sympathetic innervation in their red pulp, albeit more prominent in the younger age groups. Sporadically, small discrete nerves were observed within the red pulp, but most of the red pulp innervation was supplied either by trabecular nerves which extended to the outer margins of the trabecular connective tissue, or by nerves positioned outside the connective tissue surrounding small red pulp vascular structures. These nerves always remained in proximity with the trabeculae and vascular structures and never travelled deeper into the red pulp. In human foetuses, capsular nerves have also been observed to extend into the red pulp (Anagnostou et al. 2007). In the current study, however, capsular nerves have been observed in all age groups, but these never extended into the red pulp or reached the inner capsular margins contacting the red pulp and therefore did not contribute to red pulp innervation.

Previous studies on red pulp innervation suggest no sympathetic nerves to be present in this splenic compartment (Heusermann and Stutte, 1977)(Kudoh et al., 1979) (Anagnostou et al., 2007) (Verlinden et al., 2018). The current study, however, shows that, although rare, red pulp innervation is present in al age groups albeit it more prominent in the younger age groups. Similar to the PALS, the red pulp in humans contains significant less sympathetic innervation when compared to other animals in which red pulp innervation was already considered sparse (Bellinger et al., 1987). In these animals, most red pulp innervation was observed in the parafollicular zone, bordering venous sinuses and occasionally as discrete nerves traversing the red pulp. They also contained more abundant innervation of their capsule and trabeculae. Since little innervation is present in the red pulp in humans, comparable to the PALS, one could question whether splenic plexus stimulation would target a sufficient amount of effector cells to provoke the effect observed in animals. However,

a more elegant and subtle mechanism might be involved, which potentially requires little direct innervation. In the spleen stromal cells can be found in both the white and red pulp where they represent the main cellular components of the reticular framework, a connective tissue scaffold which provides support for splenic immune cells and guidance for their migration (Perez-Shibayama et al., 2019). As shown by a transmission electron microscopic study in guinea pigs, the reticular network is composed of an enveloping reticular cell which encloses connective tissue components and a sympathetic axon (Saito, 1990). Based on the presence of this axon, the author hypothesized that the reticular framework represents catecholaminergic canals and that migrating immune cells can be exposed to their content (Saito 1990). With the exception of follicles, the reticular cells of the spleen are represented by contractile myofibroblasts (Pinkus et al., 1986). Contraction of these myofibroblasts is thought to result in exposure of thin naked noradrenergic axons, or release of previously secreted and stored NE. In turn, this could result in innervation of migrating immune cells, either by close-association or by diffusion, and play a significant role in splenic immune function. The reticular framework might equal the more recent discovered splenic conduit system in mice; an interconnected tubular network that functions as a transport system for fluid, small molecules and particles (including antigens) and is covered with fibroblast reticular cells which support migratory lymphocytes (Nolte et al., 2003)(Roozendaal et al., 2008). Whether the conduit system contains cholinergic channels has not been established yet. In the present study no sympathetic nerves have been observed as a general component of the red pulp connective tissue scaffold, the tissue that most likely represents the reticular framework or conduit system. However, post synaptic sympathetic axons are thin (0.3-1.3 um) and single axons might have been missed during regular bright field or fluorescent microscopy. Future transmission electron microscopic studies of human spleens could elucidate whether the human reticular framework contains adrenergic nerve fibers.

## CONCLUSION

Overall, it can be concluded that, apparent age-related and interspecies differences in splenic sympathetic nerve distribution exists. It is however uncertain if and to what extent these differences are of significance for NE-ACh-TNFα mechanism based anti-inflammatory therapies in humans. Although experimental studies have shown an indisputable role for sympathetic nerves, $ChAT^+$ T cells and macrophages, it is however not completely understood how and where the various elements of the prevailing intrasplenic NE-ACh-TNFα mechanism interact and whether unknown intermediate elements are required. In order to be able to extrapolate experimental data to humans and to estimate whether targeting splenic sympathetic nerves in humans could be beneficial, additional experimental and morphological studies are required and alternative or additional mechanisms should be taken into consideration.

# II

# OMENTAL MILKY SPOTS

# 5

# A RAPID AND SIMPLE METHOD FOR VISUALIZING MILKY SPOTS IN LARGE FIXED TISSUE SAMPLES OF THE HUMAN GREATER OMENTUM

Bernadette Schurink[1]* and Cindy G.J. Cleypool[1]*, Ronald L.A.W. Bleys[1]

* Both authors contributed equally
[1]Department of Anatomy, Division of Surgical Specialties, University Medical Center Utrecht, Utrecht University, the Netherlands.

*Biotechnic & Histochemistry. 2019*

# ABSTRACT

Milky spots are unique lymphoid structures in the greater omentum that participate in both immune homeostasis of the peritoneal cavity and formation of omental metastases. We developed a rapid and simple staining method to enable macro- or stereomicroscopic identification of these miniscule structures in large samples of fixed human greater omentum. By immersing approximately 6 x 4 cm samples of omental tissue in hematoxylin, these samples could be evaluated quickly for the presence of milky spots. We used an alum hematoxylin variant containing 1 g hematoxylin, 50 g aluminium ammonium sulfate, 0.2 g sodium iodide, 1 g citric acid and 50 g chloral hydrate. This staining method enabled us to determine the number, location, dimensions and topographical relation of milky spots to other structures. Our method also facilitates isolation of milky spots for further investigation. Hematoxylin imparts a blue color to the milky spots, which remain in place during further processing for paraffin embedding. This enabled easy recognition of these small structures during transfer through various solutions and permitted selection of relevant paraffin slides prior to additional staining.

# INTRODUCTION

The greater omentum is important for peritoneal immune homeostasis (Hall et al., 1998). Milky spots (MS) are lymphoid structures in the omentum that contribute to this function. MS consist of small aggregates of macrophages, and B- and T-cells often arranged around omental glomerular like vascular structures directly beneath the mesothelium (Krist and Eestermans, 1995)(Liu et al., 2015) (Shimotsuma et al., 1991). MS also can be found in other serous membranes including pleura and pericardium (Cruz-Migoni and Caamano, 2016)(Michailova and Usunoff, 2004).

Owing to their small size (349–756 μm) (Shimotsuma et al., 1991) lack of clear macroscopic characteristics or distinct color, they cannot be readily identified by inspection of fresh or fixed adult human greater omentum. This hampers evaluation of their anatomical configuration, distribution and complicates isolation of MS for further microscopic studies to evaluate their role in pathological processes. We developed a rapid and simple hematoxylin staining method to optimize identification of MS in large samples of human greater omentum to facilitate determination of the number, location and topographical relation to other structures and to enable targeted isolation of MS for further microscopic investigation.

# MATERIALS & METHODS

The greater omenta of two female human cadavers (75 and 77 years old) were used. The subjects entered the Anatomy Department of the University Medical Center Utrecht, the Netherlands through the body donation program. Informed consent was obtained prior to death.

The entire body was preserved by perfusion through the femoral artery with 3% formaldehyde. Both omenta were inspected macroscopically in situ. One omentum showed adhesions to the ventral body wall that could be explained by a 10 cm midline scar running from the pubic bone toward the umbilicus. The other omentum showed no adhesions with surrounding structures. Both omenta were detached from the transverse colon, then stored in 0.1 M phosphate buffer, pH 7.4, containing 15% sucrose (PBS/Sucrose buffer) until further investigation.

Samples of omentum approximately 6 by 4 cm were removed and immersed in hematoxylin for 7 min followed by rinsing for 10 min in running tap water (Figure 1A, B). We used an alum hematoxylin variant ( Gill 2010; Baker 1962) (referred to below as “hematoxylin”) that was prepared as follows: 50 g aluminum ammonium sulfate was dissolved in 1 l distilled water after which 1 g hematoxylin (hematoxylin monohydrate, 1159380025, Merck KGaA, Darmstadt, Germany) was added while heating, then 0.2 g sodium iodide was added to the hematoxylin solution together with 1 g citric acid and 50 g chloral hydrate. This solution was stirred overnight at room temperature on a magnetic stirrer. The hematoxylin solution was filtered prior to each staining session.

A stereomicroscope (Leica EZ4, Nussloch, Germany) with both transmission and incident light was used for detailed assessment of hematoxylin stained omentum samples. MS were identified (Figure 1C), removed and placed in PBS/Sucrose buffer until further processing for microscopic investigation.

## Immunohistochemistry

MS were processed for paraffin embedding by dehydrating them through increasing concentrations of ethanol, clearing them in xylene (these steps should be no longer than 45 min to prevent wash

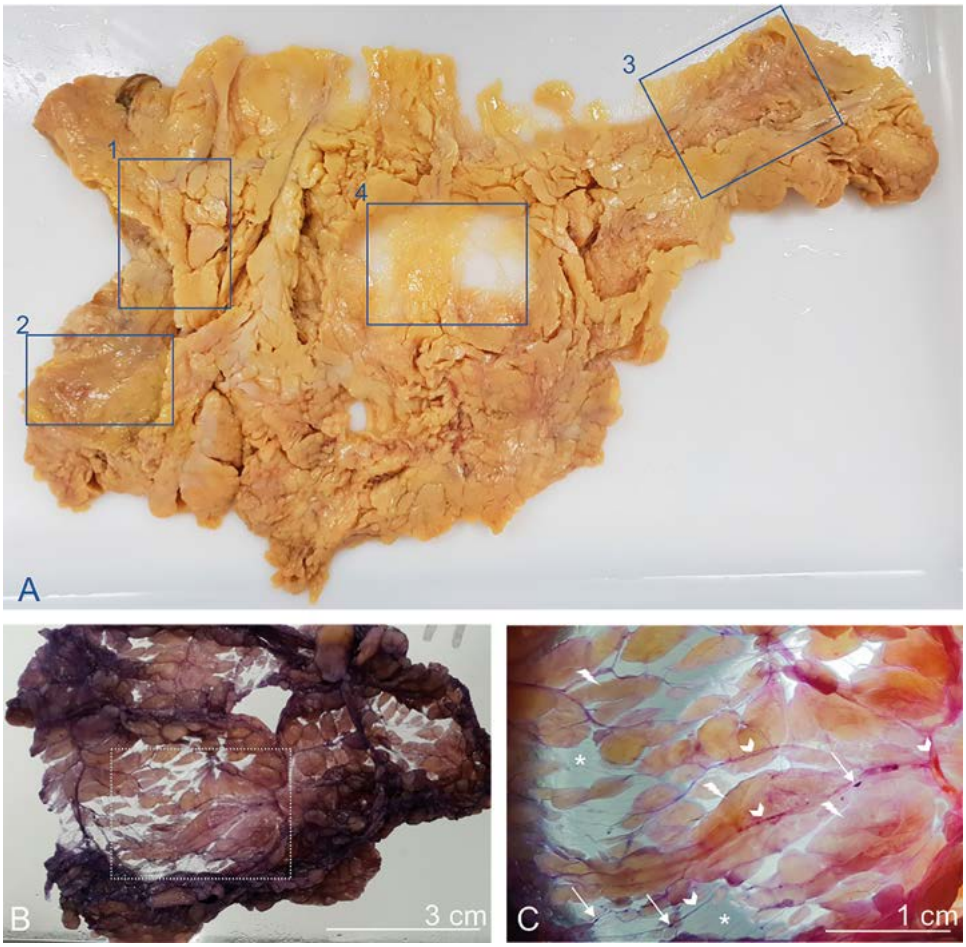


**Figure 1. Fixed omentum and a large hematoxylin stained omentum sample of 75-year-old female cadaver.** **A**) The omentum contains a moderate amount of adipose tissue and only a few translucent parts. Various large samples (1–4) were removed and stained with hematoxylin. **B**) Omental sample at location (4) after hematoxylin staining. **C**) Stereomicroscopic image of the boxed region in Panel (**B**). Blood vessels can be identified (arrowheads) as well as small yellowish adipose tissue lobes. Thunderbolts, adipose tissue lobes; *, translucent regions; arrows, small dark blue stained areas (representing MSs) surrounding blood vessels.

out of hematoxylin) and embedded in paraffin. Hematoxylin staining remained stable, which enabled easy recognition of small tissue samples that contained MS during dehydration, embedding and sectioning. Sections were cut at 5 µm using a microtome (Leica 2050 Super Cut) and placed on glass slides. After placing paraffin sections on a hot plate at 60 °C for 2 h, bright field microscopic evaluation was used to select sections that contained MS. The initial hematoxylin staining remained weakly visible, which facilitated identification of MS after paraffin embedding and immunohistochemical staining. Counterstaining with hematoxylin was applied after immunohistochemistry to enhance contrast.

To confirm that the identified structures were MS, paraffin sections were stained with antibodies raised against macrophages (CD68), T cells (CD3), and B cells (CD20), which are the main cellular constituents of a human MS (Liu et al., 2015)(Shimotsuma et al., 1991). Sections were deparaffinized and rehydrated through a descending series of alcohol followed by antigen retrieval for 20 min in 95 °C citrate buffer, which was heated on a hotplate. After washing in Tris-buffered saline (TBS) with 0.05% Tween (TBS/Tween), sections for B and T cell staining were pre-incubated with 5% normal human serum for CD 20 and 3% normal goat serum for CD3, respectively. Sections for CD68 staining for macrophages were not pre-incubated. Sections then were incubated with primary antibodies in TBS with 3% bovine serum albumin (rabbit anti-CD3 M0452; Dako, Glostrup, Denmark) diluted 1:100 for 90 min at room temperature, mouse anti-CD20 (M0755; Dako) diluted 1:400 for 60 min at room temperature, or mouse-anti CD68 (NCL-L; Nova Castra, New Castle, UK) diluted 1:25 overnight at room temperature. Sections were washed with TBS/Tween several times and incubated for 30 min at room temperature with the conjugated secondary antibody Brightvision poly-alkaline phosphatase goat-anti-rabbit (ImmunoLogic, Amsterdam, the Netherlands) for CD3 or Brightvision poly-alkaline phosphatase goat-anti-mouse (ImmunoLogic) for CD20 and CD68. After incubation with the secondary antibody, all sections were washed with TBS and incubated with liquid permanent red (LPR) (Dako) for 10 min. Sections then were washed with distilled water, counterstained with hematoxylin, prepared as described above, air dried at 60 °C for 90 min and coverslipped using Entellan (Merck). Negative controls were obtained by incubation of MS slides with TBS-3% BSA without primary antibodies. Human spleen sections were used as positive controls for all three immune cell markers.

### Image acquisition

Bright field and fluorescence single images were captured at various magnifications using a Leica DM6 microscope with a motorized scanning stage, a Leica I3 fluorescent filter, a Leica DFC7000 T camera and Leica LASX software.

## RESULTS

No MS could be identified in the samples of greater omentum prior to staining with hematoxylin. After hematoxylin staining, however, dark blue spots could be recognized as MS, (Figure 2A–C). Under the stereomicroscope, these blue spots were composed of dense clusters of cells with

moderate size round nuclei that most likely were lymphocytes (Figure 2D). By stereomicroscopy, these clusters could be categorized into three types according to their relation to other structures: 1) adjacent to reticular fibers bordering adipose tissue lobes, 2) superficial in adipose tissue lobes and 3) surrounding blood vessels (Figure 3). The second type was more common in the omentum with the most adipose tissue; the remaining two types were seen mostly in translucent areas of the omentum with the least adipose tissue. The latter two were identified most easily.

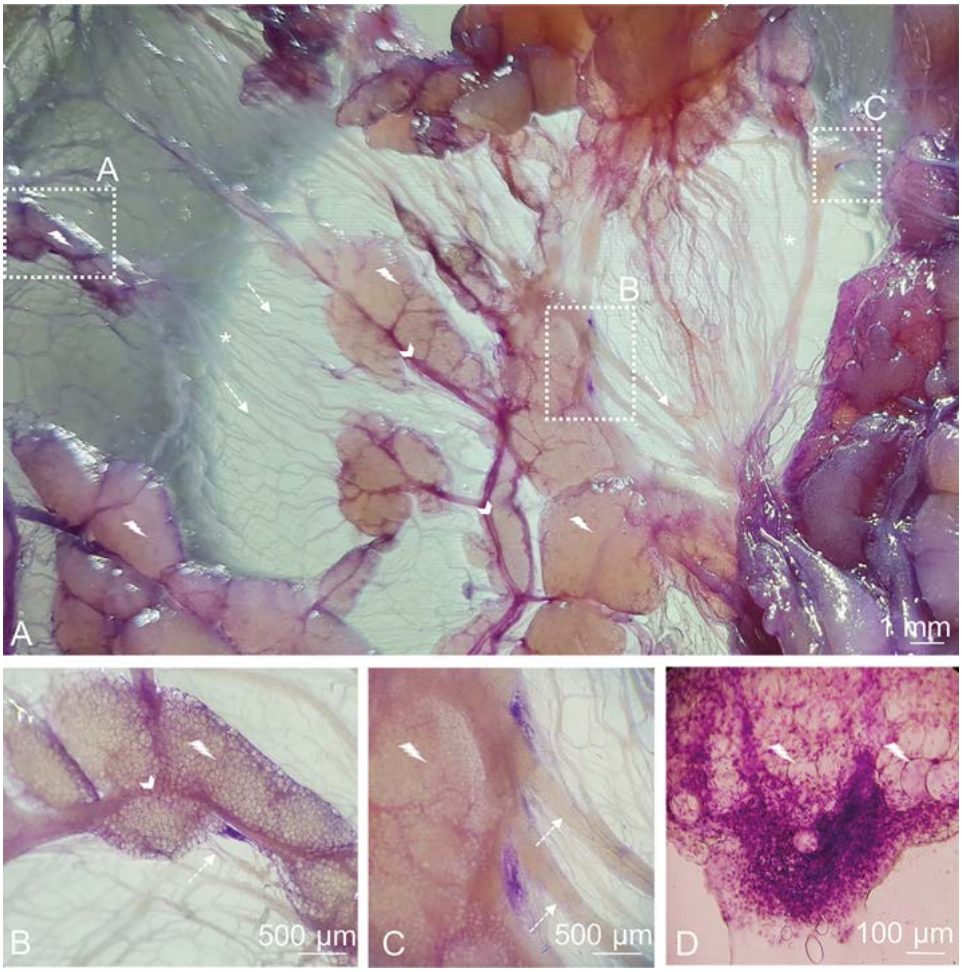


**Figure 2. Hematoxylin stained omentum at location 3 showing a small translucent area with MS. A**) Overview of omental tissue with little adipose tissue. Arrowheads, blood vessels; thunderbolts, small lobes of adipose tissue; *, translucent regions; dotted arrows, reticular fibers. Bordering translucent areas are small MS adjacent to adipose tissue lobes (dotted boxed regions). **B**, **C**) Low power magnifications of boxed regions in (**A**) and (**B**). Dotted arrows, MS adjacent to reticular fibers bordering adipose tissue (thunderbolts are positioned centrally in the adipose tissue). **D**) High power magnification of boxed region in (**C**) showing dense cluster of cells of moderate size and round nuclei at the surface of adipose tissue. Individual adipocytes are indicated by thunderbolt.

Immunohistochemical staining for CD 68, CD3 and CD 20 confirmed that the cell clusters identified were composed of the following cells in increasing number: macrophages, T-cells and B-cells, which are the main components of MS (Figure 4). The MS always were located superficially and positioned immediately beneath the mesothelium. They were in close proximity to adipocytes and contained vascular structures.

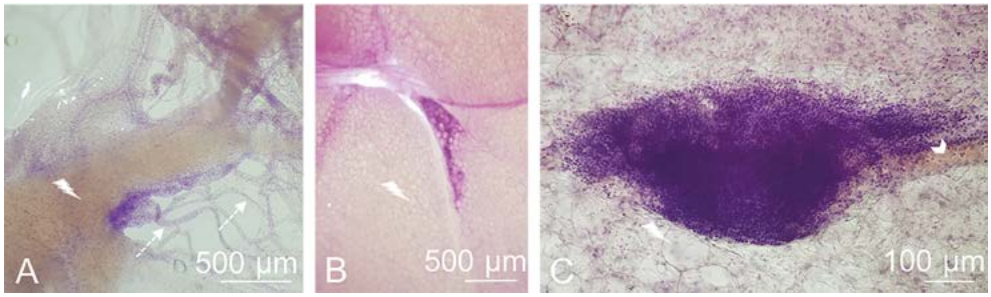


**Figure 3. Various MS types. A**) Small MS bordering a translucent area with fine reticular fibers (dotted arrows) on one side and adipose tissue (thunderbolt) on the other side. **B**) Small superficial MS at the apex of moderate adipose tissue lobe (thunderbolt). **C**) Large perivascular MS (arrowhead indicates a blood vessel), surrounded by large adipocytes (thunderbolt indicates an individual large adipocyte).

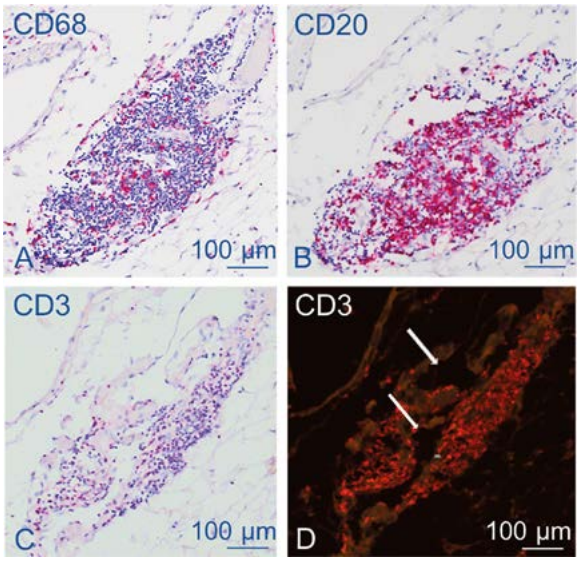


**Figure 4. Images of adjacent slides of a perivascular MS surrounded by adipose tissue. A**) Bright field image of staining with anti-CD68. Bright pink-stained cells show immunoreactivity for the specific antibody and represent macrophages. Purple/blue stained structures are nuclei. **B**) Bright field image of staining with anti-CD20. Bright pink-stained cells are B cells. Purple/blue stained structures are nuclei **C**) Fluorescent image of staining with anti-CD3. Orange-stained cells are T cells. Arrows indicate vascular structures that are identified more easily in the fluorescent images than in bright field images.

# DISCUSSION

We found that after immersing samples of human greater omentum in hematoxylin, MS could be identified readily at both macro- and stereomicroscopic levels. Our method enables determination of number of MS and their location, dimensions and topographical relations with other structures; it also enables isolation for further studies.

MS are lymphoid structures that are located directly beneath the omental mesothelium; these structures participate in peritoneal immune defence (Hall et al., 1998). In addition, MS are primary implantation sites for peritoneal exfoliated cancer cells and therefore for omental metastasis (Hagiwara et al., 1993)(Tsujimoto et al., 1995, 1996). To study the contribution of MS to the processes described above, targeted isolation and microscopic investigation of their lymphoid structures is required. Shimotsuma et al. (Shimotsuma et al. 1989) reported that MS could be identified by the naked eye as cotton wool-like structures located near the first or second branches of the gastroepiploic vessels(Shimotsuma et al. 1989)(Shimotsuma et al. 1989)(Shimotsuma et al. 1989)(Shimotsuma et al. 1989)(Shimotsuma et al. 1989)(Shimotsuma et al. 1989). We found that macro- or stereomicroscopic identification of MS was not possible. Shimotsuma et al. (Shimotsuma et al. 1989), however, included omenta from young subjects that contained more MS and less adipose tissue than older subjects, which facilitate identification of MS. Therefore, studying MS in the adult omentum, which commonly is performed at the microscopic level, requires random sampling of the omentum at different locations, followed by microscopy; this is a time-consuming process that does not ensure finding MS.

To overcome the disadvantages described above, we used hematoxylin for large fixed samples of adult greater omentum to improve visualization in situ and to enable precise sampling of MS. Hematoxylin is acidophilic and binds to acidic structures in cells such as nuclei; therefore, aggregations of cells as in MS could be identified. After staining with hematoxylin, MS were visible macroscopically as dark blue structures, whereas they could not be seen in situ without this staining. Immunohistochemical staining confirmed that these cells were macrophages and lymphocytes, which are the main cellular components of MS. During our evaluation of large pieces of greater omentum stained with hematoxylin, we observed no lymph nodes. This finding is consistent with the anatomical literature, but it is contrary to clinical articles that reported the presence of lymph nodes in the the greater omentum (Haverkamp et al., 2016)(Jongerius et al., 2014).

The method described here possesses a number of advantages. It facilitates macroscopic in situ identification of MS in large fixed tissue samples and guides isolation of these structures. Owing to the blue hematoxylin coloration, MS remained visible during dehydration prior to paraffin embedding. This facilitated recognition of minuscule isolated MS during transfer through various solutions and paraffin embedding and also helped in selecting paraffin sections that contained MS for further microscopic investigation.

Although our method enables macro- and stereomicroscopic identification of lymphoid clusters, it should be noted that hematoxylin staining does not distinguish MS from transient aggregates consisting of lymphoid cells. Additional microscopic investigation to confirm cellular composition, presence of surrounding adipocytes, covering mesothelium and vascular structures is required.

## CONCLUSION

We describe here a rapid and easy method for macro- and stereomicroscopic identification of MS in large samples of fixed adult greater omentum. Our method facilitates investigation of MS number, dimensions, distribution and three-dimensional configuration in situ, and it facilitates isolation of MS for further study.

# 6

# SYMPATHETIC NERVE TISSUE IN MILKY SPOTS OF THE HUMAN GREATER OMENTUM

Cindy G.J. Cleypool[1,*], Bernadette Schurink[1,*],
Dorinde E. M. van der Horst[1] and Ronald L.A.W. Bleys[1]

[1]Department of Anatomy, Division of Surgical Specialties, University Medical Center Utrecht, Utrecht University, the Netherlands.

*Journal of Anatomy. 2020*

# ABSTRACT

## Introduction

Omental milky spots (OMSs), small lymphoid structures positioned in the greater omentum, are involved in peritoneal immune homeostasis and the formation of omental metastases. Sympathetic nerve activity is known to regulate immune function in other lymphoid organs (e.g. spleen and lymph nodes) and to create a favourable microenvironment for various tumour types. However, it is still unknown if OMSs receive sympathetic innervation. Therefore, the aim of this study was to establish whether OMSs of the adult human greater omentum receive sympathetic innervation.

## Materials & methods

A total of 18 OMSs were isolated from 5 omenta, which were removed from 3% formaldehyde perfused cadavers (with a median age of 84 years, ranging from 64 to 94). OMSs were embedded in paraffin, cut and stained with a general (PGP9.5) and sympathetic nerve markers (TH and DBH), and evaluated by bright field microscopy. A T-cell, B-cell, and macrophage staining was performed to confirm MS identity

## Results

In 50% of the studied OMSs sympathetic nerve fibers were observed at multiple levels of the same OMS. Nerve fibers were represented as dots or elongated structures and often observed in relation to small vessels and occasionally as individual structures residing between lymphoid cells.

## Conclusion

The current study shows that 50 % of the investigated OMSs contain sympathetic nerve fibers. These findings might contribute to our understanding of neural regulation of peritoneal immune response and the involvement of OMSs in omental metastases.

# INTRODUCTION

Body cavities are lined by mesothelium and the sub mesothelial compartment of the pleura, pericardium, and peritoneum (both parietal and visceral) is known to contain lymphoid cell clusters, referred to as milky spots (MSs) (Michailova and Usunoff, 2004). The most prominently present and extensively studied MSs are the ones positioned in the omentum, hence referred to as omental MSs (OMSs). OMSs are cellular aggregates of macrophages, B-cells and T-cells (Shimotsuma et al., 1991) (J. Liu et al., 2015), which develop during ontogeny (Krist et al., 1997), are found in various animal species including humans (Michailova and Usunoff, 2004), and can be observed in large fixed omental tissue samples after staining with hematoxylin (Schurink et al., 2019) (Fig. 1). OMSs play an important role in the peritoneal immune response: 1) peritoneal fluid is absorbed via openings (stomata) in the omental mesothelial lining and gets monitored in OMSs for foreign or pathogenic substances (Wilkosz et al., 2005)(Meza-perez and Randall, 2017)(Vugt et al., 1996), and 2) OMSs form a gateway for circulating immune cells that are recruited towards the peritoneal cavity during a peritoneal immune challenge (Wijffels et al., 1992). In addition, OMSs are involved in peritoneal metastatic disease; they form primary implantation sites for peritoneal exfoliated cancer cells, which can develop into omental metastases (Krist et al., 1998)(Tsujimoto et al.,1995)(Tsujimoto et al., 1996)(Hagiwara et al., 1993).

The autonomic nervous system, and in particular sympathetic nerves, are known to be involved in local regulation of the immune response in lymphoid organs, such as the spleen and lymph nodes (Mignini et al., 2003)(Komega et al., 2018), and in creating a tumor stimulating microenvironment (Cole et al., 2015). So far only a few studies report on MS associated nerve fibers (Krist et al., 1994) (Havrlentova et al., 2017)(Yildirim et al., 2010) but none of these addressed sympathetic fibers specifically. If, like other lymphoid structures, OMSs receive sympathetic innervation, this nerve tissue, or its effectors, could hold potential as therapeutic targets to modify peritoneal immune response or tumor environment. Therefore, the aim of this study is to establish whether OMSs of the adult human greater omentum receive sympathetic innervation.

# MATERIALS & METHODS

The greater omenta of 5 human cadavers were studied. These included three male and two female cadavers with a median age of 84, ranging from 64-94 years. Bodies were donated through a body donation program to the Anatomy department of the University Medical Center Utrecht, the Netherlands. Informed consent was obtained during life, allowing the use of these bodies for educational and research purposes. No scars were observed in the abdominal region and the available medical records did not list relevant diseases such as cancerous-, immune- or neuro degenerative disease.

Whole body preservation was accomplished by perfusion with 3% formaldehyde via the femoral artery. The aprons of the omenta were resected from the transverse colon and stored in a 0.1 M

phosphate buffer, pH 7.4, containing 15% sucrose (PBS/Sucrose) at 4°C until further investigation. Of each omentum, one or two large samples of approximately 6 x 4 cm were removed. These samples were stained with hematoxylin (Schurink et al., 2019) and evaluated for the presence of OMSs with the aid of a stereomicroscope (Leica EZ4, Nussloch, Germany) (Figure 1), using both transmission and incident light. OMSs were identified, removed (with a small margin of surrounding tissue) and placed in PBS/Sucrose at 4°C until further processing for microscopic investigation. Since it is known that sympathetic nerve fibers accompany arteries towards their end organs (Mitchel 1956), omental arterial branches were studied to verify the presence of sympathetic nerve fibers in the selected omental regions. Figure 2 contains schematic images of the selected omental regions, and the amount of isolated OMSs and arterial branches per investigated omentum.

## Immunohistochemistry

OMSs and omental arteries were processed for paraffin embedding by placing them in increasing percentages of ethanol, xylene and paraffin. Paraffin blocks were cut on a microtome (Leica 2050 Super Cut, Nussloch, Germany) and 5 µm thick sections were placed on glass slides, air dried and subsequently heat fixed for two hours on a slide drying table of 60°C (Medax, 14801, Kiel, Germany).

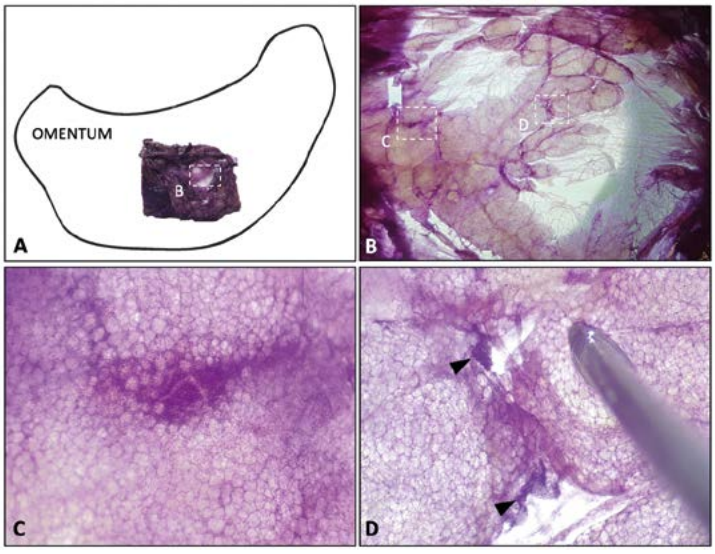


**Figure 1. Hematoxylin stained fixed human omentum.** After selection and haematoxylin staining of a large omental sample, omental milky spots (OMSs) can be observed when studied through a stereomicroscope. **A:** Schematic drawing of an omentum showing a stained area. The boxed region represents an OMS rich area that is magnified in figure B. **B:** Stereomicroscopic image of a hematoxylin stained omental sample. The omental tissue contains translucent areas and areas with fat pads composed of lobules of adipose tissue. Dark stained areas represent cell dense regions (nuclei are stained dark blue by haematoxylin). **C-D:** Magnifications of region C and D of figure B. When magnified, some dark stained areas contained dense clusters of cells with moderate size round nuclei. **C:** A moderately sized OMS composed of a cluster of lymphoid cells positioned superficial to adipocytes. A vascular structure runs through the OMS. **D:** Two smaller OMSs (black arrow heads).

Each OMS was serially cut and slides were selected at multiple levels for microscopic investigation. Of each OMS level and of each omental artery, adjacent slides were stained with antibodies against general (protein gene product 9.5 (PGP9.5)) and sympathetic (tyrosine hydroxylase (TH) and dopamine beta hydroxylase (DBH)) nerve tissue. If comparable staining patterns were present in TH- and DBH stained samples, it was assumed that immuno reactive (IR) tissue represented sympathetic nerve tissue. To confirm OMS identity, additional slides were stained for the presence of B-cells (CD20), T-cells (CD3) and macrophages (CD68), the main cellular constituents of human OMSs (Shimotsuma et al., 1991) (Liu et al., 2015). Since sympathetic regulation of splenic immune function is known to primarily involve adrenergic activation of T-helper cells (Kin and Sanders, 2006) (Olofsson et al., 2012), an additional CD4 antibody staining was performed. All slides were deparaffinized and rehydrated followed by 20 minutes of antigen retrieval in 95°C citrate buffer on a hot plate. After washing in Tris-buffered saline (TBS) with 0.05% tween (TBS/Tween), sections were pre-incubated for 10 minutes with 5% normal human or goat serum, with the exception of the ones selected for CD68 staining. After preincubation, sections were incubated with primary antibodies in TBS with 3% bovine serum albumin. Table 1 contains details of the primary antibodies. Following incubation, sections were washed with TBS/Tween and incubated for 30 minutes at room temperature (RT) with undiluted Brightvision Poly-Alkaline phosphatase Goat-anti-Rabbit (ImmunoLogic, Amsterdam, the Netherlands) in case of PGP9.5, TH, DBH and CD3 staining, or Brightvision Poly- Alkaline phosphatase Goat-anti-Mouse (ImmunoLogic, Amsterdam, the Netherlands) in case of CD20, CD68 and CD4 staining. After incubation with secondary antibodies, all sections were washed with TBS and incubated with Liquid Permanent Red (LPR) (DAKO, Glostrup, Denmark) for 10 minutes. Subsequently, tissue sections were washed with distilled water and counterstained with hematoxylin, airdried at 60°C for 90 minutes, and cover slipped using Entellan (Merck, Darmstadt, Germany). Human sympathetic trunk sections were included as positive controls for all 3 nerve markers and human spleen sections for all 4 immune cell markers. Negative controls were obtained by incubation of sympathetic trunk -, spleen - and OMSs slides with TBS-3% BSA without primary antibodies. All slides were evaluated using bright field microscopy.

### Image acquisition

Brightfield single images were captured at various magnifications using a DM6 microscope with a motorized scanning stage, a DFC7000 T camera and LASX software (all from Leica, Nussloch, Germany).

## RESULTS

OMSs could be identified in hematoxylin stained omental samples of all 5 cadavers, according to a previous description (Schurink et al., 2019). Of the 5 studied omenta, a total of 18 OMSs (2 -5 per omentum) and 7 omental arterial branches (1-2 per omentum) were sampeled and processed for microscopic evaluation. All positive controls showed expected IR patterns, whereas all negative controls were clean.

**Table 1.** Primary antibodies

| Primary antibody | | clone | Manufacturer | Reference number | Dilution | Incubation time | Temperature | Pre-incubation serum |
|---|---|---|---|---|---|---|---|---|
| PGP9.5 | Polyclonal rabbit Anti-Human | n.a. | Dako, Denmark | Z5116 | 1:2000 | 48 hrs | 4°C | 5%NHS |
| TH | Polyclonal rabbit Anti-Human | n.a. | Pelfreeze, USA | P40101 | 1:1500 | 12 hrs | RT | 5%NHS |
| DBH | Monoclonal rabbit Anti-Human | EPR20385 | Abcam, UK | AB209487 | 1:1000 | 12 hrs | RT | 5%NHS |
| CD68 | Monoclonal Mouse anti-Human | 514H12 | NovoCastra, UK | NCL-L-CD68 | 1:25 | 12 hrs | RT | NO preincubation |
| CD20 | Monoclonal Mouse anti-Human | L26 | Dako, Denmark | M0755 | 1:400 | 60 min | RT | 5%NHS |
| CD3 | Polyclonal Mouse anti-Human | n.a. | Dako, Denmark | A0452 | 1:50 | 90 min | RT | 5% NGS |
| CD4 | Monoclonal Mouse anti-Human | 4B12 | Dako, Denmark | M7310 | 1:25 | 120 min | RT | 5% NGS |

## Omental milky spots

All 18 selected OMSs showed specific microscopic morphological OMS features. They were composed of clusters of lymphoid cells, contained blood vessels, and were surrounded by adipose tissue (J. Liu et al. 2015)(Wilkosz et al. 2005)(Shimotsuma et al. 1989)(Meza-perez and Randall 2017). The median diameter of these OMSs was 379 µm, ranging from 139 to 1150 µm. TH-IR was present in 9 out of 18 OMSs (50%). Figure 2 contains schematic drawings of the investigated omenta including the number of studied OMSs and whether they contained sympathetic nerve fibers.

Four out of five omenta contained TH-IR fibers in 25-100 % of their investigated OMSs. Only 1 cadaver showed no TH-IR fibers in any of its OMSs. TH-IR in OMSs was observed as individual small spots (Fig. 3A-F), or as elongated structures with a dotted appearance resembling varicosities (encircled structures in Fig. 3B). In all TH-IR OMSs, immune labelling was observed at all studied levels of the same OMSs and in comparable regions. TH-IR structures were often closely related to small OMS blood vessels, but was also present as individual structures in close proximity to lymphoid cells (Fig. 3). TH-IR patterns were highly comparable with PGP9.5-IR patterns, suggesting that TH-IR

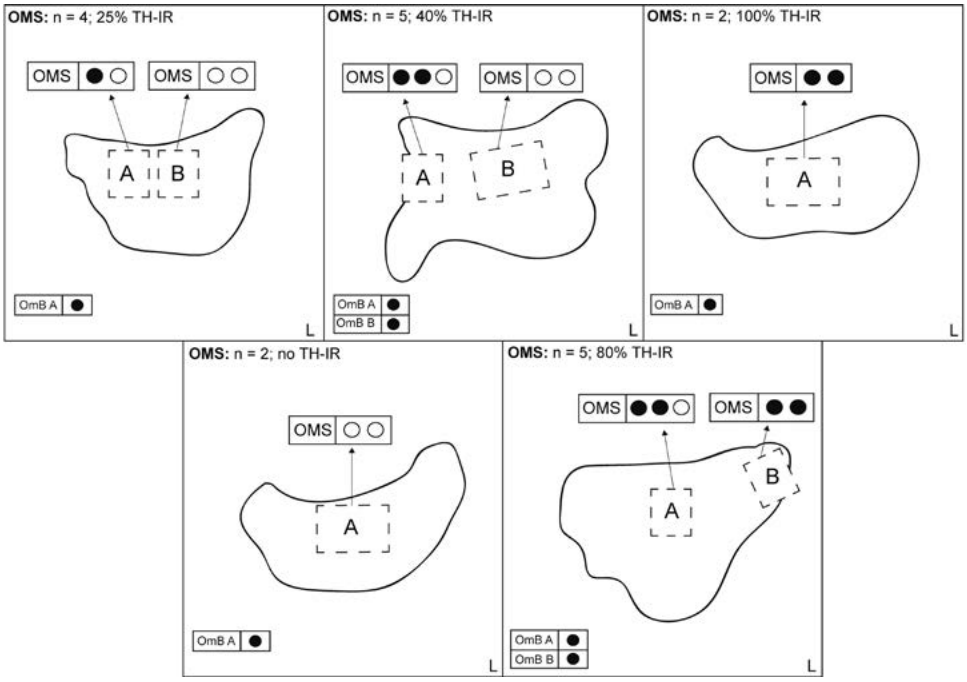


**Figure 2. Schematic representation of studied omenta.** The selected regions of each omentum are boxed and marked (**A** or **B**). Per region, the number of ometal milky spots (OMSs) is depicted by dots (black dots represent OMSs with TH-immune reactive (IR) nerve fibers). In the left upper corner of each frame, the number of stained OMSs is listed, including the % of OMSs with TH-IR nerve fibers. In the left lower corner of each frame, the number of studied omental branches is depicted as dots (black dots represent omental branches with TH-IR nerve fibers). **n**: number, **OmB**: omental arterial branch.

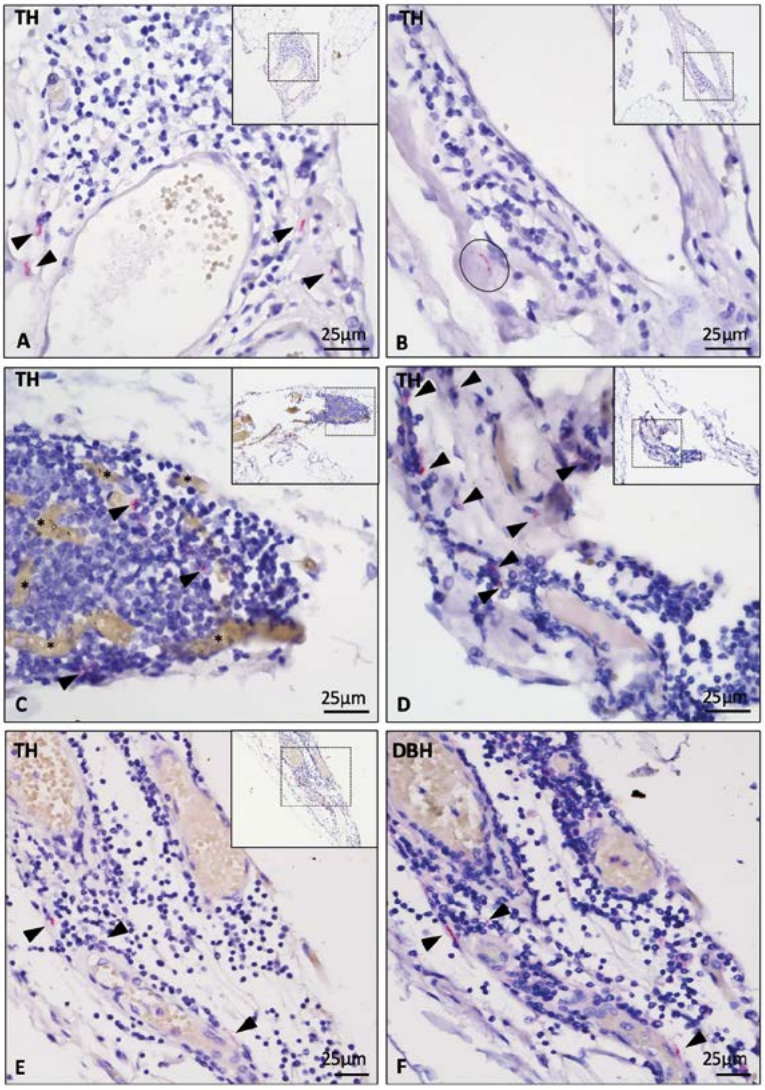


**Figure 3. Sympathetic nerve structures in different milky spots.** Each image contains an inlay with an overview image of the omental milky spot (OMS) and its surroundings. TH-IR structures are stained pink (indicated with black arrow heads) and cell nuclei are stained dark blue. **A:** OMS of a male cadaver of 94 years of age. TH-immune reactive (IR) structures can be observed as discrete structures or in close proximity to immune cells. **B:** OMS of a male cadaver of 94 years of age. An elongated TH-IR structure (encircled), with a dotted appearance, most likely representing varicosities, is present in close proximity to immune cells of the OMS. **C:** OMS with a high cellular density of a female cadaver of 84 years of age. Many vascular structures can be observed within the OMS (asterisk). TH-IR structures were observed primarily in close proximity to immune cells. **D:** OMS of a female cadaver of 84 years of age. Few TH-IR structures can be observed, which were in close proximity to lymphocytes. **E:** MS of a male cadaver of 88 years of age. TH-IR structures were observed in relation to a blood vessel, but small TH-IR structures were in close proximity to immune cells as well. **F:** The same OMS as in E but stained for DBH. Staining patterns of E and F are comparable supporting the fact that TH-IR structures represent sympathetic nerve tissue.

represented neural structures. TH-IR patterns were comparable to DBH-IR patterns. Therefore, it was confirmed that these neural structures were adrenerg and not dopaminerg.

### Immune cells

All OMSs were composed of B cells, T cells, and macrophages, confirming their OMS identity (Fig. 4B-D). CD4 staining was performed on slides of all TH-IR OMSs and CD4 positive cells were clearly present and distributed homogenously in 3/4 cadavers with TH-IR OMSs (Fig. 4E). In 1 cadaver, no CD4-IR cells could be observed in any of the 3 TH-IR OMSs.

### Omental branches

From each of the 5 cadavers, 1-2 omental arterial branches were studied, resulting in a total number of 7 branches. PGP 9.5 - , TH- and DBH-staining showed comparable patterns and sympathetic nerve fibers were observed in all studied omental arterial branch samples, either as discrete fibers or in bundles. Discrete nerve fibers were present in the adventitia up to the level of the adventitial-medial border in all omental branches, representing intrinsic vessel wall innervation (Fig. 5A-B). In 5/7 omental arterial branches, nerve bundles were observed in the adventitia or surrounding connective tissue, representing nerve fibers accompanying these arteries towards more distal omental structures (Fig. 5A-B).

## DISCUSSION

This study shows that human omental OMSs contain sympathetic nerve fibers. Often, these nerve fibers were located around small blood vessels and occasionally individual nerve fibers were observed between lymphoid cells. By means of TH, confirmed by DBH staining, sympathetic fibers were observed in 50% of the studied OMSs. The absence of TH-IR inside the other OMSs is not likely to be explained by either poor or excessive formaldehyde fixation, since TH-IR fibers and bundles have been observed in tissue surrounding these OMSs and omental arterial branches. An age related decrease of sympathetic tissue in OMS of our relatively old study subjects (median age of 84 years) would be a more plausible explanation as sympathetic nerve tissue of secondary lymphoid structures is known to decline with age (Bellinger et al., 1992).

So far, only three other studies have described nerve tissue associated with OMSs. In 2 of these studies a general nerve marker (S-100) was used and the type of nerve tissue was not further specified (Havrlentova et al., 2017)(Yildirim et al., 2010). Although these studies visualized small S-100-IR nerve bundles closely related to blood vessels, in between adipocytes or in the surrounding connective tissue, they do not describe small neural structures in close proximity to lymphoid cells. This in contrast to the results of the current study, in which fibers were observed in relation with lymphocytes. The third study, used transmission electron microscopy in combination with a dopamine (DA) marker to study innervation of OMSs in two patients under the age of 28 years with unaffected omenta. The authors observed non-myelinated nerve fibers in the OMSs of both subjects

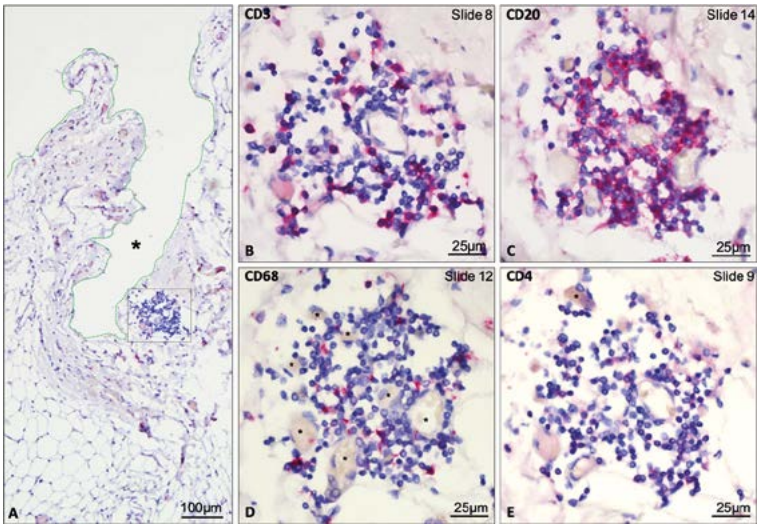


**Figure 4. Immune cells presence in an omental milky spot.** The panel is composed of images of the same omental milky spot (OMS) stained for various immune cells. **A:** Overview image of omental tissue containing a OMS (cell dense region in boxed area) with surrounding adipose tissue. The OMS is positioned directly underneath the mesothelial lining (green dotted line) of the omentum. The abdominal cavity is marked with a large black asterisk. Additional slides were stained to visualize **B:** T-cells (CD3), **C:** B-cells (CD20), **D:** macrophages (CD68) and **E:** T-helper cells (CD4). IR structures are stained bright pink and cell nuclei are stained dark blue. Small vascular structures can be discriminated inside the OMS by the presence of erythrocytes which give the vessel lumina a brownish colour (as shown with small black asterisks in D).

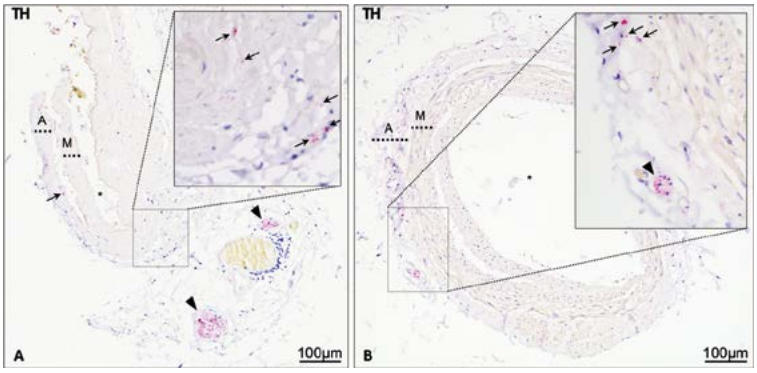


**Figure 5. Omental arterial branches supplying areas of the greater omentum of which milky spots were selected for investigation.** TH-immune reactive (IR) structures are stained pink and cell nuclei are stained dark blue. Both images (A-B) show an omental arterial branch with associated sympathetic nerve tissue. Paravascular positioned nerve bundles (arrow heads) run with arteries towards their final destination. Discrete nerve fibers (arrows) innervate the blood vessel wall and can be observed in the adventitia up to the adventitial-medial border. **A:** Omental arterial branch of a female cadaver of 84 years of age. **B:** Omental arterial branch of a male cadaver of 88 years of age with a thickened intima. **Asterisk:** blood vessel lumen, **A:** Tunica adventitia, **M:** Tunica media

(Krist et al., 1994). These nerve fibers contained DA-IR vesicles and the authors concluded them to be dopaminergic. However, DA is a precursor for NA and the nerve tissue could represent both dopaminergic and noradrenergic fibers. In the current study the commonly accepted adrenergic nerve marker TH and a marker for dopamin beta-dehydroxyase (DBH), the enzyme involved in conversion of DA to NA, were used on adjacent slides of both OMSs and omental arterial branches. TH staining patterns were comparable to DBH staining patterns suggesting the present nerve tissue to be adrenergic. However, since no double staining was performed, the presence of dopaminergic fibers could not be excluded. Furthermore, the transmission electron microscopic study of Krist *et al* revealed non-myelinated nerve endings to be in close proximity to immune cells (Krist et al., 1994), a finding which is in line with the results of the current study. Previously, this finding led to the suggestion that these nerves might modulate immune cell function by the release of their neurotransmitter. The suggestion that this nerve tissue could modify immune cell function is highly interesting since it opens new opportunities for anti-inflammatory therapies. The concept of neural structures modifying immune function is known as neuroimmunomodulation. It is acknowledged that the sympathetic nervous system plays an important role in regulation of the systemic inflammatory response via the spleen (Komega et al., 2018). Activation of sympathetic nerve tissue of the splenic plexus results in a cascade of intrasplenic events, starting with the release of norepinephrine (NE) (Kees et al., 2003) followed by adrenergic receptor activation on CD4 positive T cells (Vida et al., 2017)(Rosas-Ballina et al., 2011)(Vida et al., 2011), which results in production and secretion of acetylcholine and ultimately inhibits the release of pro-inflammatory cytokines from activated macrophages (Lu and Kwan, 2014)(Borovikova et al., 2000)(de Jonge et al., 2005)(Kox et al., 2009). This results in dampening of the systemic inflammatory response. Since OMSs are known to contain macrophages (Shimotsuma et al., 1991)(Liu et al., 2015) and the current study shows OMSs to receive sympathetic innervation, and to contain CD4 positive T cells, all required elements for neuroimmunomodulation appear to be present. Therefore, stimulation of sympathetic fibers of the greater omentum could result in dampening of the peritoneal immune response, which could be beneficial during peritoneal sepsis.

In addition to its possible role in neuroimmunomodulation, sympathetic innervation of OMSs might also be involved in the formation of peritoneal metastases. According to the seed and soil theory, as first proposed by Paget in 1889, tumor cells (seeds) have a specific affinity for certain organs or structures (soil); metastasis would only develop if both seed and soil are compatible (Paget, 1889). MSs provide such a favorable soil for certain abdominal tumors (Krist et al., 1998)(Tsujimoto et al., 1995)(Tsujimoto et al., 1996)(Hagiwara et al., 1993). Why OMSs provide a hotspot for peritoneal metastases is not fully elucidated yet. Previous studies have suggested a contributive role of OMS specific mesothelium and blood vessels (Gerber et al., 2006) or adipocytes (Ladanyi et al., 2018). We propose an additional role for sympathetic innervation of OMSs. The sympathetic nerve system and specifically its neurotransmitter noradrenalin are known 1) to contribute to a favorable tumor microenvironment by e.g. affecting stromal cells, endothelial cells, and tumor-associated macrophages (Magnon et al., 2013), and 2) to stimulate tumor cell proliferation, via beta (ß) adrenergic receptors on tumor cells (Coelho et al., 2017). Since all of these processes are mediated

via adrenergic receptors, the effects of (ß) adrenergic blocking as a potential anti-tumor therapy have been investigated in *in vitro*, animal and retrospective patient studies with promising results (Coelho et al., 2017)(Magnon et al., 2013)(Zahalka et al., 2017). Although further studies are needed to elucidate the exact antitumor mechanism, these findings suggest a potential role for ß blockers in the treatment of cancer. As a potential therapeutic application, ß blockers could be administered to the peritoneal cavity, discrete or as an adjuvant in hyperthermic intraperitoneal chemotherapy (HIPEC), which might limit or prevent intraperitoneal spread and growth of tumor cells.

In order to elucidate the role of sympathetic innervation of OMSs in the peritoneal immune response and metastatic disease, and, on its therapeutic potential, further studies are needed. These studies should include omenta from younger individuals to avoid age related decrease of innervation and investigate the amount and location of sympathetic nerve tissue. Furthermore, these studies should investigate the (synaptic) relation of sympathetic nerve fibers with various OMS cell types such as immune – and stromal cells, as well as the presence and type of adrenergic receptors on these cells. Although the current study focused on MSs in the greater omentum, similar structures, often referred to as extraomental MSs, can be found in the peritoneum, mesenterium, mediastinum, pericardium and pleura (Cruz-Migoni and Caamano, 2016)(Michailova and Usunoff, 2004). Since these structures are involved in local immune activity (Cruz-Migoni and Caamano, 2016), including them in future studies is recommended.

# CONCLUSION

In conclusion, this study showed that human OMSs are sympathetically innervated. Nerve fibers were observed in relation to both blood vessels and lymphocytes. The presence of sympathetic fibers in OMSs contributes to our understanding of how OMS immune function might be regulated during an abdominal immune challenge and why they form primary implantation sites for peritoneal exfoliated cancer cells.

# 7

# DISCRIMINATIVE MORPHOLOGICAL HALLMARKS FACILITATING DISTINCTION OF OMENTAL MILKY SPOTS AND LYMPH NODES

Cindy G.J. Cleypool[1], Claire Mackaaij[1], Bernadette Schurink[1,2,*], and Ronald L.A.W. Bleys[1,*]

*Both authors contributed equally
[1] Department of Anatomy, Division of Surgical Specialties, University Medical Center Utrecht, Utrecht University, the Netherlands.
[2] Department of Pathology, Amsterdam University Medical Centre, Free University of Amsterdam, the Netherlands.

*Histology & Histopathology. 2020*

# ABSTRACT

## Introduction

Omental milky spots (OMSs) are the primary lymphoid structures of the greater omentum. However, the presence of lymph nodes (LNs) has occasionally been mentioned as well. Understanding which lymphoid structures are present is of significance, especially in gastric tumor metastasis; tumor deposits in omental LNs suggest local lymphatic spread, whereas tumor deposits in OMSs suggest peritoneal spread and hence extensive disease. Since LNs and OMSs share morphological characteristics and OMSs might be wrongly identified as LNs, reliable hallmarks facilitating easy discrimination are needed.

## Materials & methods

A series of microscopic morphological hallmarks unique to LNs were selected as potential candidates and were assessed for their discriminative capacity: 1) capsule, 2) trabeculae, 3) subcapsular sinus, 4) afferent lymphatic vessels, 5) distinct B and T cell regions, and 6) a layered organization with, from the outside in a capsule, cortex, paracortex, and medulla. These hallmarks were visualized by multiple staining techniques.

## Results

Hallmarks 1, 2 5 and 6 were shown to be the most efficient as these were consistent and discriminative. They were best visualized by Picrosirius red, smooth muscle actin and a B cell / T cell double staining.

## Conclusion

The presence of a capsule, trabeculae, distinct B and T cell regions and a layered organization represent consistent and reliable morphological features which allow to easily distinguish LNs from OMSs, especially when applied in combination.

# INTRODUCTION

The greater omentum is the largest peritoneal fold in the human body. In addition to functioning as a fat depot, it has an important role in peritoneal immune homeostasis (Vugt et al. 1996)(Meza-perez and Randall 2017). The lymphoid structures involved in the peritoneal immune function are omental milky spots (OMSs). These aggregates of B, T cells, and macrophages (Shimotsuma et al. 1991)(J. Y. Liu et al. 2015) are located under the mesothelial surface and are in direct contact with the peritoneal cavity via stomata (Wilkosz et al. 2005). This enables OMSs to closely monitor the peritoneal fluid and provide a swift response to imminent threat (Meza-perez and Randall 2017). Although OMSs are the primary omental lymphoid structures, the omentum is considered to contain lymph nodes (LNs) as well (Koppe et al. 2014)(Haverkamp et al. 2016). This is contradicted by anatomical reference works, which state their absence in the omentum (Liebermann-Meffert 2000). This discrepancy is most likely based on the fact that during microscopic evaluation of Hematoxylin/Eosin (HE) stained slides of resected omenta, OMSs may wrongly be identified as LNs as they share morphologic characteristics. Since LNs monitor lymph and not peritoneal fluid, their presence in the omentum might carry important consequences from both a fundamental physiological and a clinical point of view. This is especially the case when considering the role of LNs in gastric tumor metastasis; tumor deposits in omental LNs suggest lymphatic spread, whereas tumor deposits in OMSs suggest peritoneal spread and hence extensive disease, which is associated with a more severe clinical outcome. Thus, verification of the presence of omental LNs could contribute to our general understanding of omental function and in determining the radicality of oncological resections and additional therapy. Therefore, distinguishing LNs from OMSs is of significance. Although morphological differences between these structures have been mentioned in the past (Seifert 1923), these were never studied for their reliability with respect to their discriminative capacity. Therefore, this study aims to determine a set of reliable morphological criteria that facilitate their discrimination at a microscopic level.

# MATERIALS & METHODS

## Study design

The literature was studied from which a list of morphological OMS and LN characteristics was distilled (Table 1). In the past, a capsule, sinuses and germinal centers have been proposed to represent distinctive morphological characteristics that discriminate LNs from OMSs (Seifert 1923). These, and supplementary discriminative hallmarks were selected and assessed for their discriminative capacity regarding LNs and OMSs in microscopic tissue slides. The selected hallmarks were: 1) capsule, 2) trabeculae, 3) subcapsular sinus (SCS), 4) afferent lymphatic vessels in relation to the capsule / SCS, 5) distinct B- and T cell regions, and 6) a layered organization with, from the outside in, a capsule, cortex, paracortex, and medulla (Table 2 contains detailed definitions). These hallmarks are considered to be reliable, independent of the plane or level of the section, and easily recognizable at a microscopic level after staining with commonly used histochemical and

immunohistochemical staining methods. HE staining was used to provide a general tissue overview and to determine the presence of a capsule, trabeculae, and SCS. As the lymph node capsule and trabeculae are composed of dense collagen fibers, a PSR that specifically stains collagen type I, II, and III (Junqueira, Binolas, and Brentani 1979) was used to study their presence. Since the capsule and trabeculae contain smooth muscle cells (Furuta 1948)(Folse, Beathard, and Granholm 1975), a smooth muscle actin (SMA) staining was applied as well. The SCS as well as afferent - and efferent lymph vessels were distinguished from blood vessels by means of a double immunohistochemical staining that stains for Podoplanin (a lymph vessel specific endothelial protein), also referred to as D2-40, and von Willebrand factor (vWF) (a blood vessel specific endothelial marker). LNs show distinct T and B cell areas, whereas OMSs show a more homogeneous distribution of these cells. A double immunohistochemical staining method, staining for CD3 (a co-receptor on T cells) and for CD20 (a B cell specific antigen) was applied to study lymphocyte distribution pattern.

## Tissue isolation, preparation and staining

Four LNs and four OMSs were isolated from eight different 3% formaldehyde perfusion fixed cadavers which included four male and four female cadavers with a median age of 87, ranging from 83-91 years. Bodies were donated through a body donation program to the Anatomy department of the University Medical Center Utrecht, the Netherlands. Informed consent was obtained during life,

**Table 1.** Morphological characteristics of lymph nodes and omental milky spots.

| | **Lymph nodes** (Seifert, 1923; Willard-Mack, 2006; Miranda et al., 2013; Buscher et al., 2016; Tubbs, 2016) | **Omental milky spots** (Seifert, 1923; Krist and Eestermans, 1995; Liebermann-Meffert, 2000; Platell et al. 2000; Mebius 2009; Buscher et al. 2016) |
|---|---|---|
| **Location** | Spread throughout the body | Underneath the mesothelial lining of the omentum |
| **Size (cross section)** | 0.1 – 2.5 cm | 349 – 756 µm |
| **Stromal compartment** | | |
| Capsule | ✓ | — |
| Trabeculae | ✓ | — |
| Reticulum | | |
| Follicular dendritic cells | ✓ | — |
| Fibroblast reticular cells | ✓ | — |
| Layered organization | ✓ | — |
| **Lymphatic compartment** | | |
| Afferent lymph vessels | ✓ | — |
| SCS | ✓ | — |
| Efferent lymph vessel | ✓ | ✓ |
| **Vascular compartment** | | |
| High endothelial venules | ✓ | ✓ |
| Glomeruli like vessels | — | ✓ |

**Table 2.** Definitions of the selected LN specific morphological characteristics

| | |
|---|---|
| **Capsule** | A solid dense layer of fibrous connective tissue containing collagen type I and fibroblasts with some filaments of smooth muscle cells amongst them (Furuta, 1948) (Folse et al.,1975) surrounding the lymph node. This capsule is approximately 25-50 um thick and completely thins out towards the hilum, where the collagenous fibers are incorporated with those of the hilar stroma (Furuta, 1948). At the hilum the identity of the cortical capsule is lost and the fibrous connective tissue becomes areolar (Furuta, 1948). |
| **Trabeculae** | Extensions of the capsule penetrating the lymph node. Their composition is comparable to the capsule, including smooth muscles cells (Folse et al., 1975) |
| **SCS** | Located beneath the lymph node capsule and encircles the entire node. The endothelium that lines the SCS is continuous with that of the afferent lymphatic vessels, carrying the morphology of lymphatic endothelial cells (Louie and Liao, 2019). A layer of macrophages lines the SCS |
| **Afferent lymphatic vessels** | Lymphatic vessels that pierce the capsule and drain into the SCS (Young et al., 2013) (Louie and Liao, 2019) |
| **Distinct B- and T cell regions** | The outer cortex contains B-cell lymphoid follicles. They can either be in a resting state (primary follicle) or activated in response to an antigen (secondary follicle). The paracortical zone is densely packed with T-cells (Young et al,. 2013) |
| **Layered organization** | LNs show a layered organization which can be found at any part of the LNs with the exception of the hilum. This layered organization comprises, from the outside, a capsule, a cortex with spherical follicles of B-cells, a paracortex containing T-cells, and a vessel rich medulla (Willard-Mack, 2006) |

allowing the use of these bodies for educational and research purposes. LNs were collected from four different cadavers and from four different regions (one from each region): the mediastinum, mesentery, inguinal area, and pancreas. The selection of these regions was random and determined by the approachability during a gross anatomy dissection course at the time the study was initiated. OMSs were isolated from four different omenta according to a previously described procedure (Schurink et al., 2019). None of the cadavers showed clinical signs which might suggest activation of the selected LNs and OMSs. All lymphoid structures were processed for paraffin embedding by placing them in increasing percentages of ethanol, xylene and paraffin. Paraffin blocks were cut on a microtome (Leica 2050 Super Cut, Nussloch, Germany) and 5 µm thick sections were placed on glass slides, air dried, and subsequently heat fixed for two hours on a slide drying table of 60°C (Medax, 14801, Kiel, Germany). All slides were deparaffinized and rehydrated and further processed for histochemical – or immunohistochemical staining.

## Histochemical staining (HE and PSR)

HE staining was routinely performed on all specimens. PSR staining was performed by placing slides in picrosirus red solution (1 mg Sirius Red F3B (BDH Chemicals, Poole, United Kingdom) in 1.2% saturated picric acid solution for 1 hour at room temperature (RT), followed by differentiation in

0.01N hydrochloric acid for 2 minutes at room temperature (RT). Slides were dehydrated in graded ethanol and xylene, and cover slipped with Entellan (Merck, Darmstadt, Germany).

## Single immunohistochemical staining (SMA)

Antigen retrieval was performed by heating slides for 20 minutes in 95°C citrate buffer on a hot plate. After washing in Tris-buffered saline (TBS) with 0.05% tween (TBS/Tween), sections were pre-incubated for 10 minutes with 5% normal human serum. After preincubation, sections were incubated for 60 minutes with mouse-anti-SMA (1:10.000, Sigma, Darmstadt, Germany) in TBS with 3% bovine serum albumin (BSA). Following incubation, sections were washed with TBS/Tween and incubated for 30 minutes at RT with undiluted Brightvision Poly-Alkaline phosphatase Goat-anti-Mouse (ImmunoLogic, Duiven, the Netherlands). After incubation with secondary antibodies, all sections were washed with TBS/Tween and incubated with Liquid Permanent Red (LPR) (DAKO, Glostrup, Denmark) for 10 minutes. Subsequently, tissue sections were washed with distilled water and counterstained with hematoxylin, airdried at 60°C for 90 minutes, and cover slipped using Entellan (Merck, Darmstadt, Germany). Smooth muscle cells of the tunica media of blood vessels served as an intrinsic positive control for SMA. Negative controls were obtained by incubation of LN slides with TBS-3% BSA without primary antibody.

## Double (sequential) immunohistochemical staining (Podoplanin/vWF and CD3/CD20)

During a sequential double staining two immunohistochemical staining procedures, each directed against a specific antigen, are performed sequentially. In this study, a sequential double staining was performed for Podoplanin in combination with vWF and for CD3 in combination with CD20 (Table 3 & 4 contain technical details on the antibodies used and incubation procedures). Antigen retrieval was obtained by heating slides for 20 minutes in 95°C citrate buffer on a hot plate. After washing in Tris-buffered saline (TBS) with 0.05% tween (TBS/Tween), sections were pre-incubated for 10 minutes with 5% normal human serum, followed by incubation with the first primary antibodies. Sections were washed with TBS/Tween several times and incubated with the matching secondary antibodies for 30 minutes at RT (Table 3). After incubation with secondary antibodies, sections were washed with TBS/Tween and incubated with LPR (DAKO, Glostrup, Denmark) or PermaBlue Plus/AP (Diagnostics Biosystems, Pleasanton, United States of America) (Table 3). Tissue sections were then washed in distilled water and subsequently placed in 95°C citrate buffer for 15 minutes to wash out unbound antibodies and for additional antigen retrieval.

After washing in TBS/Tween, sections were pre-incubated with 3% Normal Goat Serum in TBS for 10 minutes, followed by incubation with the second primary antibodies in TBS with 1% BSA. Sections were washed with TBS/Tween several times and incubated with the matching secondary antibodies for 30 minutes at RT. After incubation, sections were washed with TBS/Tween, incubated with the corresponding chromogen, washed in distilled water, airdried at 60°C for 90 minutes and cover slipped using Entellan (Merck, Darmstadt, Germany).

**Table 3.** Order of antibodies used in sequential double staining procedures.

| Double staining | 1st Primary AB | 1st Secondary AB | Substrate | 2nd Primary AB | 2nd Secondary AB | Substrate |
|---|---|---|---|---|---|---|
| CD3/CD20 | CD20 | Brightvision Poly-AP Goat-anti-Mouse (ImmunoLogic) | PermaBlue | CD3 | Brightvision Poly-AP Goat-anti-Rabbit (ImmunoLogic) | LPR |
| Podoplanin/vWF | Podoplanin | Brightvision Poly-AP Goat-anti-Mouse (ImmunoLogic) | LPR | vWF | Brightvision Poly-AP Goat-anti-Rabbit (ImmunoLogic) | PermaBlue |

**Table 4.** Overview of used antibodies listing their clone, manufacturer, reference number (Ref#) and practical specifications including dilution, incubat ion time and – temperature.

| Staining | Antibody | Clone | Manufacturer | Ref # | Dilution | Incubation | temp |
|---|---|---|---|---|---|---|---|
| SMA | Monoclonal Mouse anti- | 1A4 | Sigma, Gernmany | A2547 | 1:10000 | 60 min | RT |
| CD20 | Monoclonal Mouse anti-Human | L26 | Dako, Denmark | M0755 | 1:400 | 60 min | RT |
| CD3 | Polyclonal Mouse anti-Human | n.a. | Dako, Denmark | A0452 | 1:50 | 90 min | RT |
| Podoplanin | Monoclonal Mouse anti Human | D2-40 | Dako, Denmark | | 1:100 | overnight | 4°C |
| vWF | Polyclonal Rabbit anti-Human | vWF | Dako, Denmark | A0082 | 1:2000 | 60 min | RT |



Since LNs contain T cells, B cells, lymph vessels and blood vessels (and hence smooth muscle cells), these structures served as internal positive controls and no additional positive controls were used in this study. Negative controls were obtained by omitting the primary antibodies. To ensure adequate removal of unbound primary antibodies of the first staining round (and hence avoiding aspecific staining in the second round) in case of a sequential double immunohistochemical staining, an additional control was performed. This control was obtained by omitting the secondary antibody and its corresponding substrate in the first staining round, followed by performing antigen retrieval, and applying the secondary antibody and corresponding substrate of the second staining round. If no color reaction was observed the primary antibodies of the first staining round were properly removed.

### Image acquisition

Brightfield single images were captured at various magnifications using a DM6 microscope with a motorized scanning stage, a DFC7000 T camera and LASX software (all from Leica, Nussloch, Germany).

## RESULTS

### Lymph nodes

Mediastinal, pancreatic, inguinal and mesenteric LNs were evaluated as non-activated since no germinal centers could be observed. All LNs showed a clear capsule and trabeculae. Both structures could be observed in HE stained slides, but were more pronounced in PSR stained slides (Fig. 1BC). Regional differences in capsule thickness were observed both within and between LNs (Fig. 1DF). Trabeculae were observed as septa which were continuous with the capsule, or as discrete patches, depending on the cutting plane of the sections (Fig. 1CDF). In all LNs, both the capsule and trabeculae contained smooth muscle cells (Fig. 1E). These cells were distributed heterogeneously and did not form a distinctive continuous tissue layer.

The SCS was observed in HE stained slides but was best appreciated in PSR stained slides where bright red stained collagen of the capsule formed a high contrast demarcating border lining the SCS on its outside (Fig. 2AB). The SCS was recognized as an area directly underneath the capsule, devoid of extracellular matrix with only a few scattered cells (Fig. 2AB). In the inguinal, mesenteric and pancreatic LNs, the SCS was observed as a predominantly continuous structure, whereas in the mediastinal LN it showed a more fragmented appearance. Podoplanin staining was observed only at a few locations of the SCS in mesenteric and mediastinal LNs (Fig. 2F), but mostly the SCS showed no Podoplanin staining at all (Fig. 2CEF). Podoplanin immune reactive (IR) vessels were observed in various parts of all LNs (Fig. 2D) and occasionally in close proximity to the capsule and inside the capsule (Fig. 2CEF). Since these vessels were never observed in continuation with the SCS, they could not be classified as afferent lymph vessels.

CD3/CD20 double staining showed clear distinct B- and T-cell areas in mediastinal, inguinal, and mesenteric LNs (Fig. 3AB). The pancreatic LN showed a more heterogeneous B- / T-cell pattern (Fig. 3C).

## Additional observations

In the mesenteric and inguinal LN, SMA-IR was clearly observed in T-cell regions, whereas Podoplanin-IR was observed in B-cell regions (Fig. 3DEF). In the mediastinal LN, Podoplanine-IR was observed in a few B-cell regions, whereas no SMA-IR was present in the T cell regions. The pancreatic LN did not show IR of either marker in any of its B or T cell regions.

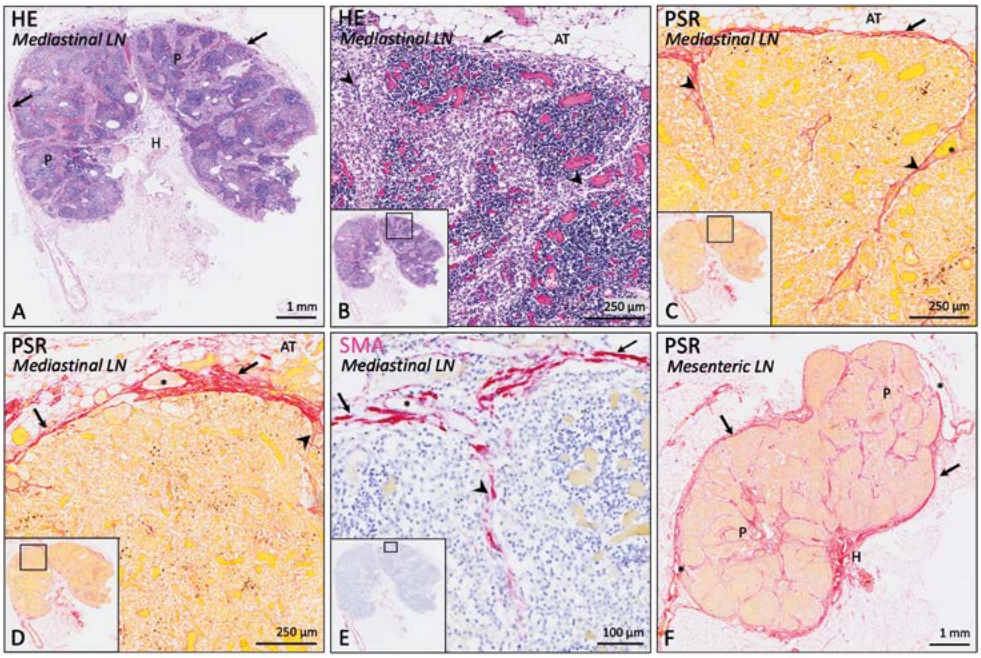


**Figure 1. Lymph node capsule and trabeculae. A:** Cross section of a mediastinal lymph node (LN) showing a capsule (arrows), parenchyma (P) and hilum (H) (hematoxylin/eosin (HE) staining). **B:** Magnified area of the mediastinal LN shown in A. The capsule can be recognized as a pink structure lining the LN parenchyma (arrow). Trabeculae (arrowheads) can be recognized but are more clearly recognizable in picrosirius red (PSR) stained slides. **C:** Similar magnified area as B (PSR staining). Connective tissue is stained red whereas other structures are stained yellow. Capsule (arrow) and trabeculae (arrowheads) are clearly recognized. Trabeculae can be observed as septa which are continuous with the capsule or as patches of connective tissue within the parenchyma (not shown in this figure), depending on the cutting plane. **D:** Magnified area of a mediastinal LN illustrating regional differences in capsule thickness (arrows) (PSR staining). Connective tissue is stained red whereas other structures are stained yellow. **E:** Magnified area of a mediastinal LN showing the presence of smooth muscle tissue in the capsule (arrow) and trabeculae (arrowheads) (smooth muscle actin (SMA) staining). SMA is stained bright pink. **F:** Cross section of a mesenteric LN illustrating regional differences in capsule thickness (PSR staining). This is a superficial cross section which shows the capsule (arrows), parenchyma (P) and a part of the hilum (H). Connective tissue is stained red whereas other structures are stained yellow. ***:** *vascular structures inside capsule and trabeculae*

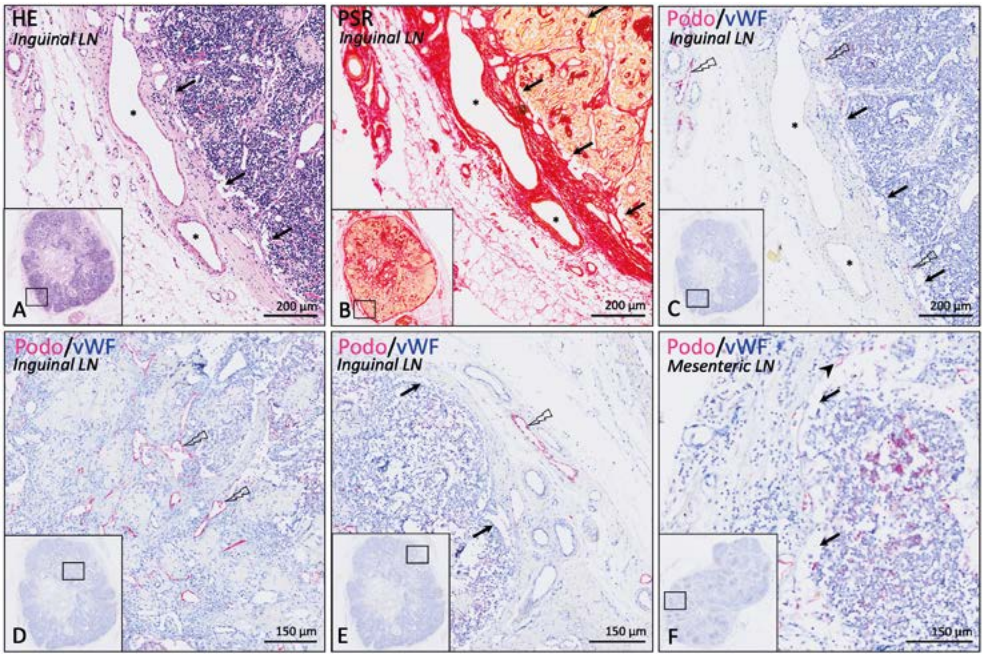


**Figure 2. Lymph node SCS and lymph vessels. A:** Magnified area of an inguinal lymph node (LN) (hematoxylin/eosin (HE) staining). Immediately underneath the capsule lies the SCS (SCS) (arrows). Large vascular structures can be observed in the capsule (*). **B:** Magnified area of an inguinal LN (picrosirius red (PSR) staining). Compare to HE stain, PSR results in a more profoundly stained capsule which forms a more demarcated border lining the SCS. In contrast to the parenchyma and capsule, the SCS forms an area devoid of extracellular matrix containing only a few scattered cells. Connective tissue is stained red whereas other structures are stained yellow. **C:** Magnified area of an inguinal LN (podoplanin and von Willebrand Factor (Podo/vWF) double staining with hematoxylin counterstaining). The SCS shows no Podoplanin-immunoreactivity (IR) whereas other lymphatic vascular structures outside the LN and inside the capsule do (thunder bolts). (Podo is stained bright pink whereas vWF is stained blue). **D:** Magnified area of an inguinal LN (Podo/vWF double staining with hematoxylin counterstaining) Podoplanin-IR is present in lymphatic vascular structures in the medulla (thunder bolts). (Podo is stained bright pink whereas vWF is stained blue). **E:** Magnified area of an inguinal LN (Podo/vWF double staining with hematoxylin counterstaining) illustrating Podoplanin-IR structures in the capsule and not in the SCS. **F:** Magnified area of an abdominal LN (Podo/vWF staining with hematoxylin counterstaining) showing sporadic Podoplanin-IR in some parts of the SCS (arrow head). Podo is stained bright pink whereas vWF is stained blue.

## Omental milky spots

All OMS were evaluated as non-activated, as no clear activation signs, such as the formation of primary follicles, were observed (Dux et al. 1986). HE staining of OMS slides showed dense clusters of cells with moderate size round nuclei resembling lymphocytes (Fig. 4A). PSR staining showed that none of the OMSs was fully enclosed by a distinct and continuous capsular structure (Fig. 4B). In one case however, a regional lining on one side (mesothelial side) with collagen rich connective tissue was observed (Fig. 4B'). In all OMSs, a substantial amount of connective tissue was present

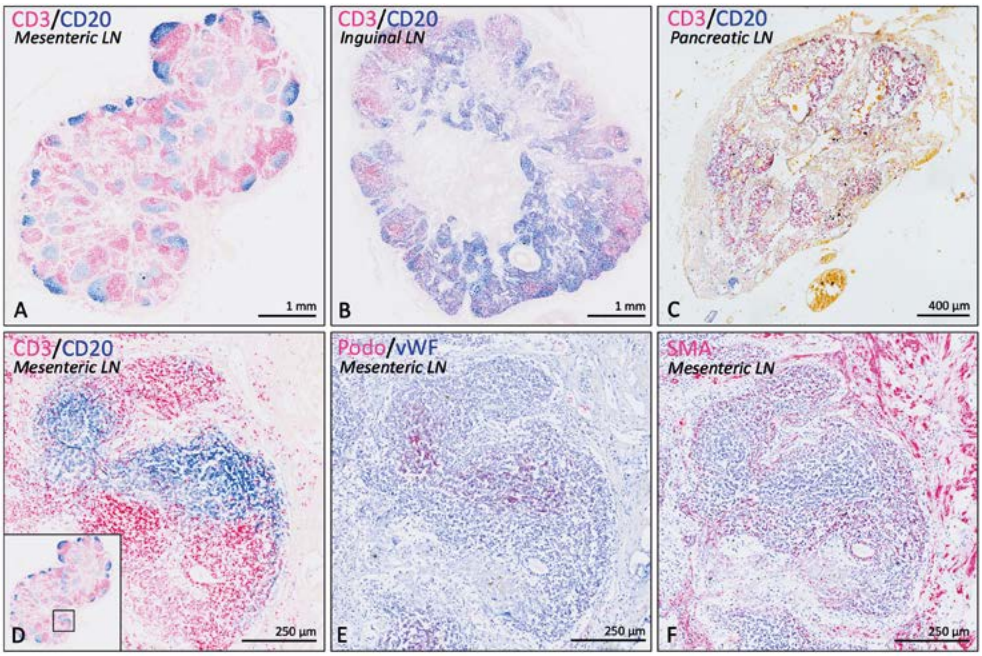


**Figure 3. Organization of T- and B-cell areas in lymph nodes. A:** Mesenteric lymph node (LN) showing distinct T- and B-cell areas (CD3/CD20 double staining). CD3 is stained bright pink whereas CD20 is stained blue. **B:** Inguinal LN showing distinct T- and B-cell areas (CD3/CD20 double staining). CD3 is stained bright pink whereas CD20 is stained blue. **C:** Pancreatic LN showing less distinct T- and B-cell areas (CD3/CD20 double staining). CD3 is stained bright pink whereas CD20 is stained blue. **D:** Magnified area of a mesenteric LN (boxed region in figure A) (CD3/CD20 double staining). Clear distinct T- and B-cell regions can be distinguished. CD3 is stained bright pink whereas CD20 is stained blue. **E:** Magnified area of a mesenteric LN (similar boxed region as in figure D (Podoplanine and von Willebrand Factor (Podo/vWF) double staining with hematoxylin counterstaining). B-cell areas show podoplanin-immunoreactivity (IR). Podo is stained bright pink whereas vWF is stained blue. **F:** Magnified area of a mesenteric LN (similar boxed region as in figure D) (smooth muscle actin (SMA) staining with hematoxylin counterstaining). SMA-IR can be observed in T-cell areas. SMA is stained bright pink. ***:** *blood vessels* ***arrows**: capsule* ***arrow heads:** trabeculae.*

within the OMSs. This connective tissue was observed in vessel walls, as discrete patches, or as small discrete fibers (Fig. 4B). No SMA-IR was present in any of the connective tissue structures mentioned above, including the regional lining observed in one OMS (Fig. 4D-D'). Small lymphatic vessels were observed in close proximity to the OMSs (Fig. 4C). Although in one OMS some Podoplanin-IR was observed in one area, no true lymphatic structures could be identified. In general, B- and T-cells were randomly distributed in OMSs (Fig. 4E), but in one OMSs T and B cells were less homogeneously spread and areas with relatively more B cells or T cells could be distinguished (Fig. 4F).

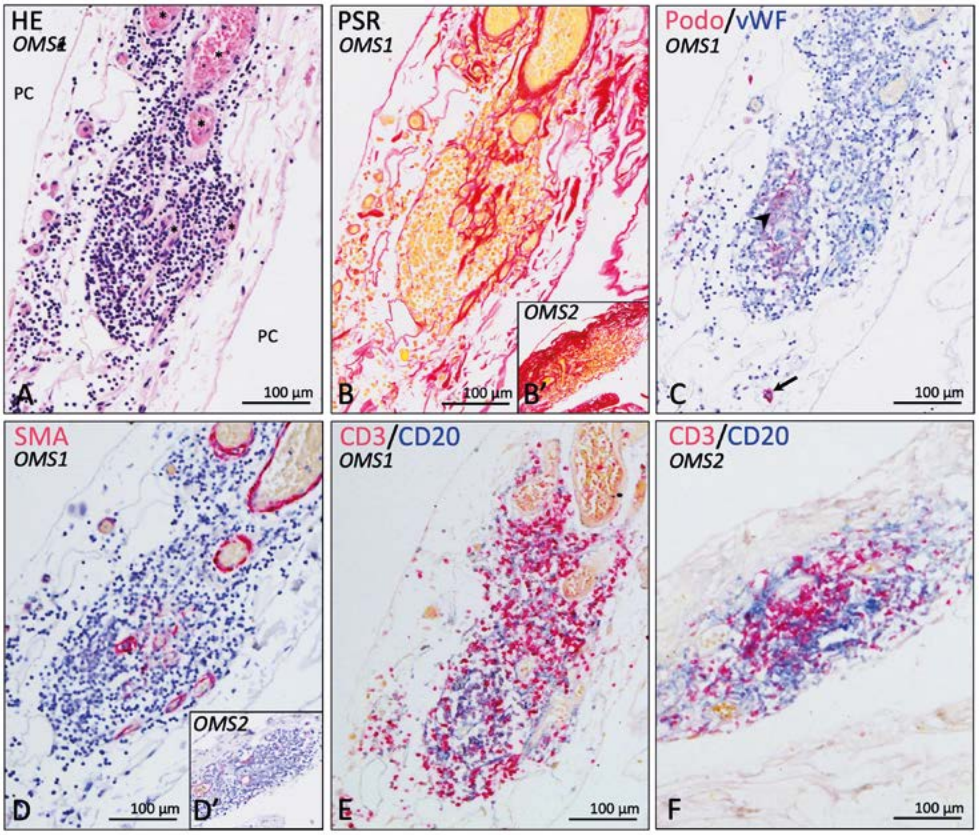


**Figure 4. Omental milky spots. A:** Omental milky spot 1 (OMS) (hematoxylin/eosin (HE) staining). The OMS is composed of a dense cluster of cells with moderate size round nuclei resembling lymphocytes. It contains various blood vessels (*), is lined by mesothelium and in close proximity to the peritoneal cavity (PC). **B:** OMS1 (picrosirius red (PSR) staining). No fully enclosing and continuous capsular structure is present. Inside the OMS, PSR staining (and therefore connective tissue) was mostly found in vessel walls, as small patches and small fibers. Connective tissue is stained red whereas other structures are stained yellow. **B':** OMS2 (PSR staining): A thick connective tissue lining is present on one side of the OMS. Connective tissue is stained red whereas other structures are stained yellow. **C:** OMS1 (Podoplanin and von Willebrand Factor (Podo/vWF) double staining with hematoxylin counterstaining). Small podoplanin-IR lymphatic structures could be observed in close proximity to the OMS (arrow), but not inside the OMS. A podoplanin-IR area (arrow head), which resembles the podoplanin-IR observed in LN B-cell areas (Figure 3E). (Podo is stained bright pink whereas vWF is stained blue). **D:** OMS1 (smooth muscle actin (SMA) staining with hematoxylin counterstaining). SMA-immunoreactivity (IR) is observed in the wall of vascular structures but not in the other connective tissue structures as observed in B. SMA is stained bright pink. **D':** OMS2 (SMAstaining with hematoxylin counterstaining). No SMA-IR was observed in the thick connective tissue lining of this OMS. SMA is stained bright pink. **E:** OMS1 showing heterogeneous organization of T- and B-cells (CD3/CD20 double staining). CD3 is stained bright pink whereas CD20 is stained blue. **F:** OMS2 shows a less heterogeneous T- and B-cell distribution compared to OMS1 (CD3/CD20 double staining). CD3 is stained bright pink whereas CD20 is stained blue, ***arrow****: lymphatic vascular structure*, ***arrow heads****: podoplanin-IR area.*

# DISCUSSION

OMSs may wrongly be identified as LNs, as they share multiple morphological characteristics. This study shows that both lymphoid structures can be distinguished microscopically by four clearly reliable recognisable morphological hallmarks, which are present only in LNs, not in OMSs. In order to visualize these hallmarks, HE, PSR, SMA and B- and T-cell staining of tissue slides appeared sufficient.

## Capsule and trabeculae

LNs are known to be fully enclosed by a compact capsule from which trabeculae penetrate into the lymph node parenchyma (Willard-Mack 2006). The presence of a capsule with trabeculae is not a common OMS feature. All the studied LNs contained a capsule and trabeculae which could be observed in HE stained slides, but were more pronounced after PSR staining. Both the LN capsule and trabeculae should contain smooth muscle cells (Folse et al. 1975), which was confirmed by the presence of SMA-IR in these structures. This study showed that OMs could regionally be lined by a layer of connective tissue, resembling a capsule-like structure, and, could have small connective tissue patches in between their lymphoid cells, resembling trabecular structures. However, compared to LNs, these structures were always less pronounced and, in the case of a lining structure, never fully enclosed the lymphoid tissue and lacked SMA-IR. The connective tissue lining as observed in one particular OMSs is most likely attributable to peritoneal fibrosis after intra-abdominal infections or after surgery, or as an age-related accumulation of extracellular matrix components (Murtha et al. 2019). Therefore, its presence should be taken into account and emphasizes the need for a SMA staining in addition to HE and PSR, for capsule and trabeculae confirmation.

## Distinct B and T cell regions

LNs are known to have distinct B and T cell regions, located in the cortex and paracortex respectively, whereas OMSs show a more random distribution of their lymphocytes. In this study, distinct B and T cell regions were observed in all but 1 LN. In this LN, lymphocyte organization was somewhat less pronounced and B and T cells were distributed more randomly, an observation which might be explained by age related involution of this lymphoid structure (Luscieti et al., 1980).Two OMSs showed a mainly heterogeneous distribution whereas there was some B/T cell clustering in one OMS. The reticular cell network of LNs provide a scaffold on which the B and T cells reside. In B-cell areas these reticular cells are represented by follicular dendritic cells (FDCs) and in T-cell areas by fibroblast reticular cells (FRCs) (Aguzzi, Kranich, and Krautler 2014)(Fletcher, Acton, and Knoblich 2015). FDCs are known to show IR with Podoplanin antibodies (Marsee, Pinkus, and Hornick 2009) whereas FRCs react with SMA antibodies (Fletcher et al. 2015), features which were observed in LNs of this study. Interestingly, some Podoplanin-IR was observed in two OMSs as well which resembled an area with relatively more B-cells upon further investigation. Although both the presence of more distinct B and T cell areas and the presence of differentiated reticular cells are not listed as common OMS characteristics, it is known that upon antigen challenge OMS can show segregation of T and

B cells (Dux et al. 1986) which might be accompanied by reticular network changes as well. These observations suggest that B and T cell distribution represents a less reliable hallmark when reviewed independently; evaluating the presence of the other three morphological hallmarks in conjunction with B and T cell staining is highly recommended.

## Layered organization

LNs are known to have a layered organization, which from the outside in comprises a capsule, a cortex with spherical follicles of B cells, a paracortex containing T cells, and a vessel rich medulla (Willard-Mack 2006). This organization can be observed in any non-superficial, non-hilar section of a LN, independent of the plane of section. When cut superficially, sections might contain a capsule and cortex only and when cut at the hilar region, the presence of a capsule, cortex, and paracortex might be less pronounced or even lacking (Furuta 1948). In this case, the lymphoid tissue might resemble an OMS. However, a section through a LN hilum should contain a relatively large artery, vein and lymph vessel and their presence could help to distinguish between a LN and OMS, although evaluating additional slides of another level of the lymphoid tissue would be recommended. In this study, all LNs showed this layered organization, whereas none of the OMSs did.

In contrast with commonly known LN morphology which describes B cell areas to be positioned peripheral to T cell areas (Willard-Mack 2006)(Young, O'Dowd, and Woodford 2013), in this study it was observed that B and T cell areas could reside next to each other.

## Excluded morphological hallmarks

The SCS and afferent lymph vessels were also selected as potential morphological hallmarks, but lacked discriminative capacities. The SCS could not always be identified as a clear entity in HE and PSR stained slides and in order to increase visibility, additional Podoplanin staining was performed. Podoplanine selectively stains the lymphatic endothelium (Breiteneder-Geleff et al. 1999), but in this study only parts of the SCSs showed Podoplanine-IR. Whether this was attributable to poor staining quality of the used marker, other technical staining issues, or due to damage of the lymphatic endothelium is unclear. At the moment this hallmark is considered inefficient. Similar observations account for afferent lymph vessels. Although potential lymph vessels were observed, (they were in close relation to the LN capsule and occasionally appeared to be penetrating it) their Podoplanin staining was doubtful; they were only partially stained and in some cases even showed partial vWF-IR. Therefore, compared to the SCS, this hallmark was considered inefficient.

## Limitations of the study

This study was limited to eight specimens which were obtained from donated bodies of individuals of advanced age. These numbers are small and the studied structures might have been affected by age or, clinical – or post mortem conditions. Therefore, this study should be considered as an exploratory study that can be supplemented in the future with samples from younger, recently diseased individuals with known medical history.

# CONCLUSION

This study presents morphological criteria to distinguish LNs from OMSs, which are of value when applied in combination. These morphological hallmarks are 1) the presence of a capsule, 2) the presence of trabeculae, 3) distinct B and T cell areas and 4) a layered organization comprising a capsule, cortex, paracortex and medulla from outside in. Sufficient visualization of these hallmarks can be achieved by HE, PSR, SMA and B and T cell staining of tissue slides. Distinguishing LNs from OMSs may be of importance to understand dissemination patterns of tumour cells.

# 8

# THE APRON OF THE GREATER OMENTUM OF GASTRIC CANCER PATIENTS CONTAINS VARIOUS LYMPHOID STRUCTURES INCLUDING LYMPH NODES

B. Schurink[1, 2], C.G.J. Cleypool[1], L.A.A. Brosens[3],
J.P. Ruurda[2], T.A.P. Roeling[1],
R. van Hillegersberg[2], R.L.A.W. Bleys[1]

[1] Department of Anatomy, University Medical Center Utrecht,
Utrecht University, the Netherland.
[2] Department of Surgery, University Medical Center Utrecht,
Utrecht University, the Netherlands .
[3] Department of Pathology, University Medical Center Utrecht,
Utrecht University, the Netherlands.

*Submitted to Clinical Anatomy. 2021*

# ABSTRACT

## Introduction

To gain more insight into the pattern of peritoneal cancer dissemination and optimize cancer treatment, it is important to improve our understanding of the omental lymphatic system. Although omental milky spots (OMSs) are considered the only lymphoid structures in the omentum, clinical studies mention the presence of lymph nodes (LNs) as well. In this study, diagnostic samples of the greater omentum of gastric cancer patients that were previously reported to contain LNs were re-evaluated for the presence of LNs.

## Materials & methods

Paraffin embedded omental samples from 17 gastric cancer patients, previously reported by the pathologist to contain LNs, were re-evaluated. Tissue sections were stained with Picrosirius red, smooth muscle actin and CD20 and CD3, and microscopically re-examined according to predefined criteria to distinguish OMSs from LNs.

## Results

Pathology records reported 47 LNs in 17 patients. Upon re-evaluation, 20/47 LNs could be classified as true LNs, which were located in both the upper and lower quadrants of the greater omentum. The other 27 structures could not be classified as LNs or OMSs and were defined as intermediate lymphoid structures.

## Conclusion

The omental apron of gastric cancer patients contains LNs and intermediate lymphoid structures, the latter most likely representing activated OMSs. These observations underline that our understanding of the (immune) function of the greater omentum is incomplete and requires additional studies to gain further insight in the structure and function of the omental lymphoid system in both health and disease.

# INTRODUCTION

The greater omentum is the largest peritoneal fold in the human body and is composed of layers of mesothelium enclosing a connective tissue framework, blood vessels, lymphatics, and fat pads (2). Furthermore, the greater omentum contains lymphoid structures referred to as omental milky spots (OMSs), microscopically identified as aggregates of B, T cells, and macrophages without a clear organization or surrounding capsule as is seen in lymph nodes (LNs).(J. Y. Liu et al. 2015; Shimotsuma et al. 1991) OMSs are in direct contact with the peritoneal cavity via stomata in their covering mesothelium (Wilkosz et al. 2005) and continuously monitor the composition of the peritoneal fluid, providing a swift response to imminent peritoneal threat.(Meza-perez and Randall 2017) Although LNs are located in the gastrocolic ligament, milky spots are the only lymphoid organs in the omental apron according to an anatomical reference work by Liebermann (Liebermann-Meffert 2000). However, in clinical practice pathology records frequently report the presence of LNs in the omental apron.(Haverkamp et al. 2016; Koppe et al. 2014) This difference may be explained by the fact that milky spots are highly dynamic structures: in response to inflammation they increase in number and size, and form specialized B and T cell areas, which are also present in, but not restricted to, LNs (Dux et al. 1986)(Cleypool et al. 2020). Therefore, activated milky spots may erroneously be mistaken for LNs.

Verification of the presence and location of omental LNs not only contributes to the general understanding of omental function. It is also of importance from an oncological point of view to help understand cancer dissemination patterns and guide the extent of surgical treatment. LNs monitor lymph supplied via afferent lymph vessels (e.g. for the presence of difference pathogens), while milky spots monitor peritoneal fluid. Therefore, metastasis in omental lymph nodes suggest lymphatic spread, whereas metastasis in OMSs suggest peritoneal spread and hence more widespread disease. The latter necessitates different treatment strategies.

The peritoneum, and especially the omentum, are a common location for gastric cancer metastases (Thomassen et al. 2013) and routine removal of the apron of the greater omentum during gastric cancer surgery is the standard of care in most guidelines. As mentioned above, there is a discrepancy between pathology reports of these resection specimens, which frequently list the presence of LNs in the omentum, and descriptions in anatomical reference works which mention OMSs as the only lymphoid structures. Therefore, this study aims to re-evaluate diagnostic tissue samples of the omental apron of gastric cancer patients which were previously reported to contain LNs. Predefined criteria(cleypool et al. 2020) will be used in order to ascertain the presence of lymph nodes in the omental apron. Additionally, these lymphoid structures were screened for the presence of tumor metastases.

# MATERIALS & METHODS

Institutional Review Board approval was obtained and informed consent requirement was waived. Between April 2012 and October 2018 the pathology reports of 17 gastric cancer patients reported the presence of lymph nodes in the greater omentum, resulting in a total of 47 lymph nodes.

These patients were selected from a total group of 103 patients operated in this time period, who received curative gastrectomy for gastric cancer (cT1-4 N0-3 M0/1) with omentectomy in the University Medical Center Utrecht, the Netherlands. During surgery the omentum was resected from the transverse colon, 3-4 cm below the right gastroepiploic artery (hence not including the gastrocolic ligament containing station 4 nodes). The separately removed free flap of the omentum was marked in the operating room, dividing it into 4 quadrants: left and right upper, and left and right lower quadrants (**Figure 1**). At the Pathology department, the greater omentum was fixed in 4% formaldehyde for a minimum of 12 hours. Afterwards, all 4 marked quadrants were visually inspected and palpated for the presence of lymph nodes or tumor deposits, which were sampled. When not found, at least 1 random omental sample was taken from each quadrant. After routine processing and embedding in paraffin, 4 µm sections were cut and stained with hematoxylin and eosin (HE) for diagnostic microscopic evaluation.

## Classification of lymphoid structures and presence of metastases

For this study, all microscopically observed lymphoid structures that were reported by the pathologist to represent lymph nodes during diagnostic evaluation were re-examined according to previously published (11) predefined criteria: the presence of a smooth muscle rich capsule and trabeculae, separate B and T cell regions and a layered organization with, from the outside in a capsule, cortex, paracortex and medulla. These hallmarks allowed to distinguish LNs from OMSs. Therefore, paraffin blocks were retrieved and 5 µm sections were cut and stained histochemically with Picrosirius red or immunohistochemically with antibodies raised against smooth muscle actin, and B and T cells. Staining and evaluation procedures were performed according to a previously described method (Cleypool et al. 2020). Additionally, HE sections of lymphoid structures were morphologically assessed for the presence of tumor metastases.

# RESULTS

After re-evaluation of the diagnostic tissue samples of the 17 patients, 20/47 lymph nodes were classified as lymph nodes according to the predefined criteria: showing a capsule, trabeculae, distinct B and T cell regions, and a layered organization (Figure 2). Omental LNs were present in 10 patients and located in both the upper and lower quadrants of the greater omentum (Figure 1). All other reported LNs did not meet the criteria to classify as true lymph nodes, neither could they be classified as milky spots (Figure 2). These structures were categorized as intermediate lymphoid

structures and were present in 12/17 patients. These structures showed segregation of B- and T- cell areas, but were not surrounded by a continuous distinct capsule.

## Omental metastasis

In 1 out of these 17 patients (5.9%) the greater omentum contained tumor metastases, which were located in 2/4 intermediate lymphoid structures situated in the left upper quadrant (Figure 3). No tumor deposits (solitary tumor aggregates devoid of lymphoid characteristics) were found. This

**Table 1.** Baseline characteristics of patients

| | **N = 17** |
|---|---|
| Age at diagnosis in years, median (range) | 72 (35 – 87) |
| **Sex, n (%)** | |
| Male | 8 (47.1) |
| Female | 9 (52.9) |
| **Histology** | |
| Adenocarcinoma | 17 (100) |
| **Tumor location** | |
| Gastro-esophageal junction | 1 (5.9) |
| Proximal (cardia/fundus) | 7 (41.2) |
| Middle (corpus) | 1 (5.9) |
| Distal (antrum/pylorus) | 8 (47.1) |
| **Clinical T stage** | |
| T1 | 2 (11.8) |
| T2 | 5 (29.4) |
| T3 | 9 (52.9) |
| Missing | 1 (5.9) |
| **Clinical N stage** | |
| N0 | 7 (41.2) |
| N1 | 6 (35.3) |
| N2 | 3 (17.6) |
| Missing | 1 (5.9) |
| **Clinical M stage** | |
| M0 | 16 (94.1) |
| M1 | 1 (5.9) |
| **Neoadjuvant treatment** | |
| Chemotherapy | 12 (70.6) |
| Chemoradiation | 1 (5.9) |
| None | 4 (23.5) |
| **Type of surgery** | |
| Total gastrectomy | 11 (64.7) |
| Distal gastrectomy | 6 (35.3) |

patient received upfront surgery for a pT2N2 antral adenocarcinoma with metastases in 5/15 regional gastric lymph nodes showing extracapsular growth.

## DISCUSSION

This study showed that the omental apron of gastric cancer patients contained LNs in all quadrants. This indicated that they represent true omental LNs and not LNs of the gastrocolic ligament. Intermediate lymphoid structures, which did not meet the criteria for either OMSs or LNs, were most frequently seen. Metastases of the primary gastric tumor were seen in the omental apron of 1/17 patients and located in intermediate lymphoid structures or as solitary tumor deposits.

The presence of LNs in the omental apron is in contrast with anatomical reference work that consider OMSs as the only lymphoid structures. This discrepancy can be explained by the fact that in anatomical works healthy omenta were used. LNs in these omenta are not activated and most likely smaller than LNs from the patients of the current study, and could have been missed.

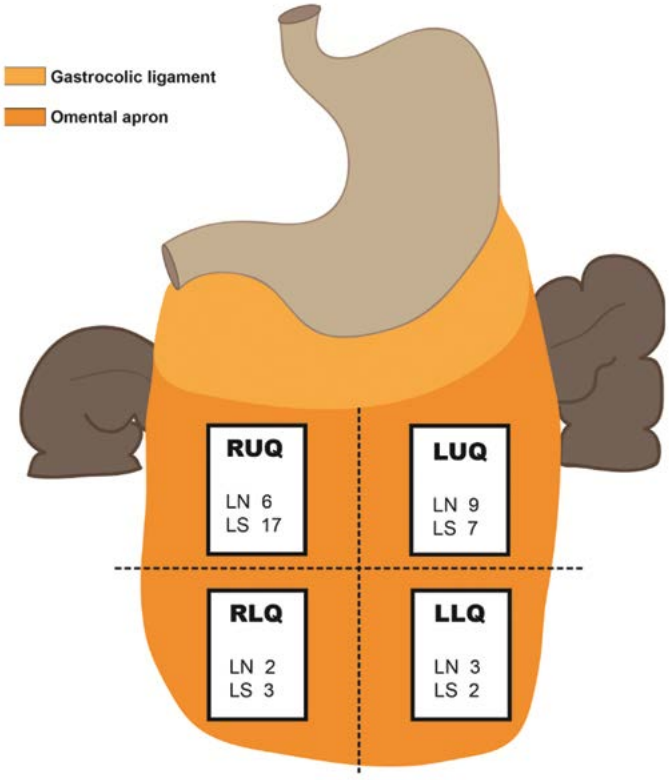


**Figure 1. Distribution and number of lymphoid structures in the omental apron of gastric cancer patients.** Abbreviations. LLQ = left lower quadrant, LN = lymph node; LS = intermediate lymphoid structure; LUQ = left upper quadrant, RLQ = right lower quadrant, RUQ = right upper quadrant.

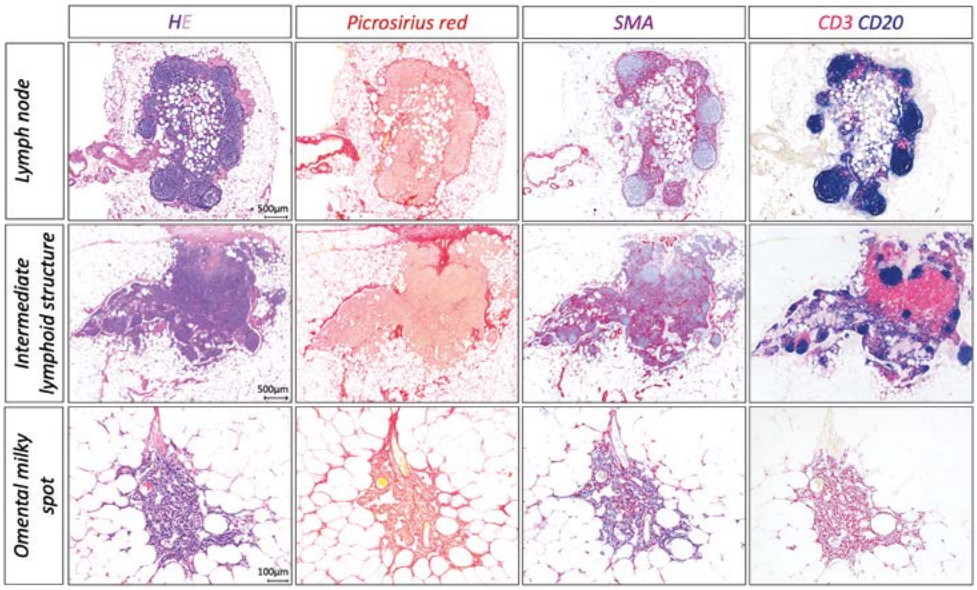


**Figure 2. Lymphoid structures in the omental apron of gastric cancer patients.** Various stainings are applied to facilitate discriminating lymph nodes (LNs) from other lymphoid structures. **Picrosirius red:** LNs show a completely surrounding connective (= capsule) tissue lining whereas this is only partial or lacking in intermediate structures and omental milky spots (OMSs), respectively. Smooth muscle actin (SMA) is present in the (partial) capsule and in T cell rich areas in both LNs and intermediate lymphoid structures. SMA can also be observed in vascular structures in all three types of lymphoid structures. **CD3/CD20:** Segregated T and B cell areas can be observed in both LNs and intermediate structures. OMSs show a more homogenous presence of both cell types. *Abbreviations.* LN = lymph node, OMS = omental milky spot, SMA = smooth muscle actin

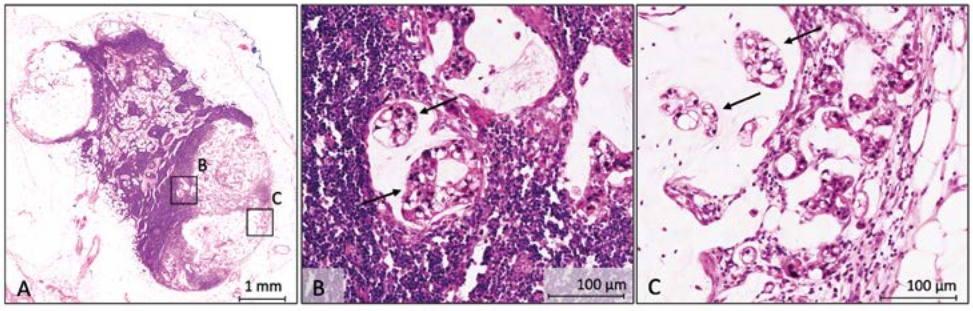


**Figure 3. Intermediate structure containing tumor metastases.** In 1/17 patients the greater omentum contained metastases, located in an intermediate lymphoid structure in the left upper quadrant. A) Low power magnification of the intermediate structure with metastases of an adenocarcinoma. B and C) high power magnification of the metastases (arrows).

Additionally, in omenta of gastric cancer patients LNs could have evolved from OMSs, and may therefore be absent in healthy omenta. OMSs are dynamic structures that are known to undergo changes upon immune stimulation and gradually gain characteristics reminiscent of lymph nodes. (Dux et al. 1986) Whether the LNs found in this study represent residential omental structures that develop during ontogeny or OMSs that have evolved into LNs, needs to be studied in developmental and experimental studies, respectively. Lymphoid structures, including OMSs and LNs, develop prior to 38 weeks of embryonic development.(Krist et al. 1997) Since the fetal omentum contains little adipose tissue, identification of LNs and the distinction between OMSs and LNs should be easy, especially when the omentum is stained with hematoxylin as a whole.(B. Schurink, Cleypool, and Bleys 2019) Experimentally, OMSs should be studied on various time periods after a stimulus (either infectious or tumor) to see if they show gradual morphological changes and evolve into intermediate lymphoid structures and eventually LNs. Parallels might exist between the mechanism behind the formation of tertiary lymphoid organs and activation of OMSs. Therefore, studies addressing tertiary structures might provide relevant insights. Tertiary lymphoid organs are organized lymphoid structures which develop *de novo* at sites of chronic inflammation and in areas with tumor. Formation of these structures is determined by site specific and inflammation dependent factors that direct stromal fibroblast to acquire LN-like properties that among others permit the retention of inflammatory cells(Gago da Graça, van Baarsen, and Mebius 2021), a process that might also occur during the activation on OMSs.

The exact drainage route of omental LNs is unknown, but of great importance for the understanding of cancer dissemination patterns, and in determining adequate therapeutic options. OMSs are known to drain into efferent lymphatic vessels originating in the proximity of OMSs. These coalesce with regional omental lymphatics, which drain toward the subpyloric or splenic lymph nodes(Liebermann-Meffert 2000) (Nylander and Tjernberg 1969) and eventually drain into the systemic circulation via the thoracic duct. When omental LNs are also linked to efferent lymphatics from OMSs and drain towards the subpyloric or splenic lymph nodes, subpyloric or splenic metastases could suggest both local lymphatic and peritoneal spread and not only local lymphatic spread as previously thought.

# CONCLUSION

Our study showed the presence of intermediate lymphoid structures in a substantial number of patients. These most likely represent activated OMSs. Remarkably, in addition to clear segregation of B and T cell regions, a feature of OMSs that has been previously described (Dux et al. 1986), the intermediate lymphoid structures in the current study frequently showed a partial covering by collagen, interspersed by smooth muscle cells. Furthermore, stroma of T cell regions of intermediate structures showed SMA immune reactivity, a feature which is also seen in fibroblast reticular cells in LNs. (Aguzzi et al. 2014)(Fletcher et al. 2015) The presence of SMA immune reactivity in OMSs might also be the result of aging, a feature commonly seen in other tissues. However, in a previous study we showed that OMSs of older patients showed no SMA immune reactivity, making

the observed changes less likely to be attributable to age.(cleypool et al. 2020) The presence of a partial capsule and segregation of T and B cell regions with corresponding stromal cells such as FRCs, suggests that OMSs are more dynamic than previously thought. Activation of OMSs and the development into intermediate lymphoid structures could be explained by the absorption of peritoneally disseminated tumor cells. However, omental metastases were only observed in 1 patient in our study. Therefore, the exact stimuli for activation of OMSs in the other patients remain unknown. It could be hypothesized that this is attributable to tumor specific circulating chemokines secreted to the peritoneal cavity by the primary tumor and surrounding stromal cells. Since OMSs represent selective implantation sites for tumor cells in peritoneal dissemination(Tsujimoto et al. 1996), these unknown substances might contribute to their activation and hence the formation of a premetastatic niche.(Kaplan, Rafii, and Lyden 2006)

The presence of intermediate lymphoid structures and the associated formation of a premetastatic niche might be detrimental for patient prognosis, as the activated OMSs might provide an optimal soil for tumor metastases. Furthermore, activated OMSs might play a role in making other parts of the peritoneum more receptive for metastases by supplying the peritoneal cavity with macrophages(Shimotsuma, Takahashi, and Hagiwara 1992) including subtype M2 that are known to generate an immunosuppressive environment and hereby promote cancer progression.(Mikuła-Pietrasik et al. 2018; Motohara et al. 2019) Interestingly, the presence of these macrophages in the peritoneal fluid appears to correlate to the occurrence of peritoneal metastases as shown in gastric cancer patients (Song et al. 2019). While the exact mechanism requires more research, this might explain why metastases develop in OMS first and only days later at other, non-OMS associated, parts of the peritoneum (Yonemura et al. 1996). Although omentectomy during gastrectomy has been debated, the aforementioned might justify omentectomy during gastric cancer surgery and necessitates thorough review during pathological assessment of the omentum for the presence of metastases.

In conclusion, the omental apron of gastric cancer patients contains LNs. Furthermore, intermediate lymphoid structures were present, which most likely represent activated OMSs. Results from the current study underline that our understanding of both immune structure and function of the greater omentum is far from complete. Further studies addressing omental lymphoid structure and function in both health and disease are required to increase our understanding of gastric tumor spread and what additional therapy would be most effective for gastric cancer patients.

# LYMPH NODES

III

# 9

# SYMPATHETIC NERVE DISTRIBUTION IN HUMAN LYMPH NODES

Cindy G.J. Cleypool[1],
Claire Mackaaij[1], Dyonne Lotgerink Bruinenberg[2],
Bernadette Schurink[3], Ronald L.A.W. Bleys[1]

[1] Department of Anatomy, Division of Surgical Specialties, University Medical Center Utrecht, Utrecht University, the Netherlands.
[2] Experimental Vascular Biology, Department of Medical Biochemistry, Amsterdam University Medical Center, the Netherlands.

*Journal of Anatomy. 2021*

# ABSTRACT

## Introduction

Various lymph node functions are regulated by the sympathetic nervous system as shown in rodent studies. If human lymph nodes show a comparable neural regulation, their afferent nerves could represent a potential therapeutic target to treat e.g. infectious or autoimmune disease. Little information is available on human lymph node innervation and the aim of this study is to establish a comprehensive and accurate representation of the presence and location of sympathetic nerves in human lymph nodes. Since previous studies mention sympathetic paravascular nerves to occasionally extent into T cell rich regions, the relation of these nerves with T cells was studied as well.

## Materials & methods

A total number of 15 inguinal lymph nodes were resected from six donated human cadavers. Lymph node sections were stained with HE and a double T/B cell staining for evaluation of their morphology and to screen for general pathologies. A triple stain was used to identify blood vessels, sympathetic nerves and T cells, and, to study the presence and location of sympathetic nerves and their relation to T cells. In order to evaluate whether the observed nerves were *en route* to other structures or were involved in local processes, adjacent slides were stained with a marker for varicosities (synaptophysin), which presence is suggestive for synaptic activity.

## Results

All lymph nodes contained sympathetic nerves, both as paravascular and discrete structures. In 15/15 lymph nodes, nerves were observed in their capsule, medulla and hilum, whereas only 13/15 lymph nodes contained nerves in their cortex. The amount of sympathetic nerves varied between compartments and between and within individuals. In general, if a lymph node contained more paravascular nerves in a specific compartment, more discrete nerves were observed as well. Occasionally, discrete nerves were observed in relation to T cells in lymphoid tissues of the cortex and medulla. Furthermore, discrete nerves were frequently present in the capsule and hilum. The presence of varicosities in a portion of these nerves, independently to their compartment, suggested a local regulatory function for these nerves.

## Conclusion

Human lymph nodes contain sympathetic nerves in their capsule, trabeculae, cortex, medulla and hilum, both as paravascular or as discrete structures. Discrete nerves were observed in relation to T cells and non-T cell rich areas such as the hilar and capsular connective tissue. The presence of discrete structures suggests neural regulation of structures other than blood vessels, which was further supported by the presence of varicosities in a portion of these nerves. These observations are of relevance in further understanding neural regulation of lymph node immune responses and in the development of neuromodulatory immune therapies.

# INTRODUCTION

Lymph nodes are strategically located secondary lymphoid organs which filter lymph and initiate local adaptive immune responses. Although long considered to function independently, nowadays it is known that this response can be regulated by the autonomic nervous system. This neural regulation predominantly occurs via the sympathetic neurotransmitter noradrenalin (NA) which influences lymph node lymphocyte proliferation, antibody secretion, blood perfusion, inflammatory cytokine production, and lymphocyte migration and egression, as shown in various rodent studies (Madden et al. 1989)(Madden et al. 1994)(Rogausch et al. 2004)(Nakai et al. 2014)(Suzuki et al. 2016)(Guyot et al., 2019). In rodents, sympathetic varicosities have been observed in relation to lymphocytes which could attribute to this neural regulation (Giron, Crutcher, and Davis 1980)(Felten et al. 1984). If human lymph nodes show a comparable neural regulation, lymph node nerves could represent a potential therapeutic target to treat e.g. infectious or autoimmune disease.

So far only two studies report on sympathetic innervation of human lymph nodes. Both studies primarily observed sympathetic nerves surrounding vascular structures and both mentioned that infrequently nerves branched off to extent into T cell specific parenchymal regions (Fink and Weihe 1988)(Panucio et al. 1998). Since the description of innervation patterns in these studies was very concise and no specific T cell staining was performed, the distribution patterns of sympathetic fibers in human lymph nodes remains unclear as well as their relation with T cells. In order to further consider therapeutic neural modulation of human lymph node immune response, understanding of the sympathetic innervation patterns of human lymph node is essential. Therefore, the aim of the current study is to establish a comprehensive and accurate representation of the presence and location of sympathetic nerves in human lymph nodes and to determine their relation to T cells.

# MATERIALS & METHODS

Inguinal lymph nodes of 6 formaldehyde perfused cadavers were studied. These included three male and three female cadavers with a median age of 75.5, ranging from 69-91 years. No scars or skin infections were observed in the inguinal- or pelvic region or on the lower extremities. Bodies were donated through a body donation program to the Anatomy department of the University Medical Center Utrecht, the Netherlands. Informed consent was obtained during life, allowing the use of these bodies for educational and research purposes. Whole body preservation was accomplished by perfusion with 3% formaldehyde via the femoral artery. For each cadaver, 2-4 inguinal lymph nodes, resulting in a total number of 15 lymph nodes, were macroscopically located, resected and further processed for paraffin embedding by placing them in increasing percentages of ethanol, xylene, and paraffin. Paraffin blocks were cut on a microtome (Leica 2050 Super Cut, Nussloch, Germany) and a series of 5 mm thick sections (originating from one level of the middle portion of the lymph nodes) were placed on glass slides, air dried, and subsequently heat fixed for two hours on a slide drying table of 60°C (Medax, 14801, Kiel, Germany). Hematoxylin/Eosin (HE)

and a double T and B cell immunostaining (using antibodies against specific membrane proteins, being CD3 and CD20, respectively) were used to evaluate technical tissue quality and to screen for general histoarchitectural changes (technical details on staining methods are listed in the following paragraphs). To evaluate the presence of sympathetic nerves in relation to T cells and blood vessels, a triple stain was performed using the markers Tyrosine Hydroxylase (TH), CD3, and von Willebrand Factor (vWF), respectively. Adjacent slides were single stained with a general nerve marker (Protein Gene Product 9.5 (PGP9.5)) to confirm neural identity of TH-immune reactive (IR) structures and with a marker for presynaptic vesicles (synaptophysin) to determine the presence of varicosities and thereby confirm that these nerves were not *en route*, but most likely innervated local tissue. Prior to histochemical and immunohistochemical staining, all tissue sections were dewaxed in xylene and rehydrated through graded alcohols and distilled water.

## HE staining

Tissue sections were stained with hematoxylin (Klinipath, Olden, Belgium) for 10 min. After rinsing in running tap water sections were dipped in ethanol 50%, stained with eosin (Klinipath) for 1 min and dehydrated in a graded series of alcohol and xylene. The slides were cover slipped with Entellan (Merck, Darmstadt, Germany). All steps were performed at room temperature (RT).

## Immune histochemical staining procedures

Tissue sections were pretreated with Heat Induced Epitope Retrieval (HIER) in citrate buffer (pH6.0) for 20 min at 95°C. Tris-buffered saline with 0.05% Tween20 (TBS-T) was used for all washing steps and were performed at room temperature (RT). Table 1 contains technical details on the used antibodies. For the sequential triple stain, the sections were incubated with 3% Normal Goat Serum (NGS) in TBS prior to incubation with Rabbit anti- human CD3 antibody (1:50 in TBS-T + 1% BSA, 90 min, RT, Dako, Glostrup, Denmark). CD3 was visualized with undiluted Brightvision Poly-AP Goat-anti-Rabbit (ImmunoLogic, Amsterdam, the Netherlands) and PermaBlue Plus/AP (Diagnostics Biosystems, Pleasanton, CA). Next, a HIER step was performed in citrate buffer (pH 6.0, 15 min, 95°C) to remove all unbound antibodies but leave the chromogen in place (van der Loos 2007). Staining was continued by incubating with 5% NHS in TBS and rabbit anti- human TH (1:1500 in TBS-T + 1% BSA, overnight at RT), Pel Freez, Rogers AR). TH was detected with Brightvision Poly-AP Goat-anti-Rabbit (ImmunoLogic) and liquid permanent red (LPR) (Dako). Next a HIER step was performed in Tris-EDTA buffer (pH9.0, 15 min, RT) to remove all unbound antibodies. Finally, the sections were incubated with 5% NHS in TBS and Rabbit anti-human vWF (1:2000 in TBS-T + 1% BSA, 60 min RT, Dako), Brightvision Poly-AP Goat-anti-Rabbit (ImmunoLogic) and PermaGreen Plus/AP (Diagnostics Biosystems). Sections were then dried on a hot plate for 15 min at 60°C and cover slipped with Entellan (Merck).

For the sequential double stain for T and B cells, sections were incubated with 5% Normal Human Serum (NHS) in TBS prior to incubation with Mouse anti-CD20 (1:50 in TBS-T + 1%BSA, 90 min, RT,

**Table 1.** Primary antibodies used for immune histochemical staining

| | Host + Clone | Vendor | Dilution, incubation time and temperature |
|---|---|---|---|
| Tyrosine hydroxylase | Rabbit Polyclonal | PelFreez (Rogers, USA) | 1:1500, o.n. RT |
| PGP9.5 | Rabbit Polyclonal | Dako (Glostrup, Denmark) | 1:2000, 48 hours, 4ºC |
| Synaptophysin | Mouse Monoclonal (SP11) | Thermo Fisher (Fremont, USA) | 1:300, o.n., 4ºC |
| CD3 | Rabbit Polyclonal | Dako (Glostrup, Denmark) | 1:50, 90 min, RT |
| CD20 | Mouse Monoclonal (L26) | Dako (Glostrup, Denmark) | 1:50, 90 min, RT |
| Von Willebrand Factor | Rabbit Polyclonal | Dako (Glostrup, Denmark) | 1:2000, 60 min, RT |

Dako). CD20 was visualized with undiluted Brightvision Poly-AP Goat-anti-Mouse and PermaBlue plus/AP (Diagnostics biosystems). To remove all antibodies but leave the chromogen in place, a HIER step in citrate buffer was performed (pH 6.0, 15 min, 95°C). Next all sections were incubated with 3% NGS in TBS prior to incubation with Rabbit anti- human CD3 antibody (1:50 in TBS-T + 1% BSA, 90 min, RT, Dako). Staining was continued with Brightvision Poly-AP Goat-anti-Rabbit (ImmunoLogic) and LPR (Dako). Sections were dried on a hotplate for 15 min at 60°C and cover slipped with Entellan (Merck).

For PGP9.5 and synaptophysin single staining, sections were incubated with 5% Normal Human Serum (NHS) in TBS prior to incubation with rabbit anti human PGP9.5 antibody (1:2000 in TBS-T + 3% BSA, 48 hr, 4°C, Dako) or Synaptophysin (1:300 in TBS-T + 1% BSA, overnight 4°C, Thermo Fisher, Fremont, CA), followed by visualization with undiluted Brightvision Poly-Alkaline Phosphatase (AP) Goat-anti-Rabbit (ImmunoLogic) and LPR (Dako). Sections were counterstained with hematoxylin (Klinipath), dried on a hotplate for 15 min at 60°C and cover slipped with Entellan (Merck).

Lymph node vessel wall innervation was used as an intrinsic positive control for both neural markers and intrinsic lymph node vessels and T cells for vWF and CD3, respectively. Human spleen sections that were previously confirmed to show proper staining for B cells, T cells and sympathetic nerves were included as a positive control for CD20, CD3, TH and PGP9.5, respectively. Beta cells in human pancreas sections were used as positive controls for synaptophysin. Negative controls were obtained by incubation with TBS-3%BSA without primary antibodies.

## Microscopic evaluation

All slides were evaluated by bright field microscopy and in case of small TH, PGP and synaptophysin-IR structures, which were visualized with the chromogen LPR, by additional fluorescent microscopy (LPR has stable fluorescent features, allowing to alternately switching between bright field and fluorescent microscopy). All samples were studied using a DM6 microscope (Leica, Nussloch, Germany) and in case of fluorescent microscopy, an I3 fluorescent filter.

### Location and quantification of sympathetic nerves

Brightfield tile scans (stitched overlapping images) were captured of all lymph nodes using a 10x objective. Tile scans were opened in 3D paint (Microsoft office) and all sympathetic nerves were encircled manually. This resulted in overview images of lymph nodes with their sympathetic nerve distribution clearly visible. The general amount of sympathetic nerves (irrespective to whether these were paravascular or discrete nerves) for each compartment, being the capsule, cortex, medulla and hilum, was then quantified by means of scoring according to the following grading scale: -: complete absence, +: minor amount, ++: moderate amount and +++: substantial amount. Prior to scoring, all lymph nodes were evaluated by the observers in order to obtain a general idea of minimal and maximal amounts for each compartment. Each sample was examined independently by two observers (CC and CM). When there was disagreement between the observers the samples were re-examined and scored by consensus.

### Image acquisition

Brightfield single images were captured at various magnifications using a DM6 microscope with a motorized scanning stage, a DFC7000 T camera and LASX software (all from Leica, Nussloch, Germany).

## RESULTS

### General observations

In total, 15 lymph nodes were evaluated. All showed typical morphological lymph node characteristics such as a capsule with trabecula, a subcapsular sinus, a cortex, medulla and a hilum (Fig. 1). Depending on the level/angle of the sections, the amount of cortical, medullar and hilar tissue slightly varied. To a certain extent all lymph nodes showed common age-related histoarchitectural changes such as lymphocyte paucity (resulting in less demarcated B- and T cell regions), fibrosis and lipomatosis (Hadamitzky et al. 2010). No significant pathologies were observed.

### Sympathetic nerve distribution

All lymph nodes contained sympathetic nerves in their capsule, cortex, medulla and hilum (Fig. 1). The amount of sympathetic nerves per lymph node compartment varied between and within individuals. Table 2 contains an overview of the studied lymph nodes, including a semiquantitative evaluation of the amount of sympathetic nerves per compartment. Adjacent PGP-stained slides confirmed the neural identity of the observed TH-IR structures. In general, it was noticed that if a lymph node contained more paravascular nerves, the more discrete nerves were present as well.

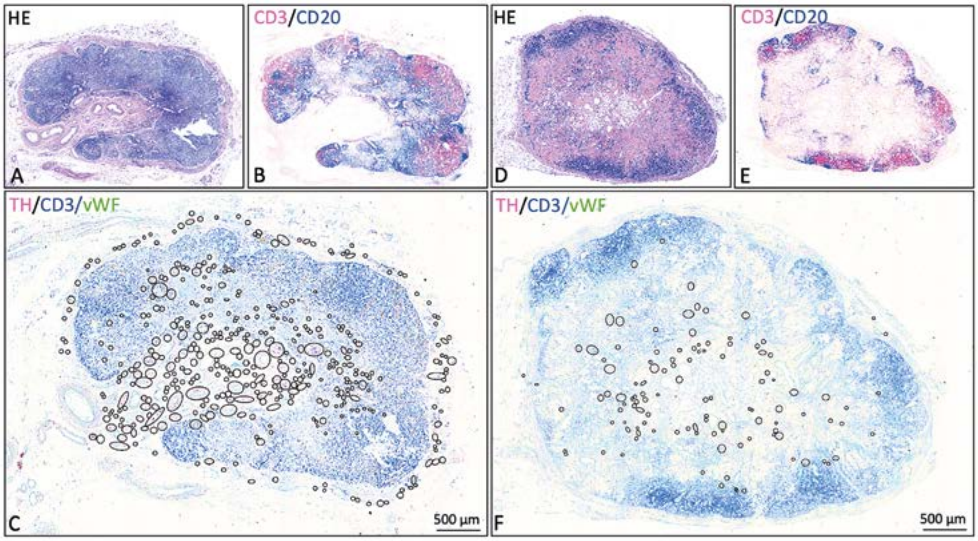


**Figure 1. Lymph nodes with different quantities of sympathetic nerves.** Hematoxylin / eosin and CD3/CD20 stained slides show the general lymph node morphology and distribution of lymphocytes, respectively. In overview images of TH/CD3/vWF stained slides, the presence of sympathetic nerves in the various compartments is indicated by black circles (in these overview images, nerves cannot be distinguished). More detailed images of sympathetic nerve distribution can be found in figure 2. **A-C:** Lymph node (# 13) with high nerve quantity. **D-F:** Lymph node (# 15) with low nerve quantity. ***Black circled structures:*** *sympathetic nerves (**Small circles:** discrete nerve fibers or small nerves **Larger circles:** clusters of nerves / blood vessels with paravascular nerves).*

## Capsule

All 15 lymph nodes showed a well-developed capsule from which occasionally trabeculae emerged that penetrated the parenchyma. All capsules, and occasionally their trabeculae, contained paravascular and discrete sympathetic nerves (Fig. 2D). Nerves were most frequently observed in the most outer layers of the capsule. Occasionally nerves were observed in deeper layers, but never in proximity to the subcapsular sinus.

## Cortex

In 13/15 lymph nodes, sympathetic nerves were present in the cortex. In most lymph nodes, cortical nerves were infrequently observed and showed a heterogeneously distribution, whereas in a few cases (the ones scored as ++ or +++), cortical nerves represented a more prominent feature with a homogeneous distribution. In the cortex nerves were observed either as paravascular nerves or as discrete nerves within T cell dense lymphoid tissue (Fig. 2C&F). Occasionally paravascular nerves were observed to extent into T cell dense lymphoid tissue.

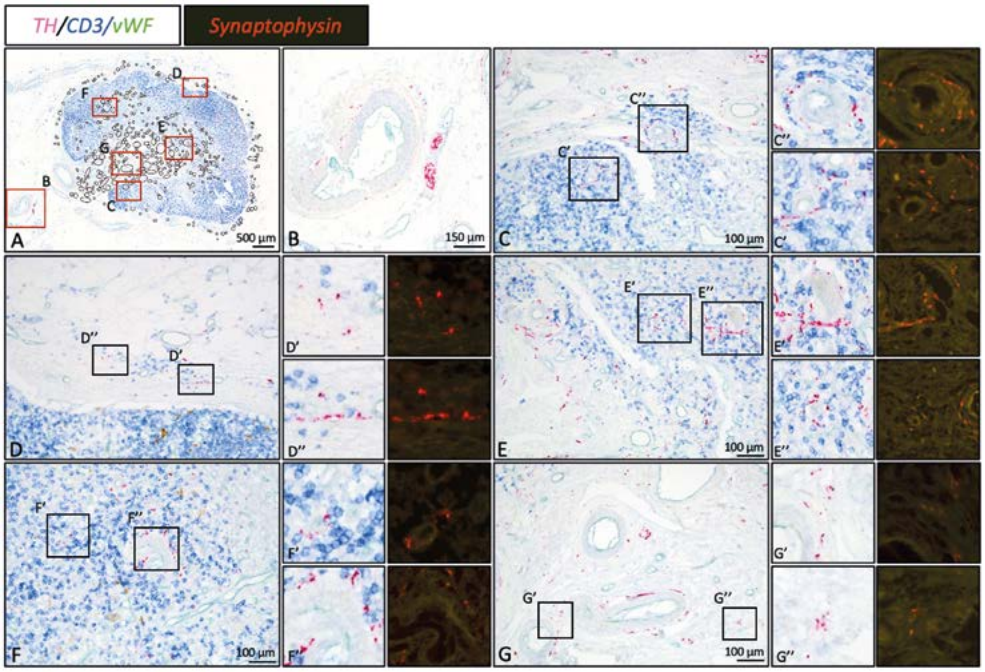


**Figure 2. Magnified images of sympathetic innervation of lymph node # 13.** Bright field images represent TH/CD3/vWF triple stained slides showing sympathetic nerves (in relation with), T cells and blood vessels, respectively. Synaptophysin stained slides show the presence of varicosities. **A:** Overview image of lymph node #13. Black circled structures represent locations with sympathetic nerves. Red boxed areas are shown in more detail in figures B-G. **B:** Large sympathetic nerve bundle running with a lymph node artery towards the hilum. **C-G:** Nerves can be observed as paravascular or as discrete entities of which some are in close proximity with T cells. **C:** Cortex, **D:** Capsule, **E:** Medulla, **F:** Cortex, **G:** Hilum.

## Medulla

Sympathetic nerves were observed in the medulla of all lymph nodes. In 2/15 LNs, medullary nerves were a rare observation whereas in other lymph nodes they appeared to represent a more residential feature. Nerves were observed surrounding vascular structures and in between the lymphoid tissue of the medullary cords (Fig. 2E).

## Hilum

All lymph nodes, contained sympathetic nerves in their hilum. In general, this compartment contained many blood vessels of various sizes with a paravascular sympathetic nerves (Fig. 2G) and many fine discrete nerves in between its connective tissue (Fig. 2G).

**Table 2.** Patient profiles and semi-quantified data of lymph node sympathetic nerve distribution

| | | | | Distribution of sympathetic nerves | | | |
|---|---|---|---|---|---|---|---|
| **Cadaver** | **Sex** | **Age** | **Lymph node** | **Capsule** | **Cortex** | **Medulla** | **Hilum** |
| I | F | 81 | 1 (L) | ++ | - | + | + |
| II | F | 91 | 2 (L) | + | + | ++ | ++ |
| | | | 3 (R) | + | _ | ++ | ++ |
| III | M | 71 | 4 (L) | ++ | + | ++ | +++ |
| | | | 5 (L) | ++ | ++ | ++ | +++ |
| | | | 6 (L) | ++ | + | ++ | +++ |
| | | | 7(R) | ++ | ++ | ++ | ++ |
| IV | M | 70 | 8 (L) | + | ++ | ++ | + |
| | | | 9 (R) | + | ++ | ++ | ++ |
| V | M | 69 | 10 (L) | ++ | ++ | +++ | +++ |
| | | | 11 (L) | +++ | +++ | +++ | +++ |
| | | | 12 (R) | +++ | ++ | +++ | +++ |
| | | | 13 (R) | +++ | ++ | +++ | +++ |
| VI | F | 86 | 14 (L) | ++ | + | + | ++ |
| | | | 15 (R) | + | + | ++ | ++ |

Each compartment is evaluated as a distinct entity and the amount of nerves were scored as none (-), the least amount of all lymph nodes (+), the most amount of all lymph nodes (+++) or valued as in between (++). This scoring method allows to compare various lymph nodes for the amount of sympathetic nerves in a specific compartment. Compartments within a lymph node cannot be compared. No distinction was made between paravascular and discrete nerves. ***(L):*** from the left inguinal region ***(R):*** from the right inguinal region.

### Synaptic activity

Synaptophysin-IR was, irrespective to the compartment, observed in a portion of paravascular nerves and in discrete nerves (Fig. 2C-G).

## DISCUSSION

The current study shows that human lymph nodes contain sympathetic nerves in their capsule, cortex, medulla and hilum, not only paravascular but also as discrete structures. Although these observations have been reported previously (Fink and Weihe 1988) (Panucio et al. 1998), this is the first study that visually showed sympathetic nerve distribution, semi-quantified the amount for each compartment and showed that a portion of these nerves was in proximity with T cells.

Although previous studies suggest sympathetic innervation of human lymph node parenchyma to be a rare finding (Fink and Weihe 1988) (Panucio et al. 1998), the current study shows this represented a more common feature, especially in the medulla. Discrete sympathetic nerves were observed to be in close proximity with T cells and the presence of synaptophysin, and thus varicosities, suggests local neural activity. T cells are known to express beta (β) 2- adrenergic receptors (AR), which upon activation can regulate T cell differentiation, activation, and effector function (recently reviewed by

Qiao et al., 2018). Although the current study focused on the relation of sympathetic nerves with T cells, other immune cells, such as macrophages, dendritic cells and B cells express adrenergic receptors (Qiao et al., 2018) and might be under direct sympathetic control as well.

In addition to immune cells, reticular cells should also be taken into consideration as a neuro immune target. These cells represent the main cellular component of the reticular fiber network of secondary lymphoid organs and play a vital role in e.g. guided migration of immune cells by the production and secretion of specific chemokines (Murray et al., 2017). For rodents it has been shown that nerve endings are in contact with these reticular cells (Villaro et al., 1987), that these cells express adrenergic receptors and that their chemokine production is regulated by sympathetic nerves (Murray et al., 2017). The presence and function of similar adrenergic signaling components in the human reticular fibre network remains to be resolved.

Thus, lymph node immune function can be regulated directly via adrenergic receptors on various immune cells and indirectly via reticular cells. However, other sympathetic innervated structures might be involved in indirect regulation as well. These structures might include SMCs in capsule, trabeculae, hilum and vascular structures. All studied lymph nodes showed discrete sympathetic nerves in their capsules and occasionally in their trabeculae. These structures are known to contain a substantial amount of smooth muscle cells (SMCs) in addition to their fibrous connective tissue (Furuta 1948) (Folse et al. 1975) which most likely represent the neural target tissue of the observed fine discrete sympathetic nerves. *In vitro* electrostimulation of bovine capsular nerves resulted in contraction of these SMCs (Lobov and Pan'Kova 2013) and hence contraction of the lymph node as a whole. Although the contribution of capsular and trabecular nerves to lymph node immune function remains to be resolved, one could assume that lymph node contraction affects e.g. lymph node lymph and blood flow, immune cell migration, and immune cell egression as described above.

A substantial amount of discrete sympathetic nerves was observed to reside in the connective tissue of the hilum. Interestingly, as shown by the presence of varicosities, these nerves are not *en route* to other structures, but most likely innervate the hilar connective tissue. Although the hilar connective tissue of normal lymph nodes does not contain nerves or cells that require neural regulation, it is known that superficial lymph nodes, and especially inguinal lymph nodes, can display SMCs as a result of local inflammation (Channer and Davies 1985). If the observed discrete sympathetic nerves innervate hilar SMCs, their activation might result in hilar contraction, which in turn could affect hilar lymph and blood flow and hence lymph node function.

Sympathetic paravascular nerves were observed in all subjects of the current study. Although, these plexuses do not directly influence lymph node immune function, they regulate blood and lymph flow, and hence play an important role in regulating the entrance of antigen presenting cells via the lymph, the influx of immune cells from the blood and the migration of immune cells through

the lymph node, all processes that should be optimal in order to conjoin the right cells for a properly aligned immune response (reviewed by Zhao et al., 2015).

Data from the current and previous studies (Fink and Weihe 1988)(Panucio et al. 1998) show that human lymph nodes do not contain a sympathetic subcapsular nerve plexus, a structure previously reported in mice (Felten et al. 1984). In mice the subcapsular plexus represents a prominent structure and varicosities have been observed in the cortical region just beneath this plexus. Although the function of this subcapsular plexus is unknown, this neural structure might be involved in species-specific lymph node immune regulatory processes and should be taken into consideration when extrapolating animal data to humans.

Although in the current study sympathetic lymph node innervation was semi quantitatively analyzed at one specific level of the lymph nodes only (middle portion), the observations were considered to be representative for the whole lymph node since sections from another level of the same lymph nodes which were used in a preceding pilot study showed comparable sympathetic innervation patterns. This assumption was further supported by the fact that multiple lymph nodes of the same individual showed comparable numbers of nerves.

The variations of lymph node sympathetic nerve distribution between individuals as observed in the current study might be explained by the use of cadavers of different ages and with different clinical and social backgrounds, all known to alter sympathetic innervation patterns in secondary lymphoid organs (Bellinger et al., 1992)(Hoover et al., 2017). However, this study indisputably shows human lymph nodes to be sympathetically innervated and that based on its close relation with T cells and various other lymph node structures, it could play an essential role in regulation of the lymph node immune response.

## CONCLUSION

Human lymph nodes contain sympathetic nerves in their capsule, trabeculae, cortex, medulla and hilum, both as paravascular or as discrete structures. Discrete nerves were observed in relation to T cells and non-T cell rich areas such as the hilar and capsular connective tissue. The presence of discrete structures suggests neural regulation of structures other than blood vessels, and was confirmed by the presence of varicosities in a portion of these nerves. These observations are of relevance in further understanding neural regulation of lymph node immune responses and in the development of neuromodulatory immune therapies.

# IV

# DORSAL ROOT GANGLIA

# 10

# A PILOT STUDY INVESTIGATING THE PRESENCE OF SYMPATHETIC SIGNALLING COMPONENTS IN HUMAN DORSAL ROOT GANGLIA

Cindy G.J. Cleypool[1], Claire Mackaaij[1],
Niels Eijkelkamp[2] and Ronald L.A.W. Bleys[1]

[1] Department of Anatomy, Division of Surgical Specialties, University Medical Center Utrecht, Utrecht University, Utrecht, the Netherlands.
[2] Center for Translational Immunology, Division Laboratories, Pharmacy and Biomedical Genetics, University Medical Center Utrecht, Utrecht University, Utrecht, the Netherlands.

# ABSTRACT

## Introduction

Doral root ganglia can contain sympathetic nerve baskets; network-like formations of sympathetic nerve sprouts surrounding ganglion cells. These sympathetic baskets are pathological and are known to contribute or exacerbate pain (also known as sympathetic maintained pain). Their occurrence and function are therefore of interest from a chronic pain perspective. This pilot study aimed to investigate the presence of sympathetic baskets and adrenergic receptors in human dorsal root ganglia. Since an influx of macrophages and T cells is known to precede the development of these baskets in rodents, the presence of these immune cells was studied as well.

## Materials & method

Dorsal root ganglia of both the left and right side and at various levels were resected from two embalmed human cadavers. Paraffin sections of each ganglion were alternatingly stained with markers for sympathetic nerves, beta-2 adrenergic receptors, macrophages and T cells. The presence of sympathetic nerves, adrenergic receptors and immune cells was evaluated microscopically and semi-quantitatively analysed using a scoring method.

## Results

The occurrence of sympathetic baskets was variable between and within individuals, the latter with respect to the side and level of the studied dorsal root ganglia. Beta-2 adrenergic receptors were abundantly present in satellite glial cells and primary sensory neuron somata, independently to the presence of sympathetic baskets. T cells and macrophages were observed in all ganglia but their presences showed a tendency to be negatively correlated to the occurrence of sympathetic baskets.

## Conclusion

Human dorsal root ganglia can contain sympathetic baskets surrounding satellite glial cells and primary sensory neuron somata and most likely directly signal to these cells directly via beta-2 adrenergic receptors. Their occurrence is variable with respect to side and level and does not correlate to aging. Further studies that allow to link their presence to pathological processes is recommended in order to increase our understanding of their occurrence and their potential role in sympathetic maintained pain.

# INTRODUCTION

Chronic pain has a prevalence of up to 30% worldwide and is defined as persistent or recurrent pain lasting longer than 3 months (Elzahaf et al., 2012). Its incurable character has increased the (mis) use of opioids and unravelling the neurobiology of chronic pain is essential in the search for less harmful therapies. It is known that chronic pain can be maintained or exacerbated by activity of the sympathetic nervous system, a phenomenon known as sympathetically maintained pain (SMP). SMP can be explained by abnormal connections between sympathetic and sensory neurons, among which at the level of the soma of primary sensory neurons in dorsal root ganglia (DRG) (Schlereth and Birklein, 2008). In DRG, these connections are represented by sympathetic sprouts forming a network around primary sensory neuron somata (PSNSs) and their surrounding satellite glial cells (SGCs). Although not commonly known, these networks have been described as early as 1885 and have been referred to as "Dogiel's arborisations", "Dogiel's nests" (both after its discoverer Alexandre Dogiel (reviewed by García-Poblete et al., 2003), or sympathetic baskets in more recent literature (Ramer et al., 1999). These sympathetic baskets were considered pathological since their occurrence is linked to neuropathy as shown in various neuropathic pain models (reviewed by García-Poblete et al., 2003). Furthermore, these baskets are considered to contribute to pain because surgical sympathectomy almost completely relieved signs of allodynia and heat hyperalgesia in rodents with neuropathic pain (Ramer and Bisby, 1998), and, sympathectomy prior to spinal nerve ligations (used to induce neuropathy) prevented the development of these baskets and pain behaviour (Chung et al. 1993). Despite the clear evidence for the presence of sympathetic baskets in the DRG and their contribution to chronic pain states in rodents, evidence in humans is more limited. Although DRGs obtained from neuropathic pain patients are known to contain sympathetic baskets (Shinder et al., 1999), both their function and the triggers causing their appearance in humans remains unsolved. Based on their potential role in pain, sympathetic baskets might represent a potential therapeutic target. This supports the need to improve our understanding of their development and function in humans. In this pilot study we used human cadaveric tissues and 1) explored the presence of sympathetic baskets and their apposition with respect to PSNs and their surrounding SGCs, 2) determined whether PSNSs and/or SGCs express beta 2 adrenergic receptors (ß2-AR) that allow for adrenergic signalling and 3) whether the presence of sympathetic baskets is associated with an increased amount of T cells and macrophages as it is known that an influx of these immune cells precedes their development (Hu and McLachlan, 2002). Data from this pilot study will be used to provide recommendations on study proceedings.

# MATERIALS & METHODS

DRGs were resected from the lumbar region of two male cadavers; one formaldehyde fixed cadaver (arterial perfusion with 4% formaldehyde) (69 years) and one fresh cadaver (88 years), of which the DRG were subsequently fixed for 24 hours in 4% formaldehyde. Table 1 contains detailed information on the included cadavers (age, sex, type of fixation and sample location). No scars

or other macroscopic observable clinical conditions were present. Bodies were donated through a body donation program to the Anatomy department of the University Medical Center Utrecht, the Netherlands. Informed consent was obtained during life, allowing the use of these bodies for educational and research purposes. Skin, dermis and muscles of the back were dissected and a lumbar laminectomy was performed. DRGs of various lumbar levels and sides were sampled (table 1). Fresh DRGs were fixed in 4% formaldehyde for 24 hours, whereas DRGs resected from the formaldehyde fixed cadaver could immediately be further processed. All DRGs were then processed and embedded in paraffin and cut into 5 µm thick sections on a microtome (Leica 2050 Super Cut, Nussloch, Germany). Sagittal sections of the middle parts of DRGs were collected on glass slides, air dried and subsequently heat fixed for two hours on a slide drying table of 60°C (Medax, 14801, Kiel, Germany). Adjacent sections of each sample were incubated with antibodies raised against Tyrosine Hydroxylase (TH), ß2-ARs, CD3 and CD68, enabling staining for sympathetic nervous tissue, a subset of adrenergic receptors, T cells and macrophages, respectively.

## Immunohistochemistry

Sections were dewaxed in xylene and rehydrated in graded alcohols, followed by 20 min of antigen retrieval in citrate buffer (pH6.0) at 95°C. After washing in Tris-buffered saline (TBS) with 0.05% Tween20 (TBS-T), sections were pre-incubated with 5% Normal Human Serum in TBS for 10 min, followed by incubation with primary antibodies: rabbit anti-TH (1:1500 in TBS-T + 3% BSA overnight at room temperature (RT), Pel Freez P40101, Rogers USA ), rabbit anti- β2-AR (1:50 in TBS-T +1% BSA overnight RT, Abcam ab182136, Cambridge UK), rabbit anti-CD3 (1:100 in TBS-T + 1% BSA , 90 min RT, Dako A0452, Glostrup, Denmark) or mouse anti-CD68 (1:25 in TBS-T +1% BSA, overnight RT, Novocastra NCL-CD68-KPI, Newcastle upon Tyne, UK). Sections were washed with TBS-T several times and incubated for 30 min at RT with Brightvision Poly-AP Goat-anti-Rabbit (ImmunoLogic, Duiven, the Netherlands) for TH, ß2-AR and CD3 or Brightvision Poly-AP Goat-anti-Mouse (ImmunoLogic) for CD68. After incubation with secondary antibodies, all sections were washed with TBS-T and incubated with Liquid Permanent Red (LPR) (Dako) for 10 min. Tissue sections were then washed with distilled water and counterstained with hematoxylin, dried on a hotplate for 15 min. at 60$^{0}$C and cover slipped using Entellan (Merck, Darmstadt, Germany). Negative controls were obtained by omitting primary antibodies. Spleen and sympathetic trunk sections were included as a positive control for immune cells (T cells and macrophages) and sympathetic nervous tissue respectively. Human stomach sections served as a positive control for the ß2-AR marker.

## Microscopic imaging

Single images were captured at various magnifications. These images were either brightfield or fluorescent images, depending on which modality appeared most suited to visualize the structures of interest. Image acquisition was performed using a DM6 microscope with a motorized scanning stage, a I3 fluorescent filter, a DFC7000 T camera and LASX software (all from Leica, Nussloch, Germany).

### Semi-quantitative analysis

The presence of Sympathetic baskets, ß2-ARs, T cells and macrophages was semi-quantitatively scored. Prior to scoring all samples were evaluated by the observers in order to obtain a general idea of minimal and maximal amounts. Each sample was examined independently by two observers (CC and CM) who were blinded for the sample origin. When there was disagreement between the observers the samples were re-examined and scored by consensus.

## RESULTS

All samples contained a substantial amount of PSNSs and SCGs (Figure 1AB). Sympathetic nerves were observed surrounding blood vessels of all studied DRGs, confirming the sympathetic nerve staining procedure was performed properly (Figure 1C). Sympathetic nerves were observed in close proximity with SGCs surrounding PSNSs, where these nerves formed distinct circumferential entities, also known as a sympathetic basket (Figure 1E, F and F'). If a sympathetic basket was observed, the connective tissue surrounding the PSNS/SGC-complex and adjacent nerve fascicles contained more sympathetic nerves as well (Figure 1E & E'). The presence and density of sympathetic baskets varied within and between the two studied cadavers. Cadaver I showed sympathetic baskets surrounding most (DRG L4) or all (DRG L5) PSNSs/SGC complexes on the left side (Figure 1 E&E') whereas their presence was significantly lower in the right DRG L4 and L5 (see table 1). Cadaver II contained either sporadic sympathetic baskets (DRG L2 and L3, on both the left and right side) or none (DRG L4 and L5 on the left side) (Figure 1D&D' shows a DRG devoid of sympathetic baskets). Table 1 contains semi-quantitative data of each sample. TH-IR was observed in the cytoplasm of a fraction of PSNSs in all studied DRGs, irrespective to study subject, presence of sympathetic baskets, side and level (Figure 1D' boxed area).

ß2-AR-IR was observed in all samples and was present in blood vessel walls (Figure 2D), in a subset of axons of nerve fascicles (Figure 2B) and in all PSNSs and SGCs (Figure 2C). The expression of ß2-AR was independently of the presence of sympathetic baskets. IR patterns in PSNSs and SGCs were granular, and could be observed in the cytoplasm and most likely on cell membranes.

All samples contained comparable numbers of T cells throughout nerve fascicles whereas the number of T cells surrounding PSNS/SGC-complexes differed amongst the DRGs and was negatively correlated to the number of sympathetic baskets (Figure 3). In areas with increased T cell numbers, T cells were also observed in between SGCs and occasionally even contacting PSNSs. CD3 is a negative regulator of dendrite neurons of young neurons and a such could be expressed by neurons (Baudouin et al. 2008). Indeed, CD3-IR granules were occasionally observed in PSNSs, independently to the cadaver, level, side or presence of sympathetic baskets.

All samples contained macrophages and their number in general exceeded the number of T cells. Macrophages were observed in nerve fascicles, but were more prominently present in the connective

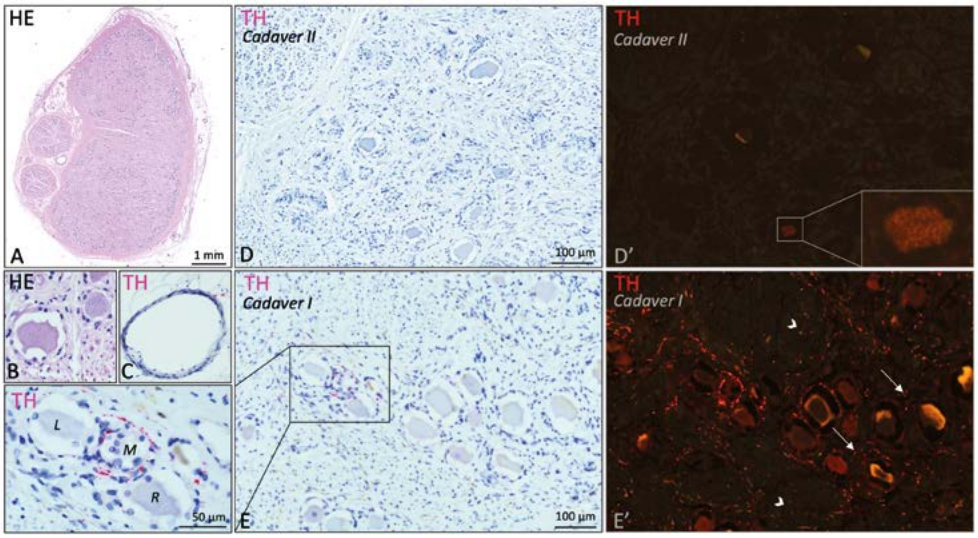


**Figure 1. Dorsal root ganglia showing variety in the presence of sympathetic baskets. A:** Cross section through a dorsal root ganglion (DRG) (H/E staining). Two large nerve bundles can be observed on the left side of the DRG. **B:** Close up image of a PSNS and its associated surrounding SGCs. There is some shrinkage of the soma, resulting is a fictive space between the neuron and the SGCs. **C:** Blood vessels were used as intrinsic positive controls for TH staining. Fine TH-IR nerves can be observed surrounding this vessel (TH staining). **D:** DRG without sympathetic baskets (TH staining). Magnified area: sympathetic baskets are clearly visible, either as a ring of small cross sectioned nerves when a PSNS/SGC-complex was cut at a deeper level (left and right complexes (L and R)) or as a more extensive neural network, when the tissue section allowed a more superficial view on these complexes (middle complex (M)). **D':** Fluorescent micrograph of D. It was noticed that some PSNSs show weak TH-IR (boxed area). **E:** DRG with many sympathetic baskets (TH staining). If baskets were present, both the surrounding connective tissue and nerve fascicles contained more sympathetic nerves as well in comparison to DRG with little to none sympathetic baskets. **E':** Fluorescent micrograph of E. ***Arrows:*** *sympathetic nerves in connective tissue surrounding sympathetic basket.* ***Arrow heads:*** *sympathetic nerves in fascicles*

tissue surrounding PSNS/SGC-complexes (Figure 4). Macrophages were also observed in between the SGCs of all samples. In each cadaver, the overall number of DRG associated macrophages was equally, independent to the level or side were the DRG was obtained. When both cadavers were compared, it was noticed that the number of macrophages in cadaver II clearly exceeded the number of macrophages in cadaver I and therefore negatively correlated to the number of sympathetic baskets. The presence of T cells and macrophages was not confined to the connective tissue immediately surrounding PSNS/SGC-complexes with sympathetic baskets only, but were also observed in relation to the other PSNS/SGC-complexes.

**Table 1.** Data semi-quantitative analysis

| | Cadaver I | | Cadaver II | |
|---|---|---|---|---|
| | Formaldehyde 69 years, male | | Fresh 88 years, female | |
| | Left | Right | Left | Right |
| **L2** | | | | |
| *TH* | | | + | +/- |
| *ß2-AR* | | | +++ | +++ |
| *CD3* | | | ++ | ++ |
| *CD68* | | | +++ | +++ |
| **L3** | | | | |
| *TH* | | | + | + |
| *ß2-AR* | | | +++ | +++ |
| *CD3* | | | ++ | ++ |
| *CD68* | | | +++ | +++ |
| **L4** | | | | |
| *TH* | +++ | + | - | |
| *ß2-AR* | +++ | +++ | +++ | |
| *CD3* | + | + | ++ | |
| *CD68* | ++ | ++ | +++ | |
| **L5** | | | | |
| *TH* | +++ | ++ | - | |
| *ß2-AR* | +++ | +++ | +++ | |
| *CD3* | + | | ++ | |
| *CD68* | ++ | ++ | +++ | |

# DISCUSSION

## Sympathetic baskets

Sympathetic baskets were observed in both cadavers and their appearance was in agreement with previous descriptions; fine sympathetic nerves covering the external surface of the PSNS/SGC-complexes with the nerves being in proximity with the SGC but never contacting the PSNSs (Shinder et al., 1999). The number of Sympathetic baskets varied between and within cadavers, the latter when comparing DRGs obtained from different sides and levels. As shown in animal experimental studies, development of the sympathetic sprouts of the baskets are known to result from physiological or pathological phenomena, related to aging or nerve damage, respectively (reviewed in (García-Poblete et al., 2003). Since the cadavers of the current study are of age, the presence of the observed sympathetic baskets might be age related. However, the youngest individual (69 years) of the current study contained more baskets than the older individual (88 years) and within each cadavers the number of baskets varied between levels and sides. These differences would more likely be explained by local pathologies such as tissue and nerve injury incurred throughout life and not by a general condition such as aging. No scars or other macroscopic observable clinical conditions

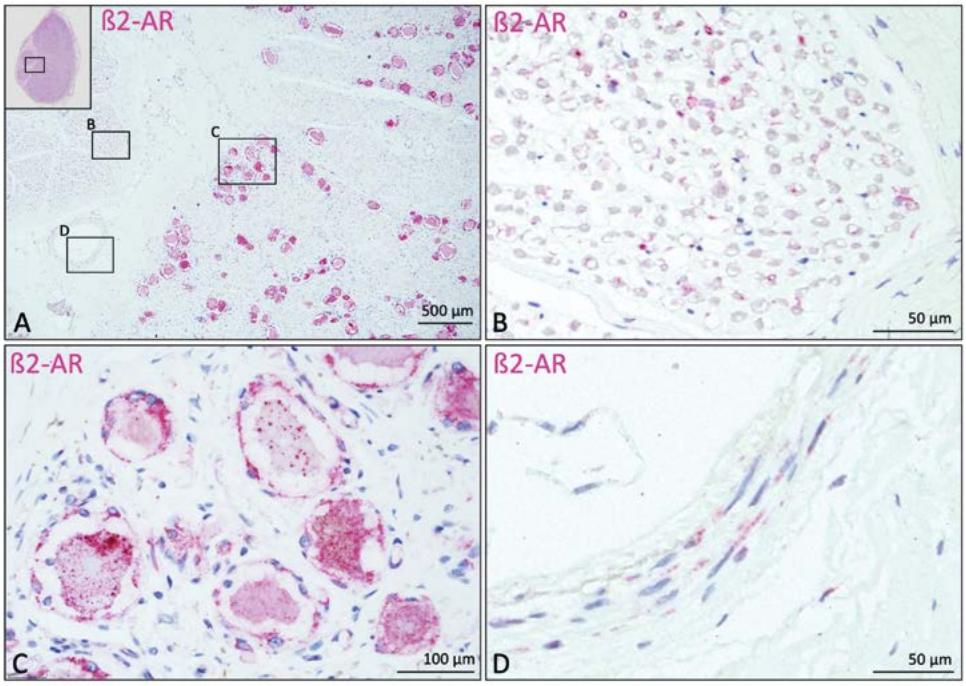


**Figure 2. Beta 2-adrenergic receptors in various dorsal root ganglion components. A:** Dorsal root ganglion (DRG) containing beta 2-adrenergic receptor (ß2-AR) immune reactive (IR) nerve fascicles (B), primary sensory nerve somata (PSNS)/satellite glial cell (SGC)-complexes (C) and blood vessels (D) (ß2-AR staining). Boxed areas marked with B, C and D correspond with figures B, C and D, respectively. The small image in the left corner shows an overview of the DRG and the area that is presented in figure A. **B:** Nerve fascicle with ß2-AR-IR axons. **C:** PSNSs and SGCs with ß2-AR-IR. The pink chromogen shows granular precipitations in the cytoplasm of both cells and potentially on their membranes. **D:** Blood vessel with ß2-AR-IR vessel wall.

were present in dermatomes corresponding with the resected DRGs which could explain the side and level related differences. Cadaver I was known with a rheumatoid arthritis which could explain the increased presence of baskets compared to the other cadaver. In order to gain more insight in local pathologies and the occurrence of sympathetic baskets in humans, it is recommended that for additional studies samples obtained from either donated bodies with unilateral scars that implicate local chronic conditions associated with pain (such as hip or knee arthroplasty) or to use tissue samples obtained via diagnostic autopsies of patients with known relevant conditions.

## Adrenergic receptors

Although variable in intensity, all observed PSNSs and SGCs showed ß2-ARs-IR. The chromogen precipitate appearance was granular and could be clearly observed in the cytoplasm whereas its presence on cell membranes was doubtful. Although ß2-ARs are present in DRG of rats as shown in western blots, so far no data could be obtained addressing the presence of these receptors on PSNSs or SGCs specifically (Zhu et al., 2015). It is however known that many, but not all PSNS in rat

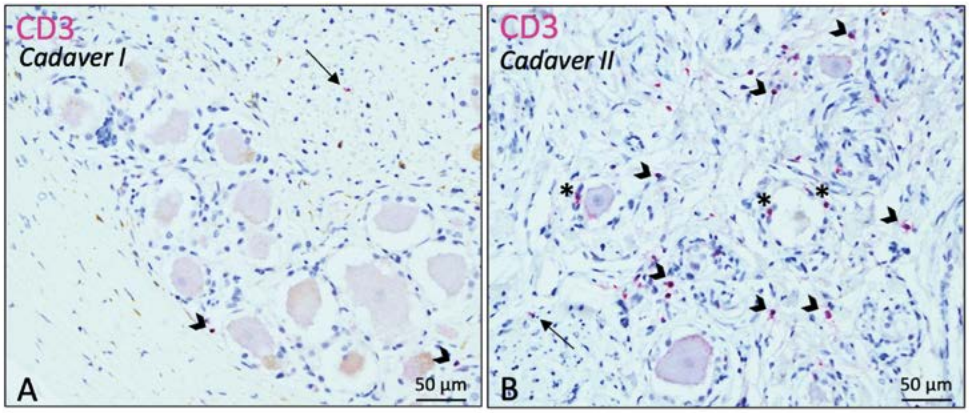


**Figure 3. T cell distribution in dorsal root ganglia.** T cells were observed in nerve fascicles, within the connective tissue between primary sensory nerve somata (PSNS)/satellite glial cell (SGC)-complexes and in between SGCs (T cell staining with CD3). **A:** Dorsal root ganglion (DRG) of cadaver I containing few T cells. **B:** DRG of cadaver II containing many T cells. T cells were more abundantly present in the connective tissue surrounding PSNS/SGC-complexes in DRG with less or none sympathetic baskets (cadaver II). ***Arrow heads:*** *T cells positioned in between PSNS/SGC-complexes.* ***Arrows:*** *T cells in nerve fascicle.* ***Asterisk:*** *T cells in between SGCs.*

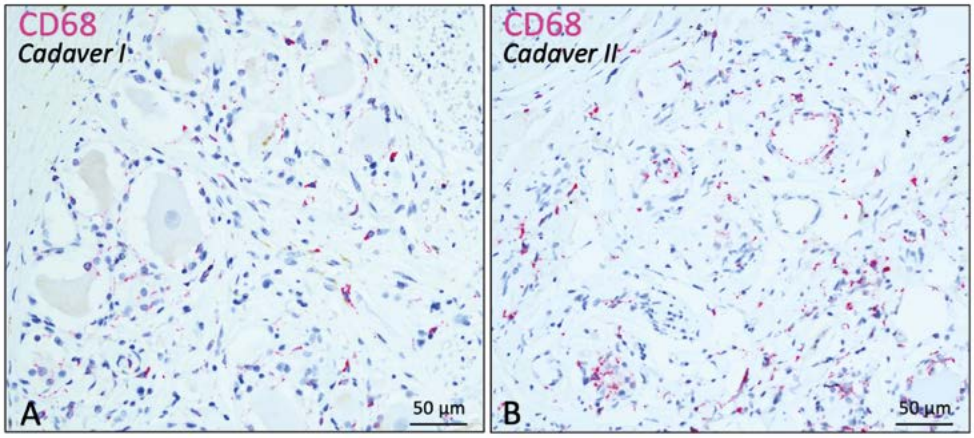


**Figure 4. Macrophage distribution in dorsal root ganglia.** Macrophages were observed in nerve fascicles, within the connective tissue between primary sensory nerve somata (PSNS)/satellite glial cell (SGC)-complexes, in between SGCs and occasionally in relation to the PSNSs (macrophage staining with CD68). **A:** Dorsal root ganglion (DRG) of cadaver I containing a moderate number of macrophages. **B:** DRG of cadaver II containing significant more macrophages compared to cadaver I. In cadaver II, macrophage numbers were primarily increased between PSNS/SGC-complexes.

DRG do show a2-ARs in their nucleus and cytoplasm, but not in their associated SGCs (Shinder et al., 1999). Functionally, a-ARs on neuronal cell membranes are hypothesized to be directly involved in acceleration of afferent discharge which occurs after systemic injection of a adrenergic agonist or sympathetic efferent stimulation (reviewed by Shinder et al., 1999). Whether ß2-ARs play a role

in sensory signal modulation remains to be elucidated. Electron microscopic studies evaluating the exact location of these ARs could help in further conceptualizing their potential role.

## Immune cells

Both cadavers of the current study contained T cells and macrophages. Although no reference of normal amounts and locations of both immune cell types in human DRGs was available for comparison, based on experience from other tissues and descriptive data from literature it is assumed that their numbers were increased in cadaver II. Within each cadaver, the number of immune cells was equally in all DRGs, independently to the side, level and presence of sympathetic baskets. According to data from an experimental study in rats, the development of sympathetic baskets is preceded by recruitment of T cells towards the DRG followed by an influx of macrophages (Hu and McLachlan, 2002). If this would apply on humans as well, the observations in cadaver II might suggest that an increase in inflammatory cells has occurred, but that the development of sympathetic baskets, of which only a few are present, is still ongoing. In cadaver I, DRGs contained many baskets but less immune cells. When evaluated in light of the suggested mechanism, one could speculate that macrophage numbers in these DRG might have been decreased but that sympathetic baskets persist. Data on longevity of sympathetic baskets is sparse, but appears to range from weeks to years in rodent experimental models (reviewd by García-Poblete et al., 2003). For humans this information is lacking and cannot experimentally be investigated. However, expanding the subject number of this pilot study, and more objectively quantify the number of baskets and immune cells, allows statistical analysis which could improve insights in their correlation.

## TH-IR in sensory neurons

All DRGs evaluated in the current study contained a fraction of TH-IR PSNSs. For various mammalian species the presence of TH, an enzyme normally only associated with noradrenergic and dopaminergic neurons, is known to be transiently or permanently expressed in a subset of PSNs of various rodent species, both during ontogeny as well as in adults (reviewed by Brumovsky, 2017). To our knowledge, their existence in adult human DRGs however, has not been previously described. So far, TH-IR sensory neurons are hypothesized to play a role in pain modulation; dopamine and/or noradrenaline might affect excitability of sensory neurons at nociceptors and/or influence neurotransmitter release from central terminals (Brumovsky, 2017). Further looking into the presence of these neurons inhuman DRGs might be of interest for future chronic pain studies. Since sensory neurons can have catecholaminergic characteristics, it should be kept in mind that, when evaluating TH stained samples for the presence of sympathetic nerves, not all TH stained nerves might be from the sympathetic lineage. For example, patients with interstitial cystitis, a condition also known as bladder pain syndrome, show increased numbers of TH-IR nerve fibers innervating the urinary bladder. These observations could be explained by outgrowth of sympathetic neuron projections (which might couple to sensory neurons and result in SMP), and / or by TH expressing sensory neurons of DRGs, which then along with sympathetic input, modulate urinary bladder sensitivity (reviewed by Brumovsky, 2017). Interestingly, newly formed tumor associated adrenergic nerves,

appear to be transdifferentiated sensory nerves as shown in a mouse model of oral cancer (Amit et al., 2020). Since adrenergic fibers promote tumor growth, this, in addition to their suggested role in pain modulation, contributes to the need to further understanding the nature of TH-IR sensory neurons and what drives or reinforce their reprogramming towards an adrenergic phenotype.

### Sympathetic baskets and chronic pain

In chronic pain, a condition in which nociceptive signals that arise from tissue damage are absent but pain persists, both the presence of immune cells and sympathetic baskets, as observed in the current study could play an important role. The influx of inflammatory cells, as observed in neuropathy experiments is suggested to contribute to neuron recovery; e.g. macrophages secrete IL-2 which in turn cause glia cells to secrete neurothrophins essential for neuronal survival. Therefore, on the short-term, these inflammatory cells appear to be beneficial, however, their long-term presence has implications for patients as the release of excitatory cytokines may generate ectopic impulse activity in sensory neurons and thereby directly contribute to chronic pain (Devor et al., 1994). With respect to sympathetic baskets, inflammatory cells can produce cytokines that initiate sympathetic neural sprouting. When sympathetic baskets are present, in turn they are believed to contribute to chronic pain via adrenergic signaling to sensory neurons (Ramer and Bisby, 1998) (Chung et al., 1993). Whether in humans the influx of immune cells and the presence of sympathetic baskets in DRG is related to chronic pain in the corresponding body part requires further studies. If a correlation can be established, both the immune and sympathetic nerve system could potentially represent new therapeutic targets in the treatment of chronic pain. Complementing this pilot study might supply data that can be supportive and guiding for further experimental studies in animals unraveling the exact involved cells, components and order of activities. Although most knowledge on sympathetic baskets originates from experimental studies on neuropathy, their development can also be linked to local, non-peripheral nerve, tissue inflammation as shown in a colitis model in rats (Xia et al., 2011). If peripheral non-neural tissue inflammation in humans evokes sympathetic basket development as well, this might explain why more sympathetic baskets were observed in the cadaver known with arthritis.

## CONCLUSION

This pilot study shows that human DRG can contain sympathetic baskets and that their occurrence is variable between and within individuals, the latter with respect to side and level of studied DRGs. These observations favour a local, most likely pathological cause instead of being the result of aging. Furthermore, ß2-ARs are present in all SGCs and PSNSs making them likely direct effector cells for adrenergic signalling in the presence of sympathetic baskets and, T cells and macrophages can occur in variable levels and their presences shows a tendency to be negatively correlated to the occurrence of sympathetic baskets.

# RECOMMENDATIONS FOR COMPLEMENTING THE CURRENT STUDY

The use of cadavers with a known medical history reporting the presence of a one-sided neuropathy, would be favorable. However, donated bodies usually lack medical files and if files can be retained, they might be incomplete. Although sympathetic baskets are known to develop as a result of peripheral nerve injury in both in rats and humans (García-Poblete et al., 2003)(Shinder et al., 1999), studies have shown that they can occur as a result of local tissue inflammation as well as shown in a colitis model in rats (Xia et al., 2011). Therefore, donated cadavers with one sided arthroplasty e.g. of the hip or knee, could represent valuable study subjects as this most likely is associated with chronic pain from the corresponding area as a result of local tissue inflammation. The presence of sympathetic baskets in the DRGs associated with the affected body area can then be compared to the DRG of the contralateral side or to DRGs of other levels. It should be kept in mind that increased numbers of immune cells and presence of sympathetic baskets were observed in DRGs of adjacent ipsilateral levels with respect to the experimentally neuropathy associated DRG (Hu and McLachlan, 2002). Most likely affected peripheral nerves project to multiple DRGs. Therefore, when comparing "affected" DRG with "non-affected" DRG, the latter should preferably be resected three levels up or down from the level of the "affected" DRG. Including cadavers from various age ranges might contribute to our understanding whether sympathetic baskets development is a physiological, age-related process. For this pilot study, semi quantitative analysis of the parameters was sufficient in order to gain a general insight. However, quantitative image analysis would be more objective and allows for sufficient statistical analysis of the data. Since TH-IR in PSNSs might be of relevance in understanding pain mechanisms, complementary studies might include this parameter as well.

No differences were observed in staining quality of DRG obtained from long term fixed or fresh cadavers.

# 11

# GENERAL DISCUSSION

# GENERAL DISCUSSION

The research described in this thesis shows that human spleens, OMSs and LNs contain sympathetic nerves, not only associated with vascular and connective tissue structures (e.g. capsule and trabeculae) but also in close proximity to T cells in their parenchyma. The implication of these findings will be discussed below for each lymphoid organ separately and focusses on *1)* the role of sympathetic nerves in immune regulation and *2)* the potential of sympathetic nerves as an anti-inflammatory therapeutic target. Furthermore, we have shown that human DRG can contain sympathetic baskets. The implications of these findings will be discussed in the "issues of concern" section.

## SPLEEN

As shown in **Chapter 4**, human spleens contain sympathetic nerves, not only surrounding vascular structures, but also in their capsule, trabeculae, red pulp and the PALS. Innervation of the PALS is considered to be of specific interest since this is the area where sympathetic nerves are in proximity to T cells and neuro modulation is thought to occur via a NE-Ach-TNFa-mechanism. Sympathetic nerve quantities of the human PALS however, seem to differ significantly from rodent species; human PALSs contain very little sympathetic innervation, even in the 10-25 age group, which represents the group that shows the highest nerve quantities in humans. These observations cast doubt on whether CAIP stimulation in humans, with only a little amount of T cells in proximity T sympathetic nerves, could target enough of these T cells to establish a similar systemic anti-inflammatory effect as observed in rodents. These doubts are partially eliminated by a clinical trial wherein the effect of VNS was studied in patients with rheumatoid arthritis and patients with epilepsy, the latter representing a control group with no known immune system dysfunction (Koopman et al., 2016). In both groups, *in vitro* LPS immune challenged whole blood samples, obtained prior and after VNS, were compared and showed significant inhibition of TNFα production after VNS. Furthermore, in the rheumatoid arthritis group improvement of symptoms was observed. Thus, although only few sympathetic nerves are present in the human PALS, electrical stimulation of the CAIP via the vagus nerve does suggest a systemic anti-inflammatory response, presumably mediated via the spleen. Since PALS innervation in humans is significant less when compared to rodents, alternative, potentially human specific alternative mechanisms might be involved, or, our understanding of where the various elements of the prevailing intrasplenic NE-ACh-TNFα mechanism interact is incomplete.

In **Chapter 4** we have discussed potential alternative mechanisms in detail and emphasize a role for the reticular framework; the spleens connective tissue scaffold which provides support for splenic immune cells and guidance for their migration (Perez-Shibayama et al., 2019). As shown by a transmission electron microscopic study in guinea pigs, the reticular framework is composed of an enveloping reticular cell, also known as a (contractile) myofibroblast, which encloses connective tissue components and a sympathetic axon (Saito, 1990). Based on the presence of

this axon, Saito suggested that the reticular framework represents catecholaminergic canals and that migrating immune cells can be exposed to their content (either naked sympathetic nerves or previously secreted and stored NE) when myofibroblasts contract (Saito, 1990). We hypothesize a similar mechanism to be present in human spleens. In our study however, we used bright field and fluorescent microscopy and might have missed out on single thin (0.3-1.3 um) sympathetic axons that run in the reticular framework. Future transmission electron microscopic studies of human spleens could provide further insight into the existence of these catecholaminergic channels.

Further support for the existence of an alternative mechanism is derived from our comparative study on an alternative splenic nerve. Studies in both rats and mice suggest that in addition to the splenic plexus, the spleen is innervated by a discrete parasympathetic nerve at its cranial pole (Buijs et al. 2008) (Guyot et al., 2019). This nerve, in mice referred to as the ASN, appeared to represent an alternative CAIP stimulation target (Guyot et al., 2019). If such a discrete ASN would be present in humans, this structure would be favored over the splenic plexus as it represents a safer and more easily accessible electrical stimulation site. In the study described in **Chapter 3** we macroscopically identified the ASN in mice and showed that it is part of a neural plexus-like configuration that interconnects the diaphragm, stomach and spleen, and that the ASN runs in the PSL towards the cranial splenic pole. Macroscopic observations in human cadavers suggest a similar structure to run in the PSL and GSL which could potentially represent equivalent structures to the ASN in mice. However, microscopic evaluation of these nerve-like structures in both mice and human did not confirm a neural identity and we concluded that these structures represent connective tissue strands. Thus, from an anatomical point of view the results of our study cast doubt on the existence of an ASN in mice and showed their absence in humans. However, from a functional point of view, the ASN does represent an interesting structure as its electrical stimulation resulted in increased levels of splenic NA and Ach and moreover provoked an anti-inflammatory response and mitigated clinical symptoms in mice. Based on these observations we considered that electric current applied to external splenic connective tissue structures could be transferred via the splenic capsule to intrasplenic structures, such as the reticular framework, and provoke an anti-inflammatory effect via e.g. release of NE from catecholaminergic channels and subsequent cellular Ach. This could imply that the splenic ligaments, or the splenic capsule, might represent easily accessible and safe stimulation sites. This assumption could be verified by e.g. electrical stimulation of splenic ligaments or capsule in mice.

Although experimental studies in rodents have shown an indisputable role for sympathetic nerves, $ChAT^+$ T cells and macrophages, studies have casted doubt on the prevailing intrasplenic NE-ACh-TNFα mechanism, both with respect to the mechanism itself and with respect to its location (Murray et al., 2017)(Rosas-Ballina et al., 2008). This, together with the above discussed indications of the existence of alternative mechanisms stresses that our understanding of splenic neuro immune regulation is incomplete. Future studies should focus on further characterizing the underlying mechanism of the CAIP and could be performed in parallel in both rodents and humans.

Since VNS stimulation is associated with side effects and might activate unknown pathways via vagal afferent fibers, the distal part of the CAIP, being the splenic plexus, was considered to serve as a more direct and safer stimulation target in humans. The efficacy of splenic plexus stimulation has been confirmed in various animal studies and during considering its feasibility in humans, questions arose regarding the anatomy of the splenic plexus. What is the configuration of this plexus, what is its neural composition and what would be the most optimal stimulation site along its course with the SA? These questions are especially of relevance for neuro electrode interface design and surgical implantation technique development and were addressed in **Chapter 2**. Tortuous parts of the SA that extend for at least 1 cm from the pancreas were referred to as SA loops and were considered to represent potential stimulation sites. Loops with these dimensions provide enough space between loop legs and the pancreas allowing introduction of surgical instruments for the purpose of exposing the site for intervention, and, for application and stabilization of a neural interface. In 83% of the studied specimens one or more SA loops were observed, suggesting that their presence is slightly variable. Previous anatomical studies show that the presence of loops is age related which might narrow the group of patients. However, a recent morphometric study analysing contrast enhanced CT images of SAs, shows that within the range of patients of 30-69 years of age, 86% of the patients showed SA loops and no age-related differences were observed (Brinkman et al., 2020). Furthermore, this study showed that CT angiography can be of use in pre-operative evaluation of their presence *in vivo* (Brinkman et al., 2020). In **Chapter 2** we showed that the splenic plexus as a whole remained in close proximity to the adventitial surface of the SA while running along the course of the SA and its loops, suggesting that the optimal neuro-electrode interface may require a circumferential device around the total neurovascular bundle of the SA loop. Surgical dissection of these loops should be carefully performed as our study showed that pancreatic, gastric and left gastroepiploic arteries can arise from these loops. Our microscopic analysis of splenic plexus nerve fiber composition showed that the plexus was predominantly composed of sympathetic nerve fibers and showed only minor amounts of parasympathetic and sensory nerves. Currently, Galvani Bioelectronics has started a clinical trial to evaluate if the SA loops and the surrounding splenic plexus are accessible, if stimulation leads can be safely placed on these nerves, whether electrical stimulation results in splenic plexus activation and what physiological responses occur (Clinical Trials NCT04171011). In this trial, patients undergoing minimal invasive surgery for esophageal cancer (esophagectomy) will be receive a short electrical stimulation via leads placed on exposed nerves of the splenic plexus. The efficacy of nerve activation and potential physiological responses will be recorded.

In **Chapter 3** we have shown that splenic sympathetic innervation in humans slightly decrease after adulthood. If these age-related variations are of significance for future splenic nerve based therapeutic applications remains to be determined.

# OMENTAL MILKY SPOTS

In the study described in **Chapter 6** we have shown that a significant part of human OMSs contain sympathetic nerves in proximity to immune cells and hence hypothesized they might be involved in regulation of OMS function. OMSs monitor peritoneal fluid and can in response supply the peritoneal cavity with immune cells, thereby playing an essential role in maintaining peritoneal immune homeostasis. Furthermore, OMSs are considered to play an essential role in intestinal immune homeostasis; OMSs represent a sort of intestinal thymus since a specific type of B cells, the CD5 B-cells or B1 cells, develop inside these lymphoid structures (Platell et al., 2000). B1 cells originating from OMSs move to the peritoneal fluid and subsequently migrate to the intestinal lamina propria (Platell et al., 2000) where they spontaneously secrete a range of antibodies (also referred to as natural antibodies) thereby supplying the baseline or resting IgM in this tissue (Rothstein et al., 2013). Further understanding of OMS function and their potential neuro immune regulation might contribute to our understanding of the development and treatment of various inflammatory conditions such as peritonitis and various inflammatory bowel diseases. If and how sympathetic nerves are involved in OMS immune modulation requires further investigation. Recently we have confirmed that OMSs in mice contain sympathetic nerves (Cleypool et al., unpublished data) and therefore these animals might represent a useful experimental model. OMS innervation originates from paravascular sympathetic nerves that run with the left and right gastro epiploic arteries and from there continue with smaller branches into the omentum (as observed in whole mount samples in mice and human fetuses, (Cleypool et al., unpublished data)). Electrical stimulation or denervation of this epiploic paravascular nerve plexuses could provide insights in its role on immune cell composition and activity in the peritoneal fluid or intestinal lining. If indeed a regulatory role for these nerves is established, these nerves or their involved AR receptors, could represent therapeutic targets in the treatment of various clinical conditions.

## Omental milky spot-like structures at locations outside the omentum

OMSs do not represent a separate entity. Although lower in number, similar structures have been observed in the parietal peritoneum, mesenteries, mediastinum, pleura and pericardium in rodents (Cruz-Migoni and Caamano, 2016)(Michailova and Usunoff, 2004). OMSs and their extra omental counterparts (by us referred to as extra-OMS, but in literature occasionally referred to as fat associated lymphoid structures or FALCs) are therefore suggested to represent a system of body cavity monitoring lymphoid structures. If extra-OMSs have comparable functions to OMSs, new findings on immune function and regulation of OMSs might be applicable to these structures as well and could contribute to our understanding of the development and treatment of e.g., pleuritis and pericarditis. Extra-OMSs in humans have been reported for newborns only wherein they have been observed in the mediastinal pleura and chest wall (Shimotsuma et al., 1993). During a pilot study in our department however, extra-OMSs were observed to be present in strips of adult peritoneum, pericardium and pleura (Cleypool et al., unpublished data). These observations justify further exploration of extra-OMSs in humans which could be accomplished by determining their location, immune cell composition and the presence of sympathetic nerves.

## OMSs and their role in omental metastatic disease

Evidence is accumulating that the sympathetic nervous system, and moreover its neurotransmitter NE *1)* contributes to a favourable tumor microenvironment by e.g. affecting stromal cells, endothelial cells, and tumour-associated macrophages (Magnon et al., 2013), and *2)* stimulates tumor cell proliferation, via ß-ARs on these cells (Coelho et al., 2017). The presence of sympathetic nerves in OMSs might therefore contribute to our understanding of why they form a preferential implantation site for peritoneal exfoliated tumor cells and hence omental metastatic disease. If tumor cells from e.g. gastric or ovarian cancer exfoliate to the peritoneal cavity, they end up in the peritoneal fluid and subsequently get absorbed by OMSs. In the presence of NE secreted by sympathetic nerves, these tumor cells might develop into metastases. The role of sympathetic nerves in omental metastatic disease development could be experimentally investigated e.g. in an omental metastatic mouse model wherein tumor cells are injected into the peritoneal cavity. Electrical stimulation or denervation of epiploic paravascular nerve plexuses could provide insights into the role of locally released NE on the formation of omental metastases. If these nerves and hence adrenergic signaling indeed play a role, this opens avenues to potential new therapies for the treatment of omental metastatic disease. Since the contribution of NE to tumor development and growth are mediated via ARs, AR blocking could serve as a potential anti-tumor therapy for patients that are at risk for exfoliation of tumor cells to the peritoneal cavity (e.g. patients with grade 4 tumors or that are about to undergo tumor surgery). Support for potential effectiveness of the use of AR blockers is derived from retrospective epidemiological and from experimental studies, which have shown reduced progression of e.g. breast, prostate and ovarian cancer after exposure to AR blockers (Cole et al. 2015).

In the study described in **Chapter 8** we have shown that the omental apron of gastric cancer patients contains various types of lymphoid structures; OMSs, LNs and intermediate lymphoid structures (the latter not meeting criteria for either OMSs or LNs). Since the presence of intermediate structures and LNs in the omentum have not been previously reported in anatomical literature, these structures might occur in association with specific diseases only, such as gastric cancer. OMSs are dynamic structures that upon immune stimulation increase in number and size (Krist et al., 1998) and undergo morphological changes including segregation of T and B cells and the formation of follicles with occasionally germinal centres (Dux et al., 1986) (Jackson-Jones et al., 2016) (Bénézech et al., 2015). In our study we have observed intermediate lymphoid structures fitting the description of activated OMSs, but noticed that some showed additional, more LN-like features. These features comprised a partial covering composed of collagen and smooth muscle cells, and SMA and podoplanin-IR in stromal cells of T and B cell regions, respectively. These observations advocate that OMSs might be more dynamic than previously thought and, as we hypothesize, sequentially evolve into intermediate lymphoid structures and LNs upon immune stimulation. If so, activated OMSs that show LN characteristics might be wrongly mistaken for e.g. subpyloric LNs. If these structures then contain metastases, local spread might be assumed, whereas this actually is a reflection of peritoneal spread and hence more severe disease. Increased understanding of which lymphoid structures reside in the healthy and diseased omentum is therefore significant and could

be assessed in developmental and experimental studies, respectively. Additional studies should also focus on mapping the lymphatic drainage pathways in the omentum as this contributes to our understanding of omental tumour spread.

Activation of OMSs has previously been suggested to be the result of absorption of disseminated tumor cells (Krist et al., 1998). However, tumor cells were observed in intermediate lymphoid structures in 1 patient only and other stimuli in the peritoneal fluid, such as tumor specific chemokines secreted by the primary tumor or surrounding stromal cells, should be considered. Since OMSs represent selective implantation sites for disseminated tumour cells in the peritoneal cavity (Krist et al., 1998)(Tsujimoto et al., 1995), these unknown substances might play a role in the formation of a premetastatic niche. The presence of intermediate lymphoid structures and / or activating substances (in the peritoneal fluid) therefore might be of prognostic value and the nature of their presence requires further studies.

## Lymph nodes

Human inguinal LNs contain sympathetic nerves in their capsule, cortex, medulla and hilum, not only paravascular but also as discrete structures (**Chapter 9**). Although previous studies suggest sympathetic innervation of human LN parenchyma to be a rare finding (Fink and Weihe, 1988) (Panucio et al. 1998), we have shown this represented a more common feature, especially in the medulla. Discrete sympathetic nerves were observed to be in close proximity to T cells and the presence of synaptophysin, a protein that is suggestive for varicosities, suggests local neural activity. T cells are known to express beta (β) 2- adrenergic receptors (AR), which upon activation can regulate T cell differentiation, activation, and effector function (recently reviewed by Qiao et al., 2018). Although the current study focused on the relation of sympathetic nerves with T cells, other immune cells, such as macrophages, dendritic cells and B cells express adrenergic receptors (Qiao et al. 2018) and might be under direct sympathetic control as well. Since LNs and the spleen share morphological and functional similarities one could assume that in addition to direct immune regulation, intermediate mechanisms as previously discussed for the spleen are involved as well, including the reticular framework. In addition to the parenchyma, sympathetic nerves were observed in LN capsules and occasionally in their trabeculae. These structures are known to contain a substantial amount of SMCs (Furuta 1948) (Folse et al. 1975) which most likely represent the neural target tissue of the observed fine discrete sympathetic nerves. *In vitro* electrostimulation of bovine capsular nerves resulted in contraction of these SMCs (Lobov and Pan'Kova 2013) and hence contraction of the LN as a whole. Although the contribution of capsular and trabecular nerves to LN immune function remains to be resolved, one could assume that LN contraction affects its lymph and blood flow, immune cell migration, and immune cell egression. Although functional studies on human LN innervation are lacking, based on rodent studies one might assume that sympathetic nerves and ARs are involved in similar processes being lymphocyte proliferation, antibody secretion, blood perfusion, inflammatory cytokine production, and lymphocyte migration and egression (Madden et al. 1989)(Madden et al. 1994)(Rogausch et al. 2004)(Nakai et al. 2014)(Suzuki et al. 2016)(Guyot et al.,

2019). Most of these studies were performed by the i.v. or i.p. administration of chemical substances that either induced sympathectomy or AR stimulation. In therapy development for humans one would preferably avoid these types of interventions as they could have various wide spread side effects. The study of Guyot et al (2019) suggest that local electrical stimulation of LN sympathetic nerves could be benificial as well. Electrical stimulation of the pancreatic nerve (a nerve that runs with the GDA) in mice resulted in accumulation of T and B cells in pancreatic LNs, inhibition of the inflammatory cytokine production and moreover, in reduced proliferation of autoreactive T cells and inhibition of disease progression in diabetic mice (Guyot et al., 2019). These observations are suggestive for the fact that LN sympathetic nerve stimulation can effect (auto) immune activity in the organ / area it drains. More data from LN sympathetic nerve stimulation studies in rodents are required to further support these assumptions and consider its therapeutic potential. In parallel, human cadaveric studies on LN nerve supply could help to estimate if and how electrical stimulation should be applied to these structures.

## ISSUES OF CONCERN FOR FURTHER DEVELOPMENT OF SYMPATHETIC NERVE BASED ANTI-INFLAMMATORY THERAPY

Electrical stimulation of sympathetic nerves might represent an anti-inflammatory therapy as its benefits have been shown in various animal models. Translating this finding into an therapeutic application in humans is challenging and in addition to general surgical risks that come with e.g. neural electrode implantation, various other issues of concerns should be kept in mind. A selection of these issues will be discussed below.

### Neural off-target-stimulation effects

In contrast to anti-inflammatory drugs, nerve mediated anti-inflammatory therapy makes use of the body's own anti-inflammatory mechanism and is considered to be more selective (especially when stimulating in the proximity of the effector). However, side effects can occur as a result of off target stimulation and should be taken into consideration. In case of splenic plexus stimulation, nerves of the splenic plexus also continue with branching arteries towards the stomach, pancreas and greater omentum, and splenic plexus stimulation can affect their physiology. Although animal studies report that no negative side effects associated with splenic plexus stimulation were observed (Guyot et al., 2019), these studies were short-term. Therefore, future, more long-term studies may provide more accurate information.

### Long term effects of implantation of perivascular neuro electrode interfaces

Permanent implantation of electrodes, such as vagus nerve stimulators, deep brain stimulators and cardiac pacemakers, has been performed for decades and is considered safe. However, there is little experience with permanent implantation of circumferential implants, also known as cuffs, that surround the whole neurovascular bundle, the preferred neural interface for e.g. splenic

plexus stimulation. In case of a vascular cuff, atherogenic risks should be considered since a tight cuff can cause disturbance of laminar blood flow or affect the perivascular adipose tissue (PVAT). Disturbed laminar blood flow results in altered shear stress which in turn represents a risk factor for plaque formation (Chatzizisis et al., 2007). Cuff design should allow for artery expansion without applying pressure on the vessel wall. The PVAT is nowadays considered to represent an integral part of the vascular wall (also referred to as tunica adiposa), to play a critical role in vascular functions (such as vasodilatation) and to produce molecules with pro-atherogenic characteristic (Qi et al. 2018) (Nava and Llorens , 2019). The PVAT is sympathetically innervated and its adipocytes express adrenergic receptors. Sympathetic nerve activation of the PVAT has been suggested to contribute to inflammation of the vessel wall (Saxton et al., 2019) and negative effects on the vessel wall at the location of electrode implantation should be closely monitored.

## Sympathetic nerve activation and pain

Sympathetic maintained pain (SMP) refers to chronic pain that is aggravated by increased sympathetic activity (e.g. during periods of stress). SMP is thought to be the result of pathological coupling of sympathetic and sensory nerves within DRGs, along peripheral sensory nerve axons or at the sensory nerve receptor ending side (Chen and Zhang, 2015). These pathological couplings are mostly studied in DRGs, where they are referred to as sympathetic baskets and are known to develop as a result of nerve damage (neuropathy) (García-Poblete et al., 2003). Interestingly, similar observations have been reported in a rat study on colitis, suggesting that the occurrence of sympathetic baskets is not restricted to neuropathy only, but is associated with non-neuronal, peripheral inflammatory diseases as well. If chronic peripheral tissue inflammation, such as the case in CIDs, results in sympathetic-sensory nerve coupling, sympathetic nerve stimulation in these patients might activate / aggravate pain. Although the presence of sympathetic baskets in human DRGs has been previously reported (García-Poblete et al., 2003), our understanding of their nature and their role in SMP is relatively concise. A pilot study was performed to increase our insights on these structures (**Chapter 10)** and showed that there was an intra and interpersonal variation in the presence of sympathetic baskets when comparing various levels and sides. Furthermore, ß2-ARs were abundantly present on both sensory neurons as well as on their associated satellite ganglion cells, making them likely effector cells for adrenergic signalling in the presence of sympathetic baskets.

Future complementing studies should preferably include cadavers with a known unilateral inflammatory pathology, as this will allow to compare DRGs from affected to non-affected body sides and potentially link their occurrence to local peripheral inflammatory processes. Although sympathetic-sensory nerve coupling is mostly studied in DRGs, it should be kept in mind that these connections can also occur along the peripheral axon of sensory nerves or at the receptor side. Although our knowledge on SMP and their underlying mechanism in humans is incomplete, CID patients with known SMP should be carefully considered for sympathetic nerve based anti-inflammatory therapy as stimulation of sympathetic nerves might worsen their pain.

## Role of sympathetic innervation in cancer

Increased release of local or systemic NE can contribute to the progression of cancer (Magnon et al., 2013)(Coelho et al., 2017). Electrical stimulation of sympathetic nerves results in the release of NE and hence should be carefully considered in cancer patients or in patients that have an increased risk of cancer development.

## Altered immune function in CIDs and hence unpredictable effects of sympathetic nerve stimulation

The anti-inflammatory effectiveness of activation of the CAIP, either via electrical VNS or splenic plexus stimulation, has been confirmed in various animal studies. These studies included either healthy animals or animals with acute induced inflammation. CIDs however, are the result of chronic, gradually developed uncontrolled immune cell activity (Furman et al., 2019) (Dhabhar, 2014) and CID patients might show a different response upon sympathetic nerve stimulation. Understanding CID related immune system alterations might be helpful in translating experimental data and predicting the effect of sympathetic nerve stimulations in humans.

Dysregulation of the immune system in CID patients might be a result of decreased efficacy of the body's own anti-inflammatory mechanisms such as loss of sympathetic innervation and hence a decreased anti-inflammatory reflex (Hoover et al., 2017) or changes in receptors involved in immune cell regulation. It is for instance known that the number of β2 -ARs on immune cells can irreversibly be decreased as shown for a subgroup of asthma patients (Miller and Chen 2006), thereby most likely making them less receptive for reflexively anti-inflammatory effect of NE secreted by local sympathetic nerves. In this specific group of patients, blocking of alpha (a)-ARs has proven to be beneficial. Potentially, in case of a decrease in b2-ARs, exposure of immune cells to NE results in activation of the low affinity a-ARs, which are known to have a pro-inflammatory effect. This might explain why acute stress, and thus increased sympathetic activity exacerbates symptoms in these patients (Miller and Chen, 2006). In addition to asthma, stress is known to exacerbate symptoms in various other CIDs as well, including Crohn's disease and ulcerative colitis (Mawdsley and Rampton, 2005) (Sun et al., 2019). How can activation of sympathetic nerves, which under normal conditions should have an anti-inflammatory effect, have a pro-inflammatory and thus opposite effect in these specific CIDs? Could this be explained by similar altered AR expression as shown in asthma patients? The double-edged sword effect of sympathetic activation on inflammation substantiates the need for studies that elucidate altered immune function characteristics of CID patients. Insights in these changed profiles can help to estimate the effect of sympathetic nerve stimulation therapy and more importantly avoid exacerbation of inflammation.

## Don't shoot the messenger

CIDs are known to result from immune driven inflammation and anti-inflammatory drugs represent the first line treatment. These therapies aim to inhibit and contain inflammation, thereby preventing irreversable tissue damage and spreading to other areas. Although of vital significance, these

therapies (including potential novel therapies such as VNS or splenic plexus stimulation) treat symptoms only and do not cure the underlying cause; a dysfunctional immune system. In order to work towards a healing approach instead of symptom relieve, further increasing our understanding of what causes the immune system to go off the rails in the first place is of considerable importance. The last decades significant progress has been made in identifying factors that underly a dysfunctional immune system and include both genetic and epigenetic factors, with epigenetic factors accounting for the majority. Major epigenetic factors represent exposure to environmental toxins (e.g. via food or air) (Yang et al., 2014), a shift in composition of the intestinal microbiome (Hand et al. 2016) and (psychological) chronic stress (Dhabhar, 2014)(Seiler et al., 2020). Exposure to toxins, such as pesticides, solvents and air pollutants can negatively alter synthesis of cytokines, immunoglobulins and inflammatory mediators thereby negatively affecting the activation and survival of immune cells (Yang et al., 2014). These toxins and other phenomena associated with large-scale urban living, such as the use of antibiotics and unhealthy diets, have been linked to significant narrowing of bacterial diversity of the microbiome. It is now known that the microbiota act as a genetically distinct organ that is critical for the enzymatic digestion of food, promotion of general immune homeostasis and prevention of enteric infection (Hand et al., 2016). Interestingly, shifts in microbiota can also occur as a result of chronic psychological stress (Siopi et al., 2020), which by itself can also directly affect the immune system. These direct chronic stress induced immune alterations (which comprise alterations as described in the previous paragraph) are caused by prolonged increased levels of stress hormones and neurotransmitters secreted by a hyperactive hypothalamic-pituitary-adrenal (HPA)-axis and sympathetic nervous system, respectively (Dhabhar, 2014). To cure CIDs, patient care should not focus on symptom relieve only, but also combat its potential cause. The latter might be accomplished by focussing on an inflammation preventive lifestyle which might include, but is not limited to, education on healthy food, avoidance of exposure to toxic substances, optimisation and re-balancing of the microbiome and prevention of chronic stress.

## Stressing an already stressed immune system

In the light of sympathetic nerve based anti-inflammatory therapy development, the contribution of chronic stress to CID development raises a significant question: Wouldn't stimulation of the sympathetic nervous system, which over activity might have partially contributed to the problem in the first place, not further contribute to disease progress? Patients, whose CID might be rooted in chronic psychological stress, should be carefully considered for sympathetic nerve based anti-inflammatory therapy until our understanding of its effect on an already stressed immune system is improved.

# FINAL CONCLUSION

The studies described in this thesis have shown that the human spleen, OMSs and LNs contain sympathetic nerves. These nerves were observed not only surrounding vascular structures but also as discrete nerves in proximity with T cells where they might reflexively regulate their immune function. The presence of these nerves is encouraging for further exploration of their potential as therapeutic intervention sites for the treatment of inflammatory diseases. Although promising, neuroimmunomodulation is a relatively new, primarily experimental discipline and further consideration of its therapeutic application in humans requires further studies. These studies should aim to increase our understanding of the underlying mechanism, provide comparative anatomical data that facilitate translation from animal studies to humans and make an inventory and assessment of all potential risks and side effects associated with surgical procedures, long term implantation of electrodes and electrical nerve stimulation.

# APPENDICES

&

# SUMMARY

Animal studies have demonstrated that various secondary lymphoid organs (including the spleen and lymph nodes) are sympathetically innervated and that these nerves play a crucial role in regulation of immune cell activity via adrenergic receptor signaling. Electrical stimulation of these nerves results in alteration of the immune response, which in case of the splenic nerves, comprises dampening of the systemic inflammatory response. These observations lead to the consideration of electrical stimulation of these nerves as an anti-inflammatory therapy for the treatment of chronic inflammatory diseases (CIDs). Further assessment of the accessibility and therapeutic potential of these lymphoid organ specific nerves in humans requires knowledge on their afferent pathways and innervation patterns. Since this relevant data on human lymphoid organs is limited, this thesis aimed to provide these anatomical details for a subset of these organs, being the spleen, omental milky spots (OMSs) and lymph nodes (LNs).

Sympathetic maintained pain (SMP) is a specific type of chronic pain which is aggravated by sympathetic activity and can be explained by pathological sympathetic sensory nerve coupling e.g. in dorsal root ganglia (DRGs). Patients with a CID, might be at risk for the development of these inflammation induced nerve connections, and increased sympathetic activity, e.g. by therapeutic electrical stimulation of sympathetic nerves, might exacerbate pain. This thesis includes a pilot study on the phenomenon of sympathetic sensory nerve coupling in human DRGs.

## Part I: The spleen

Data provided in **Chapter 2** shows that the human splenic plexus is primarily composed of sympathetic nerves which run towards the spleen in a paravascular fashion with the splenic artery (SA). The splenic plexus as a whole remained in close proximity to the adventitial surface of the SA, even at locations where SA segments extended from the pancreas. These segments, referred to as SA loops, have been evaluated as safe nerve stimulation sides; they provide enough space between SA loop limbs and the pancreas to introduce surgical instruments for the purpose of exposing the site for intervention, and, for application and stabilization of a neural interface. Furthermore, it was concluded that the most optimal neuro-electrode interface requires a circumferential device that can contain both the SA and its surrounding nerve plexus as a whole. Subsequently developed surgical implantation techniques and a nerve stimulation device are currently under evaluation in a clinical trial.

A recent study suggests that, in addition to the splenic plexus, the murine spleen is supplied with a parasympathetic apical splenic nerve (ASN), a macroscopically observational discrete white nerve-like structure entering the spleen at its cranial pole. Electrical stimulation of the ASN resulted in an anti-inflammatory response in mice and the presence of an equivalent structure in humans might, compared to the splenic plexus, provide a safer and more easily accessible stimulation

side. However, based on macro- and microscopic comparative studies as presented in **Chapter 3,** the existence of the ASN in both mice and humans is disclaimed.

The study described in **Chapter 4** shows that the human spleen contains sympathetic nerves in most of their periarteriolar lymphatic sheaths (PALSs). These nerves were observed surrounding the central artery and occasionally were in close proximity to surrounding T cells. This topographical configuration is suggestive for an immune regulatory role for these nerves. However, since splenic sympathetic nerve distribution shows interspecies variation (humans show significant less nerves compared to various rodents), it remains difficult to estimate the anti-inflammatory potential of splenic nerve stimulation in humans. Age-related variations were observed and suggest that the number of splenic sympathetic nerves slightly decreases after adulthood.

## Part II: Omental milky spots

Omental milky spots (OMSs) are omental residential lymphoid structures which play a significant role in peritoneal immune homeostasis; they absorb and monitor peritoneal fluid and, in the presence of eminent threat, provide immune cells to the peritoneal cavity. As shown in **Chapter 5,** Hematoxylin staining of large fixed samples of the omentum provides a fast and simple method that facilitates identification and isolation of these otherwise difficult recognisable structures. This method allowed for isolation of OMSs and performing additional microscopic studies. Data provided in **Chapter 6** shows that human OMSs receive sympathetic innervation and that occasionally sympathetic nerves were in proximity to T cells. If these nerves regulate the OMS immune response and hence the delivery of immune cells to the peritoneal cavity, they might represent potential therapeutic intervention sites for the treatment of various peritoneum related conditions such as peritonitis, peritoneal adhesions or the formation of peritoneal fibrosis.

Furthermore, the presence of sympathetic nerves, and moreover their neurotransmitter norepinephrine (NE), might explain why OMSs represent metastatic hotbeds for peritoneal disseminated tumour cells; NE is known to contribute to a tumour stimulating environment and can regulate tumour cells as they express adrenergic receptors. If future studies indeed confirm a role for these OMS sympathetic nerves in omental metastatic disease, these nerves, or their corresponding receptors, might represent new anticancer targets. To increase our understanding of omental cancer dissemination patterns and to optimise treatment, a clear understanding of the omental lymphatic system (lymphoid structures and lymphatic vessels) is essential. In contrast to anatomical reference work, which mention OMSs to represent the only omental lymphoid structures, clinical studies frequently report on the presence of omental LNs. Understanding which lymphoid structures are present in the omentum is of significance, especially in gastric tumor metastases; tumor deposits in omental LNs suggest local lymphatic spread, whereas tumor deposits in OMSs suggest peritoneal spread and hence extensive disease. Since LNs and OMSs share morphological characteristics and OMSs might be wrongly identified as LNs, reliable hallmarks facilitating easy discrimination are needed. **Chapter 7** provides a method that allows distinguishing LNs from OMSs. The presence of

a capsule, trabeculae, distinct B and T cell regions and a layered organization represent consistent and reliable LN specific morphological features and allow for easy distinction between LNs and OMSs, especially when observed in combination. Sufficient visualization of these hallmarks in microscopic slides can be achieved by picrosirius red, smooth muscle actine and a double B and T cell staining. This method was then used to re-evaluate the presence of LNs in the omental apron of gastric cancer patients **(Chapter 8)**. Interestingly, only a portion of lymphoid structures that were previously reported by the pathologist as LNs represented true LNs, the other structures showed characteristics that neither fitted LN or OMSs and hence were referred to as intermediate structures. The fact that in these patients the omentum contained, in addition to OMSs, LNs and intermediate lymphoid structures emphasizes that our understanding of both immune structure and function of the greater omentum is far from complete. Further studies addressing omental lymphoid structure and function in both health and disease are required to increase our understanding of gastric tumor spread and what additional therapy would be most effective for gastric cancer patients.

### Part III: Lymph nodes

Human lymph nodes contain sympathetic nerves in their capsule, trabeculae, cortex, medulla and hilum, both as paravascular or as discrete structures **(Chapter 9)**. Discrete nerves were observed in relation to T cells and non-T cell rich areas such as the hilar and capsular connective tissue. The presence of discrete nerves suggests neural regulation of structures other than blood vessels, which was further supported by the presence of varicosities in a portion of these nerves.

### Part IV: Dorsal root ganglia

Data provided by a pilot study in **Chapter 10** shows that human DRGs can contain sympathetic baskets (sympathetic nerve networks that surround primary sensory neuron somata) and that their occurrence is variable between and within individuals, the latter with respect to side and level of the studied DRGs. Although aging is suggested as a potential cause for the occurrence of sympathetic baskets, the observations of this pilot study favour a local, most likely pathological cause. ß2-ARs were observed in on the membranes of all satellite glial cells and primary sensory neurons, suggesting that sympathetic baskets could directly affect their functioning via release of NE. Future studies should focus on the occurrence of sympathetic baskets in association with peripheral tissue inflammation to gain more insight into whether CID patients are at risk for the development of SMP and whether sympathetic nerve based anti-inflammatory therapy should be avoided.

## CONCLUSION

The human spleen, OMSs and LNs contain sympathetic nerves, not only as perivascular structures but also as discrete nerves in proximity to immune cells, of which at least T cells. The presence of these nerves is encouraging for further exploration of their potential as immunomodulatory therapeutic intervention sites for the treatment of inflammatory diseases. Although promising,

neuroimmunomodulation is a relatively new, primarily experimental discipline and further consideration of electrical stimulation of nerves in order to modulate immune responses in humans requires further studies. These studies should aim to increase our understanding of the underlying anti-inflammatory mechanism, provide comparative neuroanatomical data that facilitate translation of data from animal studies to humans, and make an inventory and assessment of all potential risks and side effects associated with surgical procedures, long term implantation of electrodes and electrical nerve stimulation.

# NEDERLANDSE SAMENVATTING



Uit dierstudies is bekend dat diverse secundaire lymfoide organen, waaronder de milt en lymfeklieren, een sympathische innervatie (zenuwvoorziening) hebben. Deze sympathische zenuwen reguleren via specifieke (adrenerge) receptoren de immuunactiviteit van immuuncellen in deze organen. Zo resulteerde elektrische stimulatie van sympathische zenuwen van de milt in een verlaagde systemische inflammatoire respons. Deze observatie leidde tot de suggestie dat elektrische stimulatie van deze specifieke zenuwen als anti-inflammatoire therapie ingezet kan worden bij de behandeling van o.a. chronische ontstekingsziekten.

Onderzoek naar de toegankelijkheid en de therapeutische inzetbaarheid van deze sympathische zenuwen bij de mens vergt inzicht in o.a. de aanvoerroutes van deze zenuwen (waar zouden ze gestimuleerd kunnen worden?) en het innervatiepatroon van lymfoide organen zelf (bereiken deze zenuwen ook daadwerkelijk immuuncellen zodat ze deze kunnen beïnvloeden?). Omdat relevante informatie over sympathische innervatie van humane lymfoide organen beperkt is, had het onderzoek dat in dit proefschrift gepresenteerd wordt tot doel deze anatomische details te beschrijven voor een selectie van lymfoide organen, namelijk de milt, omentale milky spots (OMSs) en lymfeklieren.

Sympathische gemedieerde pijn is een vorm van chronische pijn die verergert bij activatie van het sympathisch zenuwstelsel. De verklaring van dit fenomeen zou kunnen zijn dat een ontstekingsreactie een pathologische verbinding tussen sympathische en sensibele zenuwen initieert. Dit kan onder meer in spinale ganglia voorkomen, maar ook op andere plekken langs sensibele zenuwen. Patiënten met chronische ontstekingsziekten lopen mogelijk een verhoogd risico voor het ontstaan van dit soort verbindingen en daarmee het risico dat elektrische stimulatie van sympathische zenuwen (in het kader van anti-inflammatoire therapie) de pijn verergert. Dit proefschrift bevat een pilotstudie naar het fenomeen van sympathische-sensibele zenuwkoppeling in humane spinale ganglia.

## Deel I: De milt

De resultaten van **Hoofdstuk 2** laten zien dat het aanvoerende zenuwweefsel van de humane milt voornamelijk sympathisch van aard is en dat dit paravasculair, in de vorm van een plexus (netwerk), via de milt arterie de milt bereikt. Deze miltzenuwplexus blijft in zijn gehele verloop in nauwe relatie met de milt arterie, ook op plekken waar deze arterie sterk gekronkeld is en daardoor verder van de pancreas af ligt. Deze arteriële lussen kunnen een veilige plek vormen voor stimulatie van de zenuwplexus; er is namelijk genoeg ruimte tussen de miltarterie en de pancreas voor de introductie van chirurgisch instrumentarium om de arterie en zijn zenuwplexus bloot te leggen én voor de implantatie en fixatie van een electrode. Verder kon uit deze studie geconcludeerd worden dat de meest optimale electrode een circumferentiële electrode is die rondom de milt arterie en de omringende zenuwplexus geplaatst kan worden. Deze resultaten hebben bijgedragen

aan het ontwikkelen van een chirurgische benadering en het ontwerpen van een electrode die momenteel in een eerste klinische studie worden geëvalueerd.

In een recente studie is aangetoond dat de muizenmilt behalve door sympathische zenuwen ook wordt geïnnerveerd door een separate parasympatische apicale zenuw; een macroscopisch zichtbare zenuw bij de craniale pool van de milt. Electrische stimulatie van deze apicale miltzenuw resulteerde, net als stimulatie van sympathische miltzenuwen, in een systemische anti-inflammatoire respons bij muizen. Als de humane milt ook door een dergelijke zenuw wordt geïnnerveerd vormt deze in vergelijking met de miltzenuwplexus wellicht een veiliger en gemakkelijker te benaderen aangrijpingspunt voor stimulatie. Echter, de vergelijkende macro- en microscopische studie beschreven in **Hoofdstuk 3**, ontkracht het bestaan van de apicale miltzenuw, zowel in muis als mens.

Het onderzoek beschreven in **Hoofdstuk 4** laat zien dat de humane milt sympathisch zenuwweefsel bevat in een groot deel van de peri-arteriole lymfatische schede (PALS), dit is de regio waarvan wordt gedacht dat er neuro-immuun regulatie plaatsvindt. Deze zenuwen waren zichtbaar rondom de centrale arterie van de PALS en in sommige gevallen hadden zij een nauwe topografische relatie met direct omringende T cellen. Deze topografische relatie is suggestief voor een immuun regulerende rol voor deze zenuwen. Omdat de mate van PALS innervatie soort specifiek is (de mens heeft aanzienlijk minder innervatie in de PALS dan diverse proefdieren), is het lastig om de waarde van bij proefdieren verkregen data in te schatten voor de mens en daarmee ook de anti-inflammatoire therapeutische potentie van miltzenuwstimulatie. Deze studie liet ook zien dat er leeftijdsgebonden variaties waren in zenuwkwantiteit en dat deze licht afneemt na het bereiken van de volwassen leeftijd.

## Deel II: Omentale milky spots

OMSs zijn lymfoide structuren die zich bevinden in het omentum majus en een belangrijke rol spelen bij de peritoneale immuunhomeostase; ze absorberen peritoneale vloeistof en monitoren deze op de aanwezigheid van o.a. pathogenen én ze leveren immuuncellen aan de peritoneaalholte. Zoals de studie in **Hoofdstuk 5** laat zien, is hematoxyline geschikt voor het snel en makkelijk kleuren van OMSs in grote stukken gefixeerd omentum. Door deze kleurtechniek kunnen OMSs, die ongekleurd niet zichtbaar zijn, makkelijk geïdentificeerd en geïsoleerd worden waarna ze inzetbaar zijn voor microscopisch onderzoek.

De microscopische studie beschreven in **Hoofdstuk 6** laat zien dat OMSs sympathische zenuwen bevatten waarvan sommige in nauwe relatie staan met T cellen. Als deze zenuwen, net zoals in de milt, een rol spelen bij de regulatie van OMSs-immuun activiteit dan zouden deze zenuwen een interessant therapeutisch aangrijpingspunt kunnen zijn voor de behandeling van diverse peritoneale aandoeningen waaronder peritonitis, peritoneale adhesies en fibrose.

Verder kan de aanwezigheid van sympathische zenuwen, en meer specifiek de aanwezigheid van de neurotransmitter noradrenaline, mogelijk verklaren waarom OMSs voorkeurslocaties zijn

voor de vorming van metastasen van naar de peritoneaalholte gedissemineerde tumorcellen; noradrenaline staat namelijk bekend om zijn bijdrage aan het creëren van een tumor stimulerende omgeving én het direct bevorderen van tumorgroei via adrenerge receptoren op tumorcellen.

Als toekomstig onderzoek inderdaad laten zien dat sympathische zenuwen in OMSs een rol spelen bij de ontwikkeling van omentale metastasen, dan zouden deze zenuwen of hun corresponderende adrenerge receptoren wellicht een nieuw anti-kanker doelwit kunnen vormen. Om meer inzicht te krijgen in metastaseringspatronen in het omentum en op geleide daarvan de behandeling te optimaliseren is een beter begrip van het totale omentale lymfoide systeem (lymfoide structuren en lymfevaten) essentieel. Dit begrip is voor de mens incompleet. Zo wordt in een aantal klinische studies, in tegenstelling tot in anatomische naslagwerken, de aanwezigheid van lymfeklieren in het omentum majus beschreven. Deze discrepantie kan mogelijk verklaard worden door het feit dat OMSs en lymfeklieren morfologische kenmerken delen. In **Hoofdstuk 7** wordt een studie beschreven die laat zien dat de aanwezigheid van een kapsel, separate B en T cel regio's en de aanwezigheid van een gelaagde organisatie (kapsel, cortex, paracortex, medulla) consistente en betrouwbare microscopische kenmerken zijn voor een lymfeklier, helemaal als ze in combinatie voorkomen. Deze kenmerken kunnen worden gevisualiseerd door kleuringen met Picrosirius rood of kleuringen met markers voor glad spierweefsel, T cellen en B cellen. Omdat omentale lymfeklieren regelmatig worden gezien bij maagkanker patiënten, is deze methodiek toegepast om te onderzoeken of het omentum daadwerkelijk lymfeklieren bevat. Coupes van omentale lymfoide structuren van deze patiënten, die eerder door de patholoog waren beschreven als lymfeklier, zijn geherevalueerd (**Hoofdstuk 8**). Slechts een deel van deze lymfeklieren bleek daadwerkelijk een lymfeklier te zijn, de overige lymfoide structuren vertoonden eigenschappen die noch bij een lymfeklier noch bij een OMS passen. Deze structuren zijn tot intermediaire structuur bestempeld. Het feit dat het omentum dus behalve OMSs ook lymfeklieren en intermediare lymfoide structuren kan bevatten laat zien dat onze kennis hierover nog tekortschiet en dat aanvullend onderzoek nodig is om metastaseringspatronen in het omentum te begrijpen en behandeling van omentale metastasen te kunnen optimaliseren.

## Deel III: Lymfeklieren

Humane inguinale lymfeklieren (klieren in de lies) bevatten een significante hoeveelheid sympathische zenuwen in hun kapsel, trabekels, cortex, medulla en hilum, dit in de vorm van zowel paravasculaire als separate zenuwen (**Hoofdstuk 9**). Deze separate zenuwen werden geïdentificeerd in het parenchym, waar zij veelal een nauwe relatie hadden met T cellen, maar ook in T cel arme regio's zoals het hilum en kapsel. De aanwezigheid van het eiwit synaptophysine in deze zenuwen suggereert lokale synaptische activiteit en daarmee de betrokkenheid van een deel van de sympathische lymfeklier innervatie bij andere functies dan regulatie van de vaattonus, zoals bijvoorbeeld immuun modulatie.

### Deel IV: Spinale ganglia

De resultaten van **Hoofdstuk 10** laten zien dat humane spinale ganglia "sympathetic baskets" (sympathische zenuwnetwerken rondom de somata van primair sensibele neuronen) bevatten, een fenomeen dat suggestief is voor sympathische-sensibele zenuwkoppeling aldaar. Er was sprake van inter- en intra-subject variabiliteit, dit laatste met betrekking tot de lichaamshelft en het niveau van de bestudeerde ganglia. Hoewel het voorkomen van deze "sympathetic baskets" het gevolg van veroudering zou kunnen zijn, suggereert deze pilotstudie dat dit waarschijnlijk pathologisch is. Tevens waren op het membraan van zowel de satelliet gliacellen als de neuronen (beta 2) adrenerge receptoren aanwezige waardoor beide mogelijk onder directe controle staan van door deze "sympathetic baskets" uitgescheiden noradrenaline. Uitbreiding van dit onderzoek zal zich dienen te richten op de aanwezigheid van deze sympathische zenuwnetwerken in combinatie met perifere ontstekingsreacties om zodoende meer inzicht te krijgen in de mogelijkheid patiënten met chronische ontstekingsziekten een verhoogd risico op de ontwikkeling van ""sympathetic baskets" hebben. Mocht dit inderdaad het geval zijn, dan zullen deze patiënten wellicht geëxcludeerd moeten worden van toekomstige anti-inflammatoire therapie die gebaseerd is op elektrische stimulatie van sympathische zenuwen, dit om initiatie of verergering van pijn te voorkomen.

## CONCLUSIE

De humane milt, OMSs en lymfeklieren bevatten sympathisch zenuwweefsel, niet alleen rondom bloedvaten maar ook als separate zenuwen. Een deel van deze separate zenuwen blijkt zelfs een nauwe topografische relatie te hebben met immuuncellen, waaronder in ieder geval T cellen. De aanwezigheid van deze zenuwen bepleit verdere exploratie van hun potentie als immunomodulatoir therapeutisch aangrijpingspunt in het kader van de behandeling van ontstekingsziekten. Hoewel veelbelovend is de discipline neuroimmunomodulatie een relatief nieuw en met name experimenteel vakgebied, en om verdere overwegingen te kunnen maken over de anti-inflammatoire inzetbaarheid van zenuwstimulaties is aanvullend onderzoek noodzakelijk. Dit onderzoek zal zich dienen te richten op o.a. het ontrafelen van de onderliggende anti-inflammatoire mechanismen, het verschaffen van neuroanatomische data die vertaling van experimentele data naar de mens faciliteert en een inventarisatie en evaluatie van potentiele risico's en bijwerkingen geassocieerd met chirurgische procedures, permanente implantatie van electroden en elektrische stimulatie van zenuwen.

# PROMOTION COMMITTEE/PROMOTIECOMMISSIE

## Promotor

| | |
|---|---|
| Prof. dr. R.L.A.W. Bleys | Department of Anatomy, University Medical Center Utrecht, Utrecht, the Netherlands |

## Other members/ Overige leden

| | |
|---|---|
| Prof. dr. J.H. de Boer | Department of Ophthalmology, University Medical Center Utrecht, Utrecht, the Netherlands |
| Dr. N. Eijkelkamp | Center for Translational Immunology, University Medical Center Utrecht, Utrecht, the Netherlands |
| Prof. dr. R. Goldschmeding | Department of Pathology, University Medical Center Utrecht, Utrecht, the Netherlands |
| Prof. dr. O.W. Kranenburg | Cancer Centre, University Medical Center Utrecht, Utrecht, the Netherlands |
| Prof. dr. R.J. Oostra | Department of Medical Biology, Section Clinical Anatomy & Embryology, Amsterdam University Medical Center, Amsterdam, the Netherlands |
| Prof. dr. J.P. Ruurda | Department of Surgery, University Medical Center Utrecht, Utrecht, the Netherlands |

# LIST OF PUBLICATIONS

## This thesis

Schurink B, **Cleypool CGJ**, Bleys RLAW. A rapid and simple method for visualizing milky spots in large fixed tissue samples of the human greater omentum. *Biotechnic & Histochemistry. 2019 Aug;94(6):429-434.*

**Cleypool CGJ**, Schurink B, Horst DEM van Der, Bleys RLAW. Sympathetic nerve tissue in milky spots of the human greater omentum. *Journal of Anatomy. 2020 Jan;236(1):156-164.*

**Cleypool CGJ**, Mackaaij C, Schurink B, Bleys RLAW. Discriminative morphological hallmarks facilitating distinction of omental milky spots and lymph nodes. *Histology & Histopathology. 2020 Nov;35(11):1275-1284.*

**Cleypool CGJ**, Lotgerink Bruinenberg D, Roeling TAP, Irwin E and Bleys RLAW. Splenic artery loops: Potential splenic plexus stimulation sites for neuroimmunomodulatory-based anti-inflammatory therapy? *Clinical Anatomy. 2021 Apr;34(3):371-380.*

**Cleypool CGJ**, Mackaaij C, Lotgerink Bruinenberg D, Schurink B and Bleys RLAW. Sympathetic nerve distribution in the human lymph node. *Journal of Anatomy. 2021 Aug;239(2):282-289.*

**Cleypool CGJ**, Mackaaij C, Verlinde-Schellekens SAMW and Bleys RLAW. A comparative anatomical and histological study on the presence of an apical splenic nerve in mice and humans. *Journal of Anatomy. 2021.*

**Cleypool CGJ**, Brinkman DJ, Mackaaij C, Luyer MD, Nolte MA, Nikkels PGJ, Jonge de WJ. Bleys RLAW. Age-related variation in sympathetic nerve distribution in the human spleen. *Under review at Frontiers in Neuroscience.*

Schurink B, **Cleypool CGJ,** Brosens LAA, Ruurda JP, Mackaaij C, Roeling TAP, Hillegersberg R and Bleys RLAW. The apron of the greater omentum of gastric cancer patients contains various lymphoid structures including lymph nodes. *Submitted to Clinical Anatomy.*

## Other recent publications

Bovendeert JFM, Nievelstein RAJ, Bleys RLAW and **Cleypool CGJ.** A parapagus dicephalus tripus tribrachius conjoined twin with a unique morphological pattern: a case report. *Journal of Medical case reports. 2020 Oct 3;14(1):176.*

Thunnissen LJW, **Cleypool CGJ** and Bakker BS. Where do human sperm and egg meet? *Reproduction. 2021 Jan;161(1):V1-V4.*

Mooren ERM, **Cleypool CGJ**, de Kort LMO, Goverde AJ and Dik P. A retrospective analysis of female Müllerian duct anomalies in association with congenital renal abnormalities. *Journal of Pediatric & Adolescent Gynecology. 2021 May12;S1083-3188(21)00201-1.*

Verdoorn D, **Cleypool CGJ**, Mackaaij C, Bleys RLAW. Visualization of the Carotid Body *in situ* in fixed Human Carotid Bifurcations using a xylene-based tissue clearing method. *Under review at Biotechnic & Histochemistry.*

Cox IL, **Cleypool CGJ**, Ru de JA, Bleys RLAW. A cadaveric study on the presence of sensory nerves in the trapezius. *Submitted to Clinical Anatomy.*

Mooren ERM, Roessingh T, De Bakker BS, **Cleypool CGJ**, Lambalk CB and Dik P. The Entire Spectrum of Female Paramesonephric Duct Anomalies: A Review of the Embryogenesis and Dysmorphogenesis of Paramesonephric Ducts. *Submitted to Journal of Anatomy.*

## Earlier publications

Lindenbergh A, Van Den Berge M, Oostra RJ, **Cleypool CGJ**, Bruggink A, Kloosterman A and Seijen T. Development of a mRNA profiling multiplex for the inference of organ tissues. *International Journal of Legal Medicine. 2013 Sep;127(5):891-900.*

Schaddelee MP, Read KD, **Cleypool CGJ**, IJzerman AP, Danhof M and De Boer AG. Brain penetration of synthetic adenosine A1 receptor agonists *in situ*: Role of the rENT1 nucleoside transporter and binding to blood constituents. *European Journal of Pharmacological Science. 2005 Jan;24(1):59-66.*

Kemper EM, **Cleypool CGJ**, Boogerd W, Beijnen JH and Van Tellingen O. The influence of the P-glycoprotein inhibitor zosuquidar trihydrochloride (LY335979) on the brain penetration of paclitaxel in mice. *Cancer Chemothery and Pharmacology. 2004 Feb;53(2):173-178.*

Schaddelee MP, Groenendaal D, DeJongh J, **Cleypool CGJ**, IJzerman AP, De Boer AG, et al. Population pharmacokinetic modeling of blood-brain barrier transport of synthetic adenosine A1 receptor agonists. *Journal of Pharmacology and Experimental Therapeutics. 2004 Dec;311(3):1138-1146.*

Kemper EM, Van Zandbergen AE, **Cleypool CGJ**, Mos HA, Boogerd W, Beijnen JH and Van Tellingen O. Increased penetration of paclitaxel into the brain by inhibition of P-glycoprotein. *Clinical Cancer Research. 2003 Jul;9(7):2849-2855.*

# DANKWOORD

Het anatomiezaadje is waarschijnlijk geplant tijdens bezoekjes aan natuurhistorische musea. De schoonheid van de objecten zelf, de wijze van presentatie en de wetenschap die ermee gepaard ging vond ik als kind uitermate fascinerend. Dit leidde al jong tot ontleedsessies van langs de slootkant gevonden dode vissen, het vrijwillig helpen van mijn moeder bij het voorbereiden van braadkip of paling en het eindeloos kijken van "vieze" plaatjes in de medische encyclopedie van mijn ouders. Biologie werd mijn lievelingsvak op de middelbare school en ik had wisselende ambities die varieerden van patholoog-anatoom, bioloog, onderzoeker, fysiotherapeut, orthodontist of kunstenaar, een mix van inhoudelijk onderzoekend en praktisch bezig zijn binnen een biomedisch wetenschappelijke context. Als ik destijds wist dat het beroep anatoom bestond had deze waarschijnlijk bovenaan mijn lijstje gestaan en was mijn carrièrepad een rechte lijn geweest. Echter, na de middelbare school volgde een lange zwerftocht. Die begon bij de opleiding tot biomedisch research analist aan de Polytechnische faculteit van de Hogeschool van Rotterdam (locatie HLO in Delft) en eindigde met een promotieonderzoek bij de afdeling Anatomie van het UMC Utrecht. Deze tocht was niet zonder hobbels, bobbels, doodlopende steegjes, stappen terug en omwegen, maar het geplante zaadje ontkiemde en kwam tot wasdom. Hoewel dit in de natuur overwegend vanzelf gaat, wordt dit wel vergemakkelijkt door een optimale omgeving, de juiste voeding en aandacht. Graag wil ik iedereen bedankten die hier een bijdrage aan leverde.

Op de eerste plek zijn dat natuurlijk mijn ouders, **Jos en Len Cleypool**. Lieve pap en mam, ik heb me nooit beperkt of geremd gevoeld en jullie steun, waarop ik ook nu nog steeds kan rekenen, zijn me heel veel waard. Jullie zijn altijd trots geweest op wat ik deed en hebben altijd oprechte interesse getoond. Het is fijn om te mogen zijn wie je bent en vanuit intrinsieke kracht en interesse je eigen pad te kunnen uitstippelen. Jullie zijn de liefste.

Mijn grote liefde en beste vriend **Roel van de Wal** (Loejo). Zo mooi hoe na meer dan 25 jaar ons samenzijn nog altijd als een kabbelend beekje voelt; rustig en puur. Bij jou heb ik altijd helemaal mezelf mogen én kunnen zijn, jouw liefkozende term "vuilniszak" zegt mij genoeg. Hoewel anatomie niet helemaal jouw ding is, zeker niet het praktische deel ervan, ben je altijd oprecht geïnteresseerd in wat ik doe en ben je een welkom klankbord geweest voor een groot deel van mijn hersenspinsels en dus mijn onderzoek. Bedankt. Ik ben blij dat ons *wij* er nog altijd is.

**Tijl** (Schurkie) mijn kleine roze frummel met je mooie *strawberry* blonde haartjes en inmiddels super lange benen. Wat fijn dat je er bent. Samen ochtendmensen zijn is wel zo gezellig. Je zegt dat je bioloog wil worden. Geen mensenbioloog zoals ik, maar een dierenbioloog. Ik vind het prachtig en met trots en liefde help ik je bij het noteren van al je natuurvondsten in je biologenlabjournaal, koop ik wandelende takken voor je en bewaar ik de dode dieren die je voor me mee naar huis brengt.

**Rinke** (Stinkel) mijn blonde engeltje. Wij zijn elkaars liefste en wederzijds houdt de een altijd meer van de ander, dan dat de ander van jou houdt. Ik geniet van je filosofische insteek en ben gefascineerd

door het "andere leven" dat jij leidt. Jouw onuitputtelijke vragenstroom over uiteenlopende onderwerpen waaronder "Mars en Pein" en het Nederlands elfentaal en jouw berichtgeving van hoe jij dacht hoe dingen waren toen je nog klein was maken jouw gezelschap nooit saai.

Mijn zussies Angela en Renata. **Angela Cleypool**, haat-liefde met twee handen op één buik. Zo zou ik onze jeugd beschrijven. Nu is het vooral liefde en een hechte vriendschap en ben je ook als een moeder voor mijn kinderen. Sinds enige tijd heb ik eindelijk een jonger zusje, **Renate Cleypool Lima**. Zo fijn en gezellig dat je er bent. Warm tropisch bloed en een heel fijn thuisland met lieve vrienden en familie. Het was kort maar heel bijzonder om ze te ontmoeten. Hopelijk normaliseren dingen en kunnen we de drie dagen Rio nog eens uitgebreid overdoen en dan met de jongens erbij.

**Hans en Loes van de Wal**, al meer dan 25 jaar de liefste schoonouders. Ik heb me altijd welkom en gesteund gevoeld in wat ik doe. Promoveren moet je zelf doen, maar het helpt enorm als je op bepaalde dingen wordt ontlast. De vele klusjes, wasjes, maaltijden en zorgen voor de kindjes hebben hier zeker aan bijgedragen alsmede de fijne skivakanties, kampeerweekendjes, kerstdiners en familiefeestjes. COVID gooit roet in het eten voor ongedwongen samenzijn. ik hoop dat dit snel voorbij is en we elkaar weer vaker in een variatie aan omgevingen kunnen zien.

Ook in mijn dagelijkse leven voel ik me rijk. Overige **familie**, de vele **vrienden** uit diverse fasen van mijn leven en mijn **lieve buren** uit de Amsterdamse Platostraat en omstreken maken dat ik me nooit alleen voel en voor iedere facet van mijn persoonlijkheid wel medestanders heb met wie ik dingen kan delen. Te veel om iedereen bij naam te noemen, maar als je dit leest hoor jij daar zeker bij.

Onderzoeken en vooral ook het filosoferen erover doe ik het liefst samen. Ik wil daarom de mensen bedanken die hierbij een belangrijke rol in mijn dagelijks en/of professionele leven spelen.

Het autonome zenuwstelsel is uitermate fascinerend en **Sander Kales** ik ben blij dat we samen enthousiast kunnen zijn. Je was er eerder, toen weer uit beeld en nu weer terug. Ik waardeer jouw oprechte interesse in mijn onderzoek en ben blij met onze autonome zenuwstelsel nerdenclub met twee leden waarin we ongestructureerd toch een soort van structuur hebben. Wat zitten we altijd lekker op dezelfde golflengte. Of moeten we het *inter-brain neural synchronization* noemen?

Ik ben super trots op je **Babs Bakels**! En wat ben ik blij dat ik je in je opnieuw uitgevonden vorm weer mag vergezellen, nu bij je eigen kunstprojecten en podcast (*Kassiewijle*) over de dood. Jouw fascinatie deel ik en jouw kijk op dingen vind ik enorm inspirerend. Wat een feest om een vriendin te hebben om op wetenschappelijk niveau over "vieze" dingen te praten, dieren op te zetten, broodjes moeder met kind te eten, gelatine te maken, met een schedel op pad te gaan, over het wiel van ontbinding te filosoferen en botten tot stof te vermalen. Jouw interesse in alles wat ik doe sterkt me enorm en ik droom van een gezamenlijk project. Iets met de dood, terror management, innerlijke spraak, stress en psychoneuroimmunologie?

**Bernadette Schurink** wat ben ik je dankbaar dat je mij introduceerde in de wondere wereld van de milky spots. Zo fijn om met goed gezelschap in een bijzondere niche te zitten. Wat begon als het visualiseren van "spijkerbroekenpluisjes" heeft *in concreto* geleid tot vier publicaties. Milky spots (tegenwoordig verwijs ik naar ze als omentale SALCs, afgeleid van serosa associated lymphoid clusters) vervelen nooit en als we al onze ideeën tot uitvoering gaan brengen zijn we nog jaren onder de pannen. Ik ben blij dat je voor het vakgebied pathologie gekozen hebt. Jouw nieuw opgedane kennis en expertise gaat vast heel goed van pas komen bij de uitvoering van onze plannen.

**Wouter de Jonge** Zo knap hoe jij doet wat je doet. Ik ben dankbaar je aan mijn collectie mooie mensen te mogen toevoegen. Bedankt dat ik bij diverse netwerk meetings me als adoptie-collega welkom mocht voelen bij jouw onderzoeksgroep en dat we de traditie van netwerkmeetings voortzetten. Jouw bijzondere persoonlijkheid, brede interesse, pragmatische aanpak en eigenzinnige humor zijn toch een soort van slinger die ons wetenschappelijk overleg tot een feestje maken.

**Daphne Verdoorn** Fijne collega, wat ben ik blij dat ik samen met jou aan het visualiseren van het glomus caroticum mag werken. Zou ik dan toch nog via jou mijn *paraganglionic playground* krijgen? De eerste stap is in ieder geval gezet en er staan inmiddels wat interessante lijntjes uit voor samenwerkingen met de Vasculaire Chirurgie en diverse beeldvormende disciplines. Jouw eerste onderzoekshobbel zijn we samen overgegaan en ik ben blij dat je me het vertrouwen hebt gegeven je te mogen helpen. Chocotoffs en Roosvicee, dat is alles wat we nodig hebben.

Jumbolino, hartlopen en darmrace. **Marcel Nederhoff**, nu je als staflid in dienst ben gekomen bij onze afdeling en meer onderwijs gaat geven, ook op snijzaal, zie ik het toch wel een keer echt gebeuren. Je bent een fijne collega en ik kijk uit naar het gezamenlijk opstellen van een onderzoeksmissie, -visie en -strategie. Hopelijk kunnen we onze kennis, interesse en kunde bundelen en mooie dingen gaan doen. Wanneer mag de *Vagus stimulation lounge* weer open voor informeel overleg?

**Dyonne Koopmans- Lotgerink Bruinenberg**. Je begon onder mijn begeleiding als master student biomedische wetenschappen aan een onderzoeksproject waarbij we samen de studie omtrent de zenuw plexus van de milt hebben opgezet. Alles was nieuw en ik ben trots op hoe we dat samen hebben aangepakt. Jouw rustige karakter en focus, en het feit dat je uit mijn vage plannen altijd precies wist te extraheren wat ik bedoelde maakt ons tot een perfect team. Ik ben ook oprecht blij dat je weer terug bent en we verder kunnen gaan waar we waren gebleven.

Schrijven is zoveel fijner met de juiste partners in crime. Bij deze wil ik dan ook mijn co-auteurs bedanken en in het bijzonder degene waarmee ik wat intensiever heb samengewerkt en die op een andere plek nog niet aan bod gekomen zijn.

Geen idee hoe we het precies moesten aanpakken met het onderzoeken van de innervatie van de humane milt, maar **Daan Brinkman**, we hebben er echt een mooie studie van gemaakt. Nog een

kleine revisie en dan is het hopelijk echt van ons bord. Succes met jouw verdere avontuur als AIOS bij de Chirurgie en het afronden van je proefschrift. Hopelijk tot ziens, hier of daar.

**Peter Nikkels**. Een patholoog met een zeer brede interesse, daar moest ik maar eens vrienden mee worden riep ik vanaf het begin tegen mijn collega's. Ik ben blij dat ik voor allerlei onderzoeksgerelateerde vragen bij je terecht kan, je altijd bereid bent om mee te denken en te helpen. Ik heb alweer allerlei nieuwe plannen dus ik kom binnenkort weer even buurten.

**Niels Eijkelkamp** De samenwerking is nog pril, maar onze gedeelde interesse in *dorsal root ganglia* (DRGs), lymfoide structuren en de translationele waarde van humaan stoffelijk overschotmateriaal vormt vast een goede basis voor de voortzetting hiervan. We gaan het zien. Vanaf september in ieder geval twee gedeelde DRG gerelateerde projecten. Ik ben zo benieuwd naar wat we gaan ontdekken.

Het aantal studenten dat ik heb begeleid op scripties, miniscriptie, bachelorstages en masterstages hebben me veel geleerd. Expliciet wil ik degene bedanken die voor langere tijd op de afdeling hebben vertoefd. Dit zijn **Lianne Coppen**, **Dyonne Koopmans**, **Sefica Barakci**, **Dorinde van der Horst**, **Pepijn van Driel** en **Jo Anne van den Bergh**. Studenten brengen leven in de brouwerij en hebben ook weer een eigen inbreng en visie wat onderzoek dynamisch houdt.

The research of this theses started with a project initiated by Galvani Bioelectronics. Therefore, I would like to thank Galvani Bioelectronics for this opportunity and more specific its involved representatives **Margriet Vervoordeldonk**, **Eric Irwin**, **Isha Gupta** and **Daniel Chew** for their pleasant cooperation. I am looking forward to a more informal meeting.

De oppositie (deskundigen die de oppositie voeren bij een wetenschappelijke promotie) bestaat uit afgevaardigden van diverse vak- en expertisegebieden waar het anatomisch onderzoek van dit proefschrift raakvlakken mee heeft, namelijk de chirurgie, oncologie, pathologie, (neuro) immunologie en vergelijkende anatomie. Ik hoop dan ook van harte dat er een interessante discussie ontstaat bij de verdediging van mijn proefschrift. Bij voorbaat wil ik de leden van de oppositie (prof. dr. **Jelle Ruurda**, prof. dr. **Onno Kranenburg**, prof. dr. **Roel Goldschmeding**, prof. dr. **Joke de Boer**, dr. **Niels Eijkelkamp** en prof. dr. **Roelof-Jan Oostra**) hartelijk danken voor hun bijdrage en betrokkenheid. Het verdedigen van mijn proefschrift lijkt me super spannend maar tegelijkertijd kijk ik er naar uit. Wat is er mooier dan over je onderzoek discussiëren met enthousiaste experts uit het veld?

**Roelof-Jan Oostra,** voorheen collega en leidinggevende, nu gastdocent in mijn keuzeblok Algemene en Toegepaste Embryologie én opponent bij de verdediging van mijn proefschrift. Dit laatste vooral als eerbetoon en dank. Jouw brede wetenschappelijke interesse is namelijk altijd een bron van inspiratie geweest gedurende het bewandelen van mijn niet-geijkte carrière pad;

van jou heb ik geleerd dat je je als anatoom niet tot één discipline hoeft te beperken maar prima ongegeneerd mag buurten bij aanverwante fundamentele disciplines (waaronder de embryologie, ontwikkelingsbiologie, vergelijkende anatomie, evolutionaire ontwikkeling, fysische antropologie, forensische wetenschap, genetica en teratologie). Anatomie in zijn breedste zin leidt met jou altijd tot leuke discussies. Zo hopelijk ook op 5 oktober en snel daarna.

Mijn lieve paranimfen **Suzanne Verlinde-Schellekens** en **Claire Mackaaij.** Ik ben gezegend met twee zulke fantastische rechterhanden die luisteren naar al mijn vage hersenspinsels en vervolgens het vermogen hebben om hier samen met mij concrete studies uit te destilleren en deze tot publiceerbare artikelen te brengen. Van milky spots tot DRGs, van muizensoep tot viscarpaccio, van dansend omentum tot transseksuele vagina's. Geen dier of weefsel is jullie te vreemd en met vol enthousiasme toveren jullie het onzichtbare om in het zichtbare. Laatjes, plankjes, plantjes, traantjes, schneiders, studenten, klankschalen, poezenposters en paraffine vingers. Geen dag op het lab (of misschien beter gezegd het kunst atelier) is hetzelfde. Ik ben blij dat jullie mijn hand willen vasthouden als ik al ons werk moet verdedigen. Samen is alles makkelijker.

Vanuit anatomisch, terminologisch perspectief bekeken suggereert het voorzetsel para bij paranimfen dat er ook nog andersoortige nimfen zijn. In het geval van mijn onderzoek is dat ook zeker het geval aangezien niet alleen onze researchanalisten (mijn paranimfen), maar ook andere medewerkers van de afdeling Anatomie een bijdrage hebben geleverd. Ik benoem ze bij deze tot mijn epi-, peri-, hyper- endo- en supranimfen.

**Marco Rondhuis, Simon Plomp** (en oud medewerkers **Fiona van Zoomeren** en **Xavier van Leening**) (epinimfen). Wat is een anatomisch bedrijf zonder goed dagelijks beheer van ruimtes, materiaal en technische ondersteuning bij diverse onderwijs en onderzoeksactiviteiten? Jullie zijn onmisbaar voor onze afdeling, maar ook voor de vele bezoekers en onderzoekers van andere afdelingen en externe partijen. Ik kijk uit naar onze verbouwing en hoop dat we het prosectoraat daarmee weer verder kunnen professionaliseren en jullie nog trotser kunnen zijn op het bijzondere werk wat jullie doen.

**Erna Beeker** en **Henriette Schakel** (perinimfen), ongelooflijk hoe jullie met liefde, aandacht, plezier en rust altijd maar klaar staan voor iedereen. Ik heb me hierdoor ook nog nooit bezwaard gevoeld om iets te vragen en heb altijd vol vertrouwen dingen uit handen kunnen geven. Door het enorme aandeel dat jullie leveren bij het beheer en de uitvoer van het lichaamsdonatieprogramma vormen jullie ook niet zomaar een regulier secretariaat, maar zijn jullie sterk betrokken bij de werving van al ons (onderwijs en) onderzoeksmateriaal. Ik realiseer me bij dit schrijven dan ook hoe onmisbaar jullie zijn geweest voor het onderzoek beschreven in dit proefschrift. Voortaan krijgen jullie een ereplaatsje in mijn manuscripten.

**Peter Heller** en **Willem van Wolferen** (hypernimfen). Beiden pensioengerechtigd (respectievelijk conservator van het museum en prosector), maar toch komen jullie nog altijd met plezier naar

de afdeling om met van alles te helpen. Dit vind ik mooi en illustreert hoe fijn en bijzonder de afdeling Anatomie is. Jullie vormen twee onuitputtelijke kennisbronnen, maar hoe gaan we jullie nou eens conserveren zodat we al jullie kennis en expertise veilig kunnen stellen? Suggesties?

Overige collegae **Marijn Zilverschoon, Tom Roeling, Isabel Thunnissen, Matty Spinder, Lieke de Wit** en de overige **Judos** (endonimfen). Onderzoek en onderwijs zijn onlosmakelijk met elkaar verbonden. Kennis helpt om onderzoek op te zetten en resultaten te interpreteren. Ik ben jullie daarom ook dankbaar dat ik voor inhoudelijke vragen, even meekijken in een preparaat, wat testweefsels uitnemen, filosoferen over een onderwerp en het kritisch meedenken over onderzoek aanpak altijd bij jullie terecht kan. Anatomie is een prachtig vakgebied, zeker als je je enthousiasme voor de inhoud kan delen.

Tot slot wil ik mijn promotor **Ronald Bleys** (supranimf) bedanken voor het zien wat anderen wellicht niet zagen of niet konden bieden. Jouw vertrouwen gaf mij de kans om in mijn eigen tempo en op mijn eigen manier mijn onderzoekskwaliteiten en onderzoeksintuïtie te ontwikkelen. Ik voel me uitermate thuis op jouw afdeling waardoor het ontkiemde anatomiezaadje goed wortel heeft kunnen schieten en heeft kunnen groeien en bloeien.  Nu is het tijd om de vruchten te plukken. Eerst nog wat laaghangend fruit, beginnende met de SALCs en DRGs en daarna hopelijk in samenwerkingsverband met andere afdelingen de overige vruchten.

Naast het verrichten van onderzoek bevatte mijn ambitiedrieluik (zoals destijds opgesteld voor mijn sollicitatie) ook management en onderwijs. Ook hierin heb je mij de ruimte gegeven en kan ik zeggen dat deze ambities na acht en een half jaar grotendeels zijn verwezenlijkt. Ik kijk ernaar uit om samen met jou een nieuw invulling te geven aan dit drieluik en daarmee een bijdrage te leveren om de afdeling Anatomie tot een waar snijpaleis te maken.

# ABOUT THE AUTHOR

Cindy Gerritje Johanna Cleypool was born on the 24th of august 1976 in Zevenbergen, the Netherlands. After graduating from the Norbertus College in Roosendaal she started a bachelor in applied Biomedical Laboratory Science at the Rotterdam University of Applied Sciences. Her final internship was performed at the department of Pharmacology at the Leiden Amsterdam Center for Drug Research in Leiden. After gaining her bachelor degree, she worked as a research technician at the department Pharmacokinetics at the Netherlands Cancer Institute (NKI) studying blood brain barrier transport of the cytostatic drug paclitaxel in a brain metastasis mouse model.

Since Cindy aspired a career in Anatomical Science rather than in Pharmacology, she started working at the education section of the department of Medical Biology (previously Anatomy and Embryology) at the University Medical Center Amsterdam (UMCA), location AMC, previously Academical Medical Center (AMC). Starting as an anatomical technician, she continued her career as the head of the dissection ward, coordinating daily activities in the dissection ward and associated lab facilities, and managing the body donation program and the development and implementation of a quality management system. Furthermore she made many anatomical prosections (including plastinated specimens) and started teaching gross anatomy, neuroanatomy and embryology. In parallel she gained her master's degree in Biomedical Sciences at the University of Amsterdam for which she performed a final research internship at the department of Neuropathology at the UMCA and John Radcliffe Hospital in Oxford.

Pursuing her academic ambitions, in 2012 Cindy started as an assistant professor at the department of Anatomy at the University Medical Centre Utrecht (UMCU). Here she teached embryology and neuroanatomy in various bachelor, master and post academic courses of the Medical and Biomedical programs of the University of Utrecht.

In May 2016 she started the research as described in this thesis. Due to her broad interest she was also involved in various other research projects, including contract research for Galvani Bioelectronics, a company developing devices for electrical stimulation of peripheral nerves to treat chronic diseases. Furthermore, she coordinated foetal body donations and managed the formaldehyde project that resulted in a large scale reconstruction plan to update the dissection ward to current safety and quality standards.

After gaining her PhD, Cindy will continue her career at the UMCU as a senior anatomist, focussing on teaching and performing research.

# REFERENCES

R

Aguzzi, Adriano, Jan Kranich, and Nike Julia Krautler. 2014. "Follicular Dendritic Cells: Origin, Phenotype, and Function in Health and Disease." *Trends in Immunology* 35(3):105–13.

Amit, Moran, Hideaki Takahashi, Mihnea Paul Dragomir, Antje Lindemann, Yu Cai, Rong Wang, Erik Knutsen, Masayoshi Shimizu, Cristina Ivan, and Xiayu Rao. 2020. "Loss of P53 Drives Neuron Reprogramming in Head and Neck Cancer." (December 2018).

Anagnostou, Valsamo K., Ipatia Doussis-Anagnostopoulou, Dina G. Tiniakos, Despina Karandrea, Emmanouil Agapitos, Petros Karakitsos, and Christos Kittas. 2007. "Ontogeny of Intrinsic Innervation in the Human Thymus and Spleen." *The Journal of Histochemistry and Cytochemistry : Official Journal of the Histochemistry Society* 55(8):813–20.

Baker, By John R. 1962. "Experiments on the Action of Mordants." *The Quarterly Journal of Microscopical Science* 103:493–517.

Bardelmeyer, G. H. 1973. "Electrical Conduction in Hydrated Collagen. I. Conductivity Mechanisms." *Biopolymers* 12(10):2289–2302.

Bassi, GabrielD. O. .. Shimizu, Daniel Penteado Martins Dias, Marcelo Franchin, Jhimmy Talbot, Daniel Gustavo Reis, Gustavo Batista Menezes, Jaci Airton Castania, Norberto Garcia-Cairasco, Leonardo Barbosa Moraes Resstel, Helio Cesar Salgado, Fernando Queiróz Cunha, Thiago Mattar Cunha, Luis Ulloa, and Alexandre Kanashiro. 2017. "Modulation of Experimental Arthritis by Vagal Sensory and Central Brain Stimulation." *Brain, Behavior, and Immunity* 64:330–43.

Baudouin, S. J., J. Angibaud, G. Loussouarn, V. Bonnamain, A. Matsuura, M. Kinebuchi, P. Naveilhan, and H. Boudin. 2008. "Diacylglycerol Is Required for the Formation of COPI Vesicles in the Golgi-to-ER Transport Pathway." *Molecular Biology of the Cell* 19(June):2444–56.

Bellinger, D. L., T. J. Felten, T. J. Collier, and D. L. Felten. 1987. "Noradrenergic Sympathetic Innervation of the Spleen: IV. Morphometric Analysis i Adult and Aged F344 Rats." *Journal of Neuroscience Research* 18(1):55–63.

Bellinger, D. L., D. Lorton, R. W. Hamill, S. Y. Felten, and D. L. Felten. 1993. "Acetylcholinesterase Staining and Choline Acetyltransferase Activity in the Young Adult Rat Spleen: Lack of Evidence for Cholinergic Innervation." *Brain, Behavior, and Immunity* 7(3):191–204.

Bellinger, Denise L., Kurt D. Ackerman, Suzanne Y. Felten, and David L. Felten. 1992. "A Longitudinal Study of Age-Related Loss of Noradrenergic Nerves and Lymphoid Cells in the Rat Spleen." *Experimental Neurology* 116:295–311.

Ben-Menachem, Elinor. 2001. "Vagus Nerve Stimulation, Side Effects, and Long-Term Safety." *Journal of Clinical Neurophysiology* 18(5):415–18.

Bénézech, Cécile, Nguyet Thin Luu, Jennifer A. Walker, Andrei A. Kruglov, Yunhua Loo, Kyoko Nakamura, Yang Zhang, Saba Nayar, Lucy H. Jones, Adriana Flores-Langarica, Alistair McIntosh, Jennifer Marshall, Francesca Barone, Gurdyal Besra, Katherine Miles, Judith E. Allen, Mohini Gray, George Kollias, Adam F. Cunningham, David R. Withers, Kai Michael Toellner, Nick D. Jones, Marc Veldhoen, Sergei A. Nedospasov, Andrew N. J. McKenzie, and Jorge H. Caamaño. 2015. "Inflammation-Induced Formation of Fat-Associated Lymphoid Clusters." *Nature Immunology* 16(8):819–28.

Bennett, Jeanette M., Glenn Reeves, George E. Billman, and Joachim P. Sturmberg. 2018. "Inflammation-Nature's Way to Efficiently Respond to All Types of Challenges: Implications for Understanding and Managing 'the Epidemic' of Chronic Diseases." *Frontiers in Medicine* 5(NOV):1–30.

Bleys, R. L. A. W. and T. Cowen. 2001. "Innervation of Cerebral Blood Vessels: Morphology, Plasticity, Age-Related, and Alzheimer's Disease-Related Neurodegeneration." *Microscopic Research Techniques* 118(December 2000):106–18.

Borovikova, L. V, S. Ivanova, M. Zhang, H. Yang, G. I. Botchkina, L. R. Watkins, H. Wang, N. Abumrad, J. W. Eaton, and K. J. Tracey. 2000. "Vagus Nerve Stimulation Attenuates the Systemic Inflammatory Response to Endotoxin." *Nature* 405(6785):458–62.

Bratton, B. O., D. Martelli, M. J. McKinley, D. Trevaks, C. R. Anderson, and R. M. McAllen. 2012. "Neural Regulation of Inflammation: No Neural Connection from the Vagus to Splenic Sympathetic Neurons." *Experimental Physiology* 97(11):1180–85.

Breiteneder-Geleff, S., A. Soleiman, R. Horvat, G. Amann, H. Kowalski, and D. Kerjaschiki. 1999. "Podoplanin, a Specific Marker for Lymphatic Endothelium Expressed in Angiosarcoma." *Verein Deutsche Gesellschaft Fur Pathologie* 83:270–75.

Brinkman, David J., Stephanie Troquay, Wouter J. de Jonge, Eric D. Irwin, Margriet J. Vervoordeldonk, Misha D. P. Luyer, and Joost Nederend. 2020. "Morphometric Analysis of the Splenic Artery Using Contrast-Enhanced Computed Tomography (CT)." *Surgical and Radiologic Anatomy* (0123456789).

Brumovsky, P. R. 2017. "Dorsal Root Ganglion Neurons and Tyrosine Hydroxylase-An Intriguing Association with Implications for Sensation and Pain." *Physiology & Behavior* 176(3):139–48.

Buijs, Ruud M., Jan Van Der Vliet, Mari-laure Garidou, Inge Huitinga, and Carolina Escobar. 2008. "Spleen Vagal Denervation Inhibits the Production of Antibodies to Circulating Antigens." PLos ONE 3(9):1–8.

Cano, Georgina, Alan F. Sved, Linda Rinaman, Bruce Rabin, and John Patrick Card. 2001. "Characterization of the Central Nervous System Innervation of the Rat Spleen Using Viral Transneuronal Tracing." *Journal of Comparative Neurology* 439(1):1–18.

Channer, J. L. and J. D. Davies. 1985. "Smooth Muscle Proliferation in the Hilum of Superficial Lymph Nodes." *Virchows Archiv A Pathological Anatomy and Histopathology* 406(3):261–70.

Chatzizisis, Y. S., A. U. Coskun, M. Jonas, E. R. Edelman, Charles L. Feldman, and Peter H. Stone. 2007. "Role of Endothelial Shear Stress in the Natural History of Coronary Atherosclerosis and Vascular Remodeling." *Journa of the American College of Cardiology* 49(25).

Chavan, Sangeeta S. and Kevin J. Tracey. 2017. "Essential Neuroscience in Immunology." *Journal of Immunology* 198(9):3389–97.

Chen, Si-Si and Jun-Ming Zhang. 2015. "Progress in Sympathetically Mediated Pathological Pain." *Journal of Anesthesia and Perioperative Medicine* 2(4):216–25.

Chung, Kyungsoon, Hee Jin Kim, Heung Sik Na, Mae Ja Park, and Jin Mo Chung. 1993. "Abnormalities of Sympathetic Innervation in the Area of an Injured Peripheral Nerve in a Rat Model of Neuropathic Pain." *Neuroscience Letters* 162(1–2):85–88.

Cleypool, CGJ, C. Mackaaij, B. Schurink, and RLAW Bleys. 2020. "Morphological Hallmarks Facilitating Distinction of Omental Milky Spots and Lymph Nodes: An Exploratory Study on Their Discriminative Capacity." *Histology Histopathology* 35(11):1275–84.

Coelho, Marisa, Cátia Soares Silva, Daniela Brandão, Franca Marino, Marco Cosentino, Laura Ribeiro, S. A. M. Sympathoadrenomedullary, A. D. Adrenaline, and C. A. R. Carvedilol. 2017. "β - Adrenergic Modulation of Cancer Cell Proliferation : Available Evidence and Clinical Perspectives." *Journal of Cancer Research and Clinical Oncology* 143(2):275–91.

Cole, Steven W., Archana S. Nagaraja, Susan K. Lutgendorf, and Paige A. Green. 2015. "Sympathetic Nervous System Regulation of the Tumour Microenvironment." *Nature Reviews Cancer* 15(9):563–72.

Cristancho, Pilar, Mario A. Cristancho, Gordon H. Baltuch, Michael E. Thase, and John P. O'Reardon. 2011. "Effectiveness and Safety of Vagus Nerve Stimulation for Severe Treatment-Resistant Major Depression in Clinical Practice after FDA Approval: Outcomes at 1 Year." *Journal of Clinical Psychiatry* 72(10):1376–82.

Cruz-Migoni, Sara and Jorge Caamano. 2016. "Fat-Associated Lymphoid Clusters in Inflammation and Immunity." *Frontiers in Immunology* 7:1–7.

Devor, M., W. Janig, and M. Michaelis. 1994. "Modulation of Activity in Dorsal Root Ganglion Neurons by Sympathetic Activation in Nerve-Injured Rats." *Journal of Neurophysiology* 71(1):38–47.

Dhabhar, Firdaus S. 2014. "Effects of Stress on Immune Function: The Good, the Bad, and the Beautiful." *Immunologic Research* 58(2–3):193–210.

Dux, K., R. V. Rouse, and B. Keywski. 1986. "Composition of the Lymphoid Cell Populations from Omental Milky Spots during the Immune Response." *European Journal of Immunology* 16:1029–32.

El-Gabalawy, Hani, Lyn C. Guenther, and Charles N. Bernstein. 2010. "Epidemiology of Immune-Mediated Inflammatory Diseases: Incidence, Prevalence, Natural History, and Comorbidities." *Journal of Rheumatology* 37(SUPPL. 85):2–10.

Elzahaf, Raga A., Osama A. Tashani, Biddy A. Unsworth, and Mark I. Johnson. 2012. "The Prevalence of Chronic Pain with an Analysis of Countries with a Human Development Index Less than 0.9: A Systematic Review without Meta-Analysis." *Current Medical Research and Opinion* 28(7):1221–29.

Felten, D. L., K. D. Ackerman, S. J. Wiegand, and S. Y. Felten. 1987. "Noradrenergic Sympathetic Innervation of the Spleen: I. Nerve Fibers Associate with Lymphocytes and Macrophages in Specific Compartments of the Splenic White Pulp." *Journal of Neuroscience Research* 18(1):28–36.

Felten, D. L., S. Y. Felten, S. L. Carlson, J. A. Olschowka, and S. Livnat. 1985. "Noradrenergic and Peptidergic Innervation of Lymphoid Organs." *The Journal of Immunology* 135:755–65.

Felten, David L., Shmuel Livnat, Suzanne Y. Felten, Sonia L. Carlson, Denise Lorton Bellinger, and Pamela Yeh. 1984. "Sympathetic Innervation of Lymph Nodes in Mice." *Brain Research Bulletin* 13(6):693–99.

Felten, S. Y. and J. Olschowka. 1987. "Noradrenergic Sympathetic Innervation of the Spleen: II. Tyrosine Hydroxylase (TH)—positive Nerve Terminals Form Synapticlike Contacts on Lymphocytes in the Splenic White Pulp." *Journal of Neuroscience Research* 18(1):37–48.

Fink, T. and E. Weihe. 1988. "Multiple Neuropeptides in Nerves Supplying Mammalian Lymph Nodes : Messenger Candidates for Sensory and Autonomic Neuroimmunomodulation?" 90:39–44.

Fletcher, Anne L., Sophie E. Acton, and Konstantin Knoblich. 2015. "Lymph Node Fibroblastic Reticular Cells in Health and Disease." *Nature Reviews Immunology* 15(6):350–61.

Folse, Dean S., Gerald A. Beathard, and Norman A. Granholm. 1975. "Smooth Muscle in Lymph Node Capsule and Trabeculae." *The Anatomical Record* 183(4):517–21.

Ford, W. L. 1979. "Lymphocytes. 3. Distribution. Distribution of Lymphocytes in Health." *Journal of Clinical Pathology. Supplement (Royal College of Pathologists)* 13:63–69.

Fujii, Takeshi, Masato Mashimo, Yasuhiro Moriwaki, Hidemi Misawa, Shiro Ono, Kazuhide Horiguchi, and Koichiro Kawashima. 2017. "Expression and Function of the Cholinergic System in Immune Cells." *Frontiers in Immunology* 8(SEP):1–18.

Furman, David, Judith Campisi, Eric Verdin, Pedro Carrera-Bastos, Sasha Targ, Claudio Franceschi, Luigi Ferrucci, Derek W. Gilroy, Alessio Fasano, Gary W. Miller, Andrew H. Miller, Alberto Mantovani, Cornelia M. Weyand, Nir Barzilai, Jorg J. Goronzy, Thomas A. Rando, Rita B. Effros, Alejandro Lucia, Nicole Kleinstreuer, and George M. Slavich. 2019. "Chronic Inflammation in the Etiology of Disease across the Life Span." *Nature Medicine* 25(12):1822–32.

Furuta, William J. 1948. "The Histologic Structure of the Lymph Node Capsule at the Hilum." *The Anatomical Record* 102(2):213–23.

Fuxe, K., D. O. Borroto-Escuela, W. Romero-Fernandez, W. B. Zhang, and L. F. Agnati. 2013. "Volume Transmission and Its Different Forms in the Central Nervous System." *Chinese Journal of Integrative Medicine* 19(5):323–29.

Gago da Graça, Catarina, Lisa G. M. van Baarsen, and Reina E. Mebius. 2021. "Tertiary Lymphoid Structures: Diversity in Their Development, Composition, and Role." *The Journal of Immunology* 206(2):273–81.

Ganusov, Vitaly V. and Jeremy Auerbach. 2014. "Mathematical Modeling Reveals Kinetics of Lymphocyte Recirculation in the Whole Organism." *PLoS Computational Biology* 10(5).

García-Poblete, Eduardo, H. Fernández-García, E. Moro-Rodríguez, M. Catalá-Rodríguez, M. L. Rico-Morales, S. García-Gómez-De-Las-Heras, and M. A. Palomar-Gallego. 2003. "Sympathetic Sprouting in Dorsal Root Ganglia (DRG): A Recent Histological Finding?" *Histology and Histopathology* 18(2):575–86.

Gautron, Laurent, Joseph M. Rutkowski, Michael D. Burton, Wei Wei, Yihong Wan, and Joel K. Elmquist. 2013. "Neuronal and Nonneuronal Cholinergic Structures in the Mouse Gastrointestinal Tract and Spleen." *Journal of Comparative Neurology* 521(16):3741–67.

Gerber, Scott A., Viktoriya Y. Rybalko, Chad E. Bigelow, Amit A. Lugade, Thomas H. Foster, John G. Frelinger, and Edith M. Lord. 2006. "Preferential Attachment of Peritoneal Tumor Metastases to Omental Immune Aggregates and Possible Role of a Unique Vascular Microenvironment in Metastatic Survival and Growth." *American Journal of Pathology* 169(5):1739–52.

Ghia, Jean Eric, Patricia Blennerhassett, Harry Kumar-Ondiveeran, Elena F. Verdu, and Stephen M. Collins. 2006. "The Vagus Nerve: A Tonic Inhibitory Influence Associated With Inflammatory Bowel Disease in a Murine Model." *Gastroenterology* 131(4):1122–30.

Gill, G. W. 2010. "Gill Hematoxylins: First Person Account." *Biotechnic and Histochemistry* 85(1):7–18.

Giron, Louis T., Keith A. Crutcher, and James N. Davis. 1980. "Lymph Nodes—A Possible Site for Sympathetic Neuronal Regulation of Immune Responses." *Annals of Neurology* 8(5):520–25.

Guyot, Mélanie, Thomas Simon, Franck Ceppo, Clara Panzolini, Alice Guyon, Julien Lavergne, Emilie Murris, Douglas Daoudlarian, Romain Brusini, Hadi Zarif, Sophie Abélanet, Sandrine Hugues-Ascery, Jean Louis Divoux, Stephen J. Lewis, Arun Sridhar, Nicolas Glaichenhaus, and Philippe Blancou. 2019. "Pancreatic Nerve Electrostimulation Inhibits Recent-Onset Autoimmune Diabetes." *Nature Biotechnology* 37(12):1446–51.

Guyot, Mélanie, Thomas Simon, Clara Panzolini, Franck Ceppo, Douglas Daoudlarian, Emilie Murris, Eric Macia, Sophie Abélanet, Arun Sridhar, Margriet J. Vervoordeldonk, Nicolas Glaichenhaus, and Philippe Blancou. 2019. "Apical Splenic Nerve Electrical Stimulation Discloses an Anti-Inflammatory Pathway Relying on Adrenergic and Nicotinic Receptors in Myeloid Cells." *Brain, Behavior, and Immunity* 80(March):238–46.

Guyot, Mélanie, Thomas Simon, Clara Panzolini, Franck Ceppo, Douglas Daoudlarian, Emilie Murris, Eric Macia, Sophie Abélanet, Arun Sridhar, Margriet J Vervoordeldonk, Nicolas Glaichenhaus, and Philippe Blancou. 2019. "Brain , Behavior , and Immunity Apical Splenic Nerve Electrical Stimulation Discloses an Anti-in Fl Ammatory Pathway Relying on Adrenergic and Nicotinic Receptors in Myeloid Cells." *Brain Behavior and Immunity* 80(March):238–46.

Hadamitzky, Catarina, Hendrik Spohr, Anette S. Debertin, Saskia Guddat, Michael Tsokos, and Reinhard Pabst. 2010. "Age-Dependent Histoarchitectural Changes in Human Lymph Nodes: An Underestimated Process with Clinical Relevance?" *Journal of Anatomy* 216(5):556–62.

Hagiwara, Akeo, Toshio Takahashi, Kiyoshi Sawai, Hiroki Taniguchi, Masataka Shimotsuma, Chouhei Sakakura, Hiroyuki Tsujimoto, Kimihiko Osaki, Sadayuki Sasaki, and Morio Shirasu. 1993. "Milky Spots as the Implantation Site for Malignant Cells in Peritoneal Dissemination in Mice1." *Cancer Research* 53:687–93.

Hall, J. C., K. A. Heel, J. M. Papadimitriou, and C. Platell. 1998. "The Pathobiology of Peritonitis." *Gastroenterology* 114(1):185–96.

Hammond, B. J. 1975. "A Compartmental Analysis of Corculatory Lymphocytes in the Spleen." *Cell Tissue Kinetics* 8(2):153–69.

Hand, Timothy W., Ivan Vujkovic-Cvijin, Vanessa K. Ridaura, and Yasmine Belkaid. 2016. "Linking the Microbiota, Chronic Disease, and the Immune System." *Trends in Endocrinology and Metabolism* 27(12):831–43.

Haverkamp, Leonie, Hylke J. F. Brenkman, Jelle P. Ruurda, Fiebo J. W. ten Kate, and Richard van Hillegersberg. 2016. "The Oncological Value of Omentectomy in Gastrectomy for Cancer." *Journal of Gastrointestinal Surgery* 20(5):885–90.

Havrlentova, L., H. Faistova, M. Mazur, D. Ziak, and S. Polak. 2017. "Comparative Analysis of Human Omental Milky Spots between the Patients with Colon Cancer and the Control Group." 118(10):580–84.

Heusermann, U. and H. J. Stutte. 1977. "Electron Microscopic Studies of the Innervation of the Human Spleen." *Cell and Tissue Research* 184(2):225–36.

Hoover, Donald B., Thomas Christopher Brown, Madeleine K. Miller, John B. Schweitzer, and David L. Williams. 2017. "Loss of Sympathetic Nerves in Spleens from Patients with End Stage Sepsis." *Frontiers in Immunology* 8(DEC):1–10.

Hu, P. and E. M. McLachlan. 2002. "Macrophage and Lymphocyte Invasion of Dorsal Root Ganglia after Peripheral Nerve Lesions in the Rat." *Neuroscience* 112(1):23–38.

Jackson-Jones, Lucy H., Sheelagh M. Duncan, Marlène S. Magalhaes, Sharon M. Campbell, Rick M. Maizels, Henry J. McSorley, Judith E. Allen, and Cécile Bénézech. 2016. "Fat-Associated Lymphoid Clusters Control Local IgM Secretion during Pleural Infection and Lung Inflammation." *Nature Communications* 7.

de Jonge, Wouter J., Esmerij P. van der Zanden, Frans O. The, Maarten F. Bijlsma, David J. van Westerloo, Roelof J. Bennink, Hans Rudolf Berthoud, Satoshi Uematsu, Shizuo Akira, Rene M. van den Wijngaard, and Guy E. Boeckxstaens. 2005. "Stimulation of the Vagus Nerve Attenuates Macrophage Activation by Activating the Jak2-STAT3 Signaling Pathway." *Nature Immunology* 6(8):844–51.

Jongerius, E. J., D. Boerma, K. A. Seldenrijk, S. L. Meijer, J. J. G. Scheepers, F. Smedts, S. M. Lagarde, O. Balague Ponz, M. I. Van Berge Henegouwen, J. W. Van Sandick, and S. S. Gisbertz. 2014. "Role of Omentectomy as Part of Radical Surgery for Gastric Cancer." *United European Gastroenterology Week* 1497–1503.

Junqueira, LCU, G. Binolas, and RR Brentani. 1979. "Picrosirius Staining plus Polarization Microscopy, a Specific Method for Collagen Detection in Tissue Sections." *Histochemical Journal* 11:447–55.

Kalson, Nicholas S., Tobias Starborg, Yinhui Lu, Aleksandr Mironov, Sally M. Humphries, David F. Holmes, and Karl E. Kadler. 2013. "Nonmuscle Myosin II Powered Transport of Newly Formed

Collagen Fibrils at the Plasma Membrane." *Proceedings of the National Academy of Sciences of the United States of America* 110(49).

Kaplan, Rosandra N., Shahin Rafii, and David Lyden. 2006. "Preparing the 'Soil': The Premetastatic Niche." *Cancer Research* 66(23):11089–93.

Kees, Martin G., Georg Pongratz, Frieder Kees, Jürgen U. Schölmerich, and Rainer H. Straub. 2003. "Via β-Adrenoceptors, Stimulation of Extrasplenic Sympathetic Nerve Fibers Inhibits Lipopolysaccharide-Induced TNF Secretion in Perfused Rat Spleen." *Journal of Neuroimmunology* 145(1–2):77–85.

Kin, Nicholas W. and Virginia M. Sanders. 2006. "It Takes Nerve to Tell T and B Cells What to Do." *Journal of Leucocyte Biology* 79:1093–1104.

Klein, R. L., S. P. Wilson, D. J. Dzielak, W. H. Yang, and O. H. Viveros. 1982. "Opioid Peptides and Noradrenaline Co-Exist in Large Dense-Cored Vesicles from Sympathetic Nerve." *Neuroscience* 7(9):2255–61.

Komega, Evilin Naname, David George Stephen Farmer, Virginia Leah Brooks, Michael Joseph McKinley, Robin Michael McAllen, and Davide Martelli. 2018. "Vagal Afferent Activation Suppresses Systemic in Flammation via the Splanchnic Anti-Inflammatory Pathway." *Brain Behavior and Immunity* 73(December 2017):441–49.

Koopman, Frieda A., Sangeeta S. Chavan, Sanda Miljko, Simeon Grazio, Sekib Sokolovic, P. Richard Schuurman, Ashesh D. Mehta, Yaakov A. Levine, Michael Faltys, Ralph Zitnik, Kevin J. Tracey, and Paul P. Tak. 2016. "Vagus Nerve Stimulation Inhibits Cytokine Production and Attenuates Disease Severity in Rheumatoid Arthritis." *Proceedings of the National Academy of Sciences of the United States of America* 113(29):8284–89.

Koppe, Manuel J., Iris D. Nagtegaal, Johannes H. W. De Wilt, and Wim P. Ceelen. 2014. "Recent Insights into the Pathophysiology of Omental Metastases." *Journal of Surgical Oncology* 110(6):670–75.

Kox, Matthijs, Jeroen F. van Velzen, Jan C. Pompe, Cornelia W. Hoedemaekers, Johannes G. van der Hoeven, and Peter Pickkers. 2009. "GTS-21 Inhibits pro-Inflammatory Cytokine Release Independent of the Toll-like Receptor Stimulated via a Transcriptional Mechanism Involving JAK2 Activation." *Biochemical Pharmacology* 78(7):863–72.

Krist, L. F. G., I. L. Eestermans, H. W. M. Steinbusch, M. A. Cuesta, S. Meyer, and R. H. J. Beelen. 1994. "An Ultrastructural Study of Dopamine Imunoreactive Nerve Fibers in Milky Spots." *Neuroscience Letters* 168:143–46.

Krist, Lambert F. G., Donna M. Broekhuis-fluitsma, Inge L. Eestermans, and Sybren Meyer. 1998. "Milky Spots in the Greater Omentum Are Predominant Sites of Local Tumour Cell Proliferation and Accumulation in the Peritoneal Cavity." *Cancer Immunology Immunotherapy* 47:205–12.

Krist, Lambert F. G. and Inge L. Eestermans. 1995. "Cellular Composition of Milky Spots in the Human Greater Omentum: An Immunochemical and Ultrastructural Study." *The Anatomical Record* 404(241):163–74.

Krist, Lambert F. G., Hans Koenen, Wim Calame, Johannes J. Van Der Harten, Johannes C. Van Der Linden, Inge L. Eestermans, Sybren Meyer, and Robert H. J. Beelen. 1997. "Ontogeny of Milky Spots in the Human Greater Omentum: An Immunochemical Study." *Anatomical Record* 249(3):399–404.

Kudoh, G., K. Hoshi, and T. Murakami. 1979. "Fluorescence of the Microscopic and Enzyme Spleen Histochemical Studies Innervation of the Human." *Archives of Histology and Cytology* 42(2):169–80.

Kuntz, Albert. 1953. *The Autonomic Nervous System*. Fourth edi. Philadelphia: Lea & Febiger.

Ladanyi, Andras, Abir Mukherjee, Hilary A. Kenny, Alyssa Johnson, Anirban K. Mitra, Sinju Sundaresan, Kristin M. Nieman, Gloria Pascual, Salvador Aznar, Anthony Montag, S. Diane Yamada, Nada A. Abumrad, and Ernst Lengyel. 2018. "Adipocyte-Induced CD36 Expression Drives Ovarian Cancer Progression and Metastasis." *Oncogene* 2285–2301.

Liebermann-Meffert, Dorothea. 2000. "THE GREATER OMENTUM Anatomy, Embryology, and Surgical Applications." *Surgical, Anatomy and Embryology* 80(1):275–93.

Liu, Jiu-yang, Jing-ping Yuan, Xia-fei Geng, Ai-ping Qu, and Yan Li. 2015. "Morphological Study and Comprehensive Cellular Constituents of Milky Spots in the Human Omentum." 8(10):12877–84.

Liu, Jiu Yang, Jing Ping Yuan, Xia Fei Geng, Ai Ping Qu, and Yan Li. 2015. "Morphological Study and Comprehensive Cellular Constituents of Milky Spots in the Human Omentum." *International Journal of Clinical and Experimental Pathology* 8(10):12877–84.

Lobov, G. I. and M. N. Pan'Kova. 2013. "Involvement of α-Adrenoceptors to the Implementation of the Contractile Effects in the Capsule of Mesenteric Lymph Nodes in Response to Electrostimulation." *Bulletin of Experimental Biology and Medicine* 154(5):588–90.

van der Loos, C. M. 2007. "Multiple Immunoenzyme Staining: Methods and Visualizations for the Observation With Spectral Imaging." *Journal of Histochemistry and Cytochemistry* 56(4):313–28.

Van der Loos, C. M. 2010. "Chromogens in Multiple Immunohistochemical Staining Used for Visual Assessment and Spectral Imaging: The Colorful Future." *Journal of Histotechnology* 33(1):31–40.

Lu, Ben and Kevin Kwan. 2014. "A7 Nicotinic Acetylcholine Receptor Signaling Inhibits Inflammasome Activation by Preventing Mitochondrial DNA Release." *Molecular Medicine* 20(1):350–58.

Lundberg, Marcus, Andreas Lindqvist, Nils Wierup, Lars Krogvold, Knut Dahl-Jørgensen, and Oskar Skog. 2017. "The Density of Parasympathetic Axons Is Reduced in the Exocrine Pancreas of Individuals Recently Diagnosed with Type 1 Diabetes." *PLoS ONE* 12(6):1–10.

Luscieti, P., T. Hubschmid, H. Cottier, M. W. Hess, and L. H. Sobin. 1980. "Human Lymph Node Morphology as a Function of Age and Site." *Journal of Clinical Pathology* 33(5):454–61.

Madden, Kelley S., Suzanne Y. Felten, David L. Felten, Pavur R. Sundaresan, and Shmuel Livnat. 1989. "Sympathetic Neural Modulation of the Immune System. I. Depression of T Cell Immunity in Vivo and in Vitro Following Chemical Sympathectomy." *Brain Behavior and Immunity* 3(1):72–89.

Madden, Kelley S., Jan A. Moynihan, Gary J. Brenner, Suzanne Y. Felten, David L. Felten, and Shmuel Livnat. 1994. "Sympathetic Nervous System Modulation of the Immune System. III. Alterations in T and B Cell Proliferation and Differentiation in Vitro Following Chemical Sympathectomy." *Journal of Neuroimmunology* 49(1–2):77–87.

Magnon, Claire, Simon J. Hall, Juan Lin, Xiaonan Xue, Leah Gerber, Stephen J. Freedland, and Paul S. Frenette. 2013. "Autonomic Nerve Development Cancer Progression." *Science* 341(6142):1–10.

Marsee, Derek K., Geraldine S. Pinkus, and Jason L. Hornick. 2009. "Podoplanin (D2-40) Is a Highly Effective Marker of Follicular Dendritic Cells." *Applied Immunohistochemistry and Molecular Morphology* 17(2):102–7.

Martelli, D., S. T. Yao, M. J. McKinley, and R. M. McAllen. 2014. "Reflex Control of Inflammation by Sympathetic Nerves, Not the Vagus." *The Journal of Physiology* 592(7):1677–86.

Mawdsley, J. E. and D. S. Rampton. 2005. "PSYCHOLOGICAL STRESS IN IBD : NEW INSIGHTS INTO PATHOGENIC AND THERAPEUTIC IMPLICATIONS."

Meza-perez, Selene and Troy D. Randall. 2017. "Immunological Functions of the Omentum." *Trends in Immunology* 38(7):526–36.

Michailova, Krassimira N. and Kamen G. Usunoff. 2004. "THE MILKY SPOTS OF THE PERITONEUM AND PLEURA : STRUCTURE , DEVELOPMENT AND PATHOLOGY." *Biomedical Reviews* 15:47–66.

Michels, Nicholas A. 1942. "The Variational Anatomy of the Spleen and Splenic Artery." *The American Journal of Anatomy* 70.

Mignini, F., V. Streccioni, and F. Amenta. 2003. "Autonomic Innervation of Immune Organs and Neuroimmune Modulation." *Autonomic and Autocoid Pharmacology* 23:1–25.

Mikuła-Pietrasik, Justyna, Paweł Uruski, Andrzej Tykarski, and Krzysztof Książek. 2018. "The Peritoneal 'Soil' for a Cancerous 'Seed': A Comprehensive Review of the Pathogenesis of Intraperitoneal Cancer Metastases." *Cellular and Molecular Life Sciences* 75(3):509–25.

Miller, Gregory E. and Edith Chen. 2006. "Life Stress and Diminished Expression of Genes Encoding Glucocorticoid Receptor and B2-Adrenergic Receptor in Children with Asthma." *Proceedings of the National Academy of Sciences of the United States of America* 103(14):5496–5501.

Mitchel, G. A. G. 1956. *Cardiovascular Innervation*. Edingburgh and London: E. & S. Livingstone LTD.

Motohara, Takeshi, Kenta Masuda, Matteo Morotti, Yiyan Zheng, Salma El-Sahhar, Kay Yi Chong, Nina Wietek, Abdulkhaliq Alsaadi, Mohammad Karaminejadranjbar, Zhiyuan Hu, Mara Artibani, Laura Santana Gonzalez, Hidetaka Katabuchi, Hideyuki Saya, and Ahmed Ashour Ahmed. 2019. "An Evolving Story of the Metastatic Voyage of Ovarian Cancer Cells: Cellular and Molecular Orchestration of the Adipose-Rich Metastatic Microenvironment." *Oncogene* 38(16):2885–98.

Murray, Kaitlin, Dayn Romero Godinez, Ingrid Brust-Mascher, Elaine Nicole Miller, Melanie G. Gareau, and Colin Reardon. 2017. "Neuroanatomy of the Spleen: Mapping the Relationship between Sympathetic Neurons and Lymphocytes." *PLoS ONE* 12(7):1–17.

Murtha, Lucy A., Matthew Morten, Michael J. Schuliga, Nishani S. Mabotuwana, Sean A. Hardy, David W. Waters, Janette K. Burgess, Doan T. M. Ngo, L. Aaron, Darryl A. Knight, and Andrew J. Boyle. 2019. "The Role of Pathological Aging in Cardiac and Pulmonary Fibrosis." 10(2):419–28.

Nakai, Akiko, Yuki Hayano, Fumika Furuta, Masaki Noda, and Kazuhiro Suzuki. 2014. "Control of Lymphocyte Egress from Lymph Nodes through B2-Adrenergic Receptors." *Journal of Experimental Medicine* 211(13):2583–98.

Nance, Dwight M. and Joan Burns. 1989. "Innervation of the Spleen in the Rat: Evidence for Absence of Afferent Innervation." *Brain Behavior and Immunity* 3(4):281–90.

Nava, Eduardo and Silvia Llorens. 2019. "The Local Regulation of Vascular Function : From an Inside-Outside to an Outside-Inside Model." 10(June):1–15.

Niijima, Akira, Tetsuro Hori, Shuji Aou, and Yutaka Oomura. 1991. "The Effects of Interleukin-1?? On the Activity of Adrenal, Splenic and Renal Sympathetic Nerves in the Rat." *Journal of the Autonomic Nervous System* 36(3):183–92.

Nolte, Martijn A., Jeroen A. M. Beliën, Inge Schadee-Eestermans, Wendy Jansen, Wendy W. J. Unger, Nico Van Rooijen, Georg Kraal, and Reina E. Mebius. 2003. "A Conduit System Distributes Chemokines and Small Blood-Borne Molecules through the Splenic White Pulp." *Journal of Experimental Medicine* 198(3):505–12.

Nylander, G. and B. Tjernberg. 1969. "The Lymphatics of the Greater Omentum. An Experimental Study in the Dog." *Lymphology* 2(1):3–7.

Olofsson, Peder S., Mauricio Rosas-ballina, Yaakov A. Levine, and Kevin J. Tracey. 2012. "Rethinking Inflammation : Neural Circuits in the Regulation of Immunity." *Immunological Reviews* 248:188–204.

Paget, Stephen. 1889. "Distribution of Secondary Growths in Cancer of the Breast." *The Lancet* 571–73.

Pandey, S. K., S. Bhattacharya, R. N. Mishra, and V. K. Shukla. 2004. "Anatomical Variations of the Splenic Artery and Its Clinical Implications." *Clinical Anatomy (New York, N.Y.)* 17(6):497–502.

Panucio, A. L., S. De La Pena, G. Gualco, and N. Reissenweber. 1998. "Adrenergic Innervation in Reactive Human Lymph Nodes." *Journal of Anatomy* 194:143–46.

Pavlov, Valentin A. and Kevin J. Tracey. 2017. "Neural Regulation of Immunity: Molecular Mechanisms and Clinical Translation." *Nature Neuroscience* 20(2):156–66.

Perez-Shibayama, Christian, Cristina Gil-Cruz, and Burkhard Ludewig. 2019. "Fibroblastic Reticular Cells at the Nexus of Innate and Adaptive Immune Responses." *Immunological Reviews* 289(1):31–41.

Pinkus, G. S., M. J. Warhol, E. M. O'Connor, C. L. Etheridge, and K. Fujiwara. 1986. "Immunohistochemical Localization of Smooth Muscle Myosin in Human Spleen, Lymph Node, and Other Lymphoid Tissues. Unique Staining Patterns in Splenic White Pulp and Sinuses, Lymphoid Follicles, and Certain Vasculature, with Ultrastructural Correlations." *American Journal of Pathology* 123(3):440–53.

Platell, C., D. Cooper, J. M. Papadimitriou, and J. C. Hall. 2000. "The Omentum." *Word Journal of Gastroenterology* 6(2):169–76.

Qi, Xiao Yan, Shun Lin Qu, Wen Hao Xiong, Oren Rom, Lin Chang, and Zhi Sheng Jiang. 2018. "Perivascular Adipose Tissue ( PVAT ) in Atherosclerosis : A Double - Edged Sword." *Cardiovascular Diabetology* 1–20.

Qiao, Guanxi, Minhui Chen, Mark J. Bucsek, Elizabeth A. Repasky, and Bonnie L. Hylande. 2018. "Adrenergic Signaling: A Targetable Checkpoint Limiting Development of the Antitumor Immune Response." *Frontiers in Immunology* 9(FEB):1–15.

Ramer, Matt S. and Mark A. Bisby. 1998. "Normal and Injury-Induced Sympathetic Innervation of Rat Dorsal Root Ganglia Increases with Age." *Journal of Comparative Neurology* 394(1):38–47.

Ramer, Matt S., Stephen W. N. Thompson, and Stephen B. McMahon. 1999. "Causes and Consequences of Sympathetic Basket Formation in Dorsal Root Ganglia." *Pain* 82(SUPPL.1).

Reardon, Colin. 2016. "Neuro-Immune Interactions in the Cholinergic Anti-Inflammatory Reflex." *Immunology Letters* 178:92–96.

Rogausch, Heiner, Thomas Böck, Karl Heinz Voigt, and Hugo Besedovsky. 2004. "The Sympathetic Control of Blood Supply Is Different in the Spleen and Lymph Nodes." *NeuroImmunoModulation* 11(1):58–64.

Roozendaal, Ramon, Reina E. Mebius, and Georg Kraal. 2008. "The Conduit System of the Lymph Node." *International Immunology* 20(12):1483–87.

Rosas-Ballina, M., P. S. Olofsson, M. Ochani, S. I. Valdes-Ferrer, Y. A. Levine, C. Reardon, M. W. Tusche, V. A. Pavlov, U. Andersson, S. Chavan, T. W. Mak, and K. J. Tracey. 2011. "Acetylcholine-Synthesizing T Cells Relay Neural Signals in a Vagus Nerve Circuit." *Science* 334(6052):98–101.

Rosas-Ballina, Mauricio, Mahendar Ochani, William R. Parrish, Kanta Ochani, Yael T. Harris, Jared M. Huston, Sangeeta Chavan, and Kevin J. Tracey. 2008. "Splenic Nerve Is Required for Cholinergic Antiinflammatory Pathway Control of TNF in Endotoxemia." *Proceedings of the National Academy of Sciences of the United States of America* 105(31):11008–13.

Rothstein, Thomas L., Daniel O. Griffin, Nichol E. Holodick, Tam D. Quach, and Hiroaki Kaku. 2013. "Human B-1 Cells Take the Stage." *Annals of the New York Academy of Sciences* 1285(1):97–114.

Sahni, A. Daisy, B. Indar Jit, C. N. M. Gupta, D. Madhur Gupta, and E. Harjeet. 2003. "Branches of the Splenic Artery and Splenic Arterial Segments." *Clinical Anatomy* 16(5):371–77.

Saito, H. 1990. "Innervation of the Guinea Pig Spleen Studied by Electron Microscopy." *The American Journal of Anatomy* 189:213–15.

Saxton, Sophie N., Sarah B. Withers, and Anthony M. Heagerty. 2019. "Emerging Roles of Sympathetic Nerves and Inflammation in Perivascular Adipose Tissue." *Cardiovascular Drugs and Therapy* 33(2):245–59.

Schindelin, Johannes, Ignacio Arganda-Carreras, Erwin Frise, Verena Kaynig, Mark Longair, Tobias Pietzsch, Stephan Preibisch, Curtis Rueden, Stephan Saalfeld, Benjamin Schmid, Jean-Yves Tinevez,

Daniel James White, Volker Hartenstein, Kevin Eliceiri, Pavel Tomancak, and Albert Cardona. 2012. "Fiji: An Open-Source Platform for Biological-Image Analysis." *Nature Methods* 9(7):676–82.

Schlereth, Tanja and Frank Birklein. 2008. "The Sympathetic Nervous System and Pain." *NeuroMolecular Medicine* 10(3):141–47.

Schurink, B, C. G. J. Cleypool, and R. L. A. W. Bleys. 2019. "A Rapid and Simple Method for Visualizing Milky Spots in Large Fixed Tissue Samples of the Human Greater Omentum." *Biotechnic & Histochemistry* 0(0):1–6.

Schurink, B., C. G. J. Cleypool, and R. L. A. W. Bleys. 2019. "A Rapid and Simple Method for Visualizing Milky Spots in Large Fixed Tissue Samples of the Human Greater Omentum." *Biotechnic and Histochemistry* 94(6).

Seifert, E. 1923. "Studien Am Omentum Majus Des Menschen." *Langenbecks Archiv Fur Chirurgie* 123:608–83.

Seiler, Annina, Christopher P. Fagundes, and Lisa M. Christian. 2020. "The Impact of Everyday Stressors on the Immune System and Health." Pp. 71–92 in *Stress Challenges and Immunity in Space: From Mechanisms to Monitoring and Preventive Strategies*, edited by A. Choukèr. Cham: Springer International Publishing.

Shimotsuma, M., M. Kawata, A. Hagiwara, and T. Takahasi. 1989. "Milky Spots in the Human Greater Omentum: Macroscopic and Histological Identification." *Acta Anatomica* 136:211–16.

Shimotsuma, M., J. .. Shields, M. W. Simpson-Morgan, A. Sakuyama, M. Shirasu, A. Hagiwara, and T. Takahashi. 1993. "Morpho-Physiological Function and Role of Omental Milky Spots as Omentum-Associated Lymphoid Tissue (OALT) in the Peritoneal Cavity." *Lymphology* 26:90–101.

Shimotsuma, Masataka, Toshio Takahashi, and Akeo Hagiwara. 1992. "Activation of Omental Milky Spots and Milky Spot Macrophages by Intraperitoneal Administration of a Streptococcal Preparation, OK-432." *Cancer Research* 52(19):5400–5402.

Shimotsuma, Masataka, Toshio Takahashi, Mitsuhiro Kawata, and Kazimierz Dux. 1991. "Cellular Subsets of the Milky Spots in the Human Greater Omentum." *Cell and Tissue Research* 264:599–601.

Shinder, V., R. Govrin-Lippmann, S. Cohen, M. Belenky, P. Ilin, K. Fried, H. A. Wilkinson, and M. Devor. 1999. "Structural Basis of Sympathetic-Sensory Coupling in Rat and Human Dorsal Root Ganglia Following Peripheral Nerve Injury." *Journal of Neurocytology* 28(9):743–61.

Siopi, Eleni, Grégoire Chevalier, Lida Katsimpardi, Soham Saha, Mathilde Bigot, Carine Moigneu, Gérard Eberl, and Pierre Marie Lledo. 2020. "Changes in Gut Microbiota by Chronic Stress Impair the Efficacy of Fluoxetine." *Cell Reports* 30(11):3682-3690.e6.

Song, D., B. S. Robinson, and T. W. Berger. 2018. "Identification of Short-Term and Long-Term Functional Synaptic Plasticity from Spiking Activities." *Adaptive Learning Methods for Nonlinear System Modeling* 289–312.

Song, Hongjiang, Tie Wang, Lining Tian, Shuping Bai, Li Chen, Yanjiao Zuo, and Yingwei Xue. 2019. "Macrophages on the Peritoneum Are Involved in Gastric Cancer Peritoneal Metastasis." *Journal of Cancer* 10(22):5377–87.

Steiniger, Birte S. 2015. "Human Spleen Microanatomy: Why Mice Do Not Suffice." *Immunology* 145(3):334–46.

Sun, Yue, Lu Li, Runxiang Xie, Bangmao Wang, Kui Jiang, and Hailong Cao. 2019. "Stress Triggers Flare of Inflammatory Bowel Disease in Children and Adults." 7(October).

Suzuki, Kazuhiro, Yuki Hayano, Akiko Nakai, Fumika Furuta, and Masaki Noda. 2016. "Adrenergic Control of the Adaptive Immune Response by Diurnal Lymphocyte Recirculation through Lymph Nodes." *Journal of Experimental Medicine* 213(12):2567–74.

Sylvester, P. A., R. Stewart, and H. Ellis. 1999. "Tortuosity of the Splenic Artery." *Clinical Anatomy* 8:214–18.

Thomassen, Irene, Yvette R. Van Gestel, Bert Van Ramshorst, Misha D. Luyer, Koop Bosscha, Simon W. Nienhuijs, Valery E. Lemmens, and Ignace H. De Hingh. 2013. "Peritoneal Carcinomatosis of Gastric Origin: A Population-Based Study on Incidence, Survival and Risk Factors." *International Journal of Cancer* 134(3):622–28.

Tsujimoto, H., A. Hagiwara, M. Shimotsuma, C. Sakakura, K. Osaki, S. Sasaki, T. Ohyama, M. Ohgaki, T. Imanishi, J. Yamazaki, and T. Takahashi. 1996. "Role of Milky Spots as Selective Implantation Sites for Malignant Cells in Peritoneal Dissemination in Mice." *Journal of Cancer Research and Clinical Oncology* 122(10):590–95.

Tsujimoto, H., T. Takahashi, A. Hagiwara, M. Shimotsuma, C. Sakakura, K. Osaki, S. Sasaki, M. Shirasu, T. Sakakibara, T. Ohyama, A. Sakuyama, M. Ohgaki, T. Imanishi, and J. Yamasaki. 1995. "Site-Specific Implantation in the Milky Spots of Malignant Cells in Peritoneal Dissemination: Immunohistochemical Observation in Mice Inoculated Intraperitoneally with Bromodeoxyuridine-Labelled Cells." *British Journal of Cancer* 71(3):468–72.

Verdú, Enrique, Dolores Ceballos, Jorge J. Vilches, and Xavier Navarro. 2000. "Influence of Aging on Peripheral Nerve Function and Regeneration." *Journal of the Peripheral Nervous System* 5(4):191–208.

Verlinden, Thomas J. M., Paul Van Dijk, Jill Hikspoors, Andreas Herrler, Wouter H. Lamers, and S. Eleonore Köhler. 2018. "Brain , Behavior , and Immunity Innervation of the Human Spleen : A Complete Hilum-Embedding Approach." *Brain Behavior and Immunity* (December):1–9.

Vida, G., G. Pena, A. Kanashiro, M. del Rocio Thompson-Bonilla, D. Palange, E. a. Deitch, and L. Ulloa. 2017. "B2-Adrenoreceptors of Regulatory Lymphocytes Are Essential for Vagal Neuromodulation of the Innate Immune System." *The FASEB Journal* 25(12):4476–85.

Vida, Gergely, Geber Peña, Edwin A. Deitch, and Luis Ulloa. 2011. "Alpha7-Cholinergic Receptor Mediates Vagal Induction of Splenic Norepinephrine." *Journal of Immunology* 186(7):4340–46.

Vijayaraghavan, Swetha, Azadeh Karami, Shahin Aeinehband, Homira Behbahani, Alf Grandien, Bo Nilsson, Kristina N. Ekdahl, Rickard P. F. Lindblom, Fredrik Piehl, and Taher Darreh-Shori. 2013. "Regulated Extracellular Choline Acetyltransferase Activity- The Plausible Missing Link of the Distant Action of Acetylcholine in the Cholinergic Anti-Inflammatory Pathway." *PLoS ONE* 8(6).

Villaro, A. C., M. P. Sesma, and J. J. Vazquez. 1987. "Innervation of Mouse Lymph Nodes: Nerve Endings on Muscular Vessels and Reticular Cells." *American Journal of Anatomy* 179(2):175–85.

Vugt, Ellen V. A. N., Ellen A. M. V. A. N. Rijthoven, and Eduard W. A. Kamperdijk. 1996. "Omental Milky Spots in the Local Immune Response in the Peritoneal Cavity of Rats." *The Anatomical Record* 245:235–45.

Wang, Hongcheng, Liyu Xing, Wenjing Li, Lingfei Hou, Jingxuan Guo, and Xian Wang. 2002. "Production and Secretion of Calcitonin Gene-Related Peptide from Human Lymphocytes." *Journal of Neuroimmunology* 130(1–2):155–62.

Weibel, E. R. 1979. *Stereological Methods*. London: Academic Press.

Wijffels, J. F. A. M., R. J. B. M. Hendrickx, J. J. E. Steenbergen, I. L. Eestermans, and R. H. J. Beelen. 1992. "Milky Spots in the Mouse Omentum May Play an Important Role in the Origin of Peritoneal Macrophages." *Research Immunology* 143:401–9.

Wilkosz, Sylvia, Grenham Ireland, Nadeem Khwaja, Michael Walker, Richard Butt, Alexander Giorgio-Miller de, and Sarah E. Herrick. 2005. "A Comparative Study of the Structure of Human and Murine Greater Omentum." *Anatomy and Embryology* 209:251–61.

Willard-Mack, Cynthia L. 2006. "Normal Structure, Function, and Histology of Lymph Nodes." *Toxicologic Pathology* 34(5):409–24.

Xia, C. M., D. G. Colomb JR, H. I. Akbarali, and L. Y. Qiao. 2011. "Prolonged Sympathetic Innervation of Sensory Neurons in Rat Thoracolumbar Dorsal Root Ganglia during Chronic Colitis." *Neurogastroenterology and Motility : The Official Journal of the European Gastrointestinal Motility Society* 23(8):801–16.

Yang, San Nan, Chong Chao Hsieh, Hsuan Fu Kuo, Min Sheng Lee, Ming Yii Huang, Chang Hung Kuo, and Chih Hsing Hung. 2014. "The Effects of Environmental Toxins on Allergic Inflammation." *Allergy, Asthma and Immunology Research* 6(6):478–84.

Yildirim, A., A. Aktaş, Y. Nergiz, and M. Akkuş. 2010. "Analysis of Human Omentum-Associated Lymphoid Tissue Components with S-100: An Immunohistochemical Study." *Romanian Journal of Morphology and Embryology* 51(4):759–64.

Yonemura, Y., Y. Endo, T. Yamaguchi, T. Fujimura, T. Obata, T. Kawamura, N. Nojima, I. Miyazaki, and T. Sasaki. 1996. "Mechanisms of the Formation of the Peritoneal Dissemination in Gastric Cancer." *International Journal of Oncology* 8(4):795–802.

Young, B., G. O'Dowd, and P. Woodford. 2013. *Wheater's Functional Histology A Text and Colour Atlas*. 6th ed. Elsevier.

Zahalka, Ali H., Anna Arnal-estapé, Maria Maryanovich, Fumio Nakahara, Cristian D. Cruz, Lydia W. S. Finley, and Paul S. Frenette. 2017. "Adrenergic Nerves Activate an Angio-Metabolic Switch in Prostate Cancer Ali." *Science* 358(October):321–26.

Zhao, Lintao, Lina Liu, Bo Guo, and Bo Zhu. 2015. "Regulation of Adaptive Immune Responses by Guiding Cell Movements in the Spleen." *Frontiers in Microbiology* 6(JUN):1–6.

Zhu, Liyan, Liting Zhao, Ruobing Qu, Hong Yan Zhu, Yongmeng Wang, Xinghong Jiang, and Guang Yin Xu. 2015. "Adrenergic Stimulation Sensitizes TRPV1 through Upregulation of Cystathionine β-Synthetase in a Rat Model of Visceral Hypersensitivity." *Scientific Reports* 5(June):1–10.

Dorsal root ganglia



Spleen